AD NUMBER

AD894644

NEW LIMITATION CHANGE

TO

Approved for public release, distribution unlimited

FROM

Distribution authorized to U.S. Gov't. agencies only; Test and Evaluation; Feb 1972. Other requests shall be referred to Air Force Aero Propulsion Laboratory, Attn: SFF, Wright-Patterson AFB, OH 45433.

AUTHORITY

AFRPL ltr, 30 Jun 1975

AFAPL-TR-72-24
Volume I
Volume II

RESEARCH ON METHODS OF IMPROVING THE COMBUSTION CHARACTERISTICS OF LIQUID HYDROCARBON FUELS

Volume I
EXPERIMENTAL DETERMINATION OF IGNITION DELAY TIMES IN SUBSONIC FLOW SYSTEMS

V. J. Siminski
F. J. Wright

Esso Research and Engineering Company
Government Research Laboratory

Volume II
KINETICS MODELING AND SUPERSONIC TESTING

R. Edelman
C. Economos
O. Fortune

GENERAL APPLIED SCIENCE LABORATORIES, INC.

TECHNICAL REPORT AFAPL-72-24, VOLUME I, VOLUME II
FEBRUARY 1972

AIR FORCE AERO PROPULSION LABORATORY
AIR FORCE SYSTEMS COMMAND
WRIGHT-PATTERSON AIR FORCE BASE, OHIO

Attn: SFF

NOTICE

When Government drawings, specifications, or other data are used for any purpose other than in connection with a definitely related Government procurement operation, the United States Government thereby incurs no responsibility nor any obligation whatsoever; and the fact that the government may have formulated, furnished, or in any way supplied the said drawings, specifications, or other data, is not to be regarded by implication or otherwise as in any manner licensing the holder or any other person or corporation, or conveying any rights or permission to manufacture, use, or sell any patented invention that may in any way be related thereto.

Copies of this report should not be returned unless return is required by security considerations, contractual obligations, or notice on a specific document.

AFAPL-TR-72-24
Volume I

RESEARCH ON METHODS OF IMPROVING THE COMBUSTION CHARACTERISTICS OF LIQUID HYDROCARBON FUELS

Volume I
EXPERIMENTAL DETERMINATION OF IGNITION DELAY TIMES IN SUBSONIC FLOW SYSTEMS

V. J. Siminski
F. J. Wright

FOREWORD

This report was prepared by Esso Research and Engineering Company, Government Research Laboratory, Linden, New Jersey under U.S. Air Force Contract No. F33615-69-C-1289. The participation by General Applied Science Laboratories, Merrick Blvd. Westbury, Long Island, New York as a subcontractor is documented under Project #719110 at Esso Research and Engineering Company. The prime Air Force contract was initiated under Project No. 3048, Task 304805, and was administered under the direction of the Air Force Aero Propulsion Laboratory of Wright-Patterson Air Force Base, Ohio, by Captain S. G. Hill, Project Engineer, AFAPL/SFF.

This report, which consists of two volumes, covers work performed by Esso Research and Engineering Company (Volume I) and General Applied Science Laboratories (Volume II) during the period between January 1, 1969 and December 31, 1971.

Mr. V. J. Siminski was principal investigator and project supervisors were Dr. M. S. Cohen and Dr. D. Grafstein for Esso Research and Engineering Company. Dr. F. J. Wright a member of the Corporate Research Laboratory at Esso Research participated in the program as a technical consultant.

The technical representative of General Applied Science Laboratories during their association as subcontractor were Drs. C. Economus, R. Edelman, and Mr. O. Fortune.

An independent, voluntary Technical Board of Review comprised of recognized experts in the fields of combustion and reaction kinetics reviewed the technical progress of the program at semi-annual intervals. The members of the board to whom we are most thankful were:

J. Ortworth (Air Force Aero Propulsion Labs)
F. Billig (Johns Hopkins Univ. Appl. Phy. Lab)
W. Blackman (United Aircraft Corp.)
H. Hottel (Mass. Inst. Tech)
J. Longwell (Esso Res. & Eng. Co.)
C. Scholler (Aerospace Res. Labs., Wright Patterson Air Force Base, Ohio)

This report was submitted by the authors on February 10, 1972.

This technical report has been reviewed and is approved.

ARTHUR V. CHURCHILL
Chief-Fuel Branch
Fuels and Lubrication Division
Air Force Aero Propulsion Laboratory

ABSTRACT

The purpose of this program was to determine, analytically and experimentally the extent to which the autoignition delay times of liquid hydrocarbons could be reduced by modification of the molecular structure or through the utilization of homogeneous additives and heterogeneous catalysts. To this end the autoignition delays of a number of different hydrocarbons were determined in three different experimental apparatus; a well-stirred reactor, a constant flow subsonic duct and a supersonic detached jet or ducted flow system. At one atmosphere pressure the velocity and temperature of the test devices were varied from subsonic to supersonic and from 300° to 1600°K respectively. The ignition delays measured in a subsonic, constant flow system at 1000°K varied from 180 milliseconds for lean mixtures of Shelldyne-H to 25 milliseconds for 1,7-octadiene. Propane was observed to have an ignition lag of 34 milliseconds. No quantitative relationship could be established between the ignition lags measured in the constant flow system and the average residence times determined in the stirred reactor at the blow-out point. However, it is clear that the stirred reactor data more closely describe the total hydrocarbon combustion time than any "pseudo ignition lag" associated with the hydrocarbon. Of the more than 25 different homogeneous additives tested, the strongest ignition promoters, by far, were found to be the alkyl nitrates and nitrites or nitric oxide and nitrogen dioxide. The ignition promoting characteristics of these compounds are associated with the ease with which they thermally dissociate or oxidize to form oxygen-atoms. The chemical reactivity of the oxygen atom compared to other radicals in the preignition reactions was found to be the dominating factor. The ignition delay at 1000°K, of Shelldyne-H or H-MCPD* was reduced from 180 and 110 milliseconds to 3.5 and 5.3 milliseconds respectively, upon the addition of 25 volume percent n-propyl nitrate. Other additives such as H_2O, N_2O, CO, H_2 or peroxides, esters, polyethers and alcohols had little or no effect on promoting the autoignition of various hydrocarbons in the temperature range of 950-1300°K. Surprisingly, a synergistic effect between H_2 and NO or NO_2 was found to dramatically increase the ignition promoting character of the oxides of nitrogen (excluding N_2O) not withstanding the fact that up to 2 weight percent of hydrogen alone had no effect on the ignition delay of various fuels. The presence of a platinum surface on the walls of the combustion chamber reduced the autoignition temperature of various hydrocarbons by 350°K. The addition of 15 volume percent n-propyl nitrate to the hydrocarbons resulted in a decrease in the autoignition temperature by another 200°K. A thermal mechanism, based on the promotion of the vapor phase oxidation reactions by platinum, is discussed. Fuel blends consisting of 15 volume percent n-propyl nitrate in either H-MCPD or Shelldyne-H were ignited and combusted in a piloted supersonic flow (Mach 1.5) over a temperature range of 300 to 1300°K. An ignition model based upon quasi-global kinetics and involving 10 basic chemical reactions has been shown to be able to predict within a factor of 5, the ignition delay of neat hydrocarbons or blends of hydrocarbons with homogeneous additives. The development of the model and the experimental results of the supersonic ignition tests are discussed in Volume II of this report.

* hydrogenated dimer of methyl cyclopentadiene

TABLE OF CONTENTS

TABLES

FIGURES

FIGURES (Cont.)

SECTION I

SUMMARY

The goals of this program were to determine, both analytically and experimentally, the influence of molecular structure and homogeneous or heterogeneous additives on the autoignition delay of hydrocarbons. This volume of the final report describes the results of ignition delay measurements obtained in a Well-Stirred Reactor (WSR) and a subsonic, continuous flow system (CFS). The development of an analytical ignition delay model based on the subsonic ignition delay measurements is discussed in Volume II, together with the experimental results of supersonic, piloted ignition tests of Shelldyne-H and the hydrogenated dimer of methylcyclopentadiene (H-MCPD).

The data obtained in the WSR under kinetically limited conditions indicated that all the long chain alkanes had shorter residence times compared to other fuel structures. In the order of increasing residence times: alkenes < cyclics < polycyclics < complex hydrocarbons. Branching in either the alkanes or alkenes tended to increase the residence time (τ) for a similar number of carbon-atoms. Benzene had the longest (τ) compared to hexyne-1, the only triple-bond hydrocarbon tested, which had a residence time 2.5 times as short. The complex, high density hydrocarbons had similar average residence times as a class, and were generally longer than any of the other hydrocarbons.

The homogeneous additives which consisted of alkyl nitrates and nitrites, peroxides, epoxides and polyethers, in some instances reduced (τ) by 90%. The additive study indicated that great care must be exercised in selecting an additive/fuel blend since results show that under certain circumstances, the ignition promoters became ignition inhibitors.

The autoignition delay times of neat hydrocarbons and blends of hydrocarbons with various homogeneous additives at one atmosphere in an unvitiated subsonic air stream were determined in a constant cross section duct. Over the temperature range of 900-1250°K, the visually determined ignition lags of lean mixtures (ϕ <0.3) in their order of decreasing lag times were: Shelldyne-H, H-MCPD, JP-7, long-chain alkenes, long chain monolefins, diolefins and triolefins. Generally, the ease with which the fuel molecule was oxidized determined the magnitude of the ignition lag times. The temperature relationship to ignition delay was described by an Arrhenius expression, $\tau = Ae^{E_a/RT}$ where the global activation energies (E_a) varied depending upon the molecular structure of the fuel. The values of (E_a) determined from the experimental data for alkanes, alkenes and complex high density fuels were 19.8 KCal/mole, 22.16 KCal/mole and approximately 40 KCal/mole, respectively.

Homogeneous additives which included alkyl nitrates and nitrites, peroxides, polyethers, hydrogen, oxygen, carbon monoxide, water, nitrous oxide and an alkylated boron compound were tested in different fuels in varying concentrations. The results showed that the low molecular weight alkyl nitrates were, by far, the most effective promoters of ignition over the temperature

range of 900-1250°K. Typically 25 vol. percent n-propyl nitrate in Shelldyne-H or H-MCPD reduced the ignition lags from 180 and 110 milliseconds to 3.5 and 5.3 milliseconds, respectively at 1000°K. Nitric oxide and nitrogen dioxide were nearly as effective as the nitrogen esters. Hydrogen, in very large concentrations did not promote hydrocarbon ignitions, but when H_2 was combined with nitric oxide a synergistic effect was observed. The maximum effect was noted for H_2 concentrations of about 8 volume percent of the total fuel flow rate. N_2O, H_2O, CO, O_2 or tri-isobutyl borane did not promote the ignitions of a wide variety of hydrocarbons. The ignition promoting effects of the nitrogen esters and NO or NO_2 were postulated to be due to oxygen atoms which were generated by the thermal decomposition of the esters and the subsequent oxidation of NO or NO_2 which were the reaction products.

The minimum autoignition temperatures of various hydrocarbons, varying in structure from alkanes to polycyclics, were reduced from 1050°K to 550-650°K via heterogeneous catalysis in an air stream that varied in velocity from 85-150 feet/sec. The catalyst was a 1-inch diameter, thin walled platinum tube that was 6-inches long and located on the inside surface of the test duct. A thermal ignition model is proposed. The platinum surface catalyzed the low temperature oxidation rates of rich mixtures of hydrocarbons sufficient to achieve local platinum surface temperatures which were very near the spontaneous ignition temperatures (S.I.T.) reported in the literature.

The successfull attainment of the goals of the program has demonstrated that high density hydrocarbons can be blended with more "active" compounds to produce blends which have high densities, high space heat release rates and most importantly low autoignition delay times.

SECTION II

INTRODUCTION

Mission profile studies of hypersonic velocity vehicles have shown that in the regime of Mach 8-12, a supersonic ramjet (SCRAMJET) fueled with a storeable, high density hydrocarbon offered striking performance advantages over alternate propulsion systems (1). The utilization of this air-breathing system became even more attractive when the scramjet take-over velocity was reduced to lower Mach numbers. However, to accomplish this task, the fuel must exhibit good, low temperature ignition and combustion characteristics if the combustion chamber length was to be realistic. The metal alkyls and hydrogen satisfy these requirements, but because of logistics and toxicity problems associated with their use, alternate fuels are required. This report which is divided into two separate volumes describes the results of a three-phase experimental and analytical research program which explored the effects of molecular structure, homogeneous chemical additives and heterogeneous catalysts on the autoignition and combustion characteristics of hydrocarbon fuels in subsonic as well as supersonic flow environments at one atmosphere. Volume I of the report is concerned with the subsonic ignition characteristics of hydrocarbons in a well-stirred environment and a constant area duct. Volume II describes the piloted ignitions of hydrocarbons in supersonic streams and the development of the quasi-global autoignition model which was modified by the experimental results described in Volume I.

The First Phase was concerned with determining relative ignition delay times of various hydrocarbons and additives in an environment void of heat and/or mass transport limitations such that the chemical kinetics of the system were the limiting factors over the temperature range of 1400-1650°K. The Well-Stirred-Reactor developed by Longwell and Weiss for determining the chemical kinetics of combustion processes was utilized in this phase of the program (2). The Second Phase was devoted to measuring the absolute values of the autoignition delay times of a number of hydrocarbons which included the same fuels and additives studied in Phase One, but in a constant flow heated air system which was considered to more closely resemble a practical combustor system. The temperature was varied between 550-1300°K.

Phase Three consisted of an analytical study of the preignition chemical reactions via a quasi-global kinetics program which subsequently led to the development of a mathematical model which was shown to predict within a factor of 5, the autoignition lag times of fuels or fuel blends with homogeneous additives.

During the last phase of the program, the best fuel systems which were Shelldyne-H or H-MCPD + 15% n-propyl nitrate which were defined in the first two phases were ignited and burned in piloted supersonic free-jet and ducted flow configuration at various temperatures and one atmosphere pressure.

Criteria For Fuel Selection

Because of the nature of this research program, the successfull development of a praccical fuel for supersonic combustion was very greatly dependent upon the initial choice of hydrocarbons and additives. The potential of candidate compounds was evaluated by a set of criteria which is described.

The structure of hydrocarbon molecules has long been recognized to exert a powerfull influence on reactivity toward oxidation, particularly in the temperature regime below 1000°K.[3] Molecular structure affects all the phenomena that influence the initial phases of the combustion process--peroxidation, chain breaking, free radical formation, chain branching--as these are manifested in such observations as cool flame development, ignition lag, burning rates, flame speeds and quenching reactions. In determining fuel ranking for supersonic combustion it is worthwhile to review some of the techniques used by fuel chemists to develop a better understanding of the effects of fuel structure on these parameters.

Perhaps the first and most widely studied manifestation of hydrocarbon structure on combustion was the development of "knock" in the internal combustion engine[4]. The environment of the fuel-air mixture is at a relatively low temperature and a high pressure and is complicated by the use of a spark source to initiate the spread of flame. The preponderance of experimental data suggests that knock results from the spontaneous ignition of the compressed end gas in the cylinder.[5] The most reactive hydrocarbons in terms of "knock" are long-chain normal paraffins and the least reactive (i.e. most "knock" resistant) were the highly branched paraffins and low molecular weight gases.[6] n-Heptane has an octane number of zero compared to 2,2,4-trimethyl pentane which has an octane number of 100. The cyclic hydrocarbon structures generally exhibit high octane numbers.[7]

Many different techniques have been used in the past to determine the spontaneous ignition temperature of fuels in the absence of an ignition source. When the temperature of the surrounding environment was gradually increased the chemical reactions are manifested by the appearance of "cool" - flames[8], negative temperature coefficient regions[9], and explosions.[10] Generally, the literature reveals that there is a correlation between autogeneous ignition ranking and "knock" rating. The hydrocarbons which show the highest spontaneous ignition temperature (S.I.T.) also appear to be the most "knock" resistant, i.e., possess high octane numbers. The low molecular weight gases such as methane, ethane and propane have (S.I.T.) of 537, 515 and 466°C respectively. Straight-chain paraffins such as heptane and octane have (S.I.T.) of 123 and 206°C respectively. The cycloparaffins, isoparaffins and aromatic hydrocarbons generally have higher (S.I.T.) than the straight-chain alkanes.

In experimental situations more closely resembling a ramjet environment many researchers have observed the same general relationships between fuel structure and auto-ignition lag.[11] The determination of ignition delays via shock tube techniques offers the best source of "kinetically controlled" data.[12] In all of these techniques the qualitative ranking of the ignition lags as a function of molecular structures are similar, but because of the nature of each experimental method, the quantitative agreement is poor.

The practical application of the candidate fuel demands long-term liquid storeability, high density and optimum ignition and combustion characteristics. Low temperature flow properties and liquid boiling temperatures are also taken into account before the fuels are considered as candidates. There are other fuel properties which may be of importance in specialized applications, but are not of direct interest in this investigation. Probably the most outstanding example within this special category is the heat-sink properties of the fuel and its cooling-characteristics as related to a regeneratively cooled engine or air frame. The ignition characteristics of a fuel which has undergone partial oxidation or pyrolysis as a result of its cooling application may be significantly different from the ignition delay of the unexposed fuel.[13]

Table I summarizes the different types of fuels studied in the kinetically controlled Well-Stirred-Reactor (WSR) the Continuous Flow Auto Ignition Test System (CFS) and piloted Supersonic Flow Facility.

Criteria for Homogeneous Additive Selection

A survey of the literature revealed that many different types of homogeneous chemical additives had been tested as hydrocarbon ignition promoters, in numerous types of experimental apparatus.[14,15] The large majority of the cited references was concerned with the promotion or inhibition of hydrocarbon ignitions in Otto-Cycle Engines where the temperature and pressure conditions were drastically different from a ramjet's combustor environment. Research on diesel engine ignition promoting additives has been extensively reviewed by Bogen and Wilson[16] and many others [17]. All these references as well as our proprietary technology indicated that the following classes of compounds are, to some degree, promoters of ignition of hydrocarbons under varying local conditions.

- Peroxides
- Alkyl Nitrates and Nitrites
- Nitro Parrafins
- Oxygen and Oxidation Products
- Oximes and Nitroso Compounds
- Aldehydes, Ketones, Ethers and Esters
- Metal Alkyls
- Boron Hydrides, Silicone Hydrides
- Nitrogen Oxides

TABLE I

PHYSICAL AND CHEMICAL PROPERTIES OF NEAT HYDROCARBONS

Fuel	Formula	B.P. °C	S.I.T. °C	M.A.T [a] on Platinum (°C)	Sg.	Flammability Limits (Vol % in Air) Lean	Rich
Methane	CH_4	-161.6	632		0.555	5.3	14
Ethane	C_2H_6	-88.6	510		1.047	3.0	12.5
Propane	C_3H_8	-42.1	468		1.550	2.2	9.5
Butane	C_4H_{10}	-0.5	405		2.076	1.9	8.5
Octane	C_8H_{18}	125	220		0.707	0.95	(7.0)
Tetradecane	$C_{14}H_{30}$	253	202 232		0.767	0.5	(4)
2-Methyl Pentane	C_6H_{14}	60.5	306		0.669	1.2	(7.7)
2,4-Dimethyl Pentane	C_7H_{16}	80.5	338		0.677	(1.0)	(7.0)
Octene-1	C_8H_{16}	123	230		0.718	0.9	6.6
Hexene-1	C_6H_{12}	63.5	253	405	0.678	(1.2)	(7.7)
1,7-Octadiene	C_8H_{14}	126	(240)		0.761	(1.0)	(6.6)
1,3,6-Heptatriene	C_7H_{12}	114.5	(245)		0.823	(1.2)	(9)
1 - Hexyne	C_6H_{10}	71.5	(275)		0.721	(1.8)	(10)
Benzene	C_6H_6	80	548		0.885	1.4	7.1

TABLE I (Cont.)

PHYSICAL AND CHEMICAL PROPERTIES OF NEAT HYDROCARBONS (Cont'd)

Fuel	Formula	B.P. °C	S.I.T. °C	M.A.T. (a) on Platinum (°C)	Sg.	Flammability Limits (Vol % in Air) Lean	Rich
Cyclohexane	C_6H_{12}	81	251	280	0.783	1.3	7.8
Cyclohexene	C_6H_{10}	83	244	300	0.816	(1.2)	(7.1)
Methyl Cyclohexane	C_7H_{14}	101	265	330	0.774	1.2	6.7
Methyl Cyclohexene	C_7H_{12}	103	(258)		0.804	(1.1)	(7.2)
Decalin	$C_{10}H_{18}$ trans.	185	250	300	0.872	0.7	4.9
Tetralin	$C_{10}H_{12}$ trans.	194	384	405	0.870	0.8	5.0
J.P.-7	$C_{12}H_{27}$	182	--		0.779-0.806	--	--
Shelldyne "H"	$C_{14}H_{18.375}$	260	--	515	1.095	--	--
"H"-M.C.P.D.	C_9H_{16}	206	--	460	0.93	--	--
Hexane	C_6H_{14}	68.5	227	350	0.664	1.2	7.7
4-Vinylcyclohexene	C_8H_{12}	129	269	415	0.834	(1.0)	(7.2)

( ) :parentheses indicates calculated data.

(a) M.A.T.: minimum auto ignition temperature catalyzed by platinum in the continuous flow system.

Other investigators have reported the ignition promoting efficiencies of chemical additives in shock tube(18) studies, in flash photolyzed reactions of gaseous mixtures of hydrocarbons in oxygen or air (19) and in continuous air flow systems having design characteristics similar to subsonic or supersonic combustion ramjets(20).

The chemical additives reported in the literature were divided into two categories. The most widely tested class of chemicals consisted of compounds which produced free radicals upon thermal decomposition over a broad temperature range depending upon the individual compound. The additives that promoted ignitions by rapidly increasing the temperature of the stream via exothermic chemical reactions were combined in the second class of compounds. The most effective type of additives in this class has been reported to be the metal alkyls which are either pyrophoric or toxic and have high heats of combustion.(21)

Table II is a summary of all the homogeneous chemical additives evaluated in either the WSR, the Continuous Flow Facility and the Piloted Supersonic System.

The ignition promoting effects of additives could not be economically determined in every hydrocarbon so a procedure was developed which would indicate the ignition promoting effects of the additives in hydrocarbons as a function of the fuel's molecular structure.

Additive Screening Procedure

Upon completion of the fuel ranking tests in the WSR, it was possible to select the fuel candidates which would most readily be improved by the addition of homogeneous combustion promoters because they already exhibited short ignition delays. Of secondary importance in selecting the base fuels for the additive screening tests were the cost and availability of the fuels. The most attractive fuels were the long-chain n-paraffins such as octane and tetradecane, which although expensive, were available in sufficient quantities to evaluate many different additives. Therefore, using these criteria as a guide, the additives were evaluated in n-octane. Since the mono-olefin, 1-octene, also showed promise as a good fuel, the most interesting additives found from the octane tests were then screened with octene-1. These data obtained with high purity, relatively simple hydrocarbons, provided the basic understanding of additive effects in various molecular structures.

The low density of the pure hydrocarbons reduced the number of practical applications for which they were considered. For this reason dense fuels such as Shelldyne-H, H-MCPD and JP-7, received more attention and were therefore of most interest in terms of the effectiveness of homogeneous additives. The additives most effective in simple hydrocarbons were therefore tested in JP-7, as representative of this family of dense, mixed hydrocarbon fuels. The most promising additives found from the JP-7 tests were then tested in in high density fuels with closed ring molecular structures.

TABLE II

HOMOGENEOUS ADDITIVES TESTED IN THE WSR OR CFS

Compound	B.P. (°C)	Formula
n-Butyl Nitrite	78	$n\text{-}C_4H_9ONO$
t-Butyl Nitrite	63	$t\text{-}C_4H_9ONO$
n-Amyl Nitrite	104	$n\text{-}C_5H_{11}ONO$
i-Amyl Nitrite	99	$i\text{-}C_5H_{11}ONO$
n-Octyl Nitrite	176	$C_8H_{17}ONO$
Methyl Nitrate	65	CH_3ONO_2
Ethyl Nitrate	87.5	$C_2H_5ONO_2$
n-Propyl Nitrate	111	$C_3H_7ONO_2$
n-Butyl Nitrate	123	$C_4H_9ONO_2$
i-Amyl Nitrate	147.5	$C_5H_{11}ONO_2$
Nitroethane	113	$C_2H_5NO_2$
Nitrobenzene	211	$C_6H_5NO_2$
Oxygen	-183	O_2
Carbon Monoxide	-191.5	CO
Nitric Oxide	-151.5	NO
Nitrogen Dioxide	21	NO_2
Nitrous Oxide	-89.5	N_2O
Propylene Oxide	34.5	CH_2CHCH_3O
Ethyl Oxalate	185	$(C_2H_5CO_2)_2$
t-Butyl Peroxide	--	$C_7H_{17}COOH$
t-Butyl Hydroperoxide	--	C_3H_9COOH
Cumene Hydroperoxide	--	$C_8H_{11}COOH$
Hydrogen	-253	H_2
Water	100	H_2O
Hydrazine (98%)	113	N_2H_4
Carbon Disulfide	46	CS_2
Benzaldehyde	180	C_6H_5CHO
Triisobutyl Borane	188	$C_{12}H_{27}B$
1,2-Dimethoxyethane	84	$C_2H_4(OCH_3)_2$
1,2-Bis (2-Methoxyethoxy) Ethane	212	$C_5H_{10}O_2(OCH_3)_2$
2-Ethoxy Ethanol	134	C_4H_9OOH
2-Butoxy Ethanol	174	$C_6H_{13}OOH$
2-(2-Ethoxyethoxy) Ethanol	213	$C_6H_{13}O_2OH$
2-(2-Ethoxyethoxy) Ethyl Acetate	227	$C_6H_{11}O_3O.C_2H_5$

All the additives except N_2H_4 were completely miscible in the fuels tested. Since some of the additives of interest were costly and in short supply it was decided to limit the concentration to five-volume percent in each test fuel. This concentration was arrived at by reviewing the literature and by internal consultation which revealed that if the additives were effecting the ignition-combustion processes, their effects would be evident at this concentration.

SECTION III

APPARATUS DESCRIPTION

A. The Well Stirred Combustor

The well-stirred reactor used during the First Phase of the program has been characterized by many researchers as an adiabatic, homogeneously mixed reactor virtually free of heat and mass transfer limitations[22]. The device more closely conformed to this description in the lean mixture region, the area of interest in this program. The reactions were limited by the chemical kinetics of the particular fuel being evaluated, as opposed to plug flow, or hot surface ignition test techniques where physical phenomena limited the reactions.

The principle of the device shown in Figure 1 was to direct turbulent, premixed jets of fuel and air into a chamber designed to maximize the entrainment of the burning mixture and thus cause sufficient recirculation to establish a uniform concentration and temperature throughout the reactor.

Figure 2 shows how the preheated fuel and air were metered separately through carefully calibrated rotometers and homogeneously mixed prior to being introduced into a 1/2" diameter perforated spherical injector which was situated at the center of a 3-inch hemispherical reactor built of insulating fire-brick. The combustible mixture issued from forty, .020" holes drilled radially in the injector at sonic velocity and kept the burning gases inside the fixed volume of the reactor vigorously stirred at all times. The products of combustion were exhausted through 1/8" diameter holes symmetrically arranged in the wall of the reactor, mixed with a large volume of external air, cooled by water injection and discharged into the atmosphere. The reactor walls were 1.75 inches thick and were made of high temperature fire brick which had an upper service temperature of 3300°F. The thermal conductivity of the brick at temperatures of 800 to 2000°F was 3.33 and 4.69 BTU/ft^2/hr/°F/in. respectively. The majority of the brick material was Al_2O_3 with 22 percent SiO_2. The outer shell of the reactor was made of stainless steel and was equipped with mounting brackets and various parts to facilitate mounting. Previously it was determined with an injector sphere only 1/2 inch in diameter, attaching 1/4" feed lines to it seriously upset the symmetry of the jet pattern. The use of a hemispherical reactor overcame this problem. Furthermore, because the injector was half-embedded into the solid upper half of the reactor, the entire injector and more particularly the critical region where the inlet tubing was welded to it, was kept cooler, thus greatly reducing the chances of failure.

To ignite the reactor, propane and air flow rates were set and the hydrogen pilot light was lit. When the test fuel was introduced into the pre-heater section, the hydrogen pilot and propane sources were turned off. Liquid fuels, including mixtures of additives with hydrocarbon fuels, were metered in calibrated rotameters and injected into a stream of nitrogen by means of an atomizing nozzle placed upstream of the pre-heater. A short period of time was allowed to stabilize the flow of test fuel and then the following procedure was initiated to determine the lean-blow-out points.

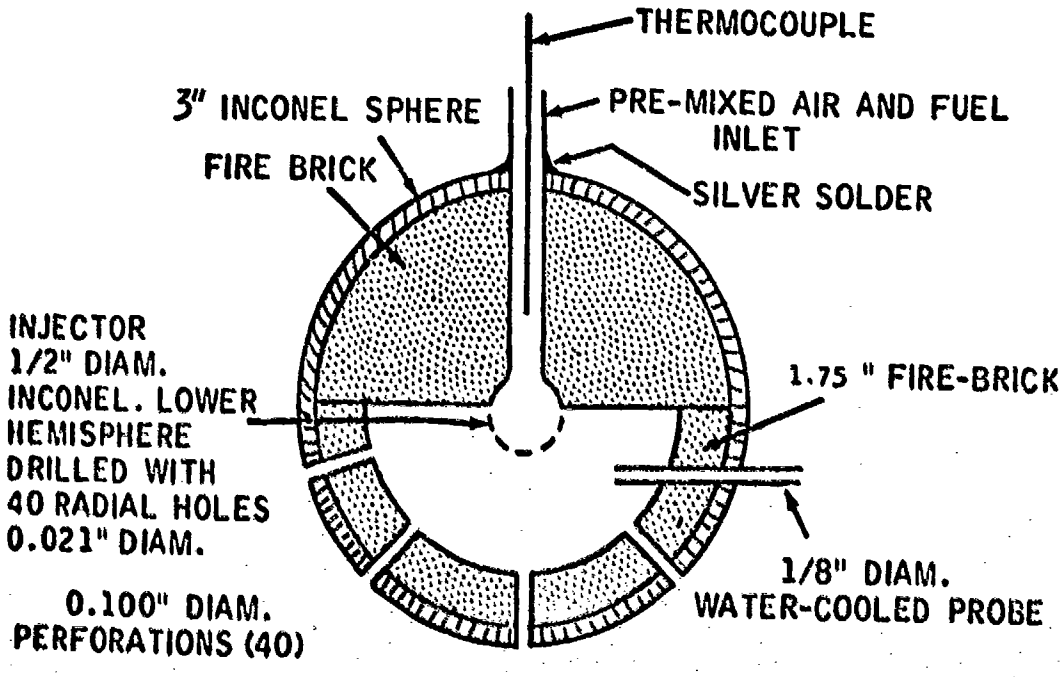

FIGURE 1 HEMISPHERICAL HIGHLY-STIRRED REACTOR

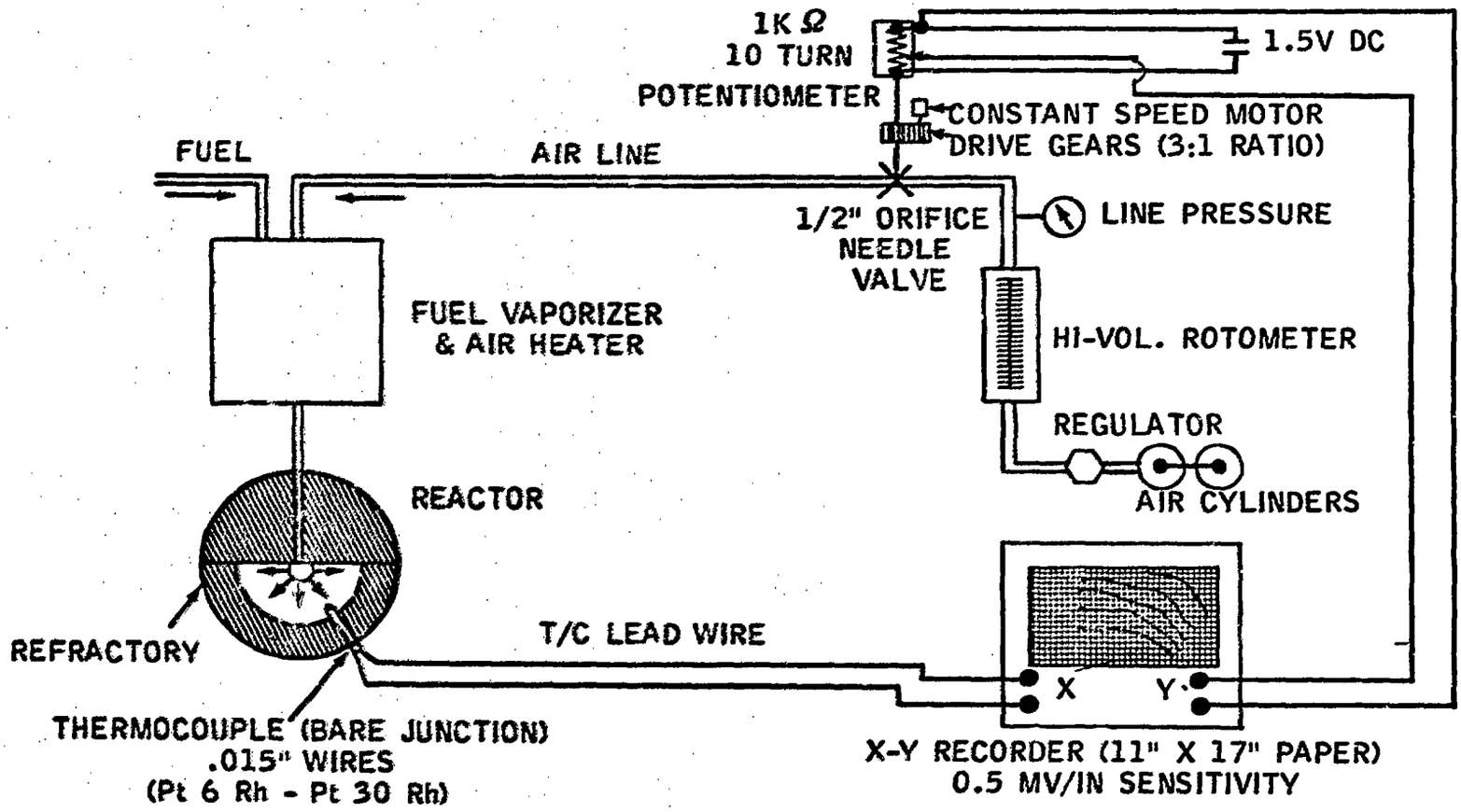

FIGURE 2 WELL-STIRRED-REACTOR INSTRUMENTATION

The procedure consisted of simultaneously recording the combustion temperature and volumetric air flow of the reactor on the X and Y-axis, respectively of a calibrated X-Y plotter. The temperature was measured by an unshielded, bare junction thermocouple housed in a pure alumina insulator which traversed the 1.75" thick firebrick wall of the lower half of the reactor. The thermocouple consisted of either Pt-Pt10Rh or Pt6Rh-Pt30Rh junctions made from wires .015" or .020" in diameter. Previous studies had shown that the temperature inside the reactor is essentiall uniform except for a small volume close to the injector. Positioning of the thermocouple inside the reactor was not critical. The thermocouples were calibrated in an electrically heated furnace, where the temperature was measured by means of a thermocouple secondary standard and an optical pyrometer.

The volumetric air flow was monitored by an in-line rotometer and simultaneously indicated on the Y-axis of the X-Y recorder. The air rotometer was calibrated with a wet-type test meter. The displacement voltage on the Y-axis was derived from a 10-turn linear potentiometer whose shaft was attached to the stem of the main air control needle valve by means of a series of reduction gears. The movement of the valve stem was automatically controlled by a constant speed, high torque, 1 RPM electric motor, which was also attached to the gear-train of the potentiometer shaft. The electro-mechanical system was such that the voltage change indicated by the potentiometer was proportional to the air volume flow rate. The combustion temperature was recorded on the X-axis of the recorder.

This technique for determining the blow-out points proved to be much more accurate and repeatable than the standard method of visually observing the cooling of the reactor's inner walls. The visual observation of a blow-out was especially uncertain at low air flow conditions due to the very slow cooling rate of the reactor's walls.

During a test run, the fuel flow was held constant and the air flow was slowly increased at a constant rate. The reactant flow conditions were such that, at the beginning of a test, the equivalence ratio* (ϕ) was near 1.0. As the air flow was increased, the equivalence ratio slowly decreased to a value between 0.1-0.5 at which point the lean limit was reached and the flame temperature-air flow curve, recorded on the X-Y recorder, suddenly changed slope due to the rapid quenching of the reaction. The "knee" of the curve graphically depicted the temperature and volumetric air flow at the blow-out point whose equivalence ratio was readily calculated. To change the total temperature of the system, it was necessary to increase the fuel and air flows to overcome the heat losses. It was therefore possible to vary the blow-out temperatures over a range of about 1400-1600°K while maintaining the equivalence ratio between 0.1 and 0.5.

---

* Equivalence ratio = $\frac{\text{F/A (Actual)}}{\text{F/A (Stoich.)}}$

As discussed by Longwell and Weiss:[2] to account for blowouts qualitatively, consider combustion to be a chemical reaction between fuel and oxygen whose rate depends on temperature and fuel and oxygen concentrations. For combustion approaching completion--that is, after a relatively long combustion time--the temperature is near a maximum, thus favoring a rapid reaction. However, the reactants have largely been consumed and their concentrations are small, thus favoring a slow reaction. If less time is allowed, the reaction will not have proceeded so far toward completion. The temperature will be lower but, more important, the reactant concentrations will be higher; the net result will be a faster overall rate. As reaction time is still further reduced, the increase of reactant concentrations continues to more than offset temperature decrease and the overall reaction rate still increases. However, a point is eventually reached such than an additional reduction in reaction time causes a temperature lowering with greater effect than the corresponding concentration increase. This point represents the shortest possible reaction time and the fastest reaction rate. Further reduction in reaction time makes continued reaction impossible; the reaction thus stops and in effect, the flame has blown out.

Longwell and Weiss showed that such a device, with sufficiently small mass transfer resistance, the determination of the composition of the burning mixture coupled with a knowledge of input conditions, temperature, pressure and blow-out data, allowed the determination of the global kinetics of lean mixtures via the following:

$$\frac{N}{V P^n} = \frac{4.76k}{R^n} \frac{e^{-E/RT}}{T^{n-1/2}} \frac{[2\phi(1-\varepsilon)]^{n-f} [1-\phi\varepsilon]^{n-f}}{\phi [4.76+\phi(1.36-\varepsilon)]^n}$$

Where N = air rate, g. moles/sec

V = reaction volume, liters

P = pressure, atm

n = overall reaction order

k = rate constant, $e^{n-1}/(°K)^{1/2}(g.\ moles)^{n-1}(sec)$

E = activation energy, cal/mole

R = gas constant, cal/(g. mole) (°K)

T = reaction temperature, °K @ blow-out

ϕ = equivalence ratio @ blow-out

ε = available oxygen

f = combustible concentration exponent

Lean blow-out data for a wide variety of fuel structures[23] has shown that the pressure exponent adapted to best fit the data was 1.8.

It was clear that the blow-out measurements carried out under controlled conditions in the well-stirred reactor can yield residence time or "quasi-ignition delay time" values, at some equivalence ratio ϕ, when the value, $N/V^{1.8}$ was known. Since all of the data reported here were obtained at one atmosphere pressure, the ratio V/N is a measure of the average time the combustible mixture spends in the combustor for ignition to occur. The average "residence time" τ at blow-out conditions was obtained from the relation:

$$\tau = 273\ V_R/T_F V_{air}$$

where		Typical Values
τ =	average gas residence time (sec)	$0.8 - 5.0 \times 10^{-3}$
V_R =	hemispherical reactor vol. (liters)	.014 - .015
V_{air} =	air flow (liters/sec.) at N.T.P.	.50 - 3.85
T_F =	flame temperature at blow-out (°K)	1390 - 1650

In the equation which describes the average residence time, the total volume of reactants is taken as the air flow (V_{air}) since the fuel flow rates are approximately 50 times less for lean mixtures.

B. Continuous Flow Autoignition Test System (CFS)

The high temperature, continuous flow ignition test apparatus shown in Figures 3 and 4 was designed so that the autoignition characteristics of a wide variety of fuels and additives could be studied at one atmosphere under a variety of experimental conditions such as air temperature, mixture ratio, additive concentration, etc.

Concentric injection of vaporized fuels into the hot air stream via a multi-hole, flat face injector shown in Figure 5 was chosen over other fuel injection techniques for the following reasons:

(1) minimum test section wall effects
(2) better fuel-air mixing at subsonic air velocities but high Reynolds Number
(3) ease of analytical treatment of results
(4) fuel vapor injection

Also of importance was the physical state of the fuel in the hot air/fuel injector mixing region. The liquid fuels were vaporized in a flow-through heater having a large surface area heat transfer medium. Vaporization of the fuel in this system prevented or greatly reduced the thermal-cracking of the fuel which could occur in a batch-type vaporizer where the light hydrocarbons would be separated from the heavier portion. A constant flow of nitrogen through the vaporizer prevented oxidation and assured constant flow.

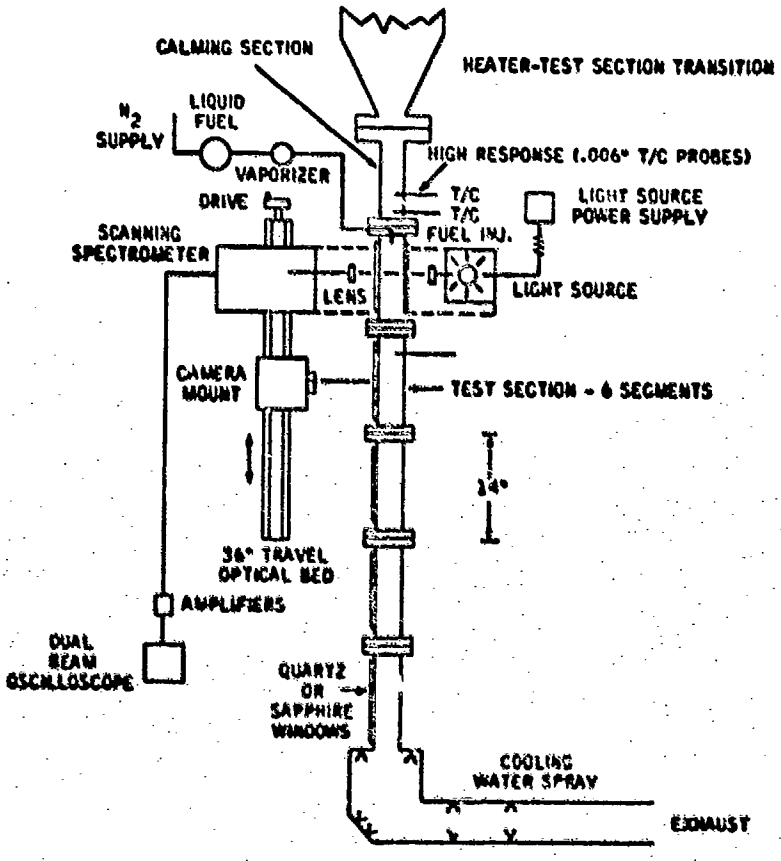

FIGURE 3 SCHEMATIC DIAGRAM OF THE CFS

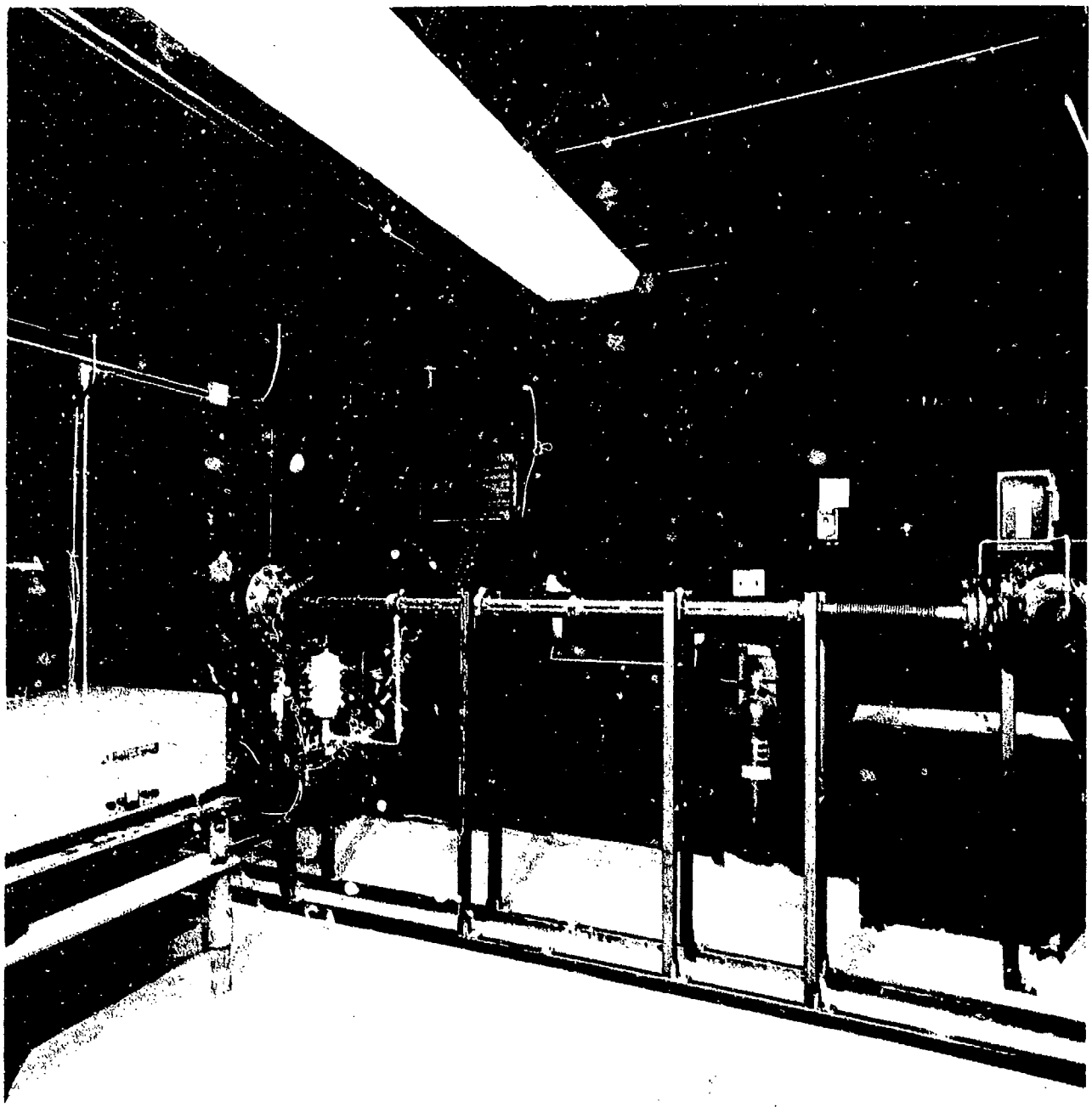

Photo (69-4822)

FIGURE 4. PHOTOGRAPH OF THE CFS

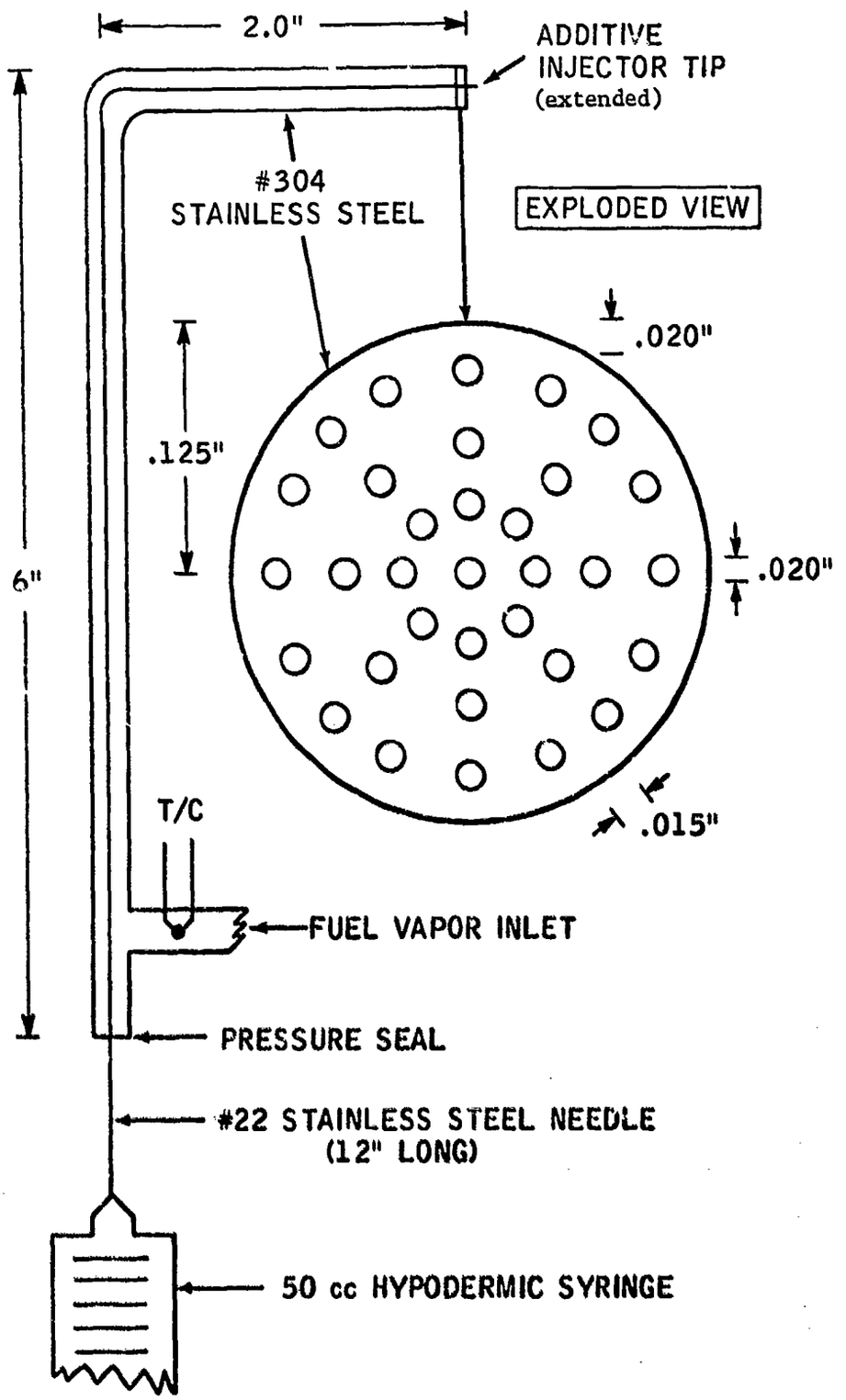

FIGURE 5 FUEL-ADDITIVE INJECTOR

The 1.065 inch-internal diameter test section was thermally insulated and was made of type 304 stainless steel and equipped with one quarter-inch thick quartz windows along the entire length of 75 inches. The test section was composed of 5, fifteen inch-long flanged segments bolted together. This feature allowed flexibility of the test section length. Inconel shielded thermocouples were mounted in the walls of the test section at fifteen-inch intervals. The tips of the thermocouples penetrated into the air stream by one-sixteenth-inch thereby reducing the perturbation to the flow and yet provided reasonably reliable internal wall temperature. The air temperature measured on the centerline of the flow, two test-section diameters upstream (2-inches) of the fuel injector was reported as the inlet air temperature. The ignition delay time was computed from the air flow rate, which was accurately measured in a calibrated rotometer, the inlet air temperature and the observed distance between the exit plane of the fuel injector and the stationary flame front. The average equivalence ratio was calculated from the known total air flow and fuel flow rates.

The liquid fuel system consisted of a 1.5 liter stainless steel cylinder which was pressurized with dry nitrogen in order to feed the fuel, at a controlled rate, through a calibrated rotameter into the fuel vaporizer. A series of solenoid valves were programmed via electronic time-delay-relays so that the liquid fuel flow was pulsed at 20-30 second periods with a much longer time between fuel pulses. The minimum fuel flow time was dictated by the volume of the fuel vaporizer which was filled with one eight-inch diameter stainless steel balls and the time required for the liquid fuel to flow from the control valve to the vaproizer. The continuous nitrogen flow through the vaporizer during the fuel flow constantly purged the bed of any fuel which remained from the previous fuel pulse. Thus, the uniformity of the fuel composition from one pulse to another was assured.

The air used in the test facility was obtained from a 150 CFM compressor which pressurized a 3000 ft^3 sphere to 100 psig. This large volume reservoir provided an abundant supply of clean, dry air for the two propane-air fired pebble-bed burners. The pebble-bed consisted of a fourteen-foot long, 18-inch O.D. pipe which was internally lined with a monolithic high temperature refractory insulator. The bed was comprised of one-inch and one-half inch diameter pure alumina balls which were randomly packed and retained in place at either end by inconel grids. The total heat transfer surface area of the bed was about 800 ft^2. Approximately 1000 pounds of alumina balls were used.

The bed was heated by two propane-air burners which were designed and fabricated especially for this system. The burners, which operated at flame temperatures of about 3000°F, were mounted at either end of the bed and each burner had a capacity of about 250,000 BTU/hr. The normal heat-up procedure called for the firing of the primary burner for about 3-4 hours which heated the bed to about 2300°F. The primary burner was then shut-off and the secondary burner, which was located downstream of the bed, was fired-up. This burner heated the pebble-bed transition section which coupled the air heater to the autoignition test section. Since all of the exhaust gases from both burners exited through the test section, it was simultaneously heated.

When the test section temperature reached a pre-determined level, the secondary burner was shut off and the combustion air diverted through the inlet of the pebble bed. Because the test section was not externally heated there was a natural cooling curve associated with its radiative and conductive losses. This cooling rate determined the time interval before the pebble-bed and test section must be reheated to the initial high temperature conditions. Normally, the actual time available for the autoignition tests was about 2 hours when the air temperature decreased to 800°K.

A schematic drawing and photograph of the experimental facility are shown in Figures 6 and 7 respectively.

Experimental Procedures in THE-CFS

The autoignition delay times at one atmosphere pressure were measured by visually observing the location of the stationary flame-front with respect to the location of the fuel injector. In the majority of cases the flame front, once established, remained stationary, but occasionally its location fluctuated by 10-15%. Observation of the ignition reaction was accomplished through a number of one-quarter-inch high quartz viewing windows. Typical air velocities in the test section were varied up to 1000 ft/sec. over a temperature range of 850-1250°K.

The prevaporized fuel--nitrogen mixture--was concentrically injected, for time intervals of 15-20 seconds, into the continuously-flowing air stream through a shower-head injector designed to assure critical fuel flow (Figure 5). Although Figure 5 shows the end of the hypodermic needle as being outside the tip of the fuel injector, it was found in subsequent tests that similar ignition characteristics were obtained when the needle tip was inside the fuel injection. Occasionally the small holes of the injector were plugged with carbon due to the pyrolysis of the fuels. However, the injector was easily cleared by injecting water into the injector while it was hot. The overall equivalence ratio was maintained between .01 and 0.3 since it was found that autoignition of richer mixtures were erratic and sometimes violent.

The liquid additive candidates were injected by an electrically driven 50 cc. glass hypodermic syringe and fine needle arrangement into the fuel injector before mixing with the heated air. The residence time of the fuel-additive mixture in the injector was 2-3 milliseconds. This was sufficiently long for thorough mixing of the fuel vapors and the additive to occur. This arrangement ensured that the effluent combustible stream was truly representative of a bulk fuel blend. The average mixture temperature was generally the boiling temperature of the fuel.

After the preliminary additive screening was completed via syringe injection, the most promising compounds were blended with the fuels in various concentrations. Blends of the neat fuel with various additives in concentrations up to 50 volume percent were prepared and successfully tested. When ignition of the mixture occured, the distance between the tip of the fuel injector and the flame front was measured by means of a scale permanently mounted on the test section.

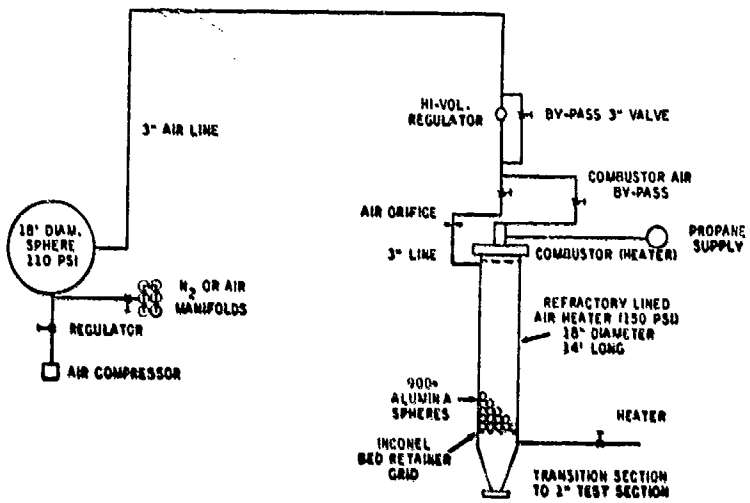

FIGURE 6. SCHEMATIC DIAGRAM OF AIR SUPPLY

FIGURE 7. PEBBLE BED AIR HEATER

Gaseous ignition promoting candidates such as NO, NO_2, N_2O, CO, H_2, and O_2 were injected into the vaporized fuel-nitrogen mixture through a calibrated orifice which was located 4 inches upstream from the tip of the fuel injector. This distance translated to an average residence time of about 3 milliseconds at the flow conditions. Candidate additives such as H_2, CO, NO, N_2O and O_2 were easily handled by conventional metering techniques. However, a separate control and metering system was used for nitrogen dioxide because of its physical and chemical properties such as high vapor pressure, high density, strongly oxidizing and corrosive nature. The NO_2 was metered as an equilibrium mixture of N_2O_4 and NO_2 @ 70°F through a calibrated pyrex rotometer fitted with teflon pressure seals throughout. The N_2O_4 was 99.5% purity and was procured from the Matheson Company. The shipping container was equipped with a full length eductor tube which allowed the cylinder to be pressured with gaseous nitrogen. A constant nitrogen pressure was maintained over the liquid N_2O_4 expelled the liquid through a stainless steel line to the pyrex rotometer tube. The liquid flow was controlled by a set of fine metering valves. One of the valve bodies contain a short length of a #22 hypodermic needle (.013 inch O.D.) which served as the critical pressure metering element in the flow system.

C. The Platinum Catalyzed Autoignition Test System (PCS)

The experimental arrangement illustrated in Figure 8 was utilized to determine the hydrocarbon autoignition promoting characteristics of a noble metal surface over the temperature range of 500-1150°K. The .008-inch thick platinum metal tube was six-inches long and had a one-inch bore diameter. The tube was inserted into the 1.065-inch diameter test section such that the leading edge (edge nearest fuel injector) of the catalytic device was 10 inches downstream of the concentrically positioned fuel injector. The platinum tube was held in position by a thin metal shim which was .020" thick x .5" long and located in the narrow annulus between the platinum liner and inner test section wall. The stainless steel test section which was the first of the five segments of the 75 inch long device previously described in Section IIIB, was attached directly to the heated-air source. The exit of the short test section was open to the atmosphere so that the products of the hydrocarbon--air reactions were exhausted into a 6-inch diameter steel duct. The entrance to the exhaust duct was 8-inches downstream of the test section exit. The location of the platinum tube within the test section was arranged in such a manner as to allow observation of the thermal history by color change, of the catalyst through the quartz windows which were located along the length of the test device. The test section was well instulated. An inconel sheathed, chromel-alumel thermocouple located 2 inches upstream of the fuel injector, on the axis of the duct, was utilized as the source of air inlet temperature data. The thermocouple's output was recorded on a dual channel, variable speed potentiometric recorder having a 10-inch span. The temperature resolution was 2.5 degrees centigrade with an accuracy of 0.25% of full scale.

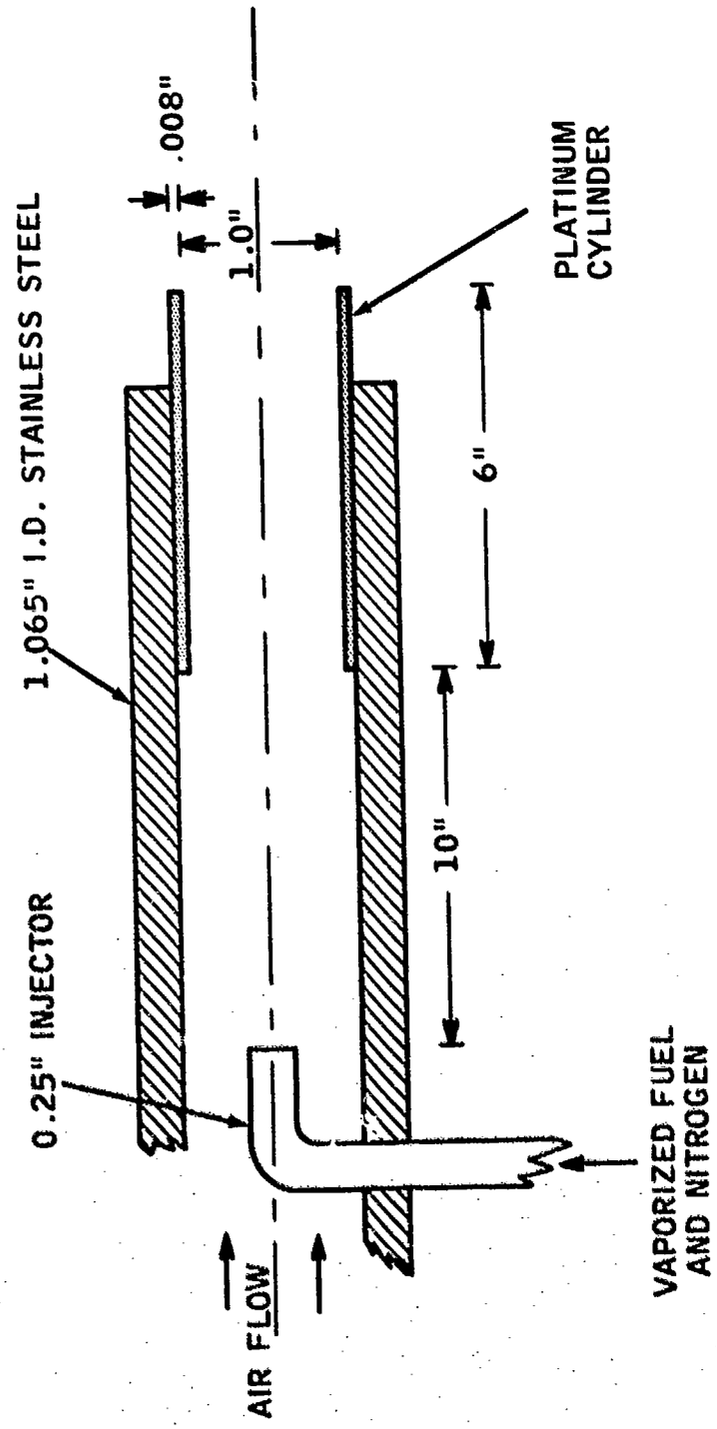

FIGURE 8. SCHEMATIC DIAGRAM OF AUTOIGNITION TEST DEVICE UTILIZING A PLATINUM LINER

The fuels tested in this device were all liquids at room temperature and their flow rates were accurately determined by a calibrated rotometer. The entire fuel system was exactly the same as described in Section IIIB.

The experimental procedure consisted of observing the equivalence ratio (ϕ) at which autoignition of the fuel occurred as a function of temperature over the range of 500-1150°K. The air stream velocity was calculated from the measured flow rate and temperature through the duct. The maximum velocity occuring at the highest temperature was about 150 feet per second. The corresponding ignition delay times were proportional to the flow velocity and varied from 5 to 10 milliseconds. Ignition was defined by the establishment of a flame front within the test duct. Although "cool" flames, characterized by their light blue appearance, were observed for all of the fuels tested, their appearance was not considered as an ignition-point.

The effect of n-propyl nitrate addition in a 15 volume percent concentration mixture with ten different hydrocarbon fuels was also evaluated in the catalytic test apparatus. The equivalence ratios of the fuel blends were corrected for the presence of the n-propyl nitrate. The liquid fuel rotometer was recalibrated for each fuel-additive blend because of the large increase in the liquid mass flow due to the improvement of the fuel viscosity by n-propyl nitrate. An example of this improvement was that Shelldyne-H, had a viscosity of nearly 13.5 cs at 100°F and with 15% addition of n-propyl nitrate the viscosity was reduced to 4.8 cs. Table III is a summary of the viscosity improvement characteristics of n-propyl nitrate in Shelldyne-H as a function of additive loading and bulk liquid feed temperature.

TABLE III

PHYSICAL AND COMBUSTION CHARACTERISTICS OF SHELLDYNE-H BLENDS WITH n-PROPYLNITRATE[a]

	Neat Shelldyne-H	Weight Percent -($C_3H_7ONO_2$)					
		5	10	15	20	25	100
$-\Delta H_c$							
BTU/gallon	160,700	157,400	153,600	149,200	143,000	138,000	71,500
BTU/pound	17,860	17,520	17,100	16,630	16,000	15,600	8,100
τ @ 1000°K (millisec.)	180	17	8	5.2	4.5	3.5	2.5
	Ignition delays measured in Continuous Flow System ($\phi < .3$)						
Viscosity (C.S.) @ °F							
100	13.47	9.07	6.34	4.8	3.75	3.0	0.74
0	214.7	93.5	52.8	32.4	21.8	15.2	1.20
-30	1037.0	333.1	160.8	89.3	55.1	32.2	1.60
-65	14097.0	3040.0	1087.0	503.0	--	--	
Boiling Temp. (°F)	506	228	226	226	228	227	222
Flash Point (°F)	240	102	88	84	82	80	74
Freezing Temp. (°F)	-80	-82	-84	-71	-63	-60	-100

(a) The information given in this table was generated at the AF Aerospace Fuels Lab. employing standard test procedures.

SECTION IV

RESULTS

A. Fuel Ranking Under WSR Conditions

The residence times or "pseudo ignition delay" times (τ) measured at lean-blow out points in the Well-Stirred Reactor for all of the hydrocarbons tested were correlated to the combustion temperature by the simple Arrhenius relationship

$$\tau = A\ (e^{E_a/RT})$$

where A is a constant, E_a is the "overall" activation energy of the reaction, R is Universal Gas Constant and T was the absolute combustion temperature measured at the point of blow-out. The residence time, τ was measured in milliseconds. "Best-fit" curves were drawn through the experimental points for the sake of clarity. This method of ranking the chemical activity of hydrocarbons is at best only qualitative, therefore any implications which can be drawn from the apparent change of the global activation energy was considered to be superfluous within the bounds of this study.

Normal Paraffins

The Arrhenius plots of the n-paraffins, methane, ethane, propane, butane, hexane, octane and tetradecane are compared in Figure 9. Propane, because of its well documented chemical kinetic behavior via other experimental techniques was the reference fuel. In the temperature range of 1400-1600°K, the residence times of all the alkanes were nearly alike and varied from 0.6 to 3 milliseconds. The global activation energies calculated from the slope of the curves varied from 18 to 28 Kcal/mole. Butane, for some anomalus reason behaved differently compared to the other members of the alkane family.

Generally, the average residence time of the normal paraffins measured for lean mixtures in the temperature range of 1400-1600°K decreased as the length of the chain increased.

Branched Paraffins

Figure 10 compares the residence times of 2-methylpentane (C_6H_{14}) and 2,4-dimethyl pentane (C_7H_{16}). Compared to the base case--propane--their "residence" times were longer over the temperature range of 1400-1600°K. Apparently the presence of the methyl group on the straight chain had the effect of foreshortening the length of the chain, thus making the molecule more resistant to chemical attack. At 1500°K, the value of τ for the C_6 and C_7 branched paraffins compared to the C_6 normal paraffin hexane, was 2.5 and 2.9 milliseconds respectively. Hexane had a value of τ of 2.2 milliseconds. The slopes of the curves of the branched paraffins were greater indicating that their activator energy was greater than the straight chain hydrocarbons.

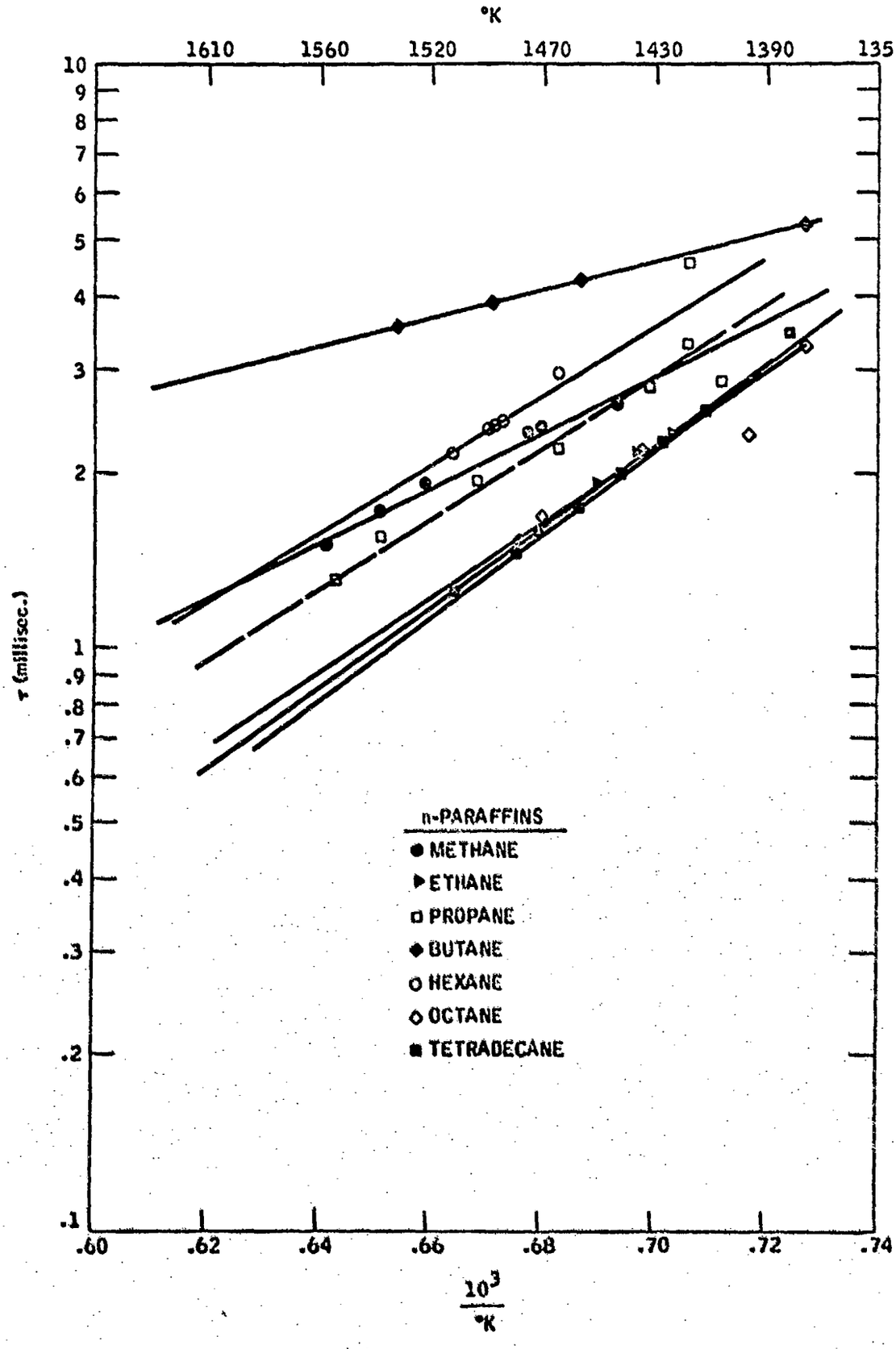

Figure 9 RESIDENCE TIME OF n-PARAFFINS

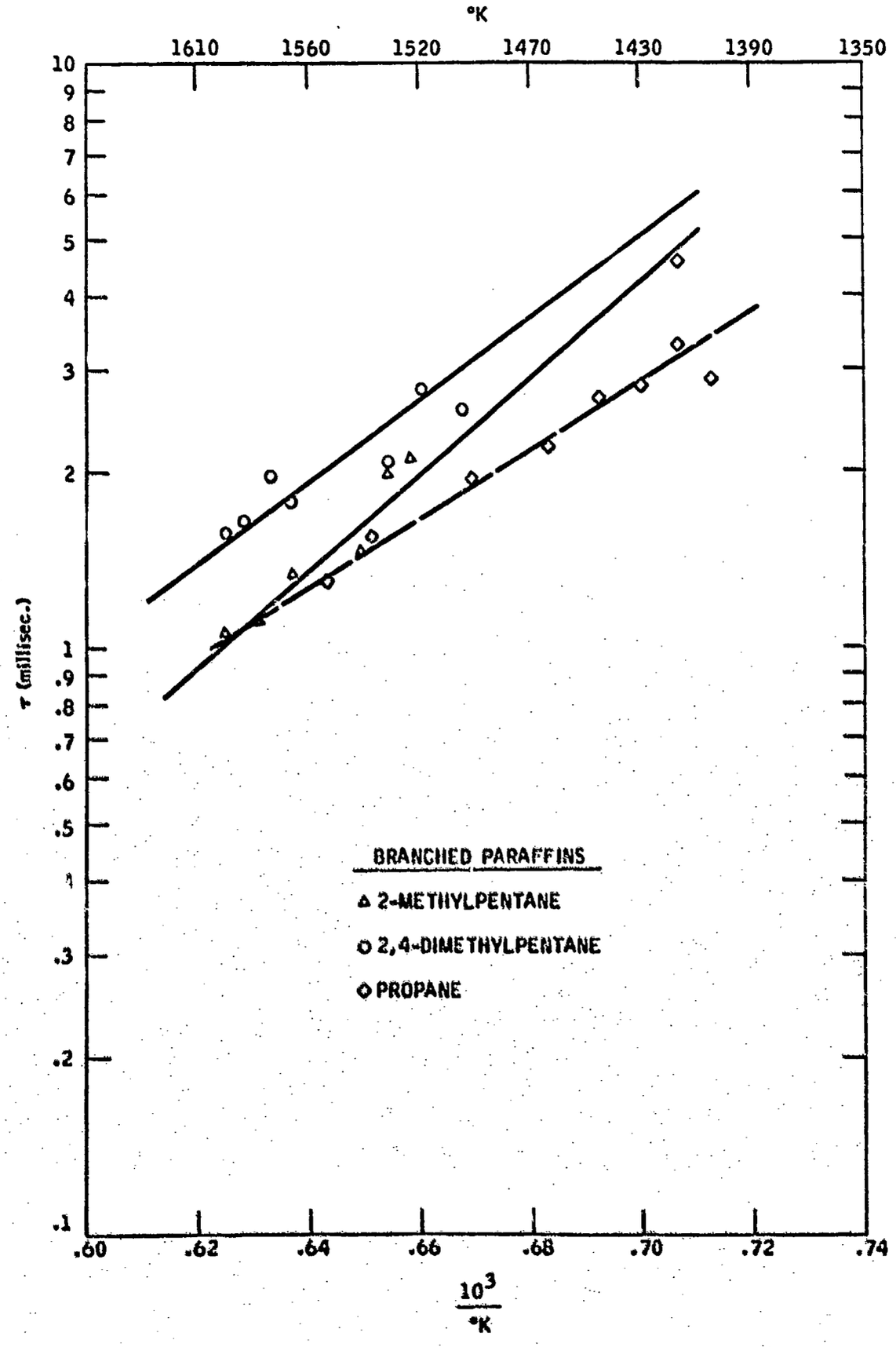

Figure 10 RESIDENCE TIME OF BRANCHED PARAFFINS

Cyclic Compounds

Generally, the hydrocarbons belonging to this family were observed to exhibit longer residence times compared to the base-fuel, propane. The computed activation energies for benzene, cyclohexane, methylcyclohexane and decalin (decahydronapthalene-trans) shown in Figure 11, were slightly greater than the energies calculated for the normal and branched paraffins. Benzene had the longest residence time compared to decalin which was observed to have the shortest τ. For any C_6 hydrocarbon tested, benzene had the longest residence time.

Olefins and Acetylenes

Figure 12 contains the "ignition-delay" data for a mono-olefin, a diolefin and an acetylenic hydrocarbon. The rather steep slope of the curve for 1-hexyne, the acetylenic fuel, [illegible]s immediate attention. Because the activation energy, computed from this curve, is so much in variance with the other fuels tested, no general remarks may be made concerning the relative ranking of the acetylenic hydrocarbons. However, referring to Figure 14 which is a composite comparison of the ignition delays of all the fuels tested at 1500°K, it appears that hexyne-1 has the shortest "ignition-delay" of all the 6-carbon molecule compounds at 1500°K.

The mono-olefin, octene-1, has similar ignition characteristics to the long chain paraffin octane. Apparently, the length of the straight chain is more important than the presence of the single double bond.

The diolefin, 2 methyl, 1,3 butadiene, is less reactive than the long-chain mono-olefin or the base case, propane, over the same temperature range. The presence of two double bonds in this molecule lengthens the "ignition-delay".

Mixed Fuels

Figure 13 compares the "ignition-delays" obtained for the mixed fuels; JP-7, Shelldyne-H and the hydrogenated dimer of methyl-cyclopentadiene (MCPD-H). Because of the high viscosity of Shelldyne-H and MCPD-H, compared to the light hydrocarbons, it was difficult to obtain the maximum fuel flow rate through the atomizing orifice which was located in the fuel vaporizer section of the WSR system. The high density and viscosity of Shelldyne-H would have required higher fuel tank expulsion pressures and alteration of the size of the vaporizer atomizing element in the WSR system, both of which were difficult to achieve. Because of the scatter in the data, the activation energies obtained from the ignition delay data were uncertain. The general behavior of this class of mixed fuels was indicative of the results obtained in the cyclic compounds shown in Figure 11.

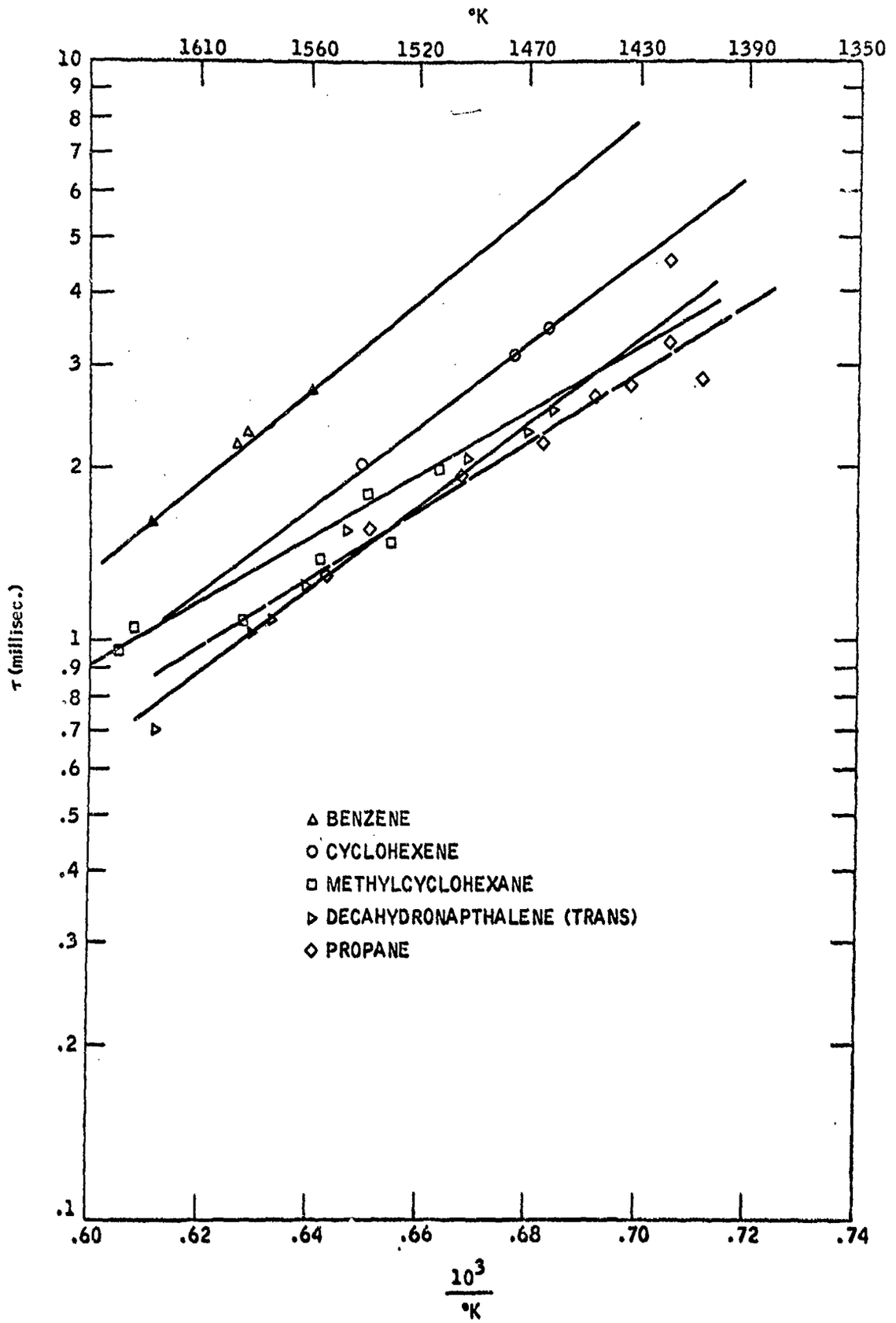

Figure 11 RESIDENCE TIME OF CYCLIC STRUCTURES

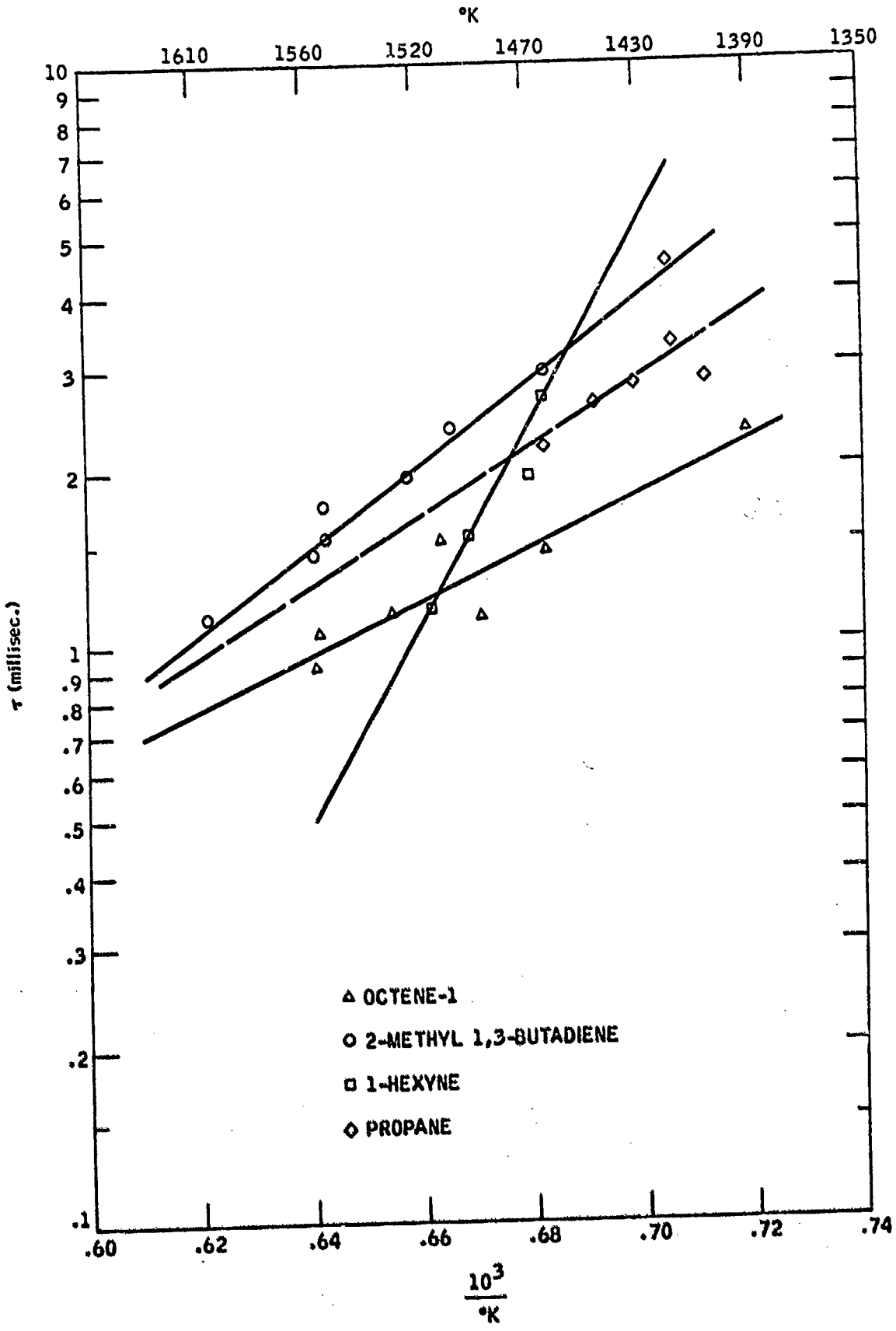

Figure 12 RESIDENCE TIME OF OLEFINS AND ACETYLENES

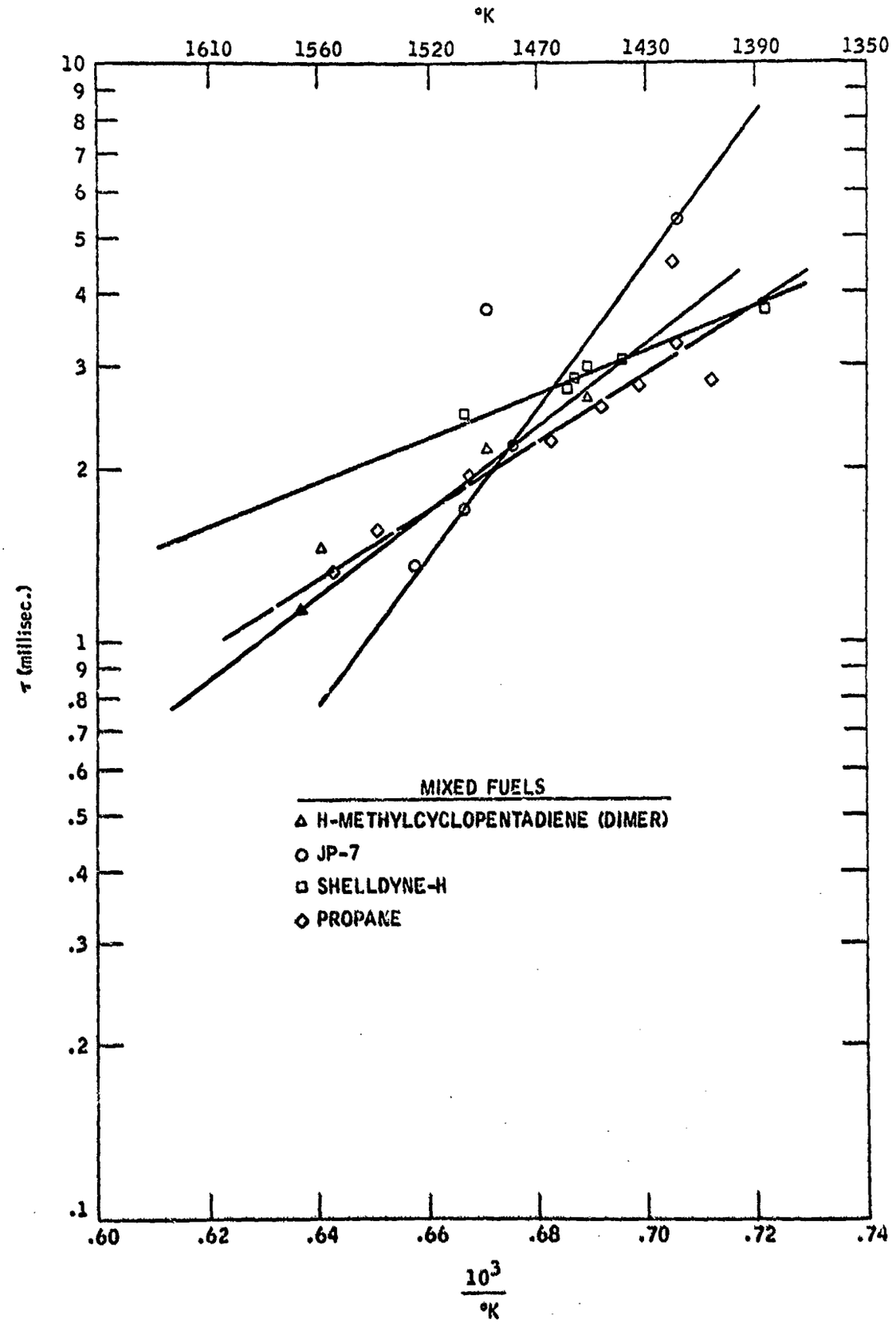

Figure 13 RESIDENCE TIME OF MIXED FUELS

The results of the neat-fuel tests are summarized in Figure 14 where the minimum reference time (τ) is plotted (f) carbon atoms. At 1500°K, the data show that the residence time decreased as the length of the straight chain alkanes increased. The erratic behavior on n-butane cannot be explained, except to say that perhaps the sample contained a large fraction of butane isomers as the remaining data show that the residence time increased as the number of methyl groups increased in branched paraffins.

B. The Effect of Heat Losses on the Equilibrium Combustion Temperature in the WSR

Table IV is a comparison of the measured and analytical combustion temperatures for propane, assuming thermodynamic equilibrium. Although propane was the fuel in this instance, the same trends were observed with the other hydrocarbons. These results show that as the loading factor ($N/VP^{1.8}$) was increased at constant equivalence ratios the measured flame temperatures increased and approached the theoretical value. The equilibrium calculations were performed for initial reactant temperatures of 450°K. The experiments were also conducted at 450°K. Even at the highest loading factor (4.5) there was a large difference between the measured and theoretical flame temperatures. Logically then, it seemed that the heat losses, although lower at large loading values compared to low values of ($N/VP^{1,8}$), were significantly affecting the combustion processes.

Table V is the result of heat loss calculations for the experimental conditions given for propane burning at one-atmosphere pressure. In the equation for spherical conduction, the presence of the exhaust holes were ignored because of their relatively small total area compared to the area of the insulating material. The thermal conductivity of the fire-brick was obtained from the manufacturer and was about .003 calories/sec-cm-°K. The ΔT across the wall thickness (X) of the thermal insulator was determined from thermocouple measurements of the inner and outer surfaces. The inner surface temperature was assumed to be the same as the measured flame temperature. The heat input (Qin) calculated from the known rate of fuel flow and its heat of combustion was compared to the conductive heat losses (Q_L) as a function of ϕ for a fixed loading value of 4.7. The percent heat loss due to thermal conduction through the walls of the reactor was observed to remain relatively constant over the range of ϕ from 0.48 to 1.08. The constantly small average heat loss at the loading value of 4.7 indicates that the large differences in combustion temperatures shown in Table 4 could not be explained by conductive heat losses. It appeared that some other mechanism was responsible for the low combustion temperatures. Longwell[2] also observed that heat losses, even very small heat losses, drastically altered the space heat release rates. He showed that heat losses of 5 and 20% reduced the maximum heat release rate by 30 and 85%, respectively. He also showed, as reported in this study, that these values were not significantly affected by ϕ. The rather small heat losses calculated for the reactor used in our study (3-5%) are responsible for the lower combustion temperatures due to the decreased chemical reaction rates which resulted in lower heat release rates.

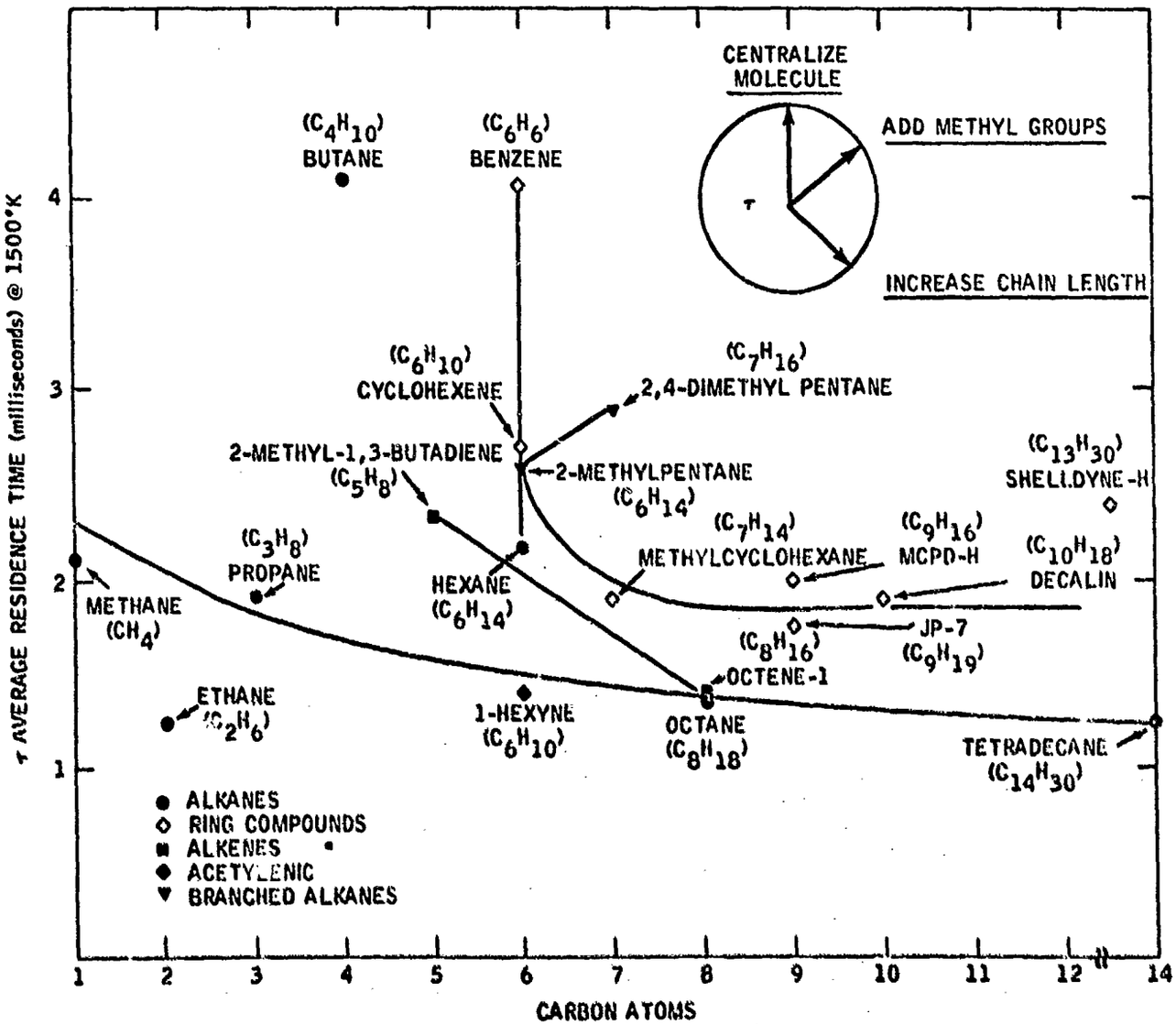

Figure 14 THE INFLUENCE OF MOLECULAR STRUCTURE ON RESIDENCE TIME

TABLE IV

Comparison of Theoretical and Experimental Combustion Temperatures for Propane at 1 ATM in the Well Stirred Reactor

ϕ	0.3	0.5	0.7	0.9	1.0
T_{THEO} (°K) @ 450°K initial state	1217	1637	2000	2273	2346
			$N/VP^{1.8} = 4.5$		
T_{MEAS} (°K) @ 450°K preheated	1250	1540	1760	1890	1940
			$N/VP^{1.8} = 3.5$		
T_{MEAS} (°K) @ 450°K preheat	1240	1530	1740	1870	1900
			$N/VP^{1.8} = 2.5$		
T_{MEAS} (°K) @ 450°K preheat	1100	1390	1610	1730	1750

TABLE V

SPHERICAL SHELL HEAT LOSS
CALCULATIONS FOR PROPANE AT 1 ATM

Initial Conditions: 450°K

$(N/VP^{1.8}) = 4.7$
Air Flow = 88 l/min

(Q_L) Cal./Sec.	ϕ	(Fuel Flow) l/sec.	(Q_L) %	(Qin) KCal/Sec
44.2	1.08	.0675	3.04	1.457
44.6	.95	.0592	3.48	1.280
46.0	.835	.0523	3.92	1.175
38.0	.735	.0458	3.84	0.990
35.2	.615	.0384	4.25	0.827
33.0	.480	.0300	5.08	0.650

C. Effects of Homogeneous
Additives on (τ) in the WSR

Because of the large number of tests required to produce the data points shown in Figures 15 through 20 the reactor volume slowly became enlarged with time. When the volume changed by more than 10 percent it was replaced. In order to take this slow variation of reactor volume into account, the base fuel, without additives, was tested before and after a series of four additive tests. Over that short period of time, the reactor volume remained essentially unchanged. The additive residence time data were normalized with respect to the τ of the neat fuel and plotted as τ (fuel + additive)/τ(Fuel) over the 1400-1600°K temperature range.

The complexity of the oxidation reactions of hydrocarbons and the effect of free radicals or other intermediate species on the total oxidation process, precluded any quantitative interpretation of the role of the additive on "ignition delay". It appeared, however, that ease of formation of free radicals upon thermal cracking was an essential prerequisite. An attempt was made to determine the qualitative effects of various classes of additives on different fuel structures. Because oxidation processes proceed in different manners in long-chain, branched molecules and cyclic structures, the response of these fuels to additives were expected to vary.

Normal Paraffins (n-Octane)

The varying effects of different classes of homogeneous additives in n-octane are plotted in Figures 15, 16 and 17 over the temperature range of 1400-1600°K. The additives found to be generally most effective in reducing τ were those compounds containing $-CH_2-CH_2-$groups such as tert-butyl hydroperoxide, cumene hydroperoxide, 2-butoxy ethanol, etc. This class of compounds was observed to decrease τ at low temperatures while promoting an increase in the residence time at higher temperatures. The other additives tested in n-octane included 4 nitro compounds, nitrate and nitrite esters and an epoxide, propylene oxide. Generally, these classes of compounds were less effective in reducing τ over the temperature range of interest °K, with the exception of n-butyl nitrite which in a 5 volume percent concentration reduced the residence time by nearly 70% at the lowest temperature, 1400°K.

Olefins (Octene-1)

The additives found to be effective in reducing τ in the straight chain mono-olefin, octene-1, were in general also observed to reduce τ in the n-octane system. However, the effect of the nitro paraffins, and nitrate or nitrite esters were much more pronounced as shown in Figures 18 and 19, in the olefin compared to the alkane. Of the nine different additives tested in octene-1 the only compound which proved to be relatively ineffective in reducing τ was ethyl nitrate. All of the additives, however, decreased τ at low combustion temperatures, by as much as 80%, and had an inhibiting effect at temperatures above 1550°K. These data seem to indicate that the presence of the double bond in the straight chain increases the effectiveness of the homogeneous additives in reducing τ.

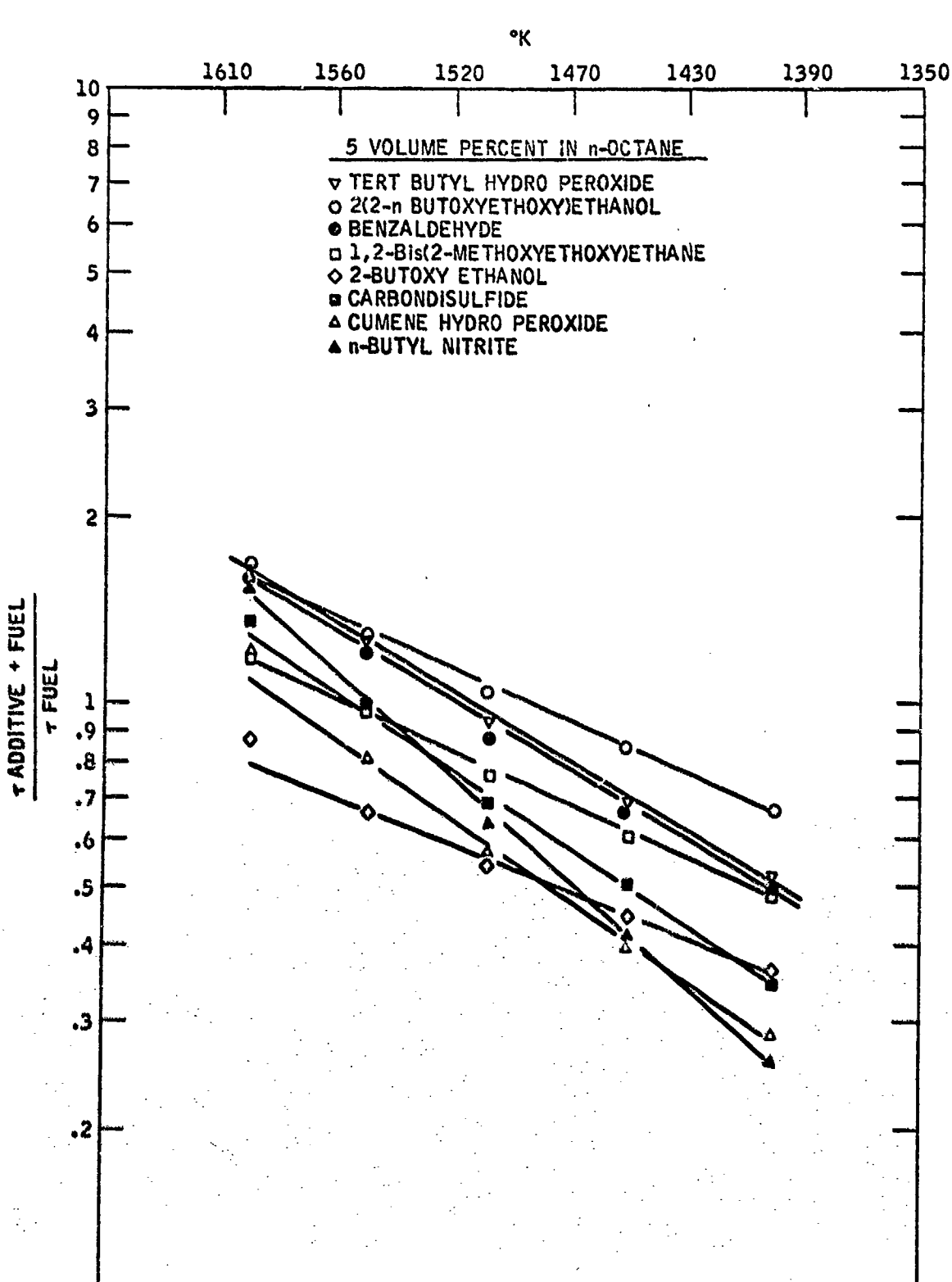

Figure 15 EFFECTIVENESS OF ADDITIVES IN n-PARAFFINS

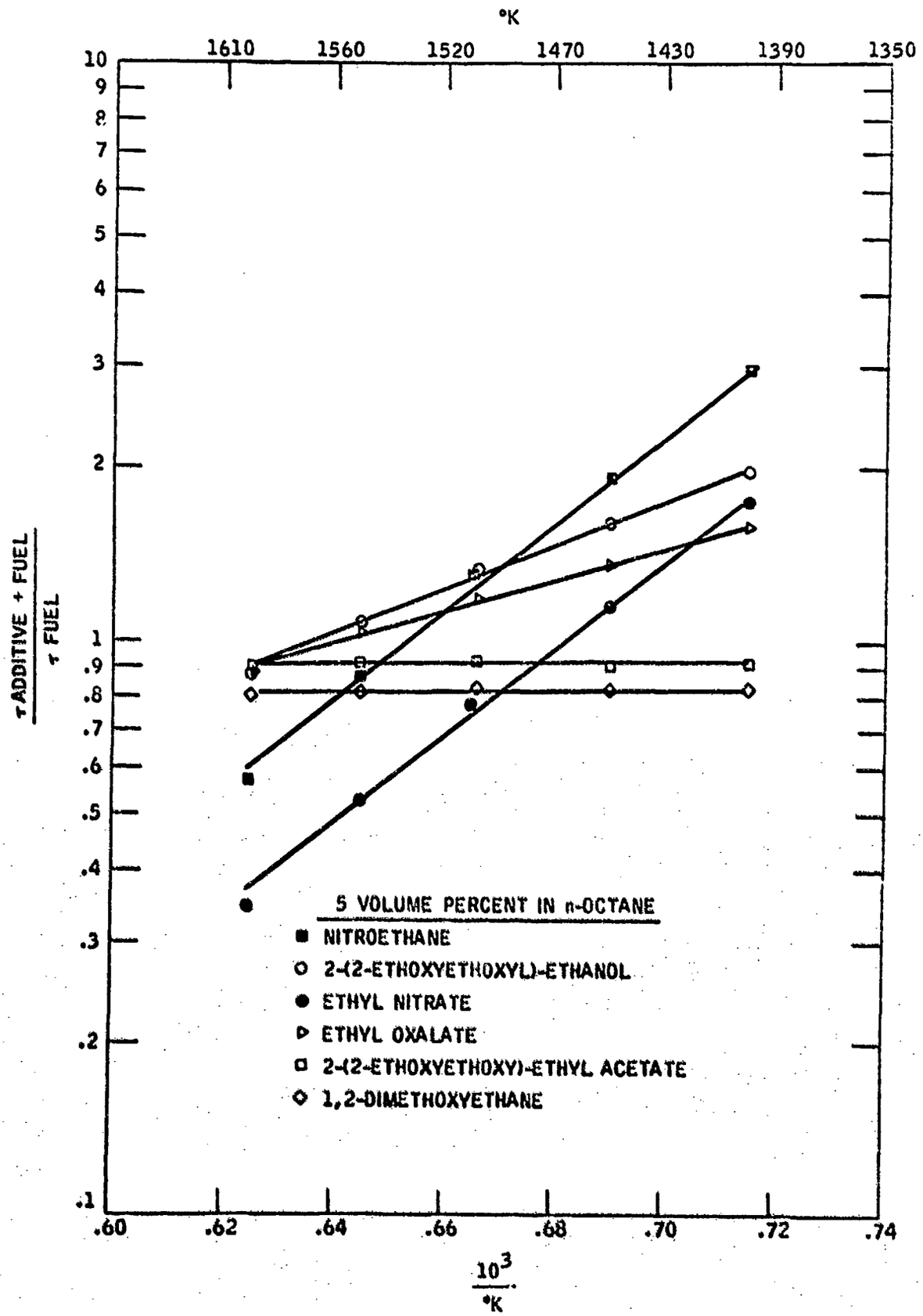

Figure 16 EFFECTIVENESS OF ADDITIVES IN n-PARAFFIN

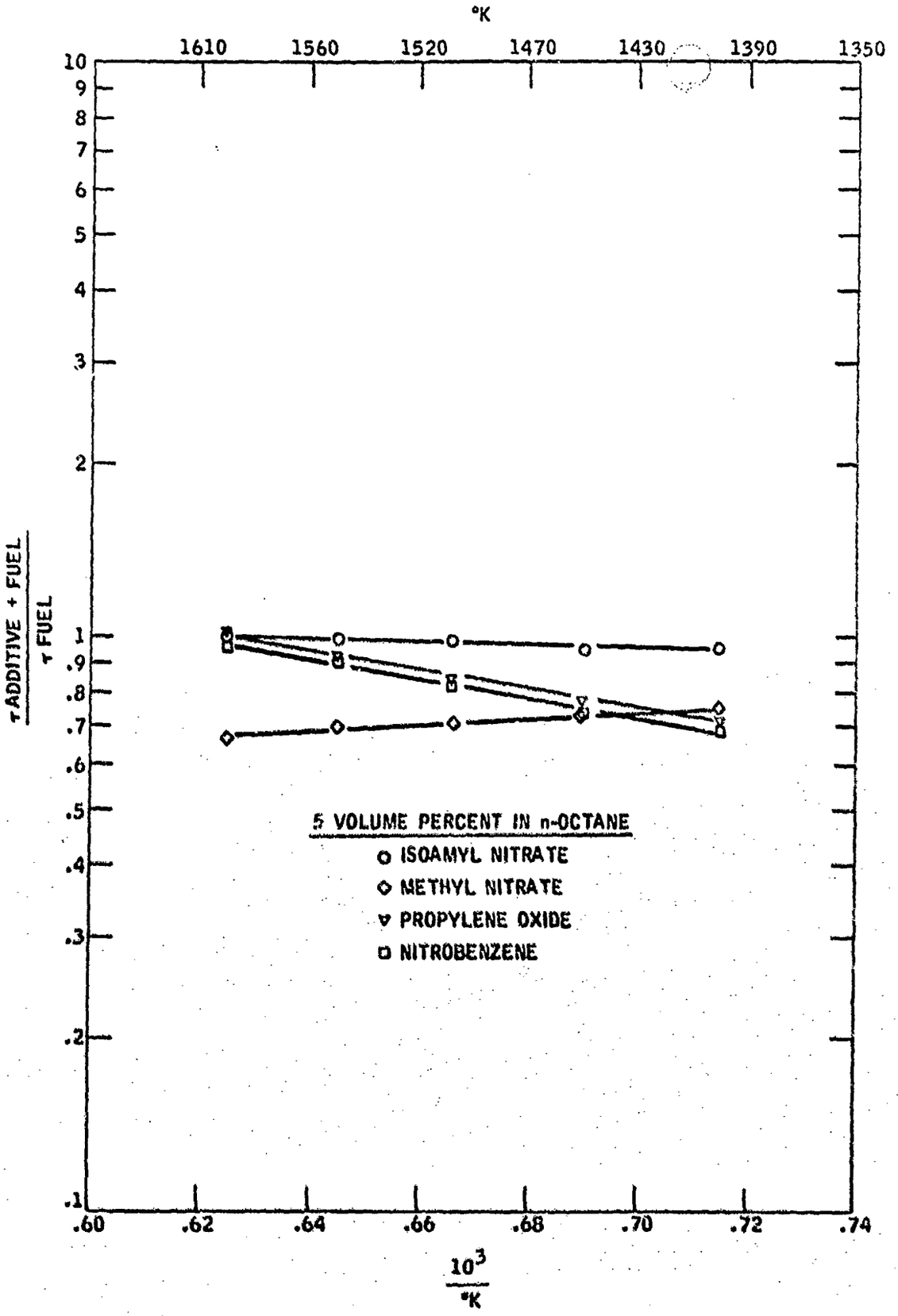

Figure 17 EFFECTIVENESS OF ADDITIVES IN n-PARAFFINS

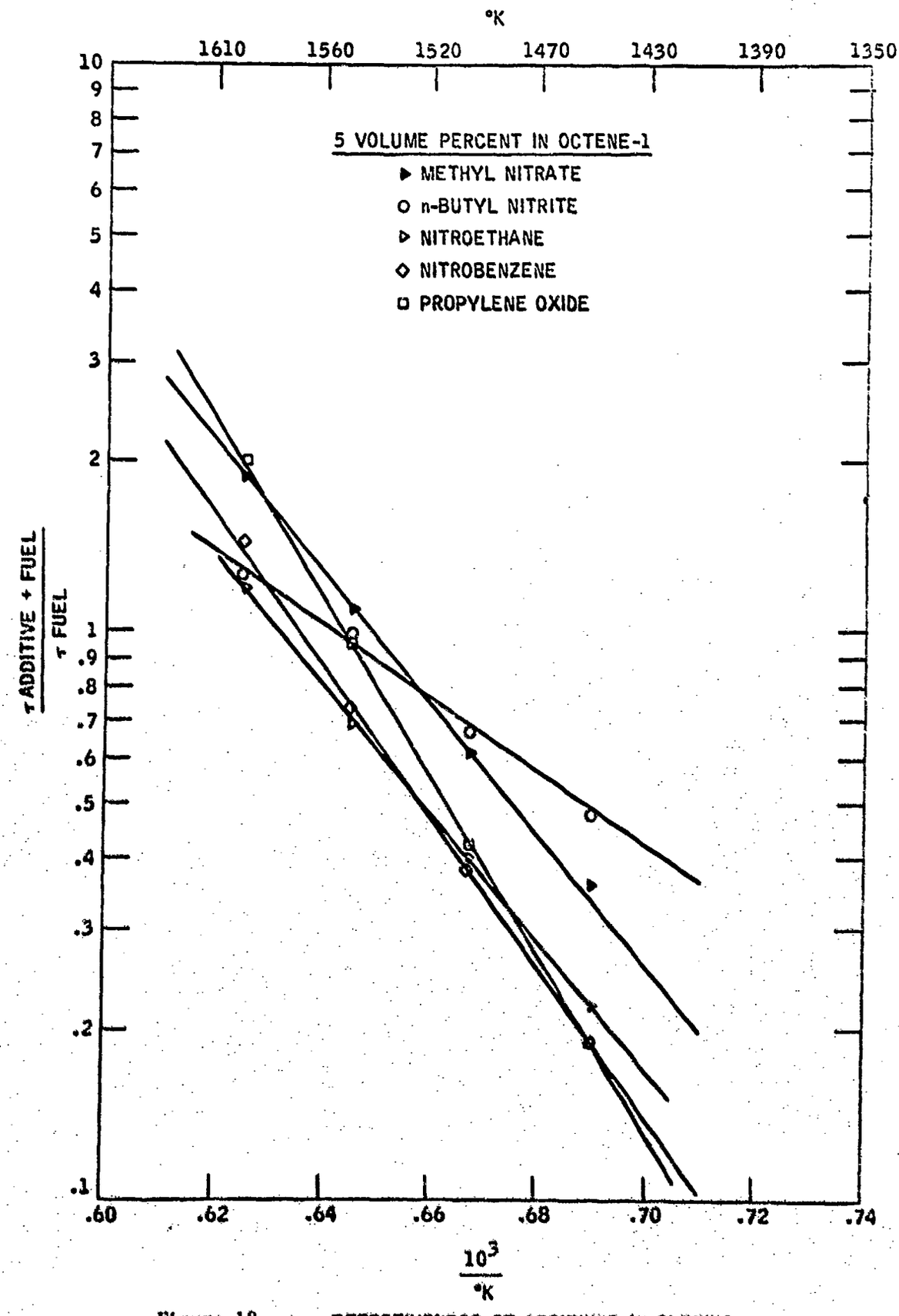

Figure 18 EFFECTIVENESS OF ADDITIVES IN OLEFINS

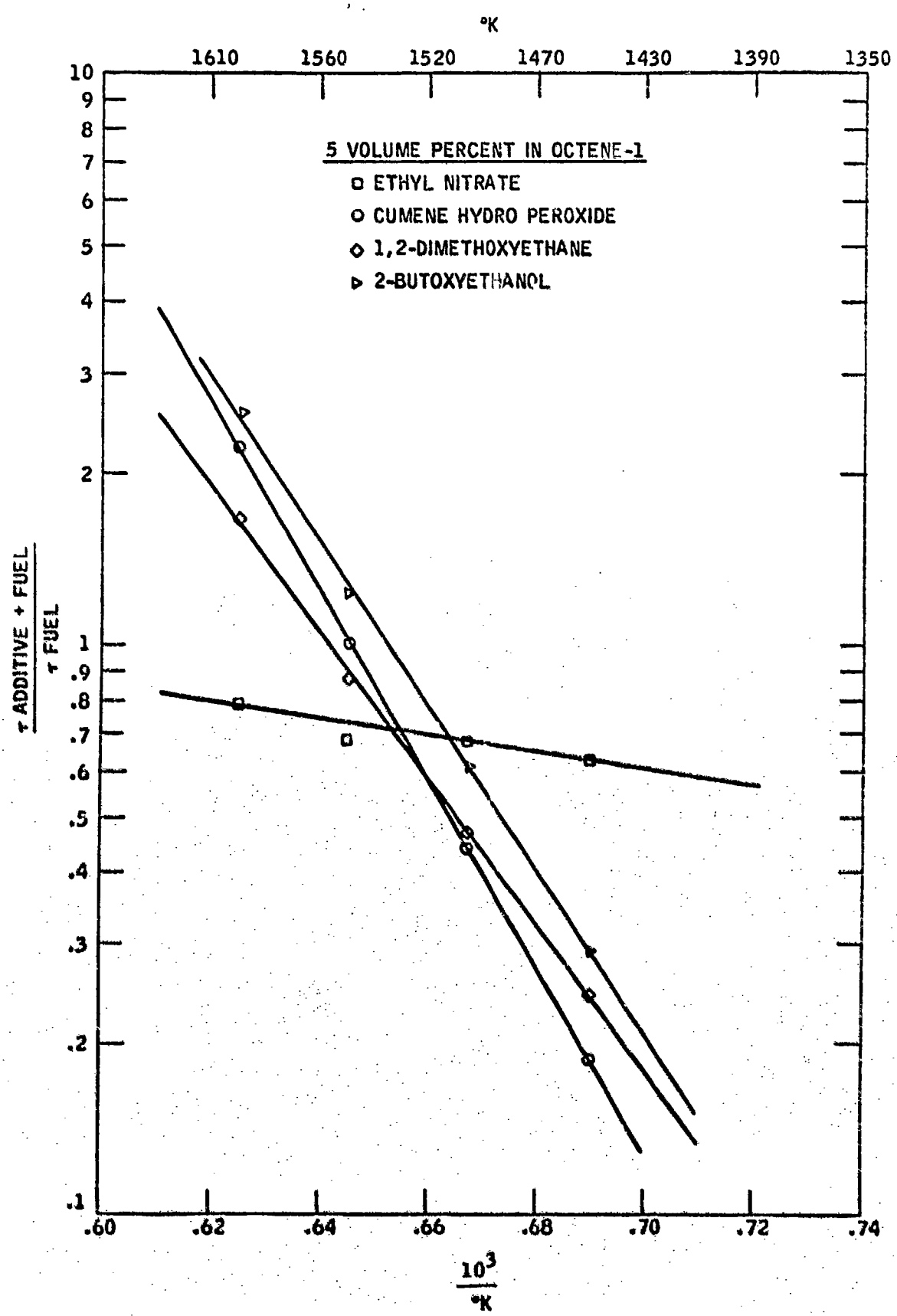

Figure 19 EFFECTIVENESS OF ADDITIVES IN OLEFINS

Complex Fuels (JP-7)

Figure 20 illustrates that those additives containing the $-CH_2-CH_2-$ groups were more efficient promoters at high temperatures. Similar effects were observed in n-octane with some of the same additives. In JP-7 the inclusion of 5 volume percent 1,2-dimethoxy ethane had an inhibiting influence on τ at low temperatures while promoting ignition at high temperatures. The most effective additive in JP-7 was observed to be n-butyl nitrite, which decreased τ by more than 50 percent at 1400°K. Cumene hydroperoxide, propylene oxide, and nitro benzene also exhibited ignition promoting characteristics, but in a somewhat less effective manner than they behaved in the olefinic fuel, octene-1.

JP-7 contains about 75 percent paraffins, mostly normal and iso compounds, an aromatic concentration of 2-4 percent and the remainder as napthenes. This high paraffinic content may explain the similarity of the effectiveness of some of the additives in JP-7 and n-octane. The difference in the relative magnitudes of the observed reductions in τ was attributed to the cyclic hydrocarbon concentration in JP-7. In the initial tests of neat fuels it was observed that compared to alkanes or alkenes, the cyclic compounds were more resistant to ignition as manifested by the longer residence times.

D. Autoignition of Neat Hydrocarbon Fuels In the Subsonic Continuous Flow Apparatus

Figure 21 contains the autoignition delay time characteristics of lean mixtures of various neat hydrocarbons observed in a subsonic, continuously flowing unvitiated air stream at one atmosphere pressure. The least-square plots were obtained from a linear regression analysis and conform to the familiar Arrhenius relationship $\tau = Ae^{E/RT}$. The ten different hydrocarbons were selected for evaluation on the basis of their performance in the WSR, previously discussed, and their practical application in ramjet propulsion systems. The data indicated that all of the complex fuels such as Shelldyne-H, JP-7, H-MCPD and cyclohexene had similar autoignition delay characteristics over the temperature range of 1050-1250°K. At the reference temperature of 1000°K, the order of activity, in terms of increasing ignition lag, was found to be: cyclohexene, H-MCPD, JP-7 and Shelldyne-H. The slopes of the curves were similar thus indicating that the overall-gradual activation energies were similar for these dense fuels.

The ignition lags of propane, n-octane and n-tetradecane were observed to increase slightly as the length of the straight alkane chain increased. At 1000°K propane had an ignition lag time of 34 milliseconds compared to 37 and 42 milliseconds respectively for n-octane and n-tetradecane.

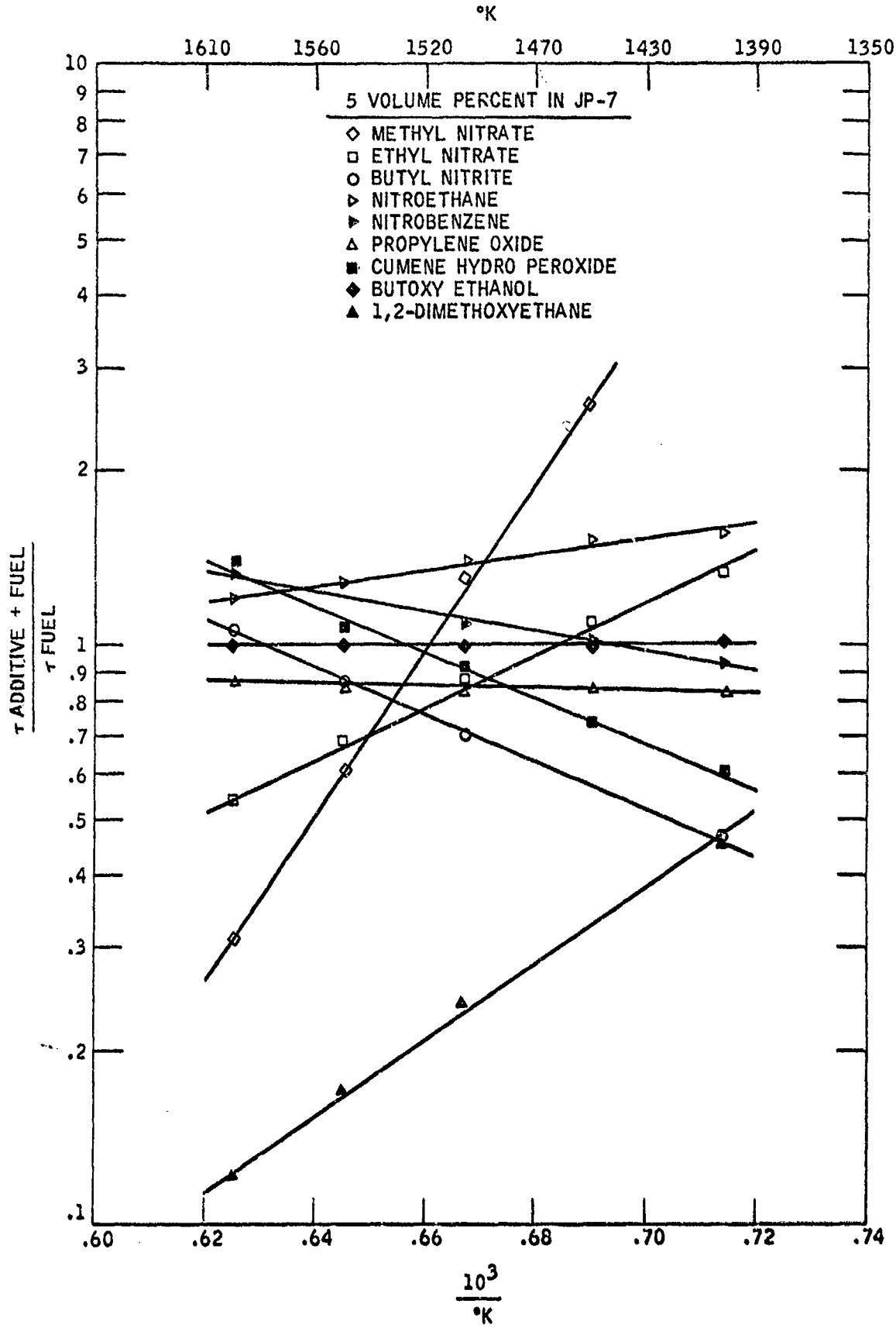

Figure 20 EFFECTIVENESS OF ADDITIVES IN JP-7

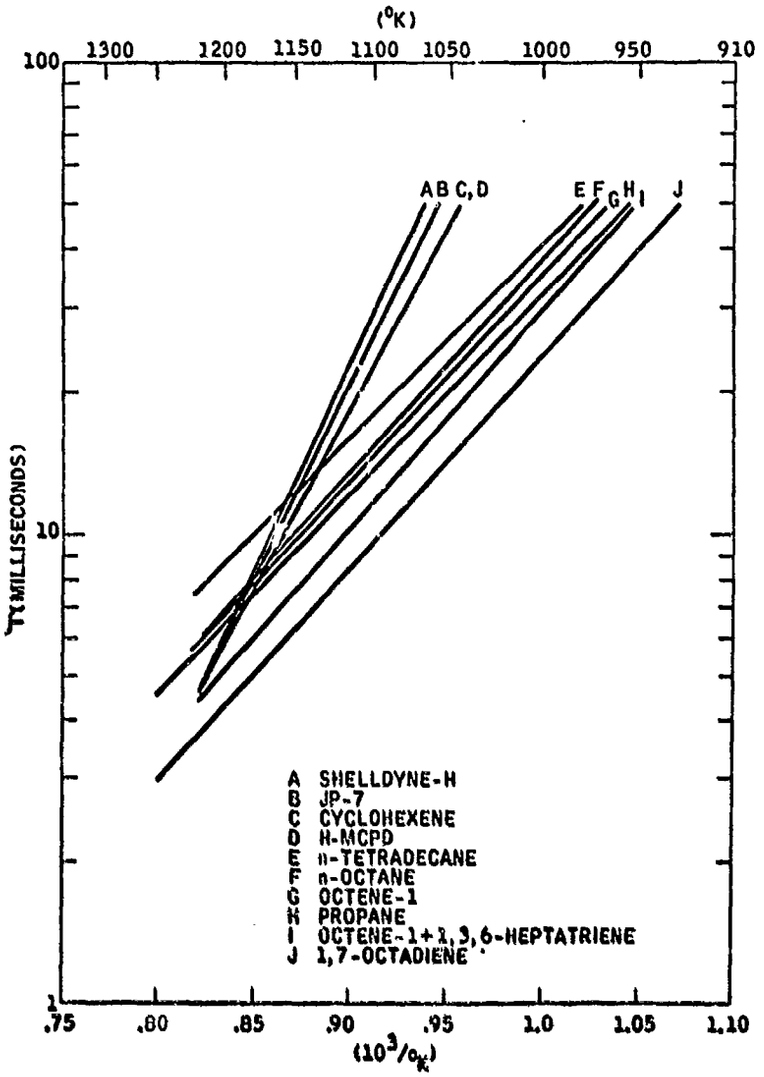

FIGURE 21 IGNITION DELAYS OF NEAT HYDROCARBONS IN THE CFS

The ignition lags of the olefins which included octene-1, and 1,7-octadiene were observed to be nearly the same or less than the lag time observed for propane. Compared to propane, the ignition lags at 1000°K were 25 milliseconds for 1,7-octadiene and 36 milliseconds for octene-1. A further indication of the effect of increasing the number of double bonds in a straight chain, on the ignition lag was ascertained by blending octene-1 with 1,3,6-heptatriene in equal concentrations. This fuel blend was observed to exhibit an ignition delay time less than observed for the octene-1 alone, indicating that the tri-olefin 1,3,6-heptatriene probably had an ignition lag shorter than the mono-olefin. Further evidence which supported this view was the fact that the ignition sequence of the blend of olefins was observed to occur in two distinct phases. Upon injection of the fuel into the hot air stream, two ignition flame fronts were simultaneously established in the duct separated from each other by a distance proportional to their individual ignition lags. In a few seconds, the flame front farthest from the fuel injector slowly propagated upstream and coalesced with the first flame front. The combined flame fronts remained fixed in that position for the duration of the test run, which lasted for 25 seconds.

Binary Fuel Blends

The ignition of all the fuel blends consisting of compounds having greatly dissimilar ignition delay characteristics were observed to occur in a two stage process as described in the previous section. The ignition delays of two fuel blends consisting of JP-7 with octene-1 or 1,3,6-heptatriene with octene-1 were compared with JP-7 or octene-1 in Figure 22. These results clearly show that the ignition lag time of JP-7, which was relatively unreactive compared to propane, was significantly reduced by blending with a fuel which had a shorter ignition lag. A blend of equal concentrations of JP-7 and octene-1 (curve B, Figure 22),was observed to ignite with a delay time of 54 milliseconds at 1000°K compared to a 36 millisecond delay for octene-1 alone and 145 milliseconds for JP-7 alone. The same results were inferred from a comparison of Curves C and D of Figure 22 which illustrated that the blend of octene-1 with 1,3,6-heptatriene exhibited significantly lower ignition delays than the most ignition resistant fuel which was octene-1. The ignition lag of 1,3,6-heptatriene by itself was not measured because a sufficient quantity was not available (cost of material was $3.40/gram).

Overall, the ignition delay characteristics of long chain olefins, especially di and tri-olefins were significantly less than long chain alkanes having the same number of carbon atoms. Figure 23 compares the ignition lags of a C_8 paraffin, monolefin and diolefin. There was a significant reduction in the ignition lag time as the number of double bonds was increased. In addition, the slope and magnitude of the ignition delay curve for the blend of octene-1 with 1,3,6-heptatriene was observed to be similar to the curve for 1,7-octadiene. This similarity indicated that the 1,3,6-heptatriene which contained three double bonds had an ignition delay lower than the diolefin since its reactivity was impaired by blending with a less reactive fuel, octene-1. It is well known that the unsaturated hydrocarbons

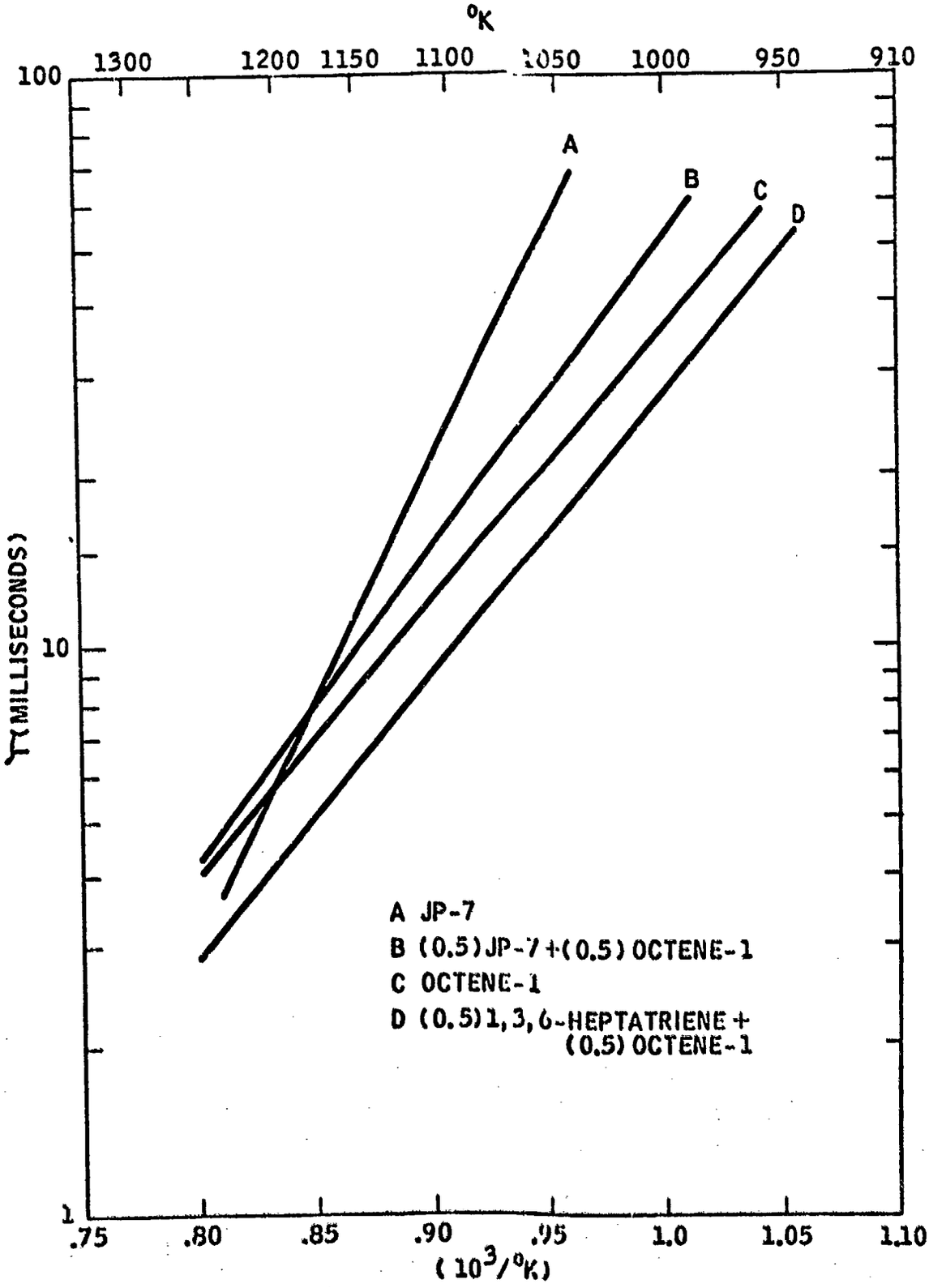

FIGURE 22 IGNITION DELAY OF BINARY FUELS IN THE CFS

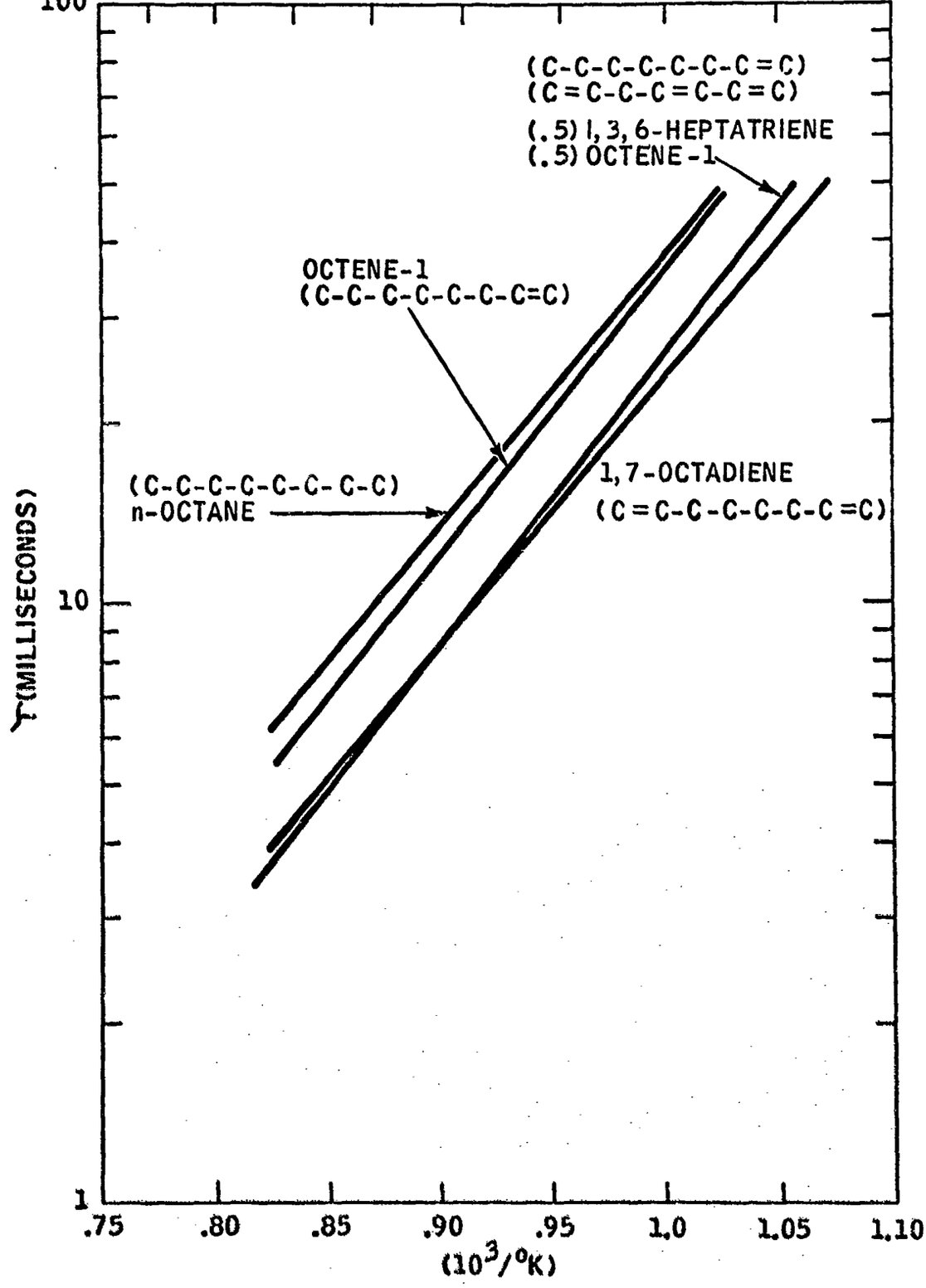

FIGURE 23 COMPARISON OF C_7 AND C_8 HYDROCARBON IGNITION DELAYS IN THE CFS

are easily oxidized at relatively mild thermal conditions; the degree of oxidation or pyrolysis increasing with the number of double bonds present on the straight chain. These facts were borne out during the experimental tests with the di and tri-olefins which were observed to pyrolyze in the tip of the fuel injector and even in the fuel vaporizer. The inclusion of homogeneous chemical additives, which affected the oxidation stability of the olefins, was observed to sharply increase the rate of coke formation in the fuel injector and vaporizer. Although these deposit formations were a nuscence, they were quickly removed by the injection of steam into the vaporizer and injector. The well known water-gas shift reaction converted the coke to CO at temperatures within the operation limits of the system.

E. The Effects of Homogeneous Additives on τ in the CFS

The magnitude of the autoignition promoting effects of the homogeneous additives were observed to depend on the chemical nature of the additive as well as the molecular structure of the fuel in which they were evaluated. Because of the large number of different fuel-additive combinations tested during the program the results are presented by discussing the additives effect as a function of the molecular structure of the hydrocarbon fuels they were evaluated with.

Generally, the magnitudes of the ignition delay of the fuel blends were inversely proportional to the log of the additive concentration.

Table II summarizes the type and number of various additives tested.

Effectiveness of Alkyl Nitrates And Nitrites in Alkanes

Although three alkane fuels were tested--propane, octane and tetradecane--the effects of the following additives were determined in only the C_8 and C_{14} normal paraffins.

nitric oxide	(NO)
methyl nitrate	(CH_3ONO_2)
ethyl nitrate	($C_2H_5ONO_2$)
iso-amyl nitrate	($i\text{-}C_5H_{11}ONO_2$)
butyl nitrite	(C_4H_9ONO)
tert-butyl nitrite	($t\text{-}C_4H_9ONO$)
amyl nitrite	($C_5H_{11}ONO$)

Methyl nitrate exploded when it was injected into the autoignition test section via the hypodermic syringe technique described in Section IIIB. The syringe contained 10 cc's of material. The eventual recovery and reconstruction of the hypodermic needle fragments clearly showed that the methyl nitrate decomposition reaction was initiated inside the needle in the vicinity when the wall temperature changed abruptly from room conditions to a temperature above the boiling point of the liquid. The 12-inch long hypodermic needle was made of type 304 stainless steel and had an internal bore diameter of .013 inch and a wall thickness of .004 inch. In retrospect, the possibility of such an explosion was evaluated prior to the test with the conclusion being that the long, small bore-diameter hypodermic needle would act as an explosion trap. Needless to say, it did not. It appeared that a high order detonation reaction may have occurred.

Auto decomposition of methyl nitrate at its boiling point (65°C) is well known to result in explosion or detonation. No further tests were conducted with methyl nitrate after that occurrence.

The other members of the alkyl nitrate and nitrite family, which have boiling temperatures which range from 63° to 177°C as summarized in Table VI, were subsequently evaluated, without incident, in n-octane and many other different hydrocarbon fuels via the hypodermic syringe injection technique. The effectiveness of these additives in promoting the autoignition of lean mixtures of n-octane in air, over a temperature range of 950°-1250°K are illustrated in Figure 24. The volumetric concentration varied from one additive to another because of their different fluid densities and viscosities. However, by comparing curves C, D, E, and F of Figure 24, all of which represent the effects of similar additive concentrations, the dramatic ignition promoting effects of the alkyl nitrates and nitrites are apparent. Curve G, which was obtained for a 50 volume percent loading of ethyl nitrate, represents an improvement in the ignition delay of n-octane by a factor of 10 at 1000°K. At 1250°K, the additives were less effective. The next most efficient ignition promoter was observed to be iso-amyl nitrate. The nitrite esters were slightly less effective than the nitrates. The tertiary isomer of the C_4 nitrite was far less effective than any of the other alkyls tested. Curve B of Figure 24 shows the effect of 25 volume percent nitric oxide.

The reduction of the autoignition delay time of n-octane by these additives was also observed to be accompanied by a drastic change in the apparent "global-activation" energy of the ignition reaction as indicated by the change in slope of the Arrhenius curves. Employing the standard equation, which describes this relationship, the activation energy (E_a) was reduced from 21 KCal/mole to less than 7 KCal/mole when 50 volume percent $C_2H_5ONO_2$ was added to n-octane.

TABLE VI

PHYSICAL AND CHEMICAL PROPERTIES
OF ALKYL NITRATES AND NITRITES

Compound	(MW)	(Sg) @ 20°C	(B.P.) °C	Cost $/Kg	(ΔH_c)[a] Kcal/mole	(ΔH_f)[a] Kcal/mole	($\cdot NO_x$) Wt. %
$n\text{-}C_2H_5ONO_2$	91.07	1.10	88	56	-313.39[26]	-45.51[26]	50.5
$n\text{-}C_3H_7ONO_2$	105.09	1.058	110	3	-470.0[26]	-57.27[26]	43.8
$n\text{-}C_4H_9ONO_2$	119.12	1.015	123	330			38.6
$i\text{-}C_5H_{11}ONO_2$	133.15	0.996	148	1.5			34.4
			Nitrites				
$r\text{-}C_4H_9ONO$	103.12	0.911	79	19			29.2
$t\text{-}C_4H_9ONO$	103.12	0.92		150			29.2
$n\text{-}C_5H_{11}ONO$	117.15	0.853	104	16		-24.5[27]	25.6
$i\text{-}C_5H_{11}ONO$	117.15	0.872	99	26			25.6
$n\text{-}C_8H_{17}ONO$	159.22	0.862	177	127			18.9

(a) Liquid @ room temperature.

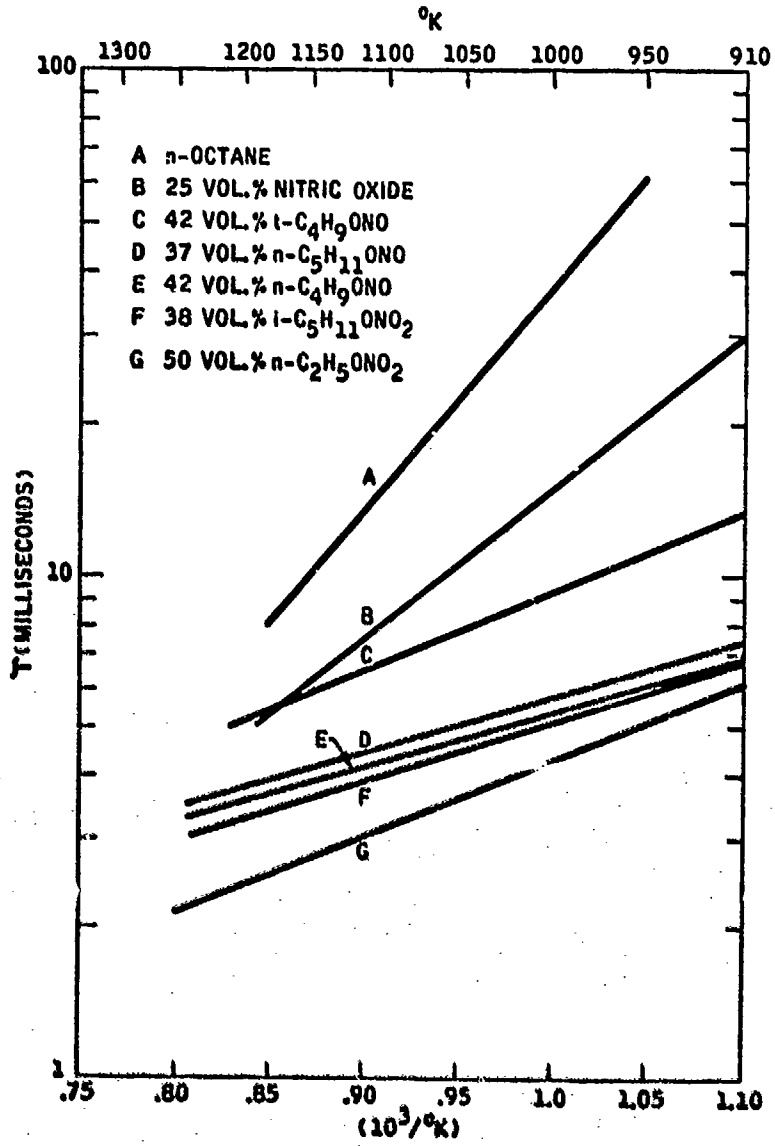

FIGURE 24 THE EFFECT OF NITROGEN ESTERS ON THE IGNITION DELAY OF n-OCTANE IN THE CFS

$$\text{Overall Activation Energy, } E_a = \left(\frac{\log \tau_1 - \log \tau_2}{1/T_1 - 1/T_2} \right) R \cdot 2.3$$

where τ_1 and τ_2 are the ignition lags (millisec.) measured at temperatures (°K), T_1 and T_2. R is the gas constant (1.987 cal mole^{-1} deg.$^{-1}$).

The strong ignition promoting effect of the alkyl nitrates and nitrites were also observed in the long-chain alkane--tetradecane ($C_{14}H_{30}$). The Arrhenius plots given in Figure 25 showed that the longer chain length was more greatly affected by the homogeneous additives, compared to the C_8 straight chain alkane notwithstanding that the ignition delay characteristics of neat octane and tetradecane are similar, as shown in Figure 21. The overall activation energy (E_a) of neat tetradecane was about 19.5 KCal/mole compared to 7.5 KCal/mole in curve D of Figure 25 which was for a 42 volume percent concentration of n-butyl nitrite (C_4H_9ONO). At 1000°K the ignition delays of tetradecane and octane with similar concentrations of n-butyl nitrite were 4.5 and 5.5 milliseconds, respectively.

The ignitions of the alkane-additive blends were extremely colorful to the eye. The additives were seen to thermally decompose as evidenced by their characteristic grey, electric-blue flames located at the leading edge of the stationary flame front. Attached to this decomposition zone were the blue-white reaction zones of the hydrocarbon fuels. The tail of the stationary flame had a green-yellow color, which was indicative of the well known NO+O recombination reaction.[25]

Effectiveness of Olefins

Fuels containing double bonds exhibited rapid thermal and oxidative reactions at high temperatures. The presence of double bonds leads to two significantly different effects compared to the alkanes. Hydrogen abstraction which leads to resonance stabilized radicals and addition to the double bond occurs in the olefins. The ensuing oxidation reactions are quite different than those possible in the alkanes. These effects were observed to significantly alter the autoignition delay characteristics of the neat fuels as shown in Figure 21. The superior response of olefins to the additives, compared to the paraffins, is shown in Figures 26 and 27.

The most effective additive in the monolefin, octene, for a loading of 25 volume percent was ethyl nitrate ($C_2H_5ONO_2$). The other additives, arranged in their order of decreasing effectiveness were: iso-amyl nitrate, tert-butyl nitrite, n-amyl nitrite, n-butyl nitrite, and nitric oxide. Comparison of curves B and D of Figure 26 shows that the combination of hydrogen and nitric oxide results in a synergistic effect as evidenced by the large reduction τ in the case where H_2 was added. It is interesting to compare the slopes of these two curves for it shows that although the ignition lag of octene has been reduced by nearly a factor of two by the addition of 13 volume percent H_2, with 25 percent nitric oxide, the overall activation energies derived from curves B and D remain essentially constant. The same concentration of H_2 without any nitric acid addition produced no ignition promotion.

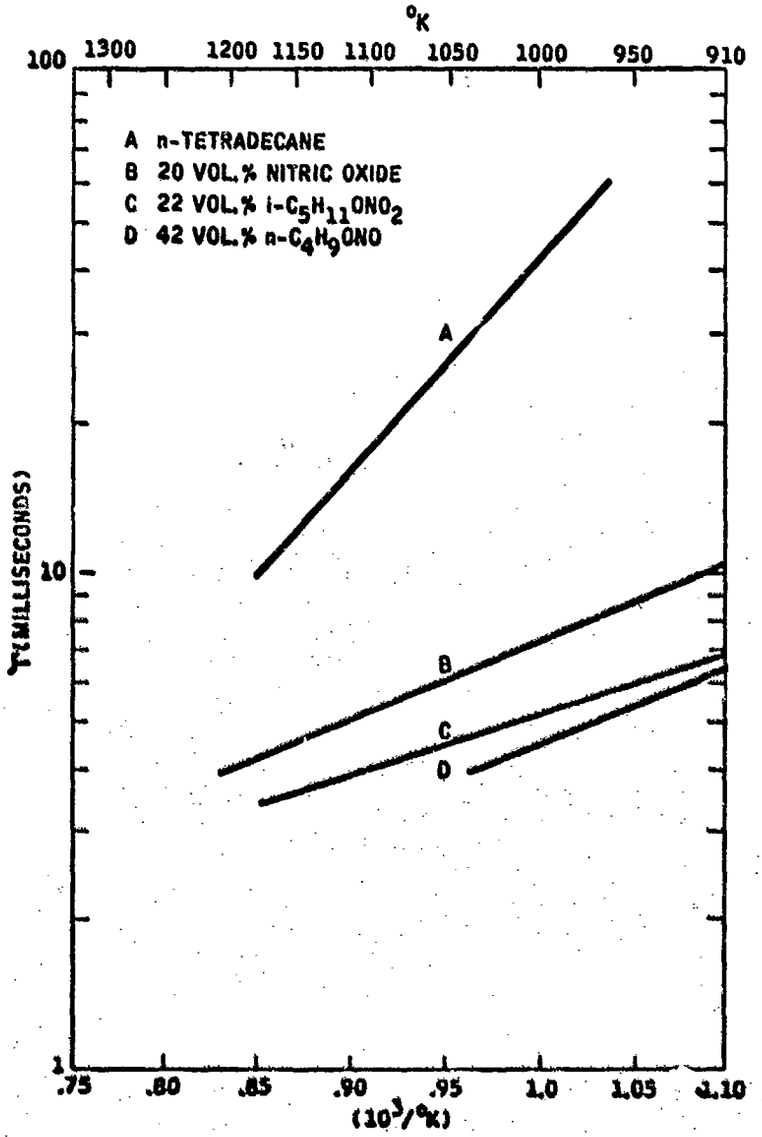

FIGURE 25 EFFECT OF NITROGEN ESTERS ON THE IGNITION DELAY OF n-TETRADECANE IN THE CFS

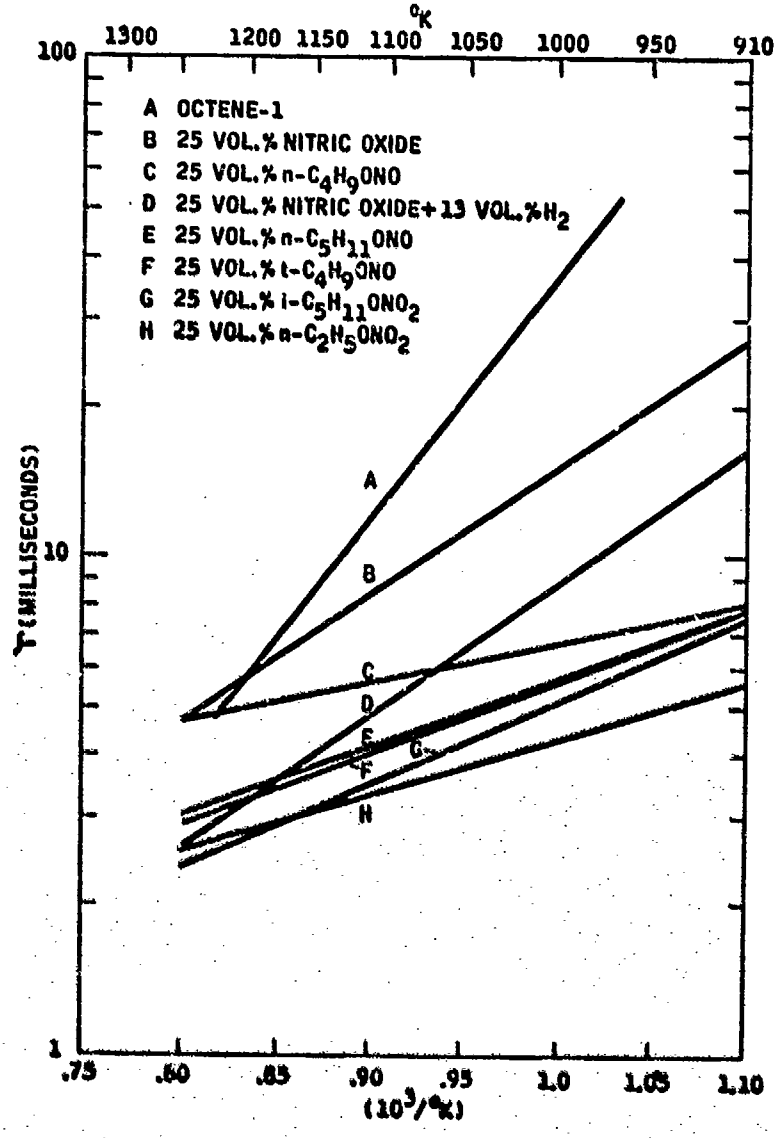

FIGURE 26 EFFECTS OF NITROGEN ESTERS IN THE IGNITION DELAY OF OCTENE-1 IN THE CFS

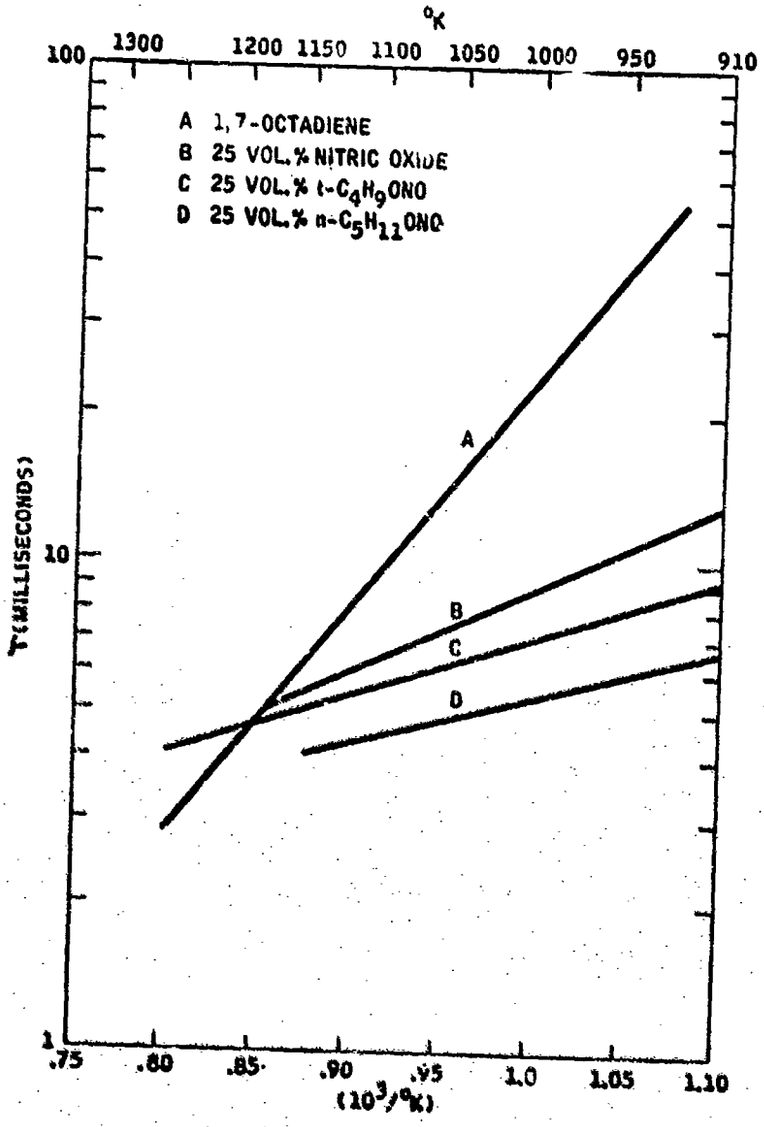

FIGURE 27 EFFECT OF NITROGEN ESTERS IN THE IGNITION DELAY OF 1,7-OCTADIENE IN THE CFS

The effect of additives in fuels containing two double bonds is shown in Figure 27. The di-olefin 1,7-octadiene was observed to be even more responsive to the ignition promoting effects of the additives tested in octene-1. Comparison of curve B of Figure 27 with curve B of Figure 26 shows that a 25 percent concentration of nitric oxide was nearly twice as effective in the di-olefin compared to the monolefin. The activity of the alkyl nitrates and nitrites in the diolefin were equal to or greater than their effects in the monolefin.

The apparent increase in the rate of oxidation of the olefin catalyzed by the homogeneous additives was also observed to promote the formation of coke inside the fuel injector. The many small holes of the fuel injector-tip often times became plugged with solid, carbonaceous deposits. The severity of this problem seemed to be dependent upon the quantity and type of additive used, generally being more severe for the best ignition promoters. The formation of coke deposits did not occur immediately but was the result of repetitive tests with olefins and alkyl nitrates or nitrites. It was found that the injection of water into the hot fuel injector (>600°C) resulted in the generation of CO and H_2O via the Water-Gas Shift Reaction, thereby purging the injection of the deposits.

The overall activation energies of the ignition reactions of neat octene-1 and 1,7-octadiene over the temperature range of 950°-1250°K were calculated to be 24 and 21 KCal/mole, respectively. The addition to octene-1, of 25 volume percent, ethyl nitrate, reduced the ignition lag by nearly a factor of 10 and lowered the activation energy to 7 KCal/mole. Similar behavior was noted for 1,7-octadiene.

The ignition reactions of the olefinic fuels promoted by the additives were characterized by the appearance of the grey,-electric-blue decomposition reaction of the alkyl nitrates and nitrites at the leading edge of the reaction zone. The reaction of the hydrocarbon was evidenced by the attachment of a blue-white flame to the grey decomposition flame of the alkyl. The characteristic green-yellow glow of the NO+O recombination reaction followed in the tail of the established flame. At temperatures below 900°K, "cool flames" were observed at the exit plane of the test section before the additive was injected. However, the alkyl nitrates and nitrites reacted in such a way as to inhibit the appearance of the "cool flame".

Another interesting effect which was observed in the tests with olefins and nitrogen esters was that the injection of tertiary butyl nitrite into the octene-1 or 1,7-octadiene flame zone did not form characteristic grey, bright-blue decomposition zone previously observed for the other nitrogen esters. Subsequent tests with just the tertiary butyl nitrite and no hydrocarbon present showed that the exothermic decomposition reaction of the tertiary nitrite isomer occurred without the appearance of any visible emission. This observation was subsequently found to pertain to all the tertiary nitrogen esters over the temperature range of 950°-1250°K. Below 950°K, their decomposition reactions were visually observed as low intensity grey flames.

Effectiveness in Complex Fuels

The category of Complex Fuels consists of Shelldyne-H, the hydrogenated dimer of methyl cyclopentadiene and JP-7. The molecular structure of Shelldyne-H was not completely identified but from the results of some simple analytical tests it was determined that the structure could be similar to the following:

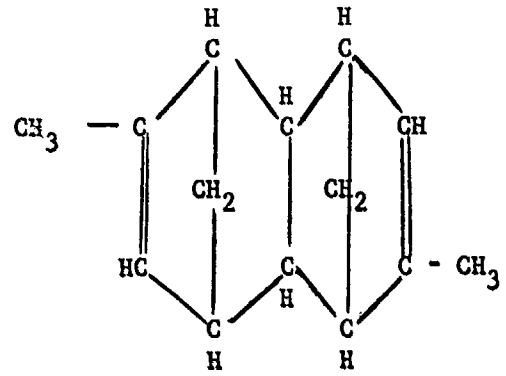

$(C_{14}H_{18})$

Based on elemental analyses and mass spectroscopy Shelldyne-H is a mixture of polycyclic unsaturated hydrocarbons with molecular masses of 184, 186 and 188. The material of mass 186 was the major constituent. Relating the elemental analysis to the mass, the carbon-hydrogen ratio for the major component was $C_{14}H_{18}$ which is in agreement with the proposed molecular structure.

It was important to ascertain the structure of Shelldyne-H after the strong ignition promoting effects of the nitrogen esters were observed in this fuel.

The effectiveness of various additives in promoting the ignition of Shelldyne-H are summarized in Figures 28 and 29 for 50 percent loadings. In Figure 28, nitric oxide and n-octyl nitrite were tested in concentrations of 25 volume percent. Compared to the very large effects the nitrogen esters had on promoting Shelldyne-H ignitions, the additives such as ethyl oxalate, tert-butyl hydroperoxide and 1,2-dimethoxy-ethane were relatively ineffective for the same volumetric loading. Of these, the most effective additive was 1,2-dimethoxyethane. The alkyl nitrates and nitrites, without exception, had very strong ignition promoting effects. The least effective of these was tert-butyl nitrite and the most effective were, in their order of decreasing effectiveness: n-butyl nitrate, n-propyl nitrate, iso amyl nitrate and ethyl nitrate.

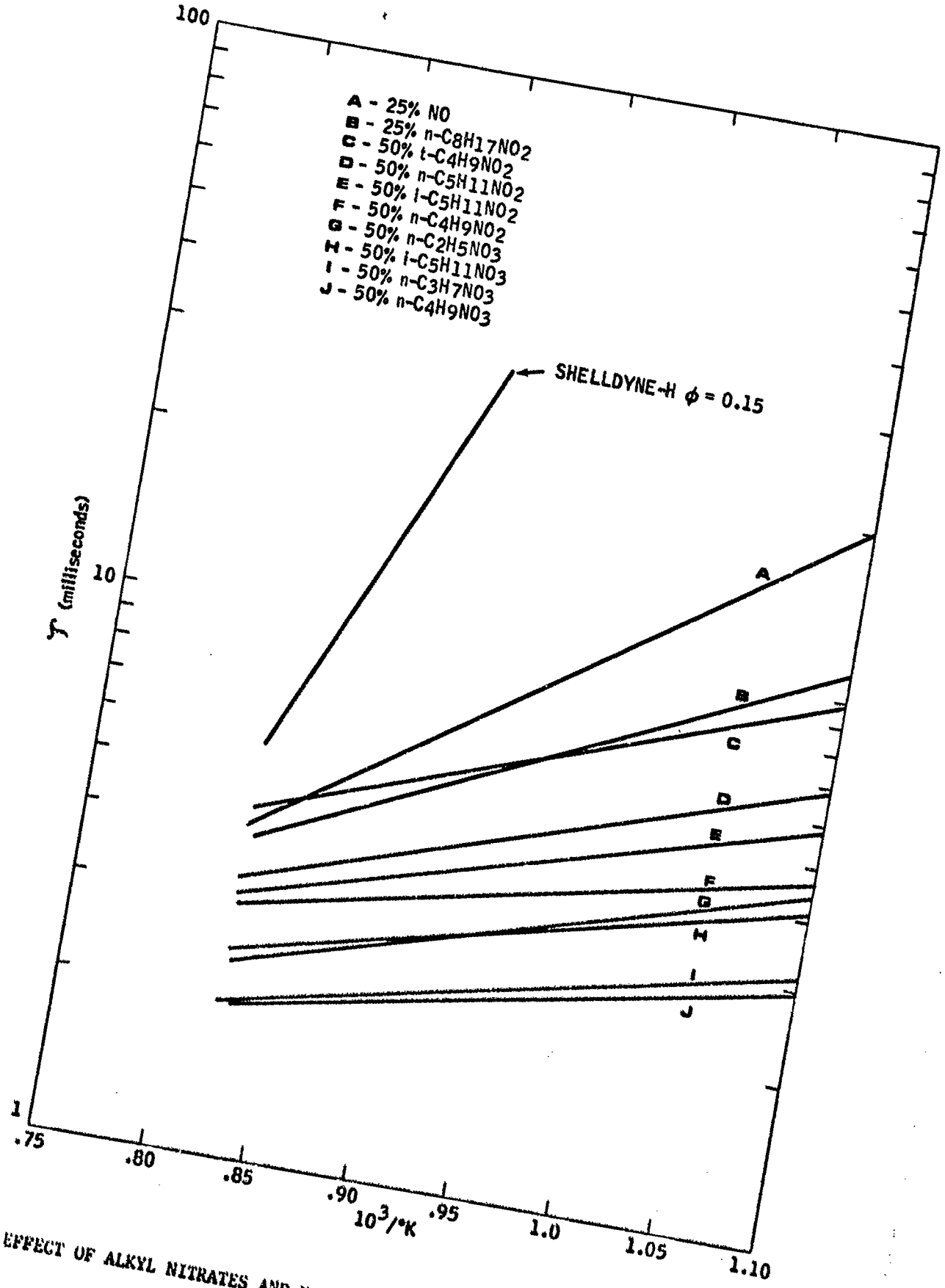

FIGURE 28 EFFECT OF ALKYL NITRATES AND NITRITES ON THE IGNITION DELAY OF SHELLDYNE-H

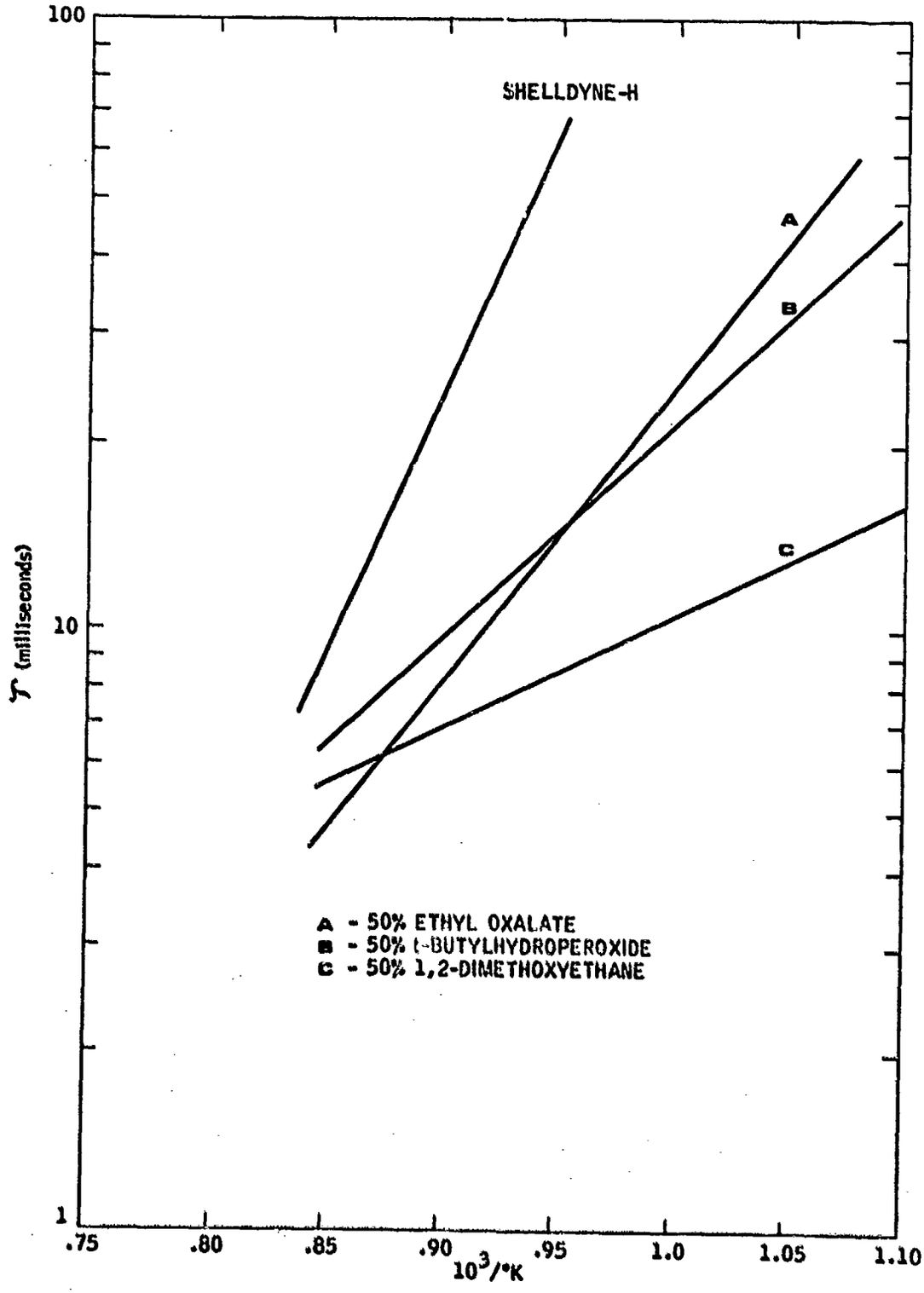

FIGURE 29 EFFECT OF LOW-TEMPERATURE ALKOXYL RADICAL ADDITIVES ON IGNITION DELAY OF SHELLDYNE-H

The overall activation energy of neat Shelldyne-H was reduced from approximately 40 KCal/mole to 12.5 KCal/mole when 50 percent n-butyl nitrate was added. The ignition delay time was likewise reduced from 180 milliseconds to 2.7 milliseconds at 1000°K.

The autoignition of neat Shelldyne-H at high inlet air temperatures was observed to occur with the emission of intense yellow-white radiation. At lower air temperatures the flame zone was less intense and resembled the typically blue-white flames observed in paraffin and olefin hydrocarbons. The partial combustion of Shelldyne-H at temperatures below about 1050°K produced gaseous products which irritated the nose and throat as well as the eyes.

The addition of any of the alkyl nitrates or nitrites to Shelldyne-H caused the severity of the irritants to be lessened since more complete combustion of the Shelldyne-H occurred at lower air temperatures. The ignition flame front of these blends were similar to the other hydrocarbon nitrogen ester flame zones except that the Shelldyne-H flame was extremely bright yellow-white. It was only after the air temperature decreased below 1000°K that the characteristic grey, bright-blue flame associated with the decomposition of the nitrogen esters was observed.

F. Optimization of Alkyl Nitrate Concentration in Shelldyne-H

The high specific gravity and high heat of combustion of Shelldyne-H made it the number one fuel candidate. In order to optimize the additive concentration and the total volumetric heat release values, the ignition promoting effects of varying concentrations of n-propyl nitrate in Shelldyne-H were determined by preparing blends. The heating values of the blends were calculated from the published thermodynamic data obtained from references 26 and 27. n-Propyl nitrate was chosen as the additive because of the following:

- Availability
- Low Cost
- Good Physical Properties - High Sg.
- Moderately High Δ Hc
- Good Ignition Promoter
- Military Applications as a Mono Fuel[28]

Upon blending varying quantities of propyl nitrate with the viscous Shelldyne-H it became apparent that the viscosity of the blend was substantially less than it was for neat Shelldyne-H. The ease with which the flow rates of the blends could be controlled as indicated by the glass rotometer flow metering device was remarkable. Subsequently, such properties as viscosity, freezing and boiling points and flash points of various blends were performed at the Fuels Laboratory of Wright-Patterson Air Force Base. The results of those tests are given in Table III. Figures 30 and 31 show the effects of n-propyl nitrate

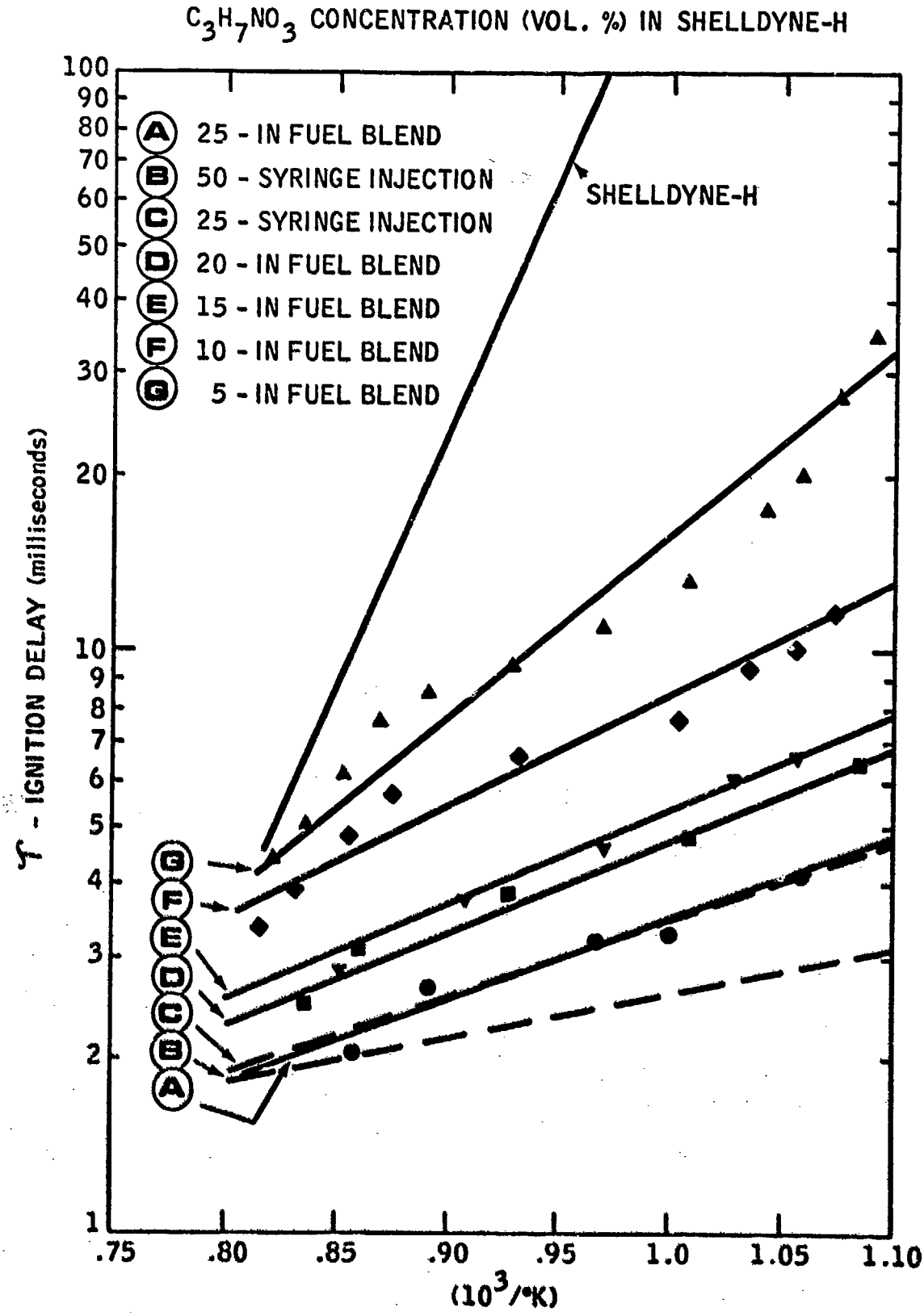

Figure 30 Effect of $C_3H_7ONO_2$ Concentration on Ignition Delay of Shelldyne-H, for either pre-mixed Bleuds or Direct Additive Injection.

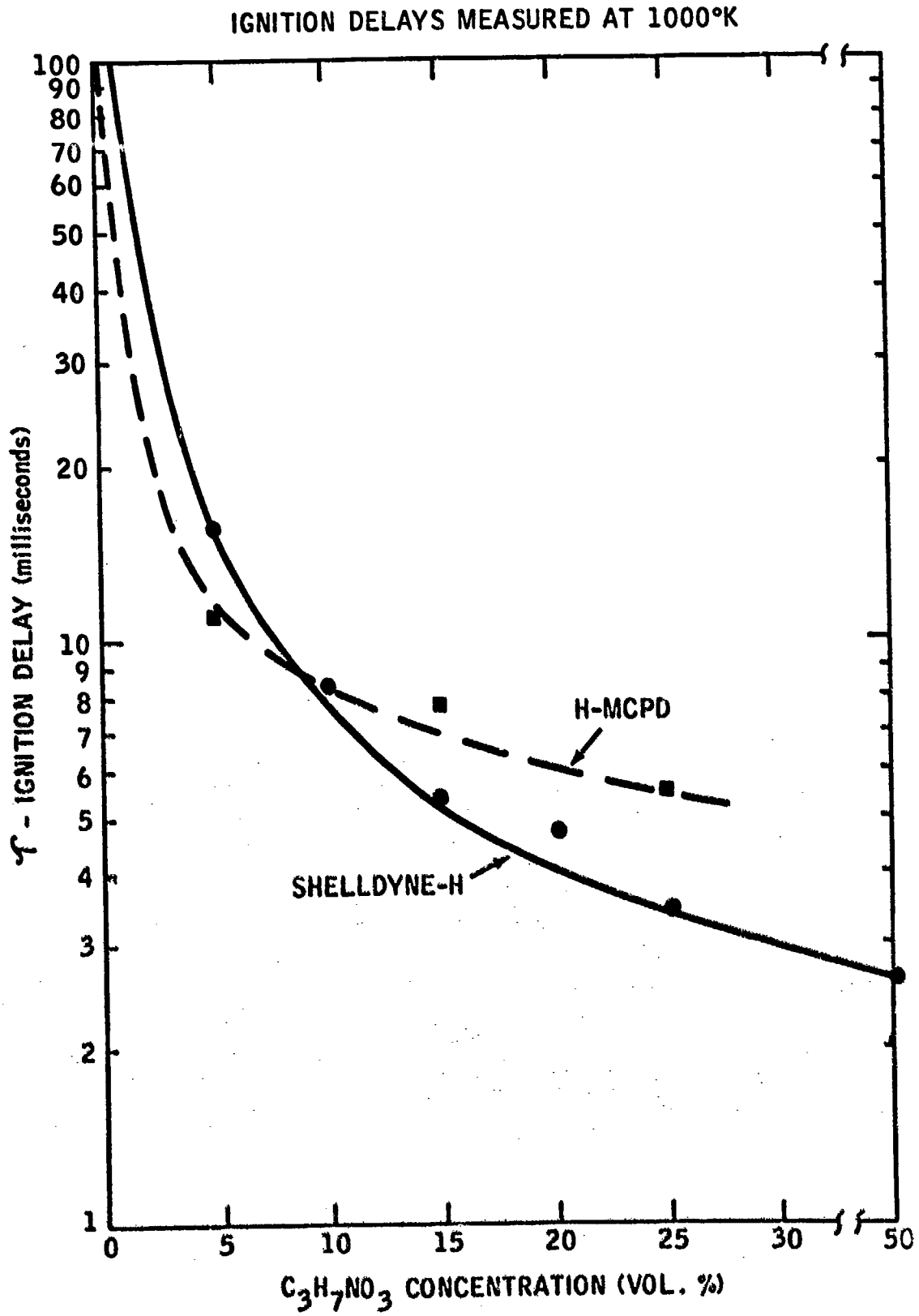

Figure 31 Comparison of Effectiveness of $C_3H_7ONO_2$ in Shelldyne-H and H-MCPD @ 1000°K Air Inlet Temperature

concentration on the ignition delay of Shelldyne-H over the air inlet temperature range of 900°-1250°K. The ignition lag was observed to vary inversely as the log of the additive concentration with the major reduction in τ being realized at a concentration of about 8 volume-percent.

The same additive concentration effect was observed for Shelldyne-H blends with n-propyl nitrate as well as for the separate injection of the additive via the hypodermic syringe technique. Curves A and C of Figure 30 clearly show the similarity. These results demonstrated that any pre-ignition reactions occurring inside the fuel vaporizer when the blends were tested were either not significant as the same results were obtained when the additive was injected directly into the hot air, vaporized fuel stream.

The superior ignition promoting characteristics of the alkyl nitrates and nitrites or nitric oxide in hydrocarbons indicated that the mechanism responsible could be attributed to either of the following:

- alkoxyl radical resulting from the thermal decomposition of the esters.
- NO or NO_2 resulting from the ester decomposition.
- Increase in heat release rate of the mixture due to the combustion of the esters.

The thermal decomposition of all the alkyl nitrates and nitrites occurs with cleavage of the O-N bond and requires about 34-36 KCal/mole.[29] The reaction products consist of alkoxyl radicals and either NO or NO_2. From the previous tests with NO as an ignition promoter, it was established that compared to other additives such as 1,2-dimethoxyethane, tert-butylhydroperoxide and other alkoxyl radical sources, the promoting effects of nitric oxide were many times greater than an equivalent amount of the peroxide compounds. On the basis, the alkoxyl radicals were ruled out as the significant ignition promoting species.

The relatively low heats of combustion of the lower molecular weight alkyl nitrates or nitrites, compared to the hydrocarbons as seen in Table 6, rules out their thermal effects as being a significant influence in promoting ignition.

The only remaining possibility was that the autoignition of the hydrocarbons was effected by nitric oxide and nitrogen dioxide which were products of thermal decomposition of the additives. Figure 37 is a compilation of all the ignition delay data obtained for Shelldyne-H blends with varying concentrations of different molecular weight alkyl nitrates and nitrites. By normalizing the ignition delay time as a function of the weight fraction of NO or NO_2 generated in the thermal decomposition of the nitrates or nitrites, the data show the following:

1. The ignition promoting effects of the esters are independent of the ester's position within the homologous series.

2. The nitrate esters, because they are the source of NO_2, are about twice as effective as the nitrite esters which produce NO upon their decomposition.

3. Generally, about 8 weight percent NO or NO_2 results in the maximum ignition promoting effect which was approximately inversely proportional to the logarithm of the additive concentration.

4. The promoting effects of equivalent amounts of neat nitric oxide compared to nitric oxide evolved during the decomposition of the alkyl nitrites have similar characteristics but neat nitric oxide is less effective than NO as the decomposition product. The same results were obtained with the alkyl nitrates and neat NO_2. The increased promotional effects of the ester's decomposition products compared to neat NO and NO_2 were attributed to the slight ignition improving properties of the alkoxyl radicals as previously observed and shown in Figure 29.

Figure 32 shows the results of the addition of large concentrations of neat NO_2 to Shelldyne-H over a broad temperature range. The ignition delay was independent of the NO_2 concentration above 8 weight percent as evidenced by the constant slope of the curve for NO_2 concentrations that varied from 23.8 to 71 weight percent.

Additive Effectiveness in H-MCPD

The high density (although somewhat lower than Shelldyne-H) and high heat of combustion of fully saturated methylcyclopentadiene also made this fuel a good candidate for volume-limited propulsion applications. The optimization of additive loading and the screening of ignition promotion effects with other types of additives was carried out much in the same manner as previously described for Shelldyne-H. Figure 33 shows that the alkoxyl radical generating additive 1,2-dimethoxyethane was almost non-effective in reducing the ignition lag time of H-MCPD in a 25 volume-percent concentration. On the other hand, the alkyl nitrates and nitrites were observed to be good promoters of H-MCPD ignition. The nitrate and nitrite esters were less effective in H-MCPD compared to Shelldyne-H for equivalent additive concentrations and the air inlet temperature range of 950°-1250°K. The overall activation energy of H-MCPD ignition derived from the Arrhenius temperature dependence was about 35 KCal/mole compared to 40 KCal/mole for Shelldyne-H. The addition of 25 volume percent n-butyl nitrate to H-MCPD reduced the activation energy to 10.5 KCal/mole. A similar reduction in activation energy was observed in Shelldyne-H.

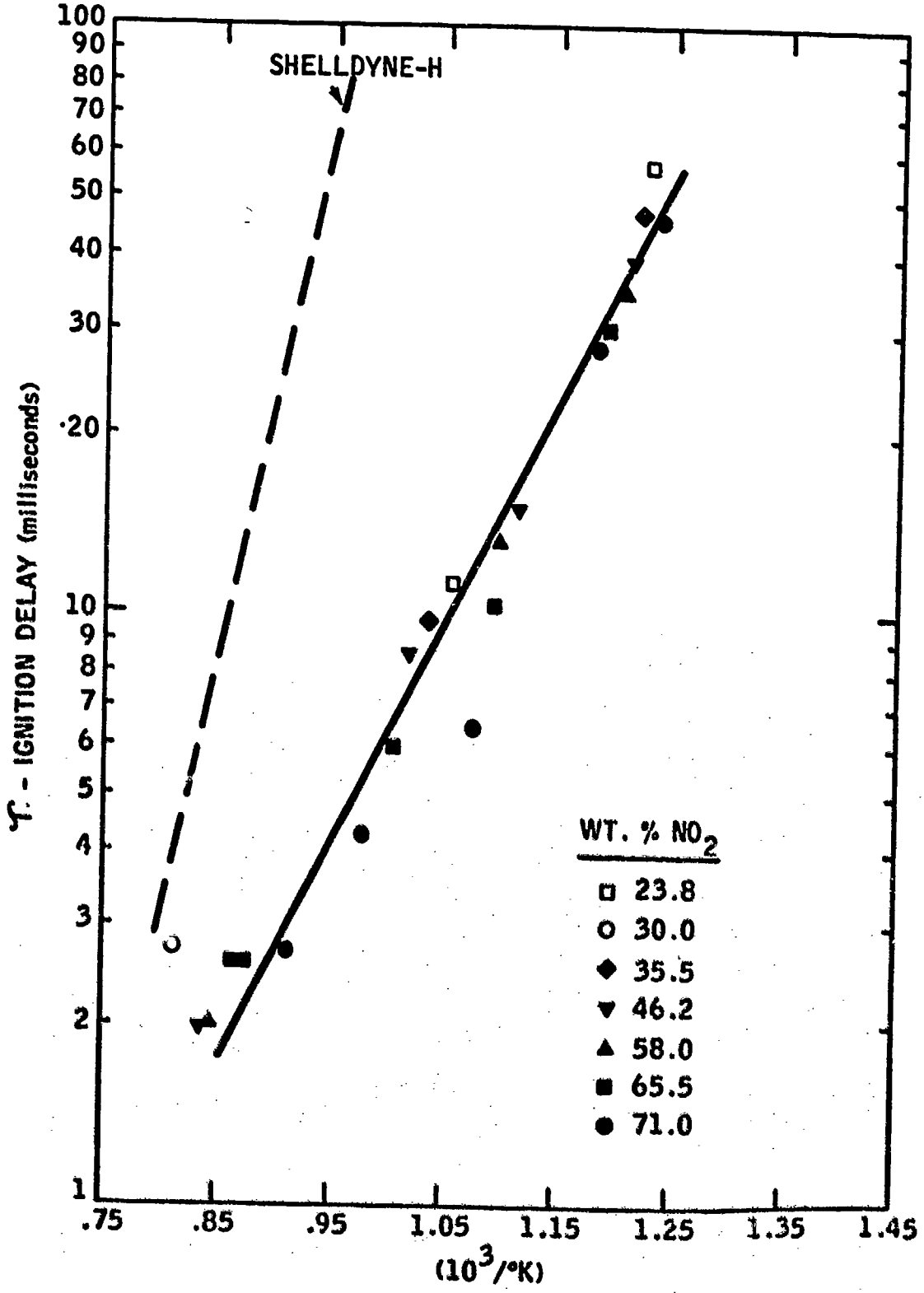

Figure 32. The Effect of NO_2 Concentration on the Ignition Lag of Shelldyne-H.

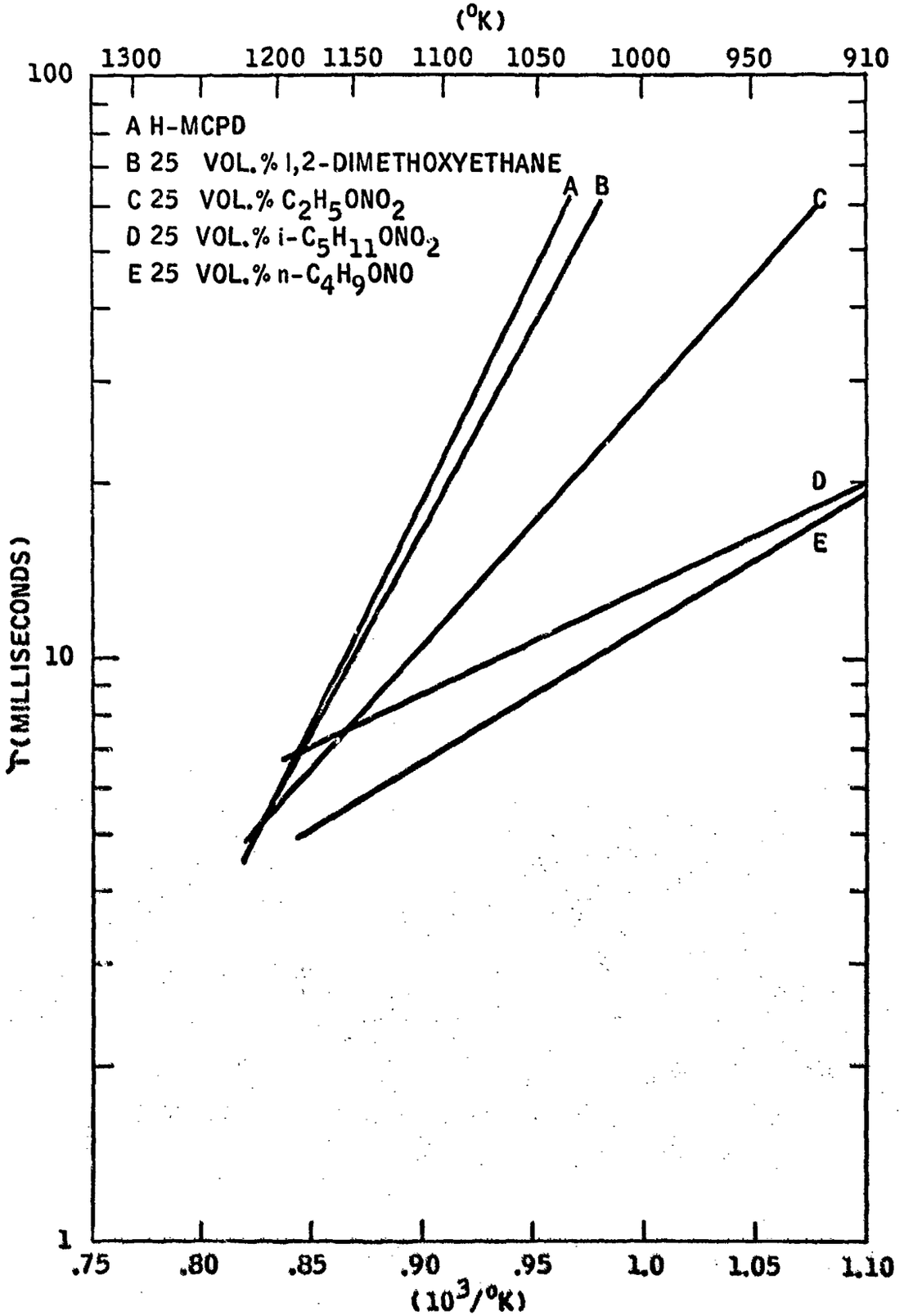

Figure 33. THE EFFECTS OF VARIOUS ADDITIVES ON THE IGNITION OF H-MCPD*

* hydrogenated dimer of methylcyclopentadiene

The visible flames of the H-MCPD with alkyl nitrates and nitrites were similar in character to the Shelldyne-H flames, except that the intensity of the latter was much greater. The fluid viscosity of H-MCPD, although only 23 centistokes at 0°F compared to 35 centistokes for Shelldyne-H, was also noticeably improved by the addition of low concentrations of the nitrate and nitrite esters.

Table VII is a comparison of the physical and combustion characteristics of neat hydrocarbon fuels and blends of n-propyl nitrate with either H-MCPD or Shelldyne-H. It was previously shown that the best homogeneous additives were the alkyl nitrates and nitrites. Since each compound within their respective homologous series thermally decompose to affect the autoignition reactions in the same manner (O-N bond fission), the exact family member chosen to represent that class of compounds was a compromise which was dictated by such factors as; cost, heat of combustion, density, flash point and weight fraction NO_x available. n-Propyl nitrate was selected as the candidate which fulfilled those properties.

Although Table VII compares propyl nitrate blends with Shelldyne-H or H-MCPD for two different concentrations, the ignition delay data and thermodynamic data given for the other fuels in Table VIII allows one to compute the effect of additive concentration on the volumetric heat release and ignition delay for other fuel blends.

Additive Effects in JP-7

The chemical composition of JP-7 is typically 90 percent normal and isoparaffins, 5 percent aromatics and the remainder as napthenes. The average number of carbon atoms is in the range of C_{11}-C_{14}. The molecular formula is best represented as $C_{12}H_{26}$. Because of the wide dispersement of JP-7 in the field, this fuel was also considered as a possible candidate for supersonic combustion propulsion applications.

Figures 34 and 35 summarize the effects of various homogeneous additives on the ignition lag of JP-7. The fuel used in all the tests was received from Air Force stores and was not identified further.

The alkyl nitrates and nitrites or nitric oxide were observed to be the most effective ignition promoters compared to such additives as 1,2-dimethoxy-ethane, tertiary butylhydroperoxide and ethyl oxolate. For 25 volume percent additive concentrations the most effective additives were n-amyl nitrite and iso-amyl nitrate. Curve G of Figure 34 shows the ignition promoting effect of n-butyl nitrite on a binary fuel blend consisting of JP-7 and octene-1, compared to the additives effect in JP-7 alone. As has been observed previously, the presence of the double-bond in octene-1, enhanced the effectiveness of the alkyl nitrite in reducing the overall ignition delay of the binary fuel blend. Figure 35 shows the same effects for various binary fuel blends for 25 volume percent nitric oxide additions. These results show that nitric oxide seems to be most effective in long chain paraffins such as n-tetradecane compared to n-octane. The two, double bonds in 1,7-octadiene clearly is more receptive to the ignition promoting effects of nitric oxide than either JP-7 n-octane or octene-1.

TABLE VII

PHYSICAL AND CHEMICAL PROPERTIES
OF HIGH DENSITY FUEL BLENDS

Fuel	Sg	BTU Gal.	BTU Lb.	τ @ 1000.K (Milisec.)
Shelldyne-H	1.1	163,000	17,800	180
50% Shelldyne-H 50% $C_3H_7NO_3$	1.08	117,250	12,950	2.5
75% Shelldyne-H 25% $C_3H_7NO_3$	1.09	139,000	15,300	3.5
H-MCPD	0.93	143,000	18,400	145
75% H-MCPD 25% $C_3H_7NO_3$	0.96	124,900	15,600	5.5
n-$C_3H_7NO_3$	1.06	71,500	8,100	2-3
JP-7	0.80	124,000	18,600	110

TABLE VIII

HEATS OF COMBUSTION OF VARIOUS HYDROCARBONS

Fuel	Mol. Wt.	$-\Delta$ Hc (KCal./Mole)
n-Propyl Nitrate	105.1	470
Cyclohexene	82.1	842.4
Cyclohexane	84.2	875.6
1-Hexene	84.2	894.2
Hexane	86.2	915.9
Methyl Cyclohexane	98.2	1018
4-Vinyl Cyclohexene	108.2	(1100)
(H-MCPD)	124	1274
Tetralin	132	1288
Decalin	138	1396
Shelldyne "H"	187	1847

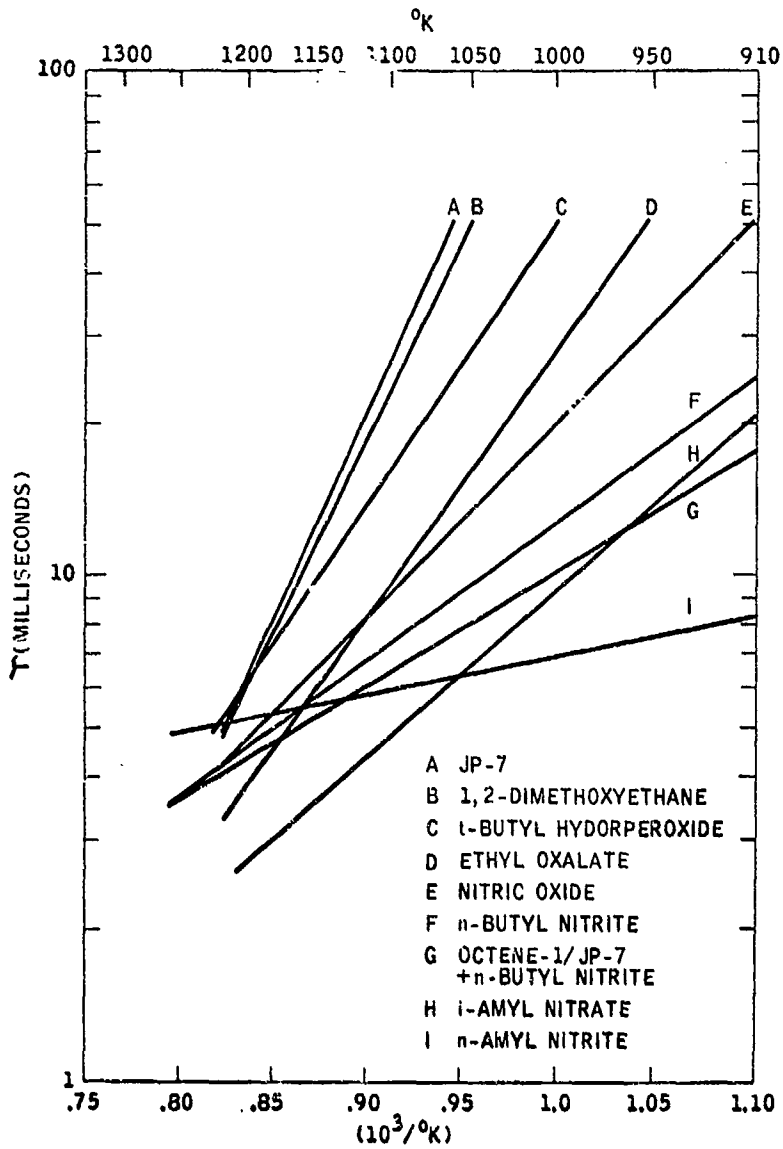

FIGURE 34. EFFECT OF VARIOUS ADDITIVES ON THE IGNITION DELAY OF JP-7 IN THE CFS

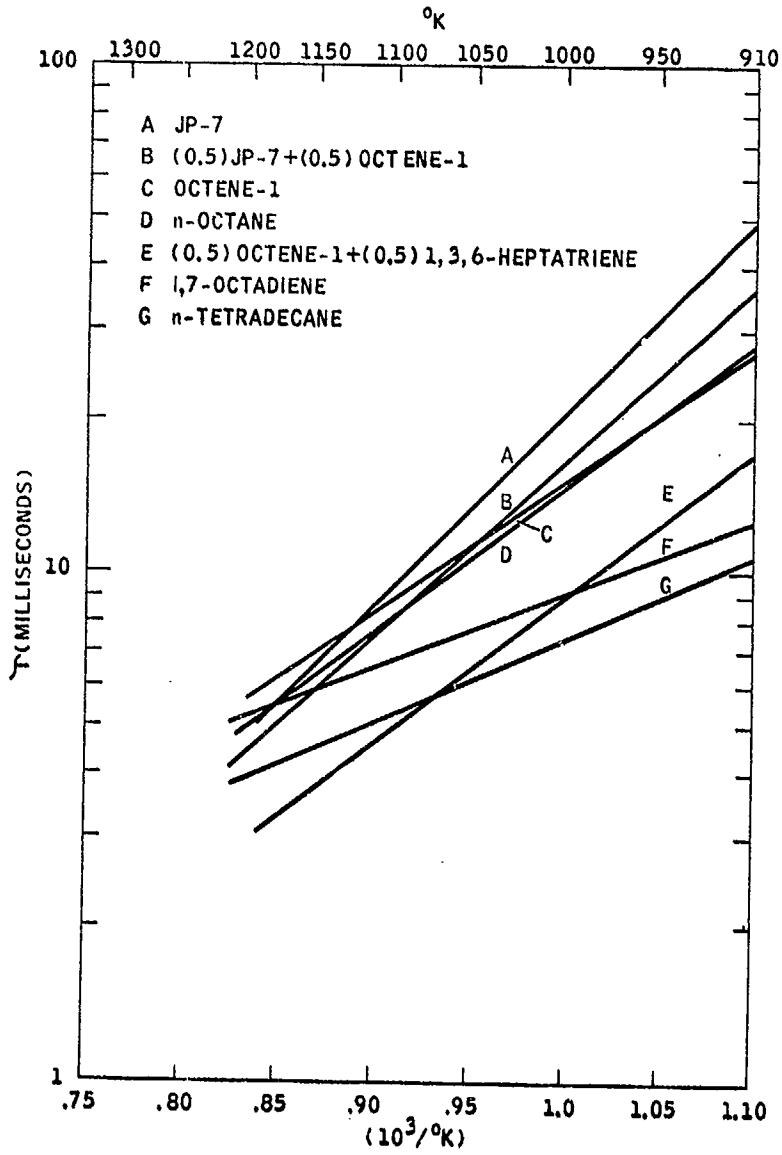

FIGURE 35. THE EFFECTS OF 25 VOLUME PERCENT (NO) ON THE IGNITION DELAY OF JP-7 IN THE CFS

The overall activation energy derived from the Arrhenius temperature relationship of JP-7 was 38.6 Kcal/mole. The best additive n-amyl nitrite reduced the activation energy to about 5 Kcal/mole. At 1000°K the ignition delay times of JP-7 and a 25% blend of n-amyl nitrite were 145 and 8 milliseconds, respectively.

The ignition of JP-7 blends with other more reactive fuels was observed to occur in a two phase process. Simultaneously, two discrete flame fronts appeared in the test duct separated from the injector by a distance proportional to the relative ignition delay of each fuel. After a short time the flame fronts merged at a longitudinal distance closer to the fuel injector compared to the location of the flame front observed for the least ignitable fuel. The alkyl nitrates or nitrites and nitric oxide exhibited their characteristic grey-blue flames when added to JP-7. The ignition of JP-7 produced a blue-white flame much the same as was observed in tests with the paraffins. The yellow-green tail, attributed to the NO+O-atom recombination reaction was always observed in varying intensities for JP-7 blends with the oxides of nitrogen (except N_2O) or the nitrogen esters.

G. Effects of Nitric Oxide in Various Fuels

Table IX summarizes the effects of nitric oxide on the autoignition delay of JP-7, Shelldyne-H, n-octane and 1,7-octadiene. Over the air inlet temperature range of 950-1150°K, and a nitric oxide concentration range of 0-50 volume percent, the ignition promoting effect of nitric oxide was outstanding. At 950°K, the addition of 10 percent nitric oxide reduced the ignition lag of all the hydrocarbon fuels by at least a factor of two. When the nitric oxide concentration was increased to between 10 and 25 percent, the ignition lag of Shelldyne-H was reduced by a factor of 100 at 950°K.

The effects of neat NO_2 on the ignition lag of Shelldyne-H was also determined and the data are shown in Figure 32. Due to limitations imposed by the experimental technique, quantities of neat NO_2 less than 23 weight percent could not be evaluated. The concentration was varied from 23-71 percent over the temperature range of 950-1250°K. The results clearly show that the ignition delay of Shelldyne-H is primarily temperature dependent for NO_2 concentrations greater than 23 percent. These results are in accordance with the previous findings concerning the dissociation of NO_2 from alkyl nitrates which are illustrated in Figure 31 which showed the ignition delay of Shelldyne-H to be inversely proportional to the logarithm of the additive concentration. The addition of up to 50 volume percent nitrous oxide (N_2O) to Shelldyne-H over the temperature range of 950-1250°K had no visible effect on the combustion process nor any ignition promoting effect.

TABLE IX

EFFECT OF NITRIC OXIDE ON THE IGNITION OF VARIOUS FUELS

IGNITION DELAY (MILLISECONDS)

AIR TEMP. (°K)	950				1000				1050				1100				1150			
VOLUME % NO	0	10	25	50	0	10	25	50	0	10	25	50	0	10	25	50	0	10	25	50
JP-7 ($C_{12}H_{26}$)	360	120	32	21	140	57	22	15	54	28	15	10	25	16	11	7.5	12	9	7	5.5
SHELLDYNE-H ($C_{14}H_{16}$)	400	--	15	14	180	--	11	11	64	--	8.5	9	23	--	6	7	8.5	--	4.5	6.0
n-OCTANE (C_8H_{18})	64	34	21	12.5	37	23	15	9.5	23	16	11	7	15	11	8	5.5	10	8	6	4.5
1,7-OCTADIENE ($C_{14}H_{16}$)	41	20	11	--	25	12	9	--	14	8	7.5	--	9	--	--	--	6	--	--	--

However, because all the alkyl nitrates and nitrites thermally decompose in the same manner with similar decomposition energies (34-36 Kcal/mole[29]) it was not surprising that the overall ignition activation energies calculated from the slopes of the Arrhenius plots were nearly identical. This similarity suggests that the pre-ignition reaction involving these compounds were associated with cleavage of the O-N bond.

H. Effectiveness of Miscellaneous Additives

The search for homogeneous ignition promoters resulted in the evaluation of many different chemical compounds in the continuous flow system. When a particular additive did not show any evidence of promoting the ignition of a test fuel, the additive was re-evaluated in a fuel having a different molecular structure. Long chain alkanes, alkenes, and complex fuels like Shelldyne or JP-7 were used as the test fuels.

In all cases the following additives did not show any ignition promoting effects in lean hydrocarbon-air mixtures, in varying concentrations over the temperature range of 900-1250°K.

oxygen
carbon monoxide
water
hydrogen
nitrous oxide
formic acid
tri-isobutyl borane
carbon monoxide + water

I. Catalytically Promoted Hydrocarbon Ignition in CFS with Platinum

Utilizing the experimental arrangement described in Section IIIC the hydrocarbon ignition promoting characteristics of platinum were evaluated over the temperature range of 500-1150°K, an air flow velocity range of 85 to 150 feet sec^{-1} and a maximum Reynolds Number of 10^4. The equivalence ratio of the fuel-air mixtures was varied from 0.1 to 5.0. Three dimensional fluid dynamic mixing calculations, which described the mixture stoichiometry, temperature and velocity of the reacting streams were performed over the range of experimental conditions studied. The analytical results indicated that one-dimensional mixing was developed approximately 10-test section diameters downstream of the fuel injector (test section diameter is 1.065 inches). Fully developed turbulent pipe-flow existed in the area of the duct where the platinum cylinder was located. The total surface area of the platinum was 18.9 $in.^2$.

The possibility that the platinum cylinder's leading edge acted as a flame holder was assumed to be unlikely because the wall thickness of the platinum tube was .008 inches. To further satisfy ourselves that the ignition promoting effects observed were due to the catalytic activity of the platinum and not due to the physical properties of the material, a duplicate cylinder made of type 304 stainless steel was inserted into the test section in place of the platinum cylinder. The hydrocarbon ignition promoting effects were only observed when the platinum cylinder insert was utilized.

An orange glow was observed to appear at the exit of the test section when NO_2 was injected into the air stream in the absence of hydrocarbons. The intensity of the glow was only slightly dependent upon the concentration of NO_2 over the air inlet temperature range of 900-1250°K. Attempts to identify the spectral content of the orange glow were not successfull. Similar tests with NO or N_2O produced no visible exhaust emissions. The nature of the glow seemed to be similar to the observations reported by other investigators who identified the glow as electronically excited (NO_2*).[30,31] Paulsen identified the mechanism as:

$$NO_2 + M \rightleftarrows NO_2^* + M$$
$$NO_2^* \longrightarrow NO_2 + hr$$

where M is N_2 or O_2.

J. The Synergistic Effect of H_2 + NO

Hydrogen, as a homogeneous additive in concentrations up to 3 weight percent of the fuel flow, had no observable ignition promoting effect in alkanes, alkenes or cyclic fuels, although the hydrocarbon flame temperatures were much higher due to the ΔH_c of hydrogen. However, when H_2 was added to the hydrocarbon fuel in the presence of nitric oxide, the ignition delay of the mixture was much less than it would be when only nitric oxide was added. The effect of varying the concentration of H_2 in octene-1 with 25 volume percent nitric oxide was determined over the temperature range of 950-1200°K, is shown in Figure 36. Clearly, with up to 35 volume percent addition of H_2 to octene, there was no improvement in the ignition lag at 950°K. However, even at a concentration of 5 percent, hydrogen was observed to synergistically decrease the ignition lageof octene when 25 percent nitric oxide was added. Fifteen percent hydrogen in a 25 percent blend of nitric oxide and octene-1 was observed to decrease the ignition lag by nearly a factor of 2 at 950°K compared to the case where no hydrogen was present.

K. Auto-Ignition Delay Times of Neat Alkyl Nitrates and Nitrites in Air

The autoignition delay times of four different nitrogen esters are plotted in Figure 38. These results were obtained under lean mixture conditions. The liquid compounds were injected into the hot air stream via the hypodermic syringe injection technique described in Section IIIB. The data show that the alkyl nitrites generally rqquire a longer time to ignite compared to the alkyl nitrates. Another distinct characteristic of these ignition delay data is the fact that the overall activation energies of all the additives were extremely low, typically about 5 Kcal/mole. The lowest ignition delay was measured for ethyl nitrate. Following in their order of increasing lag times were iso-amyl nitrate, n-amyl nitrite and n-butyl nitrite. The fact that the lowest ignition lags were measured for the alkyl nitrates, was indicative of the relatively large mass fraction of NO_x evolved during its thermal decomposition. The nitrites, containing less NO_x on a weight fraction basis than the nitrates had correspondingly longer ignition lags.

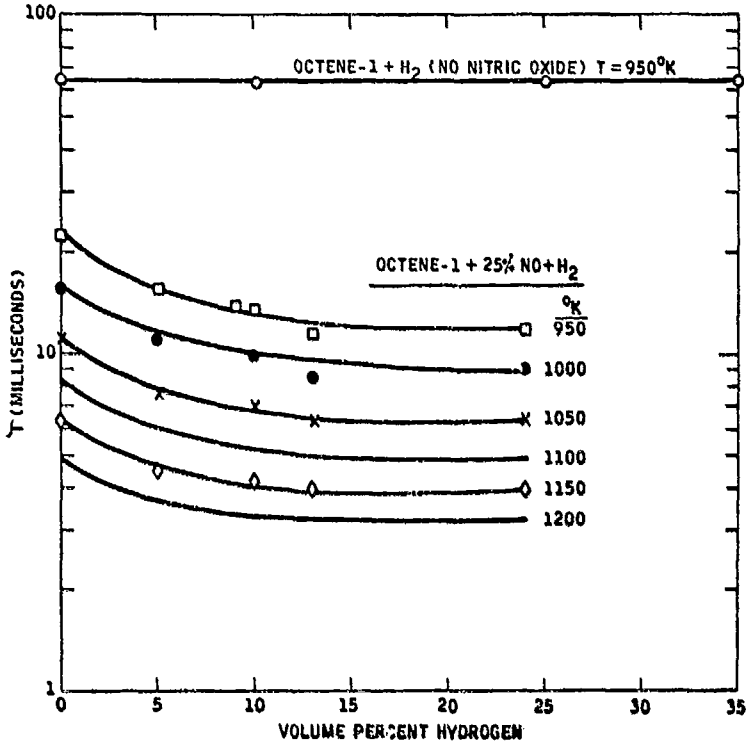

FIGURE 36. SYNERGISTIC EFFECT OF H_2 + NO ON THE IGNITION DELAY OF OCTENE-1 IN THE CFS

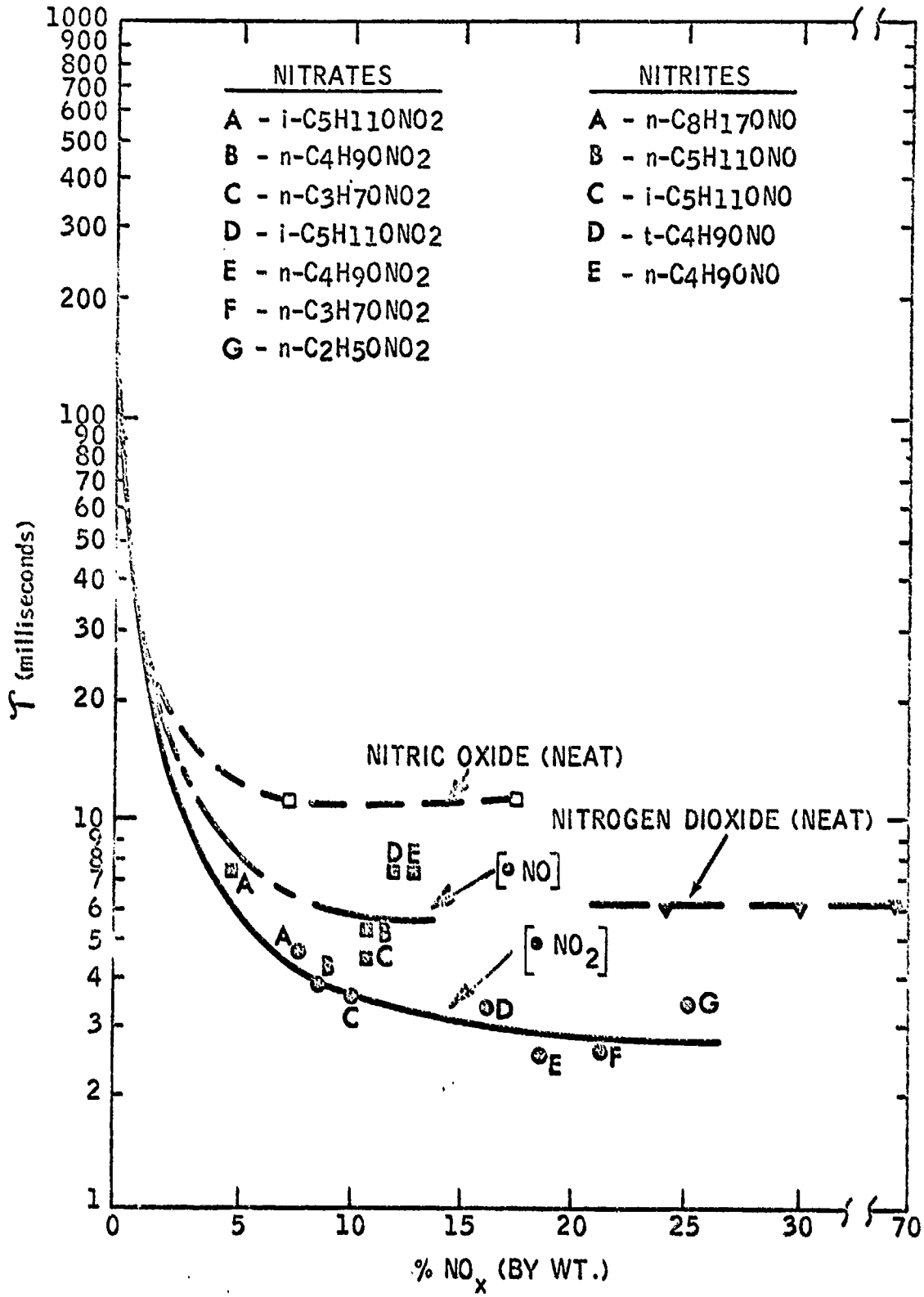

Figure 37. Comparison of Effectiveness of O-Atom Generating Additives on the Ignition Lag of Shelldyne-H at 1000°K Air Inlet Temperature

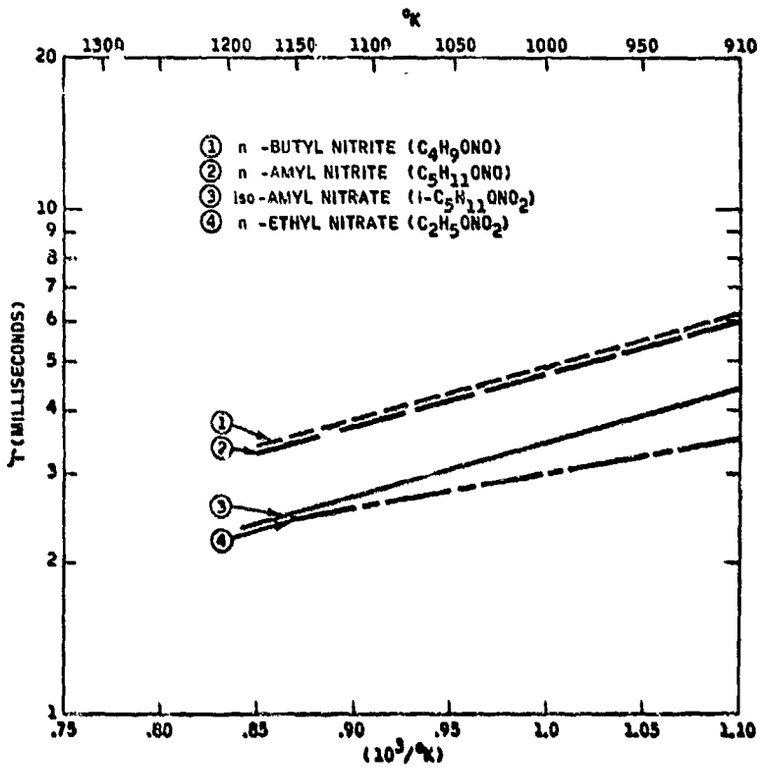

FIGURE 38. AUTOIGNITION DELAY CHARACTERISTICS OF ALKYL NITRATES AND NITRITES

When the platinum linear was initially tested, as received from the vendor[a], the ignition promoting results were very erratic and unrepeatable. Shelldyne-H was the first test fuel. In order to eliminate the cause of this erratic behavior, the platinum was cleaned in concentrated hydrofluoric acid, reduced in a hydrogen atmosphere at 600°C for 3 hours and then reinserted into the test section. The ignition promoting results were again observed to be unreproduceable and very erratic. Upon inspection of the platinum a tan-colored film was observed to be evenly dispersed over the entire surface which had been exposed to the combustion environment. Repeated attempts to remove the film by soaking in acids, solvents or by high temperature reductions with hydrogen proved to be futal. Subsequently, it was found that the only surface preparation method which produced repeatable ignition results was to "age" the platinum tube, in-situ. The "aging" process was observed to be completed when repeatable ignition results were obtained over the temperature range of interest. It is estimated that the platinum surface was exposed to high temperature oxidizing and reducing atmospheres generated by mixtures of fuel and air for a total accumulated time of about two hours. Each time an ignition reaction did occur in the test section, the platinum surface temperature was estimated to approach the flame temperature, which for most hydrocarbons was greater than 1500°C. At the termination of each day's tests the platinum tube was stored under methanol. The surface of the catalyst retained the tan-film. Continuous exposure, even to very rich products of combustion of various hydrocarbon fuels did not alter the appearance of the film nor did this exposure cause any carbonaceous deposits to accumulate anywhere on the surface. The same platinum tube was utilized in all the ignition tests reported.

The sequence of events which led to the ignition of the fuels was found to vary according to the air temperature. In the temperature range of 900-1150°K, ignition was extremely rapid and produced highly luminous flames inside the test duct. At temperatures between 500-900°K the ignition sequence consisted of a gradual heating of the platinum surface as evidenced by orange-red color, followed by the establishment of the flame front on the platinum surface. At higher temperatures the flame front anchored itself near the leading edge of the platinum tube. As the air temperature decreased the position of the flame front moved further downstream until finally, no flame was visible. However, even though no visible flame existed below 550°K, the catalytic activity was evident by the orange color of the platinum tube which resulted from exothermic reactions occurring on the surface.

The ignition data for various hydrocarbon fuels and 15 volume percent blends of n-propyl nitrate with the fuels are given in Figures 39 through 43. The tabulated ignition data are given in Table X. The curves describe the ignition limit of the mixture as a function of air temperature and equivalence ratio. The area above the curves represents the ignition region and the area under the curves defines the region of no-ignition. Table 8 gives the molecular weights and heats of combustion of the fuels tested.

(a) Englehart, Newark, N.J.

TABLE X

CATALYTICALLY PROMOTED (Pt)
IGNITION CHARACTERISTICS OF HYDROCARBONS

Equivalence Ratio (Ø)

Temperature (°K)	550	600	650	700	750	800	850	900	950	1000	1050	1100
Tetralin				1.98	1.73	1.57	1.44	1.37	1.34	1.16	0.86	
Tetralin + 15 N.P.N.(a)				(1.96)	1.23	0.77	0.48	0.32				
1-Hexene				2.08	1.49	1.18	1.01	0.88	0.79	0.71	0.65	
1-Hexene + 15 N.P.N.			1.50	(0.38)								
Methyl Cyclohexane		2.65	1.91	1.70	1.56	1.48	1.41	1.37	1.35			
Methyl Cyclohexane + 15 N.P.N.	(4.1)	(1.15)										
Cyclohexane	1.93	1.83	1.82	1.72	1.52	1.25						
Cyclohexane + 15 N.P.N.	1.54	(0.38)										
Hexane			1.97	1.48	1.21	1.04						
Hexane + 15 N.P.N.	(6.6)	1.32										
H MCPD					1.70	1.34	1.04	0.80	0.61	0.45	0.33	0.22
H MCPD + 15 N.P.N.			1.18	0.92	0.75	0.61	0.50	0.41	0.33	0.27	0.22	(0.18)
Decalin		1.83	1.46	1.26	1.14	1.05	1.00	0.90	0.70	0.64	0.51	
Decalin + 15 N.P.N.	2.28	1.52	1.16	0.95	0.78	0.67	0.56	0.45	0.36	0.27		
Cyclohexene		1.73	1.24	0.96	0.81	0.75	0.69	0.61	0.54	0.44	0.35	
Cyclohexene + 15 N.P.N.		(1.90)	1.55	1.24	0.94	0.66	0.44	0.38	0.34	0.32	0.31	0.30
Shelldyne - H						0.98	0.73	0.60	0.49	0.40		
Shelldyne - H + 15 N.P.N.		2.75	2.15	1.75	1.38	1.11	0.89	0.71	0.57	0.38	0.15	
4-Vinyl Cyclohexene				1.67	1.15	0.94	0.83	0.77	0.73	0.71	(0.69)	
4-Vinyl Cyclohexene + 15 N.P.N.				1.35	0.94	0.71	0.58					

(a) n-propyl nitrate volumetric concentration

(parentheses indicate extrapolated Ø)

Figure 39 contains the catalyzed autoignition limits of hexane, hexene-1 and 15 vol. percent propyl nitrate blends of each of the fuels. The minimum auto-ignition temperatures of the neat fuels were found to be 650°K for hexane compared to 700°K for hexene-1. The equivalence ratios of both fuel-air mixtures was about 3.0 at the rich ignition limit and less than 1.0 for the lean limit.

The addition of 15 volume percent $C_3H_7ONO_2$ to either fuel had a substantial effect in reducing the autoignition temperature at the rich mixture limits. The additive effect was most pronounced in hexane as evidenced by the reduction in ignition temperature from 650°K to 570°K. The additive concentration in the fuels was taken into consideration when the equivalence ratios were calculated. These results are quite significant when the spontaneous ignition temperatures reported in the literature are compared to the platinum catalyzed results. Table XI is a summary of spontaneous ignition temperatures (S.I.T.) and flammability limits usually obtained under static test conditions, from the literature.

The platinum catalyzed autoignition temperature limits of decalin, tetralin and 15 vol. % blends with n-$C_3H_7ONO_2$ are given in Figure 40. The lean and rich ignition limits for decalin are 1050°K and 570°K respectively compared to 1090°K and 675°K respectively for tetralin. The minimum ignition temperatures (M.A.T.) for both of these fuels occured at an equivalence ratio of 2.0-2.5. The spontaneous ignition temperatures (S.I.T.) reported in the literature and given in Table XI are 520°K for decalin and 654°K for tetralin. The platinum catalyzed minimum ignition temperatures of these fuels are in general agreement with their published S.I.T. values.

n-Propyl nitrate decreased the platinum catalyzed minimum ignition temperature of decalin to 550°K compared to only a slight improvement of tetralin's minimum ignition temperature. However, the additive was very effective in reducing the autoignition temperatures of both fuels at lower equivalence ratios, as shown in curves C and D of Figure 40.

Figure 41 compares the platinum catalyzed autoignition limits of Shelldyne-H, H-MCPD and 15% $C_3H_7ONO_2$ blends with both fuels. The minimum autoignition temperatures Shelldyne-H compared to H-MCPD were 785°K and 730°K respectively. The additive reduced the minimum temperature of H-MCPD to 625°K compared to little or no reduction for Shelldyne-H. Also, as previously shown in its effect in decalin and tetralin, the propyl nitrate substantially lowered the ignition temperatures of both fuels, over the entire range of equivalence ratios tested. There are no data available in the literature concerning the S.I.T. values for either of these dense fuels but as a generalization it may be said that the increased magnitude of the minimum autoignition temperatures of these fuels would be expected because they are completely saturated and as such relatively resistive to oxidation. Shelldyne-H and H-MCPD had the highest, minimum autoignition temperatures of any hydrocarbon evaluated in the platinum catalyzed flow device.

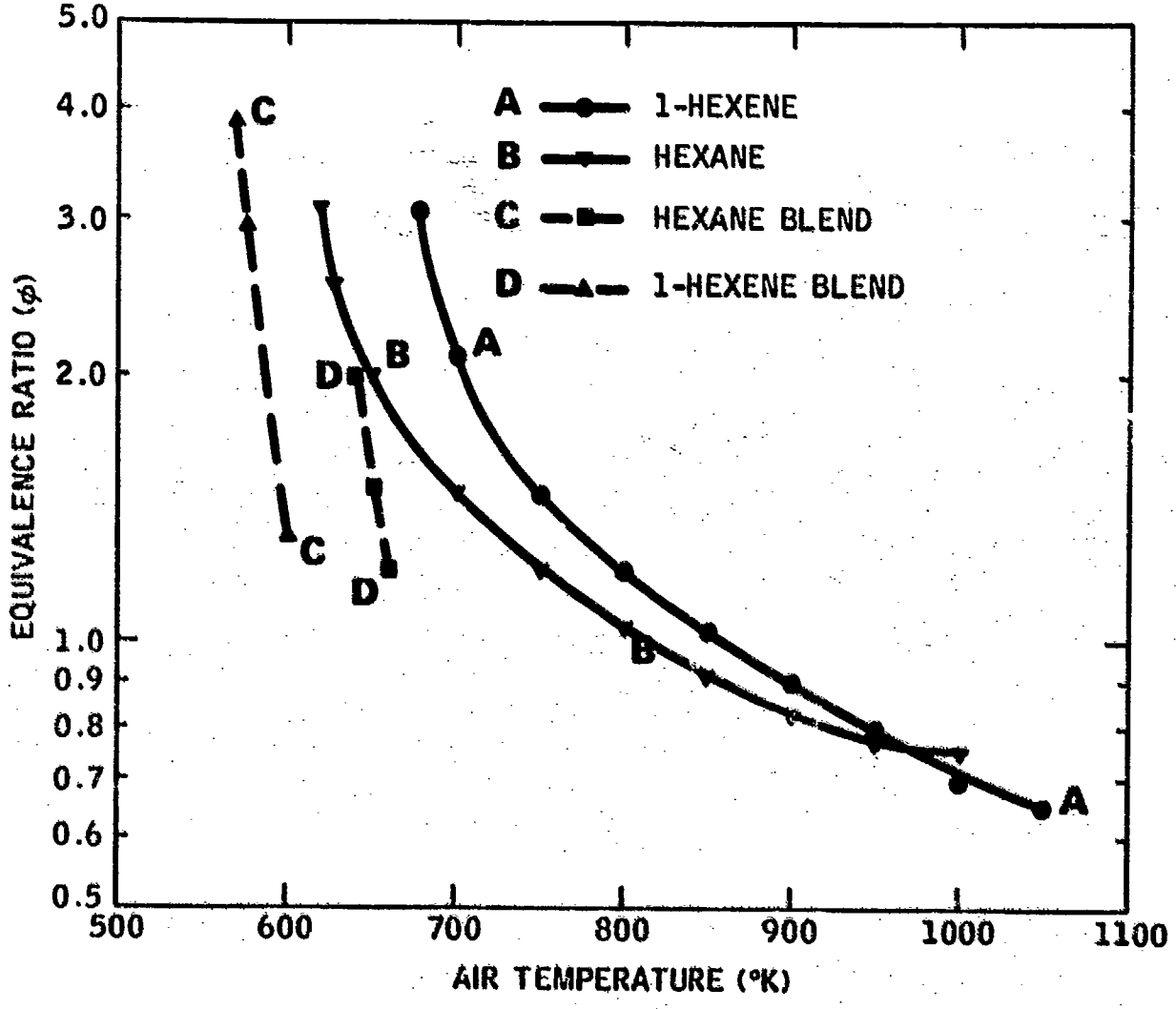

FIGURE 39.

THE EFFECTS OF 15 VOL. % $C_3H_7ONO_2$
ON THE PLATINUM CATALYZED AUTOIGNITION
TEMPERATURE OF SIMPLE HYDROCARBONS

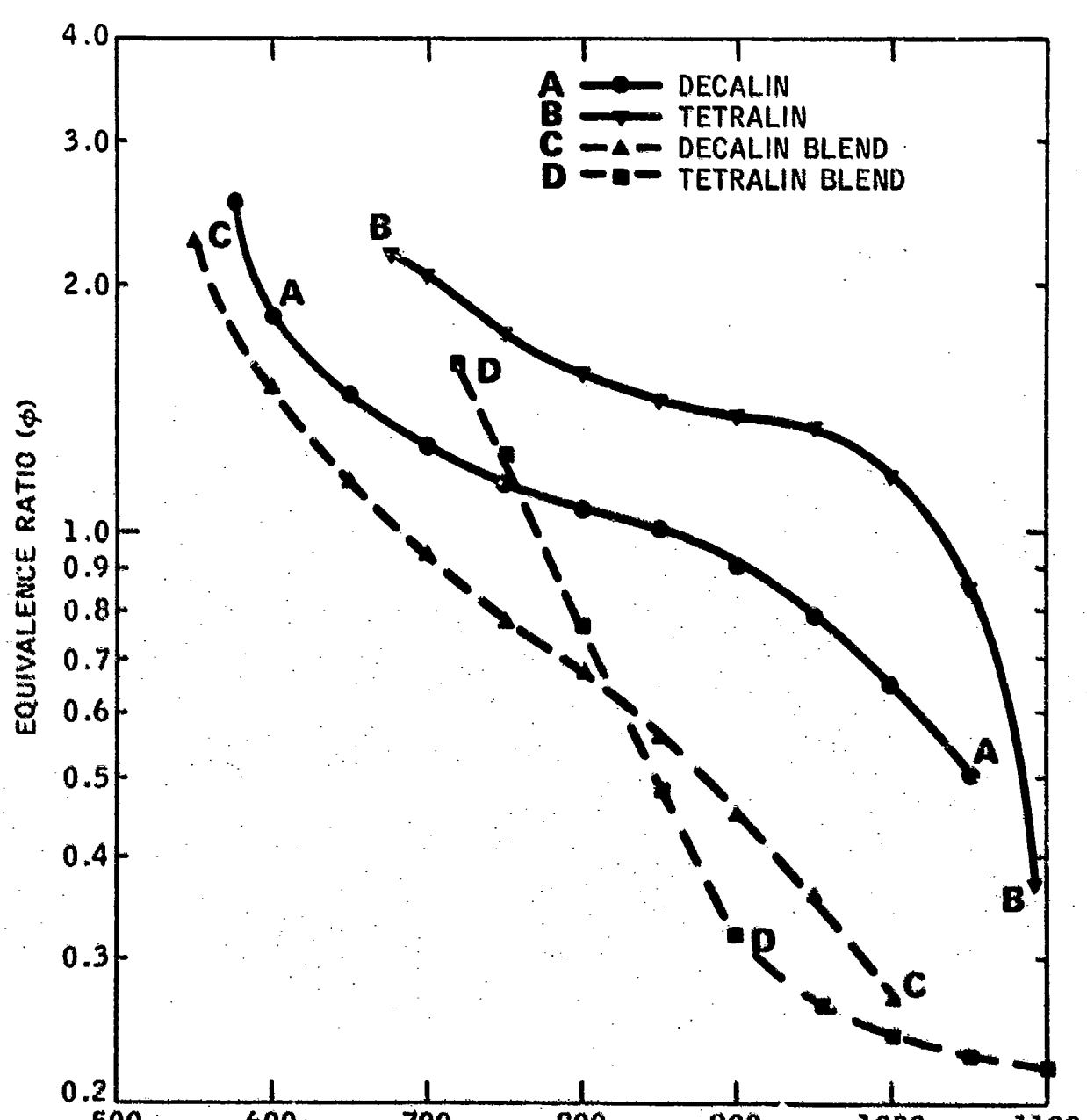

FIGURE 40. THE EFFECTS OF 15 VOL. % $C_3H_7ONO_2$ ON THE PLATINUM CATALYZED AUTOIGNITION TEMPERATURE OF NAPHTHENES

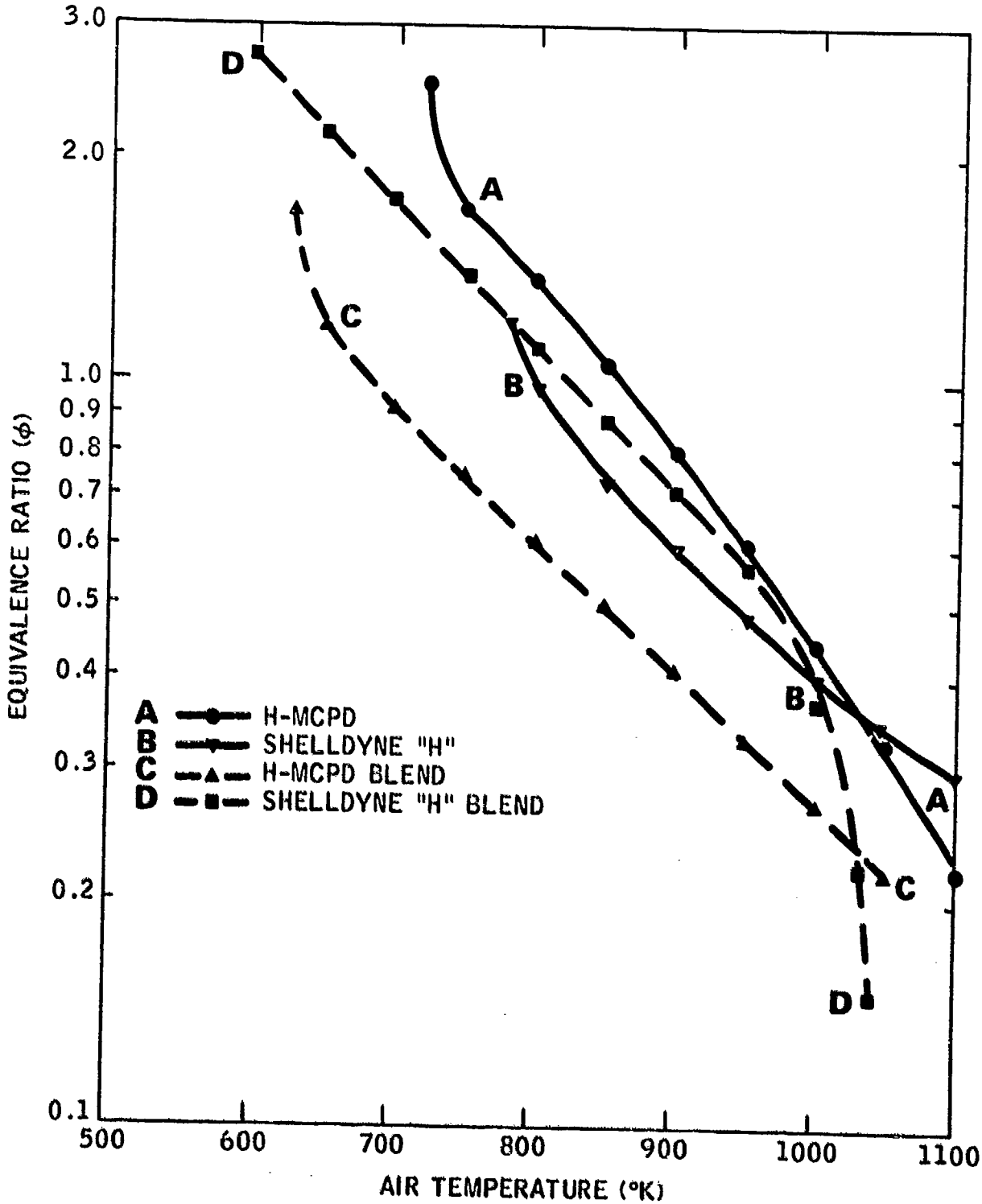

FIGURE 41.

THE EFFECTS OF 15 VOL. % $C_3H_7ONO_2$
ON THE PLATINUM CATALYZED AUTOIGNITION
TEMPERATURE OF HIGH DENSITY HYDROCARBONS

TABLE XI

COMPARISON OF SPONTANEOUS IGNITION TEMPERATURE (S.I.T.) AND CATALYZED MINIMUM AUTOIGNITION TEMPERATURE (M.A.T.) OF HYDROCARBONS

Fuel	(M.A.T.) °C	(S.I.T.) °C	(Ø) @ M.A.T.	$(-\Delta Qc)^{(a)}$ KCal sec^{-1}	$(-\Delta Q\ air)^{(b)}$ KCal sec^{-1}
Cyclohexane	280	251	1.9	11.5	.66
Cyclohexene	300	244	2.6	>12.0	.70
Decalin	300	250	2.6	10.4	.70
Methylcylohexane	330	265	2.6	14.4	.77
Hexane	350	227	3.0	>12.0	.82
Hexene-1	405	253	3.0	14.0	.92
Tetralin	405	384	2.2	12.2	.92
4-Vinylcyclohexene	415	269	2.0	10.4	.96
H-MCPD	460	--	2.5	10.5	1.07
Shelldyne-H	515	--	1.2	5.8	1.16

(a) Heat input of fuel in KCal/Sec. at Ø and (M.A.T.).

(b) Enthalpy of air stream in KCal/sec. at (M.A.T.).

Some other hydrocarbons which have rather low platinum catalyzed autoignition temperatures are cyclohexene and 4-vinylcyclohexene. Because of the chemical nature of these hydrocarbons imparted by the activity of the double bond, hydrogen abstraction and oxidation reactions at moderate temperatures are rapid. Figure 42 shows that cyclohexene had a minimum autoignition temperature of 570°K compared to 4-vinyl cyclohexene which had a value of 685°K at a similar mixture ratio. The spontaneous ignition temperatures (S.I.T.) of cyclohexene and 4-vinyl cyclohexene obtained from the literature were 514°K and 540°K respectively.

The qualitative agreement between the published values of S.I.T. and platinum catalyzed minimum autoignition temperatures of these fuels is quite good. However, the propyl nitrate additive in these fuels was observed to have virtually no effect on the minimum autoignition temperature for rich mixtures. In fact, the additive appeared to slightly increase the minimum autoignition temperature of cyclohexene.

The spontaneous ignition temperatures obtained from the literature for methyl cyclohexane and cyclohexane are 535°K and 521°K, respectively. The catalyzed minimum autoignition temperatures given in Figure 43 show that methyl cyclohexane's lowest ignition temperature was 600°K compared to 550°K for cyclohexane. The presence of the methyl group increased the autoignition temperature relative to cyclohexane in the referenced values for S.I.T. as well as for the catalyzed ignition values.

The effect of $n\text{-}C_3H_7ONO_2$ addition (15 vol.%) to either fuel reduced the minimum autoignition temperatures from 600 to 570°K in methylcyclohexane compared to a reduction from 550°K to 535°K for cyclohexane. Although Figure 43 illustrates the effectiveness of n-propyl nitrate over a rather narrow temperature range, the trends established with other fuels over a much greater temperature range, indicated that similar promoting effects could also be expected with these fuels.

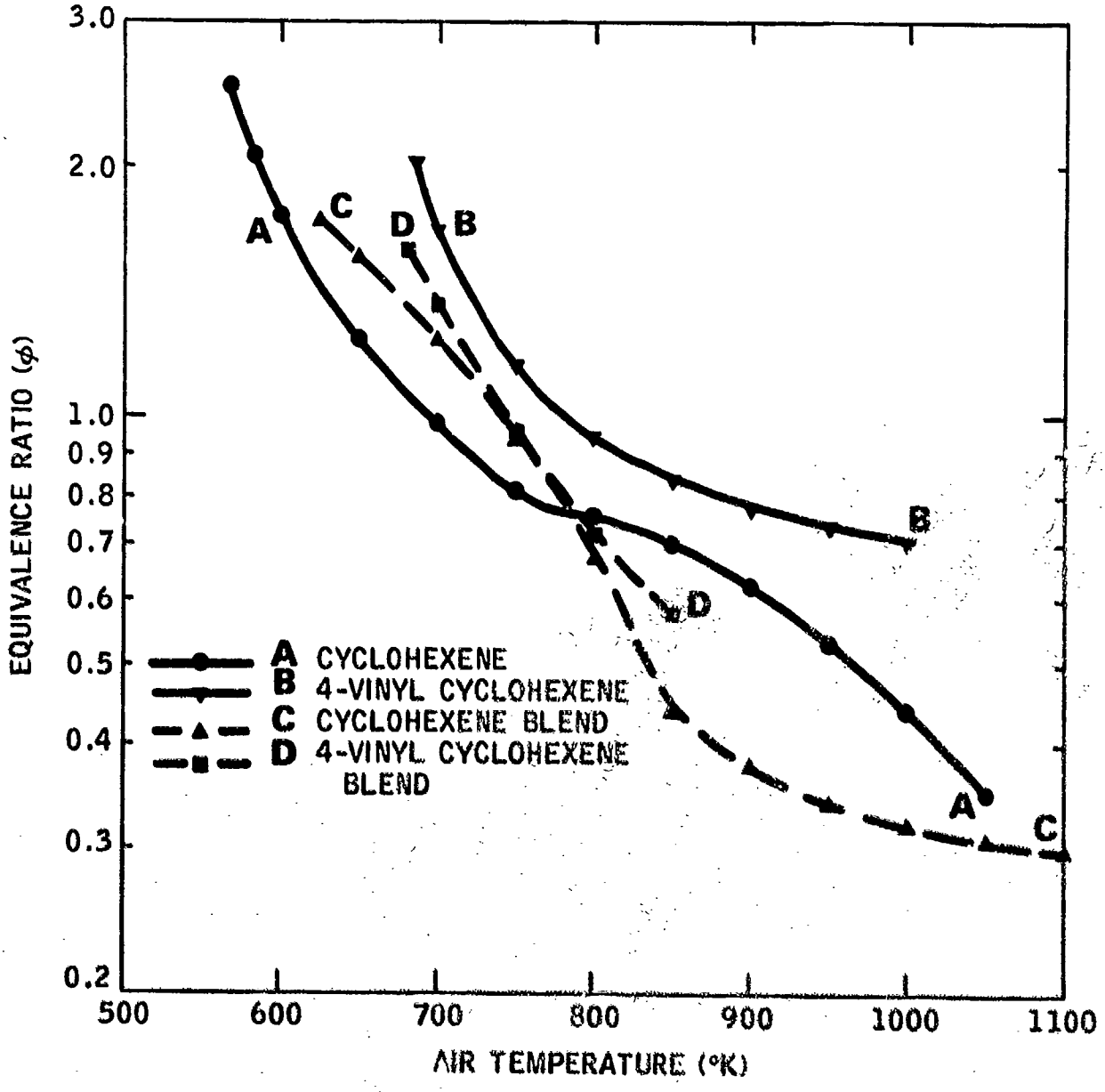

FIGURE 42. THE EFFECTS OF 15 VOL. % $C_3H_7ONO_2$ ON THE PLATINUM CATALYZED AUTOIGNITION TEMPERATURE OF CYCLIC HYDROCARBONS

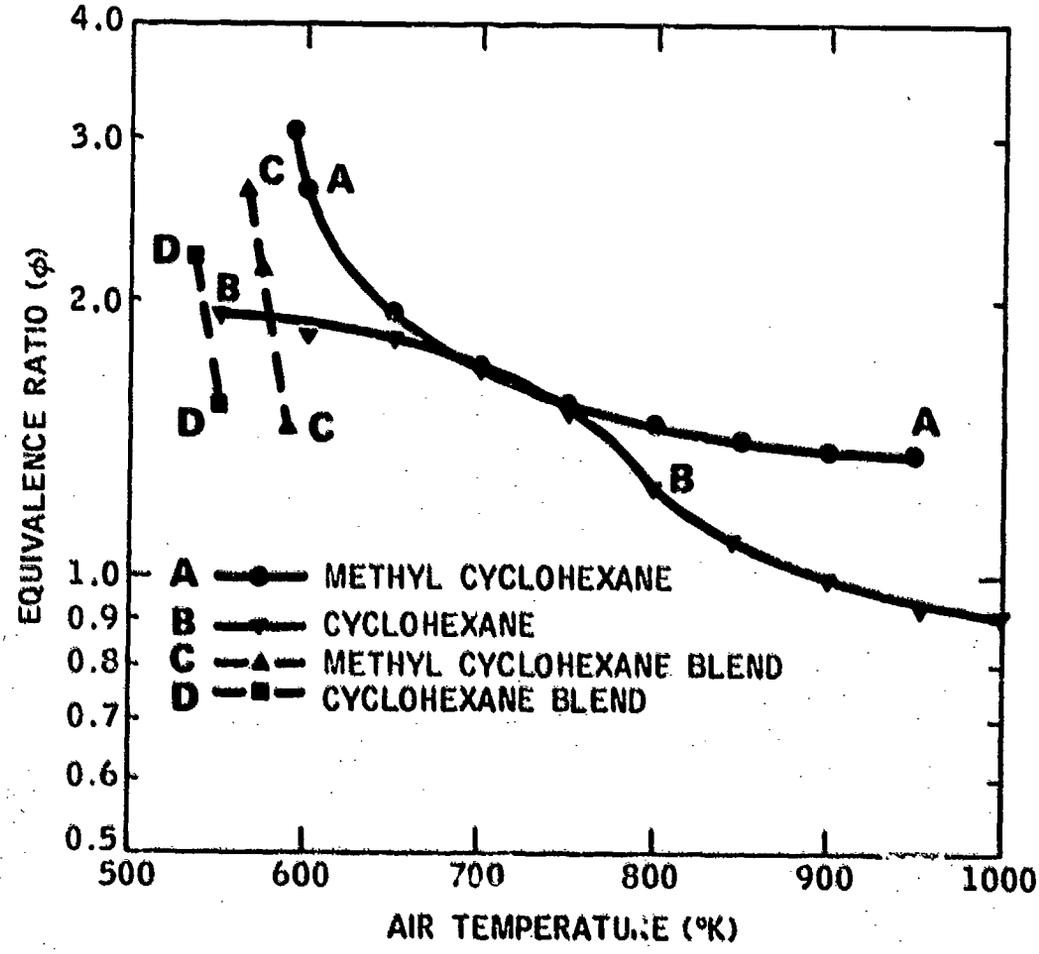

FIGURE 43. THE EFFECTS OF 15 VOL. % $C_3H_7ONO_2$ ON THE PLATINUM CATALYZED AUTOIGNITION TEMPERATURE OF CYCLIC HYDROCARBONS

SECTION V

DISCUSSION

A. Experimental Ranking of Fuels in the W.S.R.

A comparison of the WSR residence time data and the widely published octane-rating and spontaneous ignition temperature data for the same fuels indicate that the controlling mechanisms are closely associated.[32] That is the fuels exhibiting the longest delay times were also reported, in standard octane rating tests, to be least prone to "knocking". The work of Lovell and Campbell[33] showed that the critical compression ratio (C.C.R.) at which fuels could be burned without "knocking" depended heavily upon the chain length of the hydrocarbon molecule, the number and position of methyl groups, the presence of double or triple carbon bonds, etc. Similar correlation between molecular structure and the WSR data can therefore also be excepted. To verify this relationship, the experimental residence time data obtained in the stirred reactor are plotted as a function of the number of carbon atoms in the molecule. Figure 14 reveals a number of interesting generalizations for the relationship between structure and the residence time. Considering the paraffins, it can be seen that in a homologous series, τ decreased as the carbon chain was lengthened except in the case of butane which had an unexplainably larger τ. The addition of methyl groups to a straight chain paraffin caused τ to increase rapidly as evidenced by the marked change in τ observed between 2,4-dimethylpentane and 2-methylpentane and hexane. Similar trends were observed in the olefin series. The anomolous behavior of butane may be due to a similar effect if the "practical grade" material contained branched chain isomers. Unfortunately, the butane sample was never analyzed.

The presence of double bonds in the olefins with carbon chain lengths up to 8 required longer residence times than the normal, long-chain hydrocarbons which contained the same number of carbon atoms. A comparison of the monoolefin octene-1 (C_8H_{16}) and the n-paraffin octane (C_8H_{18}) revealed that τ became similar after the chain was longer than about 6 carbons. However, the diolefin, 2-methyl-1,3-butadiene (C_5H_8) which has two double bonds and a methyl group was observed to have a larger τ than the five or six carbon atom n-paraffins. The cyclic compounds from benzene to Shelldyne-H followed the same general pattern observed in the n-paraffins, except that the paraffins exhibited shorter τ's. The fact that JP-7 contained from 2-5 percent aromatics, about 75 percent paraffins and the remainder as naphthenes and exhibits a residence time similar to that measured in methylcyclohexane (C_7H_{14}) and decalin ($C_{10}H_{18}$), indicated that the presence of cyclic compounds were deleterious as far as τ was concerned. The presence of ring structures in Shelldyne-H and the MCPD-dimer were indicated by the experimental measurements where it was noted that all of the closed ring structures behaved somewhat the same.

A multitude of factors contributed to the magnitude of τ and the relative contribution of each factor doubtless varied from hydrocarbon to hydrocarbon. Fundamental reasons of general applicability for the observed correlation with structure, and the exceptions, cannot therefore be expected. It was nevertheless profitable to consider some of them. Ignition lag may be affected by the thermodynamic properties of the fuel. According to Ubbelohde[34], the higher the internal energy available the shorter the ignition lag. He has suggested that the addition of a $-CH_2-$ group to methane leads to the formation of coupled oscillators and that in this way the internal energy content of the molecule is increased. This effect is larger in longer chains. Branching or introduction of a double bond will interrupt this coupling process. Thus, n-octane had a lower heat content than iso-octane. Double bonds also lower the heat content and the nearer to the center of the molecule the greater the effect.

The rate of initial attack of the hydrocarbon by free radicals can also play a dominant role in determining the length of the ignition delay. This attack will generally occur by hydrogen abstraction from the hydrocarbon and will be determined by the number and strength of the CH bonds present. According to Rice[35], at 300°C, the relative rate of abstraction of primary: secondary:tertiary hydrogens is 1:3:33. In complex molecules, the strength of CH bonds was not always accurately known and while there can be little doubt that it was affected by substituent groups in the molecule, active qualitative estimates of this effect will not always be available. Furthermore, the rate of abstraction may also be affected by steric effects such as might arise from the presence in the molecules of a bulky group. Benzene has a very high C-H bond strength and is quite resistant to oxidative attack--it showed a long residence time.

The stability of the combustion intermediate may also be of importance. The greater reactivity of aldehydes compared with ketones has been used by Pope[36] to account for the enhanced oxidation resistance of straight chain and branch paraffin.

Similarly, the longer τ displayed by methane compared to ethane or propane or higher hydrocarbons could be rationalized on the basis of the greater strength of the C-H bond in methane. A great many factors can thus influence the chemistry of the reactions leading to ignition which one predominates in a particular situation cannot always be predicted a priori--while considerations of some of these factors can provide the general directional guidelines, they must be used with diffidence.

Longwell's earlier studies of well-stirred lean blow-out limits of various hydrocarbons and non-hydrocarbons showed that the data could not be completely explained on the basis of combustion temperature differences between various fuels.[23] His data also indicated, indeed very strongly, that chemical effects played a significant role in the combustion process leading to blow-out. Mullins[37] has reported very strong ignition promoting effects for alkyl nitrates and nitrites in kerosene, whereas Longwell found

that propyl nitrate added to iso-octane had no observable effect in altering the lean blow-out limits over the temperature range of 1200-1900°K. The ignition delay data obtained in the present study utilized a WSR as well as a continuous flow device similar to those employed by Longwell and Mullins. Similar temperature and chemical effects were observed. Figure 44 is a composite presentation of the results of these effects which are reflected in the temperature dependency of (τ) in shock tubes, continuous flow devices and well-stirred reactors.

The group of curves bunched together on the left side of Figure 44 represent the average residence time measured in stirred reactors operating at atmospheric pressure. The other curves are representative of shock tube and continuous flow devices. References associated with each of the curves in the figure are given in Table XII.

Curves 16 and 15 are the ignition data of n-heptane and kerosene, respectively, reported by Mullins. These data were obtained in a vitiated air stream at atmospheric pressure with concentric injection of atomized liquid fuels. Curve 17 represents the "combustion time" of kerosene as calculated from the length of the visible flame by Mullins. Ignition data obtained in the present study as well as by Longwell and Weiss for various hydrocarbons under well-stirred conditions are plotted in curves 1 through 7. It is obvious from a comparison of the ignition delay data obtained from shock-tubes and continuous flow devices that the characteristic times (τ) measured in the WSR are generally about 10 to 50 times longer than reported for shock tubes or continuous flow devices at the same temperature. These relationships at first seems to indicate that "combustion time" may be the rate controlling factor in the combustion process; not the ignition delay time. Delay times measured in shock tubes for propane and n-octane reported by Snyder(38), Scheller(39) and Kogarku(40) are given in curves 18, 21 and 20. The longer "combustion times" derived from stirred-reactor measurements of hydrocarbons seems to indicate that the processes important in determining (τ) via shock tube or continuous flow techniques are different from those associated with "kinetically-limited" stirred reactors. In general, the hydrocarbons and non-hydrocarbon additives seem to exhibit a larger variation in behavior due to molecular structure deriving reactions that commence at low temperatures than they showed in the high temperature stirred reactor. The low temperature oxidation reactions and thermal cracking are unimportant in the stirred reactor whereas their importance in low temperature continuous flow and shock tube devices are paramount.

The stirred reactor, when operated in the lean blow-out region under adiabatic conditions was found to be kinetically limited.(41,42) And yet, the residence times obtained in this device are 10 to 50 times longer than reported for shock tubes, which are also kinetically-limited. To explain these differences Sokaw and others have suggested that the total time required to completely oxidize (burn) a hydrocarbon is a combination of the ignition-delay time (τ_1) and the burning time (τ_2).(43,44) If the residence times measured in the stirred reactor are a combination of $\tau_1 + \tau_2$, then the difference between the stirred reaction residence times and the ignition delay (τ_1) measured in shock tubes or constant flow systems represents the burning time (τ_2) of the hydrocarbon. Figure 44 shows that in nearly all cases, the burning time (τ_2) is many times longer than (τ_1), the auto-ignition delay time of different molecular structure hydrocarbons.

TABLE XII

REFERENCE IDENTIFICATION FOR FIGURE 47

Curve #	Fuel System	Test Device	Reference
1	n-octane + 5% $C_4H_9ONO_2$ (ϕ <.5)	WSR	This work
2	Octene-1 (ϕ <.5)	WSR	"
3	n-octane (ϕ <.5)	WSR	"
4	Shelldyne-H (ϕ <.5)	WSR	"
5	n-hexane (ϕ <.5)	WSR	"
6	Isooctane (ϕ <.8)	WSR	Longwell (23)
7	JP-7 (ϕ <.5)	WSR	This work
8	Shelldyne-H (ϕ <.3)	CFS	"
9	JP-7 (ϕ <.3)	CFS	"
10	n-octane (ϕ <.3)	CFS	"
11	Octene-1 (ϕ <.3)	CFS	"
12	Propane (ϕ <.3)	CFS	"
13	n-octane + 50% $C_2H_5ONO_2$ (ϕ <.3)	CFS	"
14	Kerosene + 50% $C_2H_5ONO_2$ (ϕ <.3)	CFS	Mullins (20)
15	Kerosene (ϕ <.3)	CFS	" (20)
16	n-heptane (ϕ <.3)	CFS	" (20)
17	Kerosene Burning Time (from #15)	CFS	" (20)
18	n-octane (ϕ = .5)	ST	Snyder (38)
19	Propane (ϕ <.5)	ST	Zimont (49) (R)
20	Propane (ϕ <.5)	ST	Kogarku (40)
21	Propane (ϕ <.5)	ST	Scheller (39)

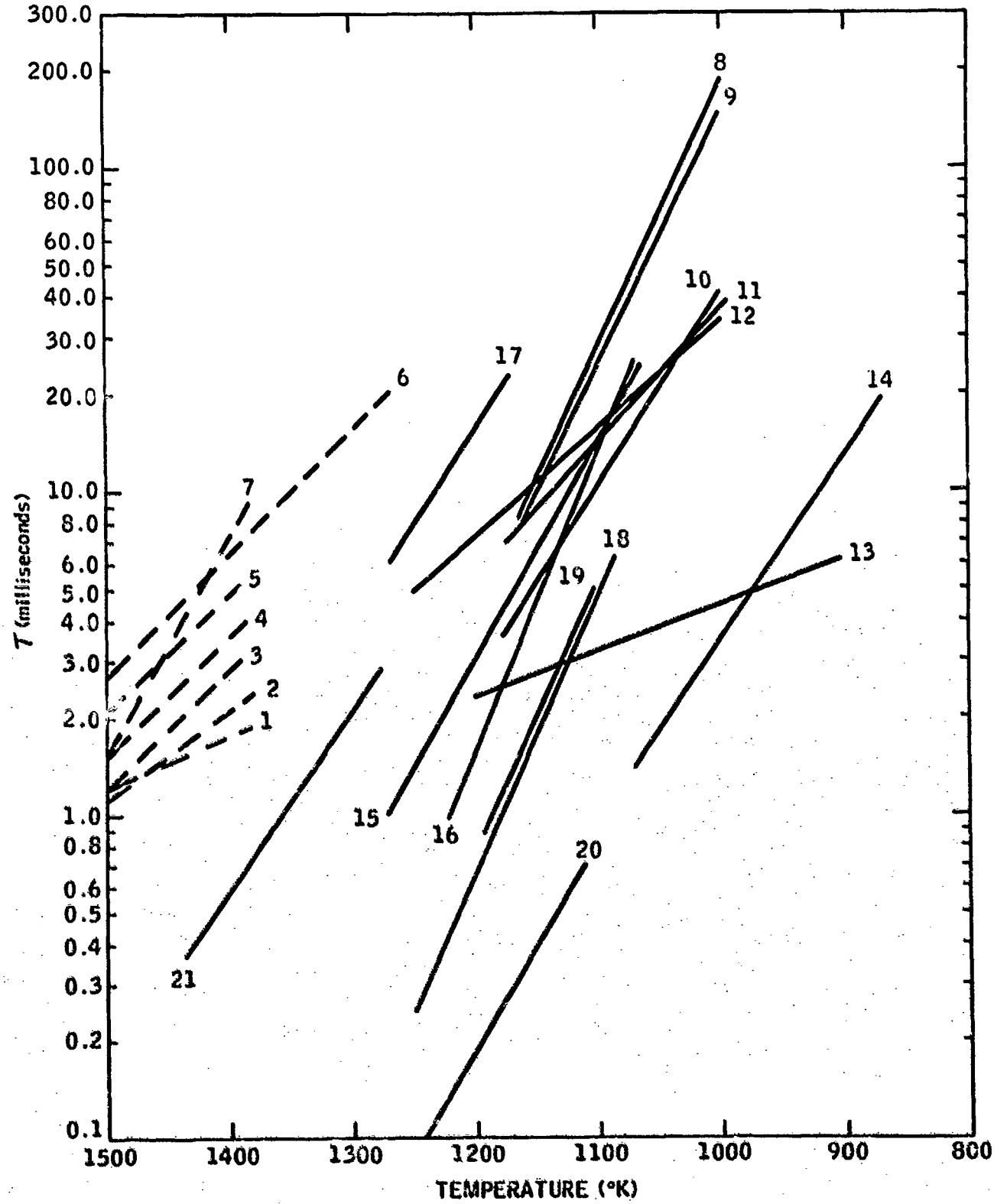

FIGURE 44. COMPARISON OF THE IGNITION DELAYS OF HYDROCARBONS DETERMINED BY DIFFERENT EXPERIMENTAL METHODS

B. The Effects of Additives in the Stirred Reactor

The effectiveness of the additives tested was found too dependent upon the molecular structure of the fuel and the flame temperature at the blow-out point. For example, in Figures 15 & 18 methyl nitrate decreased the relative residence time of n-octane by about 30 percent and appeared equally effective over the temperature range of 1450-1600°K. However, when added to octene-1, methyl nitrate increased the relative residence time by a factor of two at 1600°K and reduced it by over sixty percent at 1450°K. In JP-7, (Figure 20) this behavior was reversed in that methyl nitrate was a strong inhibitor at 1450°K, increasing the relative residence time by nearly a factor three. At 1600°K the relative residence time was reduced by seventy percent.

In JP-7, the most effective additive was 1,2 dimethoxyethane. The relative residence time was reduced by 50 percent at 1400°K and ninety-percent at 1600°K. This additive in octene-1 decreased the relative residence time by seventy-five percent at 1600°K and increased the time at 1400°K. By contrast, this additive had only a very slight effect in altering the residence time of n-octane.

In general, the nitrogen esters were less effective ignition modifiers at low temperatures compared to the peroxides and nitro paraffins. Indeed, some of the nitrogen esters exerted inhibiting effects at low temperatures and promoting ignition at higher temperatures. The chemical effects attributed to the alkoxyl radicals which are decomposition products of the thermal dissociation of the nitrogen esters were of considerable importance in the ultimate effects of these additives. Ethyl nitrate had a much greater modifying effect than methyl nitrate over the same temperature range. The alkoxyl radicals are well known as intermediates in the pyrolysis of numerous organic peroxides and in the decomposition of explosives. They initiate polymerization and take part in oxidation reactions. The rupture of the C-H bond in alkoxyl radicals is likely at high temperatures and is considered to be most likely to occur in methoxyl and ethoxyl radicals. The unimolecular mode of decomposition is described by:

methoxyl: $CH_3O\cdot \longrightarrow H\cdot + CH_2O \quad \Delta H = \frac{25\ KCal}{mole}$

ethoxyl: $C_2H_5O\cdot \longrightarrow H\cdot + CH_3CHO \quad \Delta H = \frac{13\ KCal}{mole}$

The decomposition of the alkoxyl radicals via C-C bond fission requires a somewhat lower activation energy, but at high temperatures the C-H bond rupture is thought to be relatively more important.

The alkyl nitrates and nitrites modify the combustion process in two prominent ways. First, as described by the following reactions; thermal decomposition of n-propyl nitrate, the alkoxyl radical is formed:(45)

$$n\text{-}C_3H_7ONO_2 \longrightarrow n\text{-}C_3H_7O\cdot + NO_2$$

$$n\text{-}C_3H_7O\cdot \longrightarrow C_2H_5\cdot + CH_2O$$

$$C_2H_5\cdot + NO_2 \longrightarrow (C_2H_5O\cdot + NO) + C_2H_5NO_2$$

$$C_2H_5O\cdot \longrightarrow CH_3\cdot + CH_2O$$

$$CH_3\cdot + NO_2 \longrightarrow (CH_3O\cdot + NO) + CH_3NO_2$$

$$n\text{-}C_3H_7O\cdot + NO \longrightarrow n\text{-}C_3H_7ONO$$

Nitrogen dioxide subsequently dissociates to NO+O. Second, the rupture of the C-H bond in the propyl radical evolves hydrogen atoms and alkyl radicals, which participate in the propagation of the chain reaction.

With the exception of ethyl nitrate all the homogeneous additives tested in octene-1 increased the relative residence time at 1600°K and reduced it at 1400°K. Compared to n-octane, all the additives were about twice as effective in reducing the residence time in octene-1. It is interesting to note in light of this observation that aliphatic olefins are generally much more sensitive to Otto-Cycle engine operating conditions than the corresponding paraffin when compared on the basis of "knocking" tendency. The double bond in the olefins leads to either hydrogen abstraction which results in resonance stabilized radicals or addition to the double bond. The course of the oxidation reaction which insures will therefore be quite different. It was not unexpected then, that the additive effects were different in various hydrocarbon structures.

While ease of thermal decomposition to free radicals is essential, the nature of the fragments had a very marked influence on the efficiency of the additive. It is clear that coupling between the radical fragments formed from the additives and those originating from the fuel occurs. Hence, the effectiveness of a particular additive must be considered in relation to the fuel in which it is to be used and the temperature at which it is required to perform. The sensitivity of homogeneous additives to temperature in general arises from differences in the activation energies of the thermal decomposition of the additives, and the reactions in which they participate.

The foregoing considerations make it obvious that an attempt to draw useful generalizations about the molecular structure required to significantly alter the residence time in well-stirred or highly turbulent, back mixed combustion devices is indeed difficult and cannot be attempted until more quantitative data become available. The trends which have been obtained in the WSR study satisfied the goals for which the study was originated - to qualitatively rank the combustion characteristics of hydrocarbon fuels and homogeneous additives in a high temperature kinetically limited system.

C. Results of Platinum Catalyzed M.A.T. Tests in the CFS

Tables X and XI summarize the effects of the platinum catalyst on the minimum autoignition temperatures (M.A.T.) of various hydrocarbons. Generally the M.A.T. data are in qualitative agreement with the published S.I.T. data, although the platinum catalyzed autoignition temperatures are always greater, by varying amounts. The spontaneous ignition data (S.I.T.) indicate that the order of activity from the most easily igniteable to the least igniteable was the following:

n-hexane
cyclohexene
decalin
cyclohexane
hexene-1
methyl cyclohexane
4-vinyl cyclohexene
tetralin
H-MCPD
Shelldyne-H

Many other investigators, notably Zebatakis[46] and Carhart[47] have shown in static as well as dynamic tests that the long straight chain paraffins had the lowest S.I.T. of any hydrocarbons studied. They noted that the S.I.T. decreased as a function of the length of the straight chain. Similar trends were observed for the straight chain alkenes, although as a class, the S.I.T. of alkenes were greater than an alkane of similar chain length. Other molecular structural effects on S.I.T. were found to be the degree of chain branching which in the alkanes as well as the alkenes increased the S.I.T., compared to the straight chain. The cycloparaffins had S.I.T.'s similar to straight chain alkenes, but the addition of side chains to the cyclic compounds decreased the S.I.T. whereas in the alkanes and alkenes, the side chains increased the S.I.T. Aromatics were found by both investigators to have the highest S.I.T.'s of all the hydrocarbons examined.

The relationship between fuel structure and ignition temperature found by other investigators in experimental systems which were different from the method utilized in this study are similar to the results obtained in the platinum catalyzed continuous flow system (CFS). In both situations, the reactions leading to ignition were dependent upon the ease with which the hydrocarbon fragments were oxidized. The low temperature oxidation of hydrocarbons (<300°C) has been well documented and generally occurs in the following sequence:[47]

Hydrocarbon Oxidation Below 300°C

$RH + O_2$ (initiation) $\longrightarrow$ $R^\bullet + HOO^\bullet$ (endothermic) (1)

$R^\bullet + O_2 \longrightarrow ROO^\bullet$ (2)

$ROO^\bullet + RH \longrightarrow ROOH + R^\bullet$ (3)

$ROOH \longrightarrow RO^\bullet + {}^\bullet OH$ (4)

RO or $R'CH_2O^\bullet \longrightarrow R'^\bullet + CH_2O$ (5)

$RO^\bullet + RH \longrightarrow ROH + R^\circ$ (6)

Termination Reactions

$ROO^\bullet + ROO^\bullet \longrightarrow$ (7)

$R^\bullet + R^\bullet \longrightarrow$ Non-radical products (8)

$R^\bullet + ROO^\bullet \longrightarrow$ (9)

The oxidation reactions that are considered important above 400°C are:

$RH + {}^\bullet OO^\bullet \longrightarrow R^\bullet + {}^\bullet OOH$ (10)

$RH + {}^\bullet OOH \longrightarrow R^\bullet + HOOD$ (11)

$R^\bullet + {}^\bullet OOH \longrightarrow R'CH{=}CH_2 + HOOH$ (12)

$ROOH \longrightarrow RO^\bullet + {}^\bullet OH$ (13)

Because of the complexity of the oxidation reactions and considering that both the low and high temperature reactions occur simultaneously, the relative contributions from each reaction cannot be assigned. Without reviewing the sequence of reactions which lead to the production of active radicals which initiate the chain branching reactions, the most important consideration, which significantly effects the overall oxidation rate of the hydrocarbon is the free radical concentration at the lowest temperature possible. The oxidation rates of the hydrocarbons are essentially fixed by the temperature of the environment and the hydrocarbon concentration. The addition of compounds which readily decompose to peroxy, alkyl or alkoxyl radicals can significantly increase the overall oxidation rate of the hydrocarbon. These radicals are relatively inert at high temperatures (>600°C) because of other competing reactions but their catalytic effect on the oxidation rate at lower temperatures is dramatic. The sensitivity of the hydrocarbon molecule to oxidation in the low temperature regime from the slowest to the most rapid was previously given in this section where the oxidation rates were ranked from the magnitudes of their respective S.I.T. and M.A.T. values.

The production of alkoxyl radicals and oxygen-atoms via the decomposition of $C_3H_7ONO_2$ via the following:

$$C_3H_7ONO_2 \longrightarrow C_3H_7O^{\cdot} + NO_2$$

requires approximately 37 KCal $mole^{-1}$. The subsequent dissociation of NO_2 to $NO + O^{\cdot}$ below 400°C is relatively slow compared to the lifetime of $C_3H_7O^{\cdot}$ which has been shown by Gray to be an effective catalyst for promoting low temperature oxidation reactions.(45)

The experimental data obtained in the platinum catalyzed autoignition tests of various hydrocarbons indeed show the oxidation promoting effect of n-propyl nitrate which manifested itself in the reduction of the M.A.T. The M.A.T. data also indicate that as the temperature increased, the igaition promoting effect of the n-propyl nitrate increased. This probably indicates that the oxidation reactions of the hydrocarbons promoted by oxygen atoms were dominant compared to the effects of the alkoxy, peroxy and alkyl radicals.

The possibility that thermal effects were the dominant force in decreasing the M.A.T. of the hydrocarbons has been considered. Table XI compares the equivalence ratio (ϕ), heat input for the total fuel flow sec^{-1} (Qin) and M.A.T. for each hydrocarbon in the presence of the platinum catalytic surface. The enthalpy of the inlet air was derived from its specific heat, mass flow and temperature. This quantity describes the thermal energy of the air stream in the vicinity where the fuel was injected. The heat losses through the walls of the duct were not determined but since all fuels were evaluated over the same range of temperatures and air mass flows, the heat losses were nearly the same in all cases.

Considering these circumstances the thermal effects would be associated with the heat release rates of the various hydrocarbons. The total heat released by the fuel was a combination of the slow oxidation reaction occuring in the air stream and the heat resulting from the oxidation and/or dehydrogenation reactions or the surface of the platinum.

Table XI shows that the enthalpy of the air stream over the temperature range of 280 to 515°C varied from .660 to 1.16 KCal/sec. The equivalence ratio (Ø) at the M.A.T. for each fuel was observed to be similar--typically between 2 and 3. The exception to this generalization was Shelldyne-H. The only other significant variables were the values of M.A.T. and S.I.T., the latter of which has already been determined to be dependant upon the rate of hydrocarbon oxidation at moderate temperatures (<400°C). Therefore, utilizing this relationship between S.I.T. and M.A.T., the platinum catalyzed ignitions also seem to be dependent upon the low temperature oxidation rates of the hydrocarbons. Platinum had a substantial catalytic effect on these rates as evidenced by the large temperature increase of the platinum tube, even when no flame was visible.

The effect of n-propyl nitrate in altering the M.A.T. of various fuels is more complex in that the heat of combustion generated by the decomposition of the additive significantly altered the total enthalpy of the fuel-air stream at temperatures below 700°K. The $-\Delta Hc$ of n-propyl nitrate was reported to be -470 KCal mole^{-1}.[26] Calculations show that at the experimentally measured propyl nitrate flow rates (15 vol. percent of hydrocarbon flow) the total enthalpy of the air stream was doubled. Therefore, the decrease of a particular fuel's M.A.T. below 700°K may be attributed to thermal as well as chemical effects. The rate of oxidation of the fuel would be significantly altered by the increase in the stream temperature.

The catalytic ignition promoting effects of noble metals have been reported by Grenleski and Falk where they measured the ignition delay times of JP-5 in a subsonic ramjet.[48] Their results indicated that the minimum autoignition temperature was very heavily dependent upon the equivalence ratio of the JP-5/air mixture over the temperature range of 600-830°K. Below 600°K no ignition was obtained even for mixture ratios approaching stoichiometric. They proposed a thermal model to account for the effect of the catalytic surfaces or promoting ignition. They based their mechanism on the fact that alteration of the noble metals (platinum or platinum-rhodium screens) total cross section and heat loss characteristics had significant effects on the measured ignition delays. Since JP-5 is mainly composed of iso and n-paraffins with small fractions of olefins and aromatics, the S.I.T. and M.A.T. values derived from the results of our catalytic ignition studies indicate that JP-5 behaves similar to n-hexane, which was shown to have a M.A.T. of 620°K for a Ø=3.0. The agreement between the autoignition temperatures measured by Grenliski and the M.A.T. value measured in this study are in good agreement. This agreement may be fortuitus, but since the experimental conditions were similar in both instances, the pre-ignition reactions should be similar.

D. Ignition Delays in CFS

The autoignition delays of lean ($\phi \leq 0.3$) hydrocarbon air mixtures over the temperature range of 950-1250°K at one atmosphere pressure can be approximated by the following relationship.

$$\tau = A\, e^{B/T}$$

where: τ is the ignition delay (milliseconds) A and B are constants derived from the experimental data. ($B = Ea/R$)

Ea = measured activation energy (KCal $mole^{-1}$)

R = gas constant (~2 cal/degree-mole)

T = temperature (°K)

The experimental data presented in Section IV-D shows that the global activation energies varied depending upon the structure of the hydrocarbon molecule. However, the activation energies of the straight chain alkanes were similar and had an average measured value of 19.8 KCal $mole^{-1}$. The straight chain alkenes had average activation energies of 22.16 KCal $mole^{-1}$ and the ignition delays of this class of compounds were as a class, shorter than the alkanes. The complex fuels; Shelldyne-H JP-7, H-MCPD and cyclohexene generally had much larger activation energies and longer ignition delays compared to the simple hydrocarbons. The constants, A and B derived from the experimental data are summarized in the following table.

TABLE XIII

IGNITION DELAY CONSTANTS OF HYDROCARBONS

Fuel	A	B
propane octane tetradecane	1.85×10^{-3}	9.9×10^{3}
octene-1 1,7-octadiene octene-1/1,3,6-heptatriene	5.2×10^{-4}	11.08×10^{3}
H-MCPD cyclohexene	33×10^{-7}	17.5×10^{3}
Shelldyne-H	37.2×10^{-8}	20×10^{3}
JP-7	63.3×10^{-8}	19.3×10^{3}

These relationships apply only for lean equivalence ratios, typically less than 0.3. The ignition delays of richer mixtures, especially at low temperatures were found to be erratic and greatly influenced by the average fuel concentration. If reproduceable ignition delay data could be obtained for rich mixtures at low temperatures it is likely that the delay times would be noticeably shorter. This observation is in agreement with other investigators who established the definite relationship between τ and ϕ.[50,51] Generally, τ was reported to be inversely proportional to ϕ. Mullins, in a study of the effects of droplet size and fuel concentration on τ reported that the ignition delay of kerosene was not dependent upon the fuel concentration in the lean mixture range of ϕ from 0.135 to 0.34.[52] The coarseness of the atomized spray, however, had a very pronounced effect on τ. Changing the mean diameter of the particles from 55 to 140 microns increased τ by 30 percent. The ignition delay was decreased by 25 percent when the kerosene was injected into the air stream as a vapor (450°C) over the same range of ϕ. These same effects were also recently reported by Billig in a study of the ignition of alkylated boron fuels.[53] He observed that τ decreased by 40 and 48 percent when the fuel was preheated from 330°K to 360° and 460°K respectively for lean mixtures. Foure[54] and Lezberg[55] studied fuel concentration effects of hydrocarbons, hydrogen and nitrogen esters, respectively, and they all found that the ignition delays of these different molecular structures generally decreased when the fuel concentration was increased. However, their studies were performed for richer mixtures compared to the experimental conditions described by Mullins, Billig and in the present study.

From a review of these results as well as the present work it appeared that the ignition delay of various compounds was significantly affected in mixtures where $\phi > .3$ while there was no noticeable effect of fuel concentration on τ in mixtures leaner than $\phi = .3$. It appears then, that the chemical reaction rates were more severely limited in lean mixtures compared to rich mixtures.

Thermal ignition is a delicate balance between the heat generated in the exothermic oxidation reactions and the heat lost through various physical processes. When these exothermic reactions are limited, as would be the case for lean mixtures the ignition process proceeds slowly compared to rich mixtures where abrupt and sometimes explosive ignition occurs. In the latter case the chemical reaction rates, and hence the total heat output, are many times greater than the former condition.

Flame Propagation Velocities of Hydrocarbons

In view of the relatively large magnitude of the autoignition delay times measured in the CFS it is proper to determine what, if any, relationship exists between the ignition delay and flame velocity of lean hydrocarbon-air mixtures. Various investigations (56) have reported the burning velocities of alkanes to be directly proportional to the square of the mixture's temperature at one atmosphere-pressure. Although the referenced experimental data are for 700°K, if we make the brash assumption that the same temperature effects exist at 1000°K, then the extrapolated flame propogation velocity of lean mixtures ($\phi < .6$) of n-alkanes in air would be about 40 feet per second. The ignition delay times of the alkanes

measured in the CFS were typically 30-40 milliseconds at 1000°K. The average unreacted flow velocity under these conditions was 140-150 feet per second. The fact that the lean alkane-air mixtures propogated a steady state flame in this environment implies that the flame speed was even greater than the velocity of the unreacted stream. The predominant reasons for this behavior are likely due to the flame-holding effect of the ignition-zone and an increase of the total enthalpy of the reacting flow in the wake of the ignition zone which may have flame temperatures approaching adiabatic, equilibrium values; near 2000°K. The relationship between flame propogation and autoignition in a constant area duct is not clear from these data and the complex nature of such phenomena requires much more study and thought than has been expended in this brief discussion.

Additive Effects in the CFS

The sensitivity of additives to temperature arises in general from differences in the activation energies of the thermal decomposition of the additives and the ignition reactions which they promote. Of the additives tested which included 1,2-dimethoxyethane, tert-butyl peroxide, ethyl oxalate as well as a number of nitrite and nitrate esters, it was found that by far, the most effective were the nitrogen esters.

The effectiveness of these ignition promoters appears to be largely due to the oxides of nitrogen to which they thermally decompose rather than to the alkoxy radicals which are simultaneously produced. This becomes obvious when the effect that nitrogen dioxide and nitric oxide have on ignition delays is compared with that of other additives which yield alkoxy radicals almost exclusively, such as polyethers and peroxides. While these additives are to some extent effective, their effectiveness in no way compares with that of the oxides of nitrogen.

It is pertinent at this point to ascertain whether the decomposition of these alkyl nitrates and nitrites is sufficiently rapid for them to affect ignition delays by way of the oxides of nitrogen which they generate.

The activation energies for the thermal decomposition of these esters are approximately 37 Kcal/mole and are essentially the same for all alkyl derivatives in keeping with the finding that thermal decomposition occurs principally by scission of the -O-N bond.[45] The decomposition reaction occurs very rapidly--typically in less than 1 millisecond at 1000°K. As indicated in Figure 37 the effectiveness of the various nitrite and nitrate esters is essentially the same on a mass fraction NO_x comparison.

It might also be noted that in general, unsaturated fuels are more responsive to these catalysts. The presence of a double bond in the olefin molecule leads to two important effects which are not possible in paraffins, namely hydrogen abstraction which results in resonance stabilized radicals and addition to the double bond. The course of the oxidation reaction that leads to ignition will therefore be quite different.

Because of the greater susceptibility of olefinic fuels to ignition promoters, the effect of oxides of nitrogen and of alkyl nitrites was investigated on binary blends of octene-1 with JP-7 and other fuels of practical importance such as Shelldyne and H-MCPD.

It was first established that the addition of octene-1 caused the JP-7 to ignite much more readily although the ignition delay of the blend is longer than that of the pure olefin. The ignition of this binary blend was seen to occur with the establishment in the test duct of two distinct but simultaneous flame fronts. Soon after ignition had occurred in this manner, the flame farthest from the injector eventually moved towards the first flame front and coalesced with it. Doubtless this merging of the two flame fronts is due to an increase in the stream enthalpy resulting from the combustion taking place behind the first flame front. The addition of n-butyl nitrite to a JP-7/octene-1 blend eliminated this dual ignition. At a temperature of 1000°K this is in fact equivalent to decreasing the ignition delay by a factor of 15.

A strong synergistic effect was observed when hydrogen was added to a fuel which already contained nitric oxide. A similar effect was reported by Snyder[38] in shock tube studies of H_2/air mixtures which were sensitized with NO or NO_2. The data obtained in the present study plotted in Figure 36 show very clearly the addition of hydrogen dramatically decreases the ignition delay of octene-1. This improvement in the ignition characteristics of the fuel reaches a maximum when approximately 10 vol.% of hydrogen has been added.

It is pertinent at this point to speculate in the light of these observations on the reasons for the effectiveness of oxides of nitrogen as ignition promoters. The nitrogen oxides are normally thought of as inhibitions of gas phase reactions at low temperatures and concentrations.[57] The complexity of the basic combustion processes coupled with an incompletely known high temperature chemistry of these oxides make it difficult to arrive at an unambiguous explanation for their influence on the ignition process even though it has been the topic of a number of investigations.[58] The special and positive role which they play in this temperature range is probably best rationalized in terms of the oxygen atoms which they generate either by the following reactions:

$$NO + O_2 \longrightarrow NO_2 + O \qquad \Delta H = 46 \text{ kcal} \qquad (1)$$

$$NO_2 \longrightarrow NO + O \qquad \Delta H = 72 \text{ kcal} \qquad (2)$$

or in some ways such as by reaction (4). Figure 45 is a comparison of the oxygen atom and oxides of nitrogen concentrations as a function of time, calculated for the kinetic behavior of NO and NO_2 in air at 1000°K via equations 1 and 2.

The replacement of hydrocarbon radicals by oxygen atoms as the initial chain carriers allows the pre-ignition reactions to proceed via an ordinary chain branching reaction rather by relatively slower degenerate chain branching.

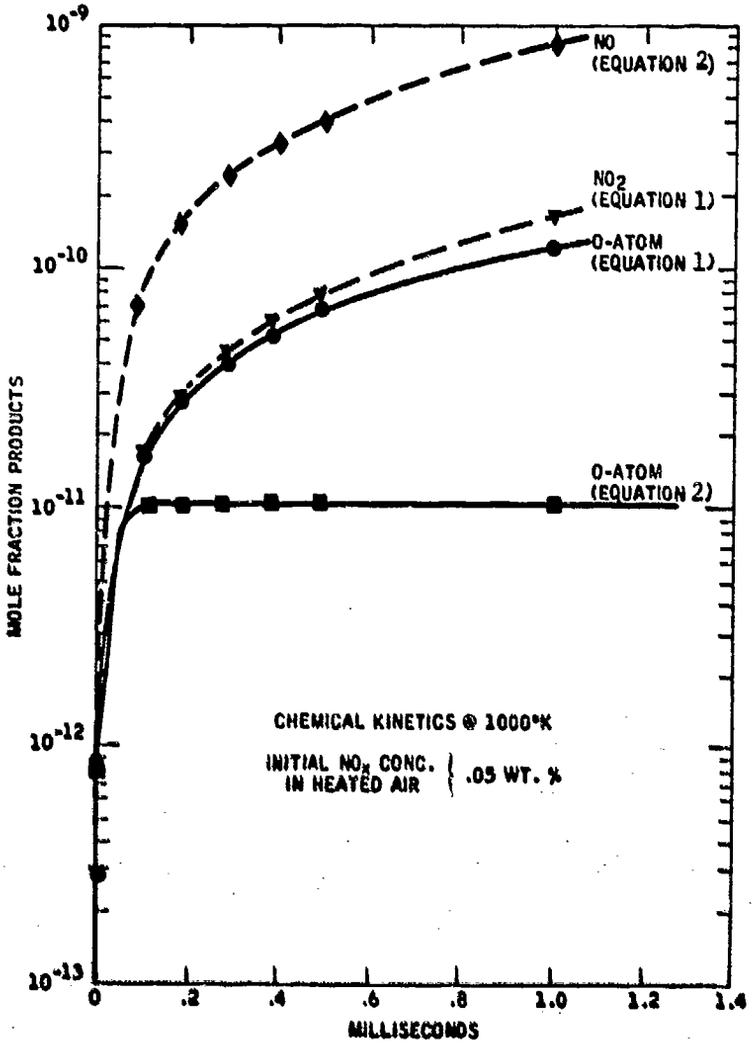

FIGURE 45. VARIATION OF O-ATOM, NO AND NO_2 CONCENTRATIONS AT 1000°K AND 1 ATM. IN HEATED AIR

It has been suggested that the role of the oxides of nitrogen(59) is to replace a relatively inert radical like HO_2 which acts as a chain terminator, by a much more reactive species like OH which is capable of propagating the oxidation chain. This substitution could occur in one of the following ways

$$HO_2 + NO \longrightarrow NO_2 + OH \quad \Delta H = -10.9 \text{ kcal/mole} \tag{3}$$

or

$$HO_2 + NO \longrightarrow HNO_2 + O \tag{4}$$

In both these reactions, nitric oxide effectively removes a chain breaking species and replaces it by a chain propagating one. The experimental evidence accumulated in this study suggests that reaction (3) as such could not account for the observed role of NO. If OH radicals are supplied from hydroperoxides the decrease in ignition delay is considerably less pronounced than when oxides of nitrogen or additives which readily yield them, are used. Another argument which can be adduced against reaction (3) is that it does not explain the synergistic influence of hydrogen which greatly reinforces the ignition promoting properties of the oxides of nitrogen. For these reasons reaction (4) is favored. Reaction (4) is even more attractive when the thermal decomposition of HNO_2 which it produces is considered. At the high temperatures at which the present study was carried out, such a decomposition will occur and result in the generation of OH radicals and the regeneration of NO to continue the cycle.

$$HNO_2 \longrightarrow OH + NO \quad (\Delta H = -50 \text{ kcal/mole}) \tag{5}$$

The alternative path for the decomposition of HNO_2 can be ruled out because of its high activation energy.

$$HNO_2 \longrightarrow H + NO_2 \quad (\Delta H = -80 \text{ kcal/mole}) \tag{6}$$

It must also be pointed out that the enthalpy changes which occur in the hydrogen abstraction by NO_2 in a reaction such as

$$RH + NO_2 \longrightarrow R + HNO_2 \tag{7}$$

are approximately 30 Kcal less endothermic than the corresponding abstraction by oxygen.

$$RH + O_2 \longrightarrow R + HO_2 \tag{8}$$

Reaction (7) could therefore also contribute to the ease of ignition by providing an easier route for the initiation reaction to occur and by producing HNO_2 which then becomes a source of hydroxyl radicals via reaction (5).

While these reactions might help shorten ignition delays, rapid chain branching via oxygen atoms would doubtless have a very much more pronounced effect. That oxygen atoms are formed where nitrate or nitrite esters or oxides of nitrogen are present in the combustible mixture was revealed by the characteristic grey, green-yellow color of the reaction zones. The greyish color was associated with the decomposition of the nitrogen esters and the green-yellow coloration was characteristic of the NO + O recombination reaction.

SECTION VI

CONCLUSIONS

The three important conclusions which resulted from characterizing the ignition and combustion behavior of hydrocarbons under subsonic flow conditions in the WSR and CFS are:

1. The chemical processes important under WSR blow-out conditions are drastically different in the CFS as evidenced by the varying effectiveness of homogeneous additives which are well known promoters of oxidation reactions via free radical chain branching initiation. The "pseudo-ignition delay" times obtained in the WSR are really the total combustion times.

2. The homogeneous additives found most effective in promoting ignition in subsonic flows (CFS) were the alkyl nitrates and nitrites or nitric oxide and nitrogen dioxide. Nitrous oxide was inert. A surprisingly large synergistic effect between H_2 and nitric xoide was observed. Although hydrogen, but itself, had no promoting effect. The oxygen atoms generated via the thermal decomposition of the nitrogen esters are thought to promote ignition via replacement of inert radicals like HO_2 with OH on an alternate reaction leading to the production of HNO_2 which at moderately high temperatures participates in a regeneration cycle where OH and NO are produced to continue the cycle. The synergistic effect of H_2 + NO observed experimentally helps support the latter reaction, as being most probable. The nitrogen esters, (n-propyl nitrate) reduced the ignition delay time of Shelldyne-H and H-MCPD by mainly a factor of 100 at 1000°K, while alkoxyl radical generating additives had relatively minor effects in promoting ignitions in the CFS. The ignition delay was found to be inversely proportioned to the logarithm of additive concentration. The well known low temperature vapor phase inhibiting reactions of the nitrogen oxides were not observed in the range of 900-1250°K.

3. In a flowing system, the platinum catalyzed vapor phase oxidation reactions of hydrocarbons reduced their minimum autoignition temperatures from about 1050°K to 700-800°K for rich mixtures. Increasing the rate of the low temperature oxidation reactions via addition of n-propyl nitrate to the hydrocarbon reduced the minimum autoignition temperatures of the dense fuels to 550-650°K which are approximately the spontaneous ignition temperatures (S.I.T.) of the fuels reported in the literature.

In summary then, the minimum autoignition temperatures (M.A.T.) and ignition delay times (τ) of Shelldyne-H or H-MCPD have been reduced by the addition of n-propyl nitrate from 1050°K to 550-650°K and from 180 and 145 milliseconds to 2.5-3 milliseconds, respectively.

The optimum fuel blends have the physical and chemical properties required of a volume-limited propulsion system propellant.

SECTION VII

RECOMMENDATIONS

Promotion of the rates of low temperature vapor-phase oxidation of hydrocarbons via heteregeneous catalysis has been shown to drastically alter their minimum autoignition temperatures. The experimental data indicate that ignition near the surface of the platinum metal occured when the exothermic oxidizing processes within the boundary layer were greater in magnitude that the local heat losses due to conduction and convection. The relatively good agreement between the measured minimum autoignition temperatures and spontaneous ignition temperatures published in the literature support the proposed mechanism. However, since these data are only qualitative, it is recommended that a program be instituted to concern itself with the quantitative identification of the reactions, their chemical rates and the effect of catalyst surface area and formulation on these parameters. The end results of such a program would be invaluable in the process of designing catalytic "flameholders" or combustion chambers for subsonic as well as supersonic flows. The enhancement of the low temperature oxidation rates of high density hydrocarbons by heteregeneous catalysis would reduce the chamber volume required for complete combustion; a worthwhile accomplishment, indeed.

Although the greatest emphasis is associated with the future study of vapor phase heteregeneous catalysis, there are other technical areas which have been identified during this study, that merit some consideration in the future.

Of most interest, from the standpoint of designing supersonic ramjets, is the effect of pressure on the autoignition delay time and the total combustion times of hydrocarbons. Although the results of this study showed that the ignition lags of dense hydrocarbons were reduced by a factor of 100 at atmospheric pressure, by the addition of homogeneous additives, it is likely that these gains would be much lower at low combustion pressures. The relative importance of the speed of the chemical reactions at low pressures - typically 0.1 atm - would be increased since the combustion times were approximately inversely proportional to the square of the pressure, as determined by Well-Stirred Reactor measurements.

It is highly recommended that the ignition promoting effects of homogeneous additives and heteregeneous catalysis on hydrocarbons be studied in a low pressure, fast flow environment, which closely approximates a subsonic ramjet. It would be premature to attempt to study these complex phenomena in supersonic flows at this time.

SECTION VIII

REFERENCES

1. Billig, F. and Pirkle, J., Research and Exploratory Development III-19. Scramjet Propulsion Research Z310BHP. Johns Hopkins University - Applied Physics Lab. Silver Spring, Md. 1968-69.

2. Longwell, J. and Weiss, M., High Temperature Reaction Rates in Hydrocarbon Combustion. Ind. & Eng. Chem. 47 (1955) 1634-1643.

3. Swarts, E.E. and Frank, C.E., Effects of Hydrocarbon Structure on Reaction Processes Leading to Spontaneous Ignition, NASA TN 3384, July 1955.

4. Walcutt, C. and Mason, J., Effect of Preflame Oxidation Reactions on Engine Knock. Ind. and Eng. Chem. 46 (1954) 1029-1034.

5. Rifkin, E. and Walcutt, C., A Basis for Understanding Antiknock Action. SAE National Fuels and Lubes Meeting, Tulsa, Oklahoma Nov., 1956.

6. Reference Data for Hydrocarbons and Petro-Sulfur Compounds. Phillips Petroleum Co. Special Products Div. Bartlesville, Oklahoma Bulletin # 521, 1962.

7. Lovell, W. and Signaigo F., Ind. and Eng. Chem. 26 (1934) 475.

8. Williams, K., Johnson, J. and Carhart, H., Probing Into Coal Flames. NRL Report 4249, December 30, 1953.

9. Carhart, H., Williams, K., Coal Flames - A Key to Ignition and Combustion of Hydrocarbons. Presented at the ONR Symposium, NRL, Washinton, D.C. March 20, 1957.

10. Zabetakis, M., Bureau of Mines Bulletin 627. U.S. Dept. Interior, Pittsburgh, Pa., 1965.

11. Neshi, J., A Survey of Experimental Methods for the Determination of Ignition Delay Times of Potential Scramjet Fuels. Technical Report AFAPL-TR-70-94 December, 1970. Wright-Patterson A.F.B., Ohio.

12. Burcat, A., Scheller, K., Shock Tube Investigation of Comparative Ignition Delay Times for C_1-C_5 Alkanes. Wright-Patterson A.F.B., Ohio, ARL (ARC) July 1970 (To be published).

13. Nixon, A., Ackerman, G., et al. Vaporizing and Endothermic Fuels for Advanced Engine Applications. AFAL-TR-67-114 Parts I and II. Sept. 1968. Shell Development Co.

14. Desmond, E., Wilson G., What Amyl Nitrate Does to Improve Diesel Fuels. Petroleum Processing. 9 (1954) 684-87.

15. Foord, S. and Norrish, R., The Hydrogen Oxygen Reaction Catalysed by Nitrogen Peroxide. Prac. Ray. Soc. 152 (1935) 196-220.

16. Bogen, J. and Wilson, G., Ignition Accelerators for Compression-Ignition Engine Fuels. Petroleum Refining. 23 (1944) 118-28 and 130-152.

17. Jones, B. and Weil, B. H., Effect of Additives on the Combustion of Petroleum - Derived Fuels. Presented before the ACS, Div., Chem., Lit., Dallas, Tex. April 10, 1956. - Ethyl Corp.

18. Mullins, B. and Penner, S., Explosions, Detonations, Flammability and Ignition. Pergamon Press, 1959.

19. Norrish, R. and Griffiths, J., The Combination of H_2 and O_2 Photo-sensitised by Nitrogen Peroxide. Proc. Ray. Soc. 139 (1933) 147-162.

20. Mullins, B.P., Studies on the Spontaneous Ignition of Fuels Injected Into a Hot Air Stream III. Fuel, 32 (1951) 327-342.

21. Billig, F. and Pinkle, J., Fuels Research for Supersonic Combustion. Report FQR/68-3 Johns Hopkins University, Applied Physics Lab. September 1968.

22. Schneider, G. R. , Kinetics of Propone Combustion in a Well Stirred Reactor. Sc. D. Thesis, M.I.T. Chem. Eng. Dept. 1960.

23. Longwell, J. and Weiss, M., Combustion Rates in Spherical Reactors. Ind. and Eng. Chem. 50 (1958) 257-264.

24. Richter, G., Organic Chemistry, Third Edition, John Wiley & Sons. 1952.

25. Kaufman, F., The Air Afterglow and Its Use in the Study of Some Reactions of Atomic Oxygen. Prac. Ray. Soc. A247 (1958) 123-139.

26. Farnbrother, et al. Trans. Faraclay Soc. 53 (1957) 779-83.

27. Benson, et al. Additivity Rules for Estimating Thermodynamic Properties. Chem. Rev. 69 (1969) 279.

28. Amster, A. and Edwards, G., Research on the Safety Characteristics of Normal Propyl Nitrate II. Terminal Report. Nav. Ord Rep 4493 March, 1957.

29. Levy, J., The Thermal Decomposition of Nitrate Esters. II. J. Am. Chem. Soc. 76 (1954) 3790-3793.

30. Paulsen, D. and Sheridan, W., Thermal and Recombination Emission of NO_2. J. Chem. Phy. 53 (1970) 647-658.

31. Fontijn, A. and Meyer, C., Absolute Quantum Yield Measurements of the NO-O Reaction and Its Use as a Standard for Chemiluminescent Reactions. J. Chem. Phy. 40 (1964) 64-70.

32. Schaad, R. and Boord, C., Effects of Knock Suppressing and Knock Inducing Substances on the Ignition of Certain Fuels. Ind. and Eng. Chem. 21 (1929) 756-62.

33. Lovell, W. and Campbell, J., Molecular Structure of Hydrocarbons and Engine Knock. Second Symposium on Combustion Sept. 1937.

34. Ubbelahde, A., Six Lectures on the Basic Combustion Process, Ethyl Corp. 1954; 53.

35. Rice, F., Aliphatic Free Radicals, Johns Hopkins University Baltimore, Md., 1935.

36. Pope, J., four. Am. Chem. Soc. 51, (1929), 2203.

37. Mullins, B., Spontaneous Ignition. Butterworths Scientific Publications London, 1955.

38. Snyder, A., et al., Shock Tube Studies of Fuel-Air Ignition Characteristics. Report AFAPL-TR-65-93. August, 1965. Monsanto Research Corp., Dayton, Ohio.

39. Scheller, K., et al., Shock Tube Investigation of Ignition in Propane-Oxygen-Argon Mixtures. Aerospace Res. Labs. Report ARL 70-0021, February, 1970. Wright-Patterson A.F.B., Ohio.

40. Kogarko, S. and Borisov, A., Bull. Acad. Sci. USSR, Div. Chem. Sci. (1960) 1255.

41. Miles, G., A Well-Stirred Reactor Investigation of the Combustion of Propane With Vitiated Air. 13th Combustion Symposium, 1970.

42. Hottel, H. and Williams, G., Eleventh Combustion Symposium (1967) 771.

43. Brokaw, R., Thermal Ignition With Particular Reference to High Temperatures. Selected Combustion Problems - Combustion Collogquim (AGARD) Belgium, December 5-9, 1955. 115-163.

44. Tipper, C., Oxidation and Combustion Review, 2 (1967) 224

45. Gray, P. and Williams, A., The Thermo-Chemistry and Reactivity of Alkoxyl Radicals Chemical Reviews. 59 (1959) 239.

46. Zebatakis, M., Bureau of Mines Report 5992, (1962) Pittsburgh, Pa.

47. Carhardt, H. and Affens, W., Ignition Studies, Part VI. NRL Report 5566 November, 1960; Washington, D.C.

48. Grenleski, S. and Falk, F., An Investigation of Catalytic Ignition of JP-5 and Air Mixtures. S.A.E. National Aero & Space Eng. Meeting, October, 1964. Paper #918C.

49. Zimont, V. and Trushin, Yu. Ignition Delays of Hydrocarbon Fuels at High Temperatures. Phys. of Comb. and Expl. (Russian) 3 (1967) 86.

50. Brokaw, R. and Jackson, J., Fifth Symp. on Combustion, Reinhold, New York, 1955.

51. Anagnostou, E. and Butler, J., Selected Combustion Problems (AGARD) Dec. 5-9, 1955. Belgium

52. Mullins, B., Fuel. 32 (1951) 234-247.

53. Billig, F., Fuels Research for Supersonic Combustion. Report FQR/68-3. July 1968. Applied Physics Lab. Silver Spring, Md.

54. Faure, C., Recherche Aero. No. 42 (1954) 33.

55. Lezberg, E. and Lord, A., Unpublished work at N.A.C.A. (1953).

56. Dugger, G. L., Nat. Advisory Committee for Aero. TN 2624, February 1952 (25).

57. Pratt, G., Gas Kinetics. John Wiley & Sons, 1969.

58. Shtern, V.I., Gas Phase Oxidation of Hydrocarbons. McMillan Press, 1964.

59. Ashmore, P.G., Catalysis of Inhibition of Chemical Reactions. Butterworth Press, London (1963), 354.

AFAPL-TR-72-24
Volume II

RESEARCH ON METHODS OF IMPROVING THE COMBUSTION CHARACTERISTICS OF LIQUID HYDROCARBON FUELS

Volume II
KINETICS MODELING AND SUPERSONIC TESTING

R. Edelman
C. Economos
O. Fortune

FORWARD

This report was prepared by the General Applied Science Laboratory, Westbury, Long Island, N.Y., under subcontract to Esso Research and Engineering Company, Government Research Laboratory, Linden, New Jersey under U.S. Air Force Contract No. F33615-69-C-1289. The program conducted at General Applied Science Laboratory is documented under Project No. 5828. The prime Air Force contract was initiated under Project No. 3048, Task 304805 and was administered under the direction of the Air Force Aero Propulsion Laboratory of Wright-Patterson Air Force Base, Ohio by Captain S. G. Hill, Project Engineer, AFAPL-SFF. This report, which is Volume II of a two volume report covers the work performed during the period between January 1, 1969 and December 31, 1971. The work was performed in the Viscous Flow and Thermochemistry Section under the direction of Dr. Raymond Edelman. The analytical modeling work was conducted by Mr. Owen Fortune and the supersonic combustion experiments were performed by Dr. Constantino Economos and Mr. Stephen Schmotolocha.

This report was submitted by the authors on February 10, 1972. This technical report has been reviewed and is approved.

ARTHUR V. CHURCHILL
Chief-Fuels Branch
Fuels and Lubrication Division
Air Force Aero Propulsion Laboratory

ABSTRACT

This report presents the results of theoretical and experimental studies upon neat fuel combustion characteristics and combustion enhancement techniques for hydrocarbon fuels. The investigation covers cyclic and long-chain type fuels with emphasis on the heavy hydrocarbons including H-M&PD and Shelldyne-H.

The theoretical study is concerned primarily with the modeling of kinetic mechanisms necessary to characterize ignition delay times for neat fuel and neat fuel/additive systems. The study shows that a modest scheme comprised of a subglobal partial oxidation step coupled to a wet CO mechanism is capable of predicting the observed ignition delay times for both cyclic and long-chain hydrocarbon fuels. Furthermore, it is shown that the effect of additives upon ignition delay time can be simulated by introducing added amounts of free radicals in the initial reactant mixture.

The experimental study presented here is concerned with ignition and combustion characteristics of neat and neat/additive fuel systems under supersonic flow conditions. The investigation includes both vaporized and liquid fuel injection. For both modes of injection the experiments indicate that supersonic combustion of these heavy hydrocarbon fuels is feasible and that the neat/additive fuel system displays combustion performance which is superior to the neat system. Nevertheless, significant differences in performance between the two modes was apparent. Specifically, for the vaporized injection mode qualitative agreement between flame luminosity and temperature measurements was observed whereas, for the liquid injection mode, no such correlation between luminosity and quantitative measurements was obtained. In addition, it was found that the performance of the vaporized heavy hydrocarbons relative to the base fuel improved continuously with increasing ambient total temperature level, whereas, in the liquid injection mode, this improvement deteriorated at total temperature levels above approximately 1500°R. Possible mechanisms to explain the difference in behavior between the two modes of injection are presented and discussed.

TABLE OF CONTENTS

LIST OF FIGURES

LIST OF TABLES

LIST OF SYMBOLS

c_p	Specific Heat
E	Activation Energy
h	Static Enthalpy
H	Total Enthalpy
k	Specific Rate Constant
$\dot{m}$	Mass Flow Rate
M	Mach Number
p	Pressure
Pr	Prandtl Number
r	Radial Coordinate
R	Universal Gas Constant
Sc	Schmidt Number
T	Temperature
u	Axial Velocity
v	Radial Velocity
V	Injection Velocity
W_i	Molecular Weight of i^{th} Species
$\dot{W}_i$	Production Rate of i^{th} Species
x	Axial Coordinate
α_i	Mass Fraction of i^{th} Species
β	Pilot To Fuel Mass Flow Ratio

γ	Specific Heat Ratio
π	Duct Pressure Integral (See Figure 48)
ρ	Density
φ	Equivalence Ratio

SUBSCRIPTS

f	Fuel
p	Pilot
t	Stagnation
T	Tunnel
∞	Nozzle Exit

I

INTRODUCTION

Theoretical performance studies have established the potential operational gains offered by airbreathing ramjets, SCRAMjets and composite systems flying in the hypersonic regime at moderate altitudes. Perhaps the single most important consideration in terms of system characteristics is that of achieving the potential performance with the minimum possible hardware volume. Thus, high volumetric heating value fuels which are highly reactive with air are necessary to optimize the system within the volume limitation requirements.

In terms of combustion performance overall combustion times in the low-to-sub millisecond range at, say, 1000°k and 1 atmosphere is desirable. Although hydrocarbon fuels are of particular interest because of their general availability and handling characteristics they do not meet the necessary combustion time characteristics.

However, because of the continued interest in hydrocarbons particularly in the newer, high density candidates such as Shelldyne-H and Esso's Pentadimer (H-MCPD) emphasis has been placed on combustion enhancement techniques. A number of such methods have been suggested and a number of these have been explored to varying degrees. Hot gas piloting, photo irradiation, heterogeneous catalysts, and homogeneous catalysts are typical of the techniques that have been considered for combustion enhancement particularly under conditions where ignition would not otherwise occur. Thermal and highly reactive free radical mechanisms are responsible for the catalytic effect and the techniques cited above involve either one or both of these mechanisms.

An attractive feature of the homogeneous catalyst is the fact that it is carried along as part of the fuel and as such provides the potential of eliminating special hardware that is inherent with the other techniques.

Accordingly, the theoretical and experimental study presented here is based primarily upon the use of homogeneous catalysts as a means of enhancing the combustion characteristics of hydrocarbon fuels. This work was performed in conjunction with work carried on at the Esso Research and Engineering Company under Air Force Contract F33615-69-C-1289, Reference 1.

II

THEORETICAL ASPECTS

1. INTRODUCTORY REMARKS

The definition of the combustion characteristics of practical hydrocarbon flames involves a complex interaction of fluid dynamical and chemical kinetics mechanisms. The fluid mechanics includes the convection and diffusive transport of mass, energy, and momentum while the kinetics of the oxidation process involves the generation and depletion of a variety of hydrocarbon fragments, partially oxidized species, and free radicals.

Since the kinetics appear to be the limiting mechanism in the heat release process in high-speed hydrocarbon fueled systems the emphasis here will be on the modeling of the kinetic mechanisms. The mixing processes will be considered, however, as this is required to treat flame propagation in piloted premixed configurations and flame spreading in diffusion flames. In addition to the analysis of these more practical flame configurations the fluid mechanical aspects associated with the various basic kinetics experiments need also be considered to aid in data interpretation.

2. KINETICS

Most often, the combustion of hydrogen-air and hydrogen-oxygen systems have been examined (Refs. 2-6), although methane-air oxidation has also been studied (Ref. 7). In the case of the nozzle recombination problem, expansion of the equilibrium products of the following systems have been examined: hydrogen-air (and oxygen) (Refs. 5-7), hydrogen-fluorine (Refs. 8-9), hydrogen-fluorine-oxygen (Ref. 9), and hydrocarbon-oxygen (i.e., H_2, H_2O, CO, CO_2, H and OH) (Ref. 4).

Although the systems cited above constitute the simplest to analyze from theoretical and numerical viewpoints, since substantial data concerning the relatively few elementary reactions involved are available, current interest in the use of hydrocarbon fuels requires an examination of the non-equilibrium behavior of these fuels as well. As a result of

previous studies at GASL (Ref. 10), it was hypothesized that the chemical kinetics describing the combustion of gaseous, paraffin hydrocarbons up through propane might reasonably be applied to the analysis of the combustion of straight-chain paraffin hydrocarbons of higher molecular weight (at least through the kerosene range), provided that the vaporization kinetics are separately coupled into the problem. The implication here is that in considering the kinetics of the oxidation of a given mass of gaseous hydrocarbon fuel of high molecular weight, the chemical analysis can be approximated with sufficient accuracy (e.g., for obtaining ignition delay and chemical reaction times) by assuming instead the combustion under the same conditions of the same mass of propane. This hypothesis is predicated on the argument that in a real system at high temperature, involving a high-molecular-weight hydrocarbon, some of the fuel will undergo rapid thermal cracking to yield significant quantities of C_1 to C_3 hydrocarbon radicals. Furthermore, it was demonstrated (Ref. 10) that the higher radicals produced in the initial cracking reactions will themselves quickly degrade to additional C_1 to C_3 hydrocarbon species. In order to demonstrate that these initial cracking reactions must occur quickly, lending credence to the above hypothesis, Ref. 10 may be cited, in which experimental ignition delay times for paraffin hydrocarbons from ethane (C_2H_6) through kerosene are shown to be of the same order of magnitude under the same initial conditions.

Propane itself is of considerable interest as a fuel in advanced air-breathing engines. This stems from the fact that propane has been shown to be an effective endothermic heat sink fuel (Ref. 11). That is, in engines where regenerative cooling of the combustion chamber walls is required, propane, either thermally cracked or catalytically dehydrogenated, acts as a highly efficient heat sink.

A considerable amount of experimental work with laminar, premixed, high temperature Bunsen-type flames of propane-air mixtures has been carried out (Refs. 13-20) under flame zone conditions which correspond closely with those of interest here. As a result, it may be anticipated that the species observed in significant quantities in these experiments (Ref. 18) will indicate the kinetic mechanism by which the oxidation proceeds. The 31 species which are considered to be involved are listed in Table I.

TABLE I Species Considered in the Detailed Mechanism for the Oxidation of Propane (Reference 7)

Species No.	Species	Species No.	Species
1	H	17	C_2H_5
2	H_2	18	C_2H_4
3	O	19	C_2H_2
4	O_2	20	C_2H
5	OH	21	C_2H_5O
6	H_2O	22	C_2H_5OH
7	CO	23	CH_3CO
8	CO_2	24	CH_3CHO
9	CHO	25	C_3H_3
10	HCHO	26	C_2H_7
11	CH_3	27	C_3H_6
12	CH_4	28	C_2H_5CHO
13	CH	29	C_2H_5CO
14	CH_3O	30	C_3H_4
15	CH_3OH	31	N_2
16	C_2H_6		

When a complete tabulation of possible elementary kinetic reactions is made involving these 31 species, a list of over 200 reactions results. Many of these may be eliminated as a result of one or more of the following considerations:

a. The activation energy for the indicated reaction is excessively high when compared with the alternative paths which are available for continuing the chain. When available, activation energies were obtained from the literature. When unavailable the empirical correlation of Semenov (Ref. 20) was used:

$$E = 11.5 - 0.25\ \Delta H_R \quad \text{(exothermic reactions)} \qquad (1a)$$

$$E = 11.5 - 0.75\ \Delta H_R \quad \text{(endothermic reactions)} \qquad (1b)$$

which is approximately valid for reactions involving radicals such as H, CH_3, and OH with a wide variety of molecules (e.g., derivatives of methane, aldehydes, ethylene, propylene).

b. The elementary reaction involved the collision of two relatively rare chemical species. As a result, it was considered unlikely that the reaction was important in continuing the chain.

c. The reaction required an unlikely orientation of the molecules on collision in order to proceed to completion; that is, the steric (probability) factor would also be quite low.

When the above considerations are made, and alkyl radical recombination reactions are neglected, the likely kinetic mechanism in which the 31 chemical species participate involves 69 elementary reactions (Ref. 7). Here again, when available, suitable reaction rate constant data were taken from the literature. When such data were not available, the ideal gas kinetic theory was used to obtain the frequency factor (Ref. 7), steric factors were estimated by the method discussed in Ref. 30, and activation energies were obtained from Eq. (1). The rate constant is then expressed in the usual form.

$$k = A \exp(-E/RT) \qquad (2)$$

in which A is the product of frequency factor and steric factor. The ratio of the forward and reverse rate constants was assumed to be equal to the equilibrium constant when the latter data were available.

The above analysis has been programmed for high-speed digital computations using solution techniques developed at GASL (Ref. 21). Such a tool is invaluable in making rapid calculations for comparison with basic kinetic data and is necessary when such kinetic systems are coupled to multi-dimensional flows involving diffusive transport processes.

One of the principal uses of the detailed chemical kinetic analyses has been their use in arriving at overall reaction rate expressions for the combustion of hydrocarbons (Ref. 22 and 23). In this work, what are called "quasi-overall" or "quasi-global" reaction rate expressions were deduced, since it was found more accurate to assume that the reaction proceeds to partially oxidized species (e.g., CO, H_2) rather than to CO_2 and H_2O. The oxidation is then completed via a more detailed kinetic mechanism. For example, in Reference 21, the assumed "overall" reaction is

$$C_nH_{2n+2} + \frac{n}{2} O_2 - n\,CO + (n+1)\,H_2 \qquad (3)$$

and is coupled to a sequence of elementary steps as indicated in Tables II and III where the subglobal stop, reaction 1, proceeds according to the rate given by:

$$\frac{dC_F}{dt} = - AC_F^{\alpha} C^{\beta}O_2 \, e^{-E/RT} \qquad (4)$$

where C_F and CO_2 are the concentrations of fuel and oxidizer, respectively, E^2 is the apparent activation energy, $A=A(p,T)$ and α and β are constants. Thus, a total of 10 species entering into 10 reactions results from the formulation.

TABLE II

C-H-O CHEMICAL KINETIC REACTION MECHANISM

$$k_f = AT^b \exp(-E/RT)$$

REACTION	Forward A	b	E/R
1. $C_nH_m + \frac{n}{2} O_2 \rightarrow \frac{m}{2}H_2 + nCO$	$\frac{6 \times 10^9 a}{p^{.825}} . C^{\frac{1}{2}}_{C_nH_m} C_{O_2}$	1	EQG/R
2. $CO+OH = H+CO_2$	5.6×10^{11}	0	$.543 \times 10^3$
3. $OH+H_2 = H_2O+H$	2.19×10^{13}	0	2.59×10^3
4. $OH+OH = O + H_2O$	5.75×10^{12}	0	$.393 \times 10^3$
5. $O+H_2 = H+OH$	1.74×10^{13}	0	4.75×10^3
6. $H+O_2 = O+OH$	2.24×10^{14}	0	8.45×10^3
7. $M+O+H = OH+M$	1×10^{16}	0	0
8. $M+O+O = O_2+M$	9.38×10^{14}	0	0
9. $M+H+H = H_2+M$	5×10^{15}	0	0
10. $M+H+OH = H_2O+M$	1×10^{17}	0	0

Reverse reaction rate, k_r, is obtained from k_f and the equilibrium constant, K_c.

TABLE III

N-O CHEMICAL KINETIC REACTION MECHANISM

$$k_f = AT^b \exp(-E/RT)$$

REACTION	Forward A	Forward b	Forward E/R
11. $O+N_2 = N+NO$	1.36×10^{14}	0	3.775×10^4
12. $N_2+O_2 = N+NO_2$	2.7×10^{14}	-1.0	6.06×10^4
13. $N_2+O_2 = NO+NO$	9.1×10^{24}	-2.5	6.43×10^4
14. $NO+NO = N+NO_2$	1.0×10^{10}	0	4.93×10^4
15. $NO+O = O_2+N$	1.55×10^9	1.0	1.945×10^4
16. $M+NO = O+N+M$	2.27×10^{17}	-0.5	7.49×10^4
17. $M+NO_2 = O+NO+M$	1.1×10^{16}	0	3.25×10^4
18. $M+NO_2 = O_2+N+M$	6.0×10^{14}	-1.5	5.26×10^4
19. $NO+O_2 = NO_2+O$	1×10^{12}	0	2.27×10^4

Reverse reaction rate, k_r, is obtained from k_f and the equilibrium constant, K_c.

Now, as previously cited, the similar behavior of the hydrocarbons suggests that the quasi-global representation can be effectively used to represent the overall combustion history of a variety of hydrocarbons. The differences that do exist between the fuels being accounted for through the available constants in the sub-global rate equation, Eq. 4, as determined empirically.

This technique also has potential for the simulation of the effects of additives upon the ignition and combustion times of a given fuel system. In terms of the effects of additives upon ignition delay there are other means of accounting for their presence in the fuel. The actual mechanisms that are responsible for the behavior of additives is promoting ignition are not fully understood although a combination of thermal and reactive radical mechanisms are known to play roles in the process. The thermal mechanism arises in cases where the additive is highly reactive with the oxidizer and if present in sufficient quantities will act as an in situ thermal ignition source for the main fuel component. Such a process provides for a "staged" mode of ignition. The reactive radical mechanism is associated with the decomposition of the particular additives with the attendent "early" release of species which readily initiate the chain carrying and branching reactions crucial to the induction phase of the overall reaction process. Thus, in summary the simulation of the effect of additives is offered by: 1. Defining a set of constants including an effective activation energy for the subglobal step for each fuel system (neat fuel plus additive), and 2. Defining an initial "added" amount of a free radical which is available for this purpose in the quasi-global scheme.

The application of some of these notions to the experimental data is discussed later.

3. FLUID MECHANICS

To complete the backgound necessary to evaluate the experimental data a fluid mechanical framework is required. Now, the bulk of the experimental techniques employed is the program involved continuous flow devices where the fuel was injected coaxially into the flowing air stream. For the treatment of such reacting flows a parabolic mixing analysis is appropriate and for ducted flows the describing equations are given by:

Continuity:

$$\frac{\partial(\rho u r)}{\partial x} + \frac{\partial(\rho v r)}{\partial r} = 0 \qquad (5)$$

Momentum:

$$\rho u \frac{\partial u}{\partial x} + \rho v \frac{\partial u}{\partial r} = \frac{1}{r} \frac{\partial}{\partial r} \left(\mu r \frac{\partial u}{\partial r}\right) - \frac{dp}{dx} \qquad (6)$$

Energy:

$$c_p \rho u \frac{\partial T}{\partial x} + c_p \rho v \frac{\partial T}{\partial r} = u \frac{dp}{dx} + \mu \left(\frac{\partial u}{\partial r}\right)^2 +$$

$$+ \frac{1}{r} \frac{\partial}{\partial r} \left(\frac{c_p}{Pr} \mu r \frac{\partial T}{\partial r}\right) +$$

$$+ \frac{\mu}{Sc} \frac{\partial T}{\partial r} \sum_i c_{pi} \frac{\partial \alpha_i}{\partial r}$$

$$- \sum_i h_i \dot{W}_i \qquad (7)$$

Species Diffusion:

$$\rho u \frac{\partial \alpha_i}{\partial x} + \rho v \frac{\partial \alpha_i}{\partial r} = \frac{1}{r} \frac{\partial}{\partial r} \left(\frac{\mu}{Sc} r \frac{\partial \alpha_i}{\partial r}\right) + \dot{W}_i \qquad (8)$$

In Eqs. (5) through (8), the transport coefficients μ, Pr, and Sc, can be taken either as the laminar (molecular) values or as the "effective" turbulent counterparts depending upon the specific problem under analysis. For the present purpose, of course, the latter is appropriate and a variety of semiempirical "viscosity" models can and have been implemented at GASL. The specific models utilized to perform the various calculations conducted during this program are described in the next section.

To supplement these conservation equations, relations among the thermodynamic variable are required, viz.:

State:

$$\rho = \frac{p}{RT \sum_i \frac{\alpha_i}{W_i}} \qquad (9)$$

also

$$H = h + \frac{u^2}{2} \tag{10}$$

where

$$h = \sum_i \alpha_i h_i \tag{11}$$

with

$$h_i = h_i\,(T) \tag{12}$$

Chemical Production Rate, $\hat{W}_i$: Consider a chemical system containing N species entering into R elementary reactions:

$$\sum_{i=1}^{N} \nu'_{ip} M_i \quad \underset{k_{bp}}{\overset{k_{fp}}{\rightleftharpoons}} \quad \sum_{i=1}^{N} \nu''_{ip} M_i \,, \qquad p = 1, \text{---}R \tag{13}$$

Then the production rate of the i^{th} specie is given by:

$$\hat{W}_i = W_i \sum_{p=1}^{R} (\nu''_{ip} - \nu'_{ip}) k_{fp} \rho^{mp} \prod_{i=1}^{N} \left(\frac{\alpha_i}{W_i}\right)^{\nu'_{ip}} \left[1 - \frac{\rho^{Np}}{k_{c,p}} \prod_{i=1}^{N} \left(\frac{\alpha_i}{W_i}\right)^{\nu''_{ip} - \nu'_{ip}}\right] \tag{14}$$

where

$$m_p \equiv \sum_i \nu'_{ip}$$

$$n_p \equiv \sum_i^N (\nu''_{ip} - \nu'_{ip})$$

Π denotes the running product

k_{fp} ≡ forward specific reaction rate constant for reaction ρ

$k_{c,p} \equiv \frac{k_{fp}}{k_{bp}}$ ≡ equilibrium constant

$k_{b,p} \equiv \frac{k_{fp}}{k_{bp}}$ backward specific reaction rate constant

W_i ≡ molecular weight of i

Initial and Boundary Conditions The following conditions represent initial and boundary conditions required to set the problem for steady axisymmetric ducted flow configurations:

Initial Conditions

@ x = 0

$$T = T_f(r)$$

$0 \le r \le r_w$ $\quad u = u_f(r)$

$$\alpha_i = \alpha_i(r)$$

$$v = 0$$

Boundary Conditions

@ $x \geq 0$

$$r=r_w \quad \begin{cases} \dfrac{\partial u}{\partial r} = -\dfrac{\rho u^2}{\mu} cf/_2 \\ T = Tw, \text{ or } \dfrac{\partial H}{\partial r} = -\ q(x)\ \dfrac{Pr}{\mu} \\ \dfrac{\partial \alpha_i}{\partial r} = 0 \end{cases} \tag{15}$$

$$r = 0 \quad \begin{cases} \dfrac{\partial u}{\partial r} = \dfrac{\partial T}{\partial r} = \dfrac{\partial \alpha_i}{\partial r} = 0 \quad \text{(symmetry)} \\ v = 0 \end{cases} \tag{16}$$

Note that in the first of the conditions (15) the "no slip" condition $u = o$ is <u>not</u> applied directly but is replaced by imposing a shearing force on the fluid by specification of an appropriate average value of skin friction coefficient. Note also that the adiabatic wall case follows from the remaining conditions for $q(x) = o$ since in that case, $\partial H/\partial r = \partial \alpha_i/\partial r = 0$ imply $\partial T/\partial r = 0$.

The preceding models for the kinetics and the coupled kinetics/mixing processes have been applied to the analysis of the data reported upon in Reference 1. These results are described in the next section.

III

COMPARISON OF THEORY WITH EXPERIMENTS

This section describes the application of the preceeding theoretical methodology to the prediction and interpretation of the basic low speed ignition data obtained during related studies performed at Esso Research and Engineering Company, Reference 1. Specifically, the comparison covers neat fuels, simulation of additives, and two dimensional effects.

1. NEAT FUEL EVALUATION

In the early part of the program both a well stirred reactor and a continuous flow facility were employed for the determination of ignition delay times, Reference 1. A variety of fuel types have been tested including long chain paraffins (alkanes) and olefins (alkenes), and cyclic structured fuels. Now, a basic part of the model development involved the determination of the activation energies (and pre-exponential factors) required in the subglobal reaction rate to characterize the various neat fuels. An example typifying the results of this study is shown in Figure 1. The predictions were based upon the coupled fluid mechanical/kinetics model as discussed in the preceeding section, with the assumption of uniform inviscid adiabatic flow at constant pressure. This assumption is shown later to be valid for Esso's continuous flow facility. Now, Figure 1 shows data for octane and propane along with predictions for various assumed activation energies ($E_{Q.G.}$'s). Here, the pre-exponential factor, a (see Table II), is unity. As expected these long chain type hydrocarbons do indeed behave in a similar way and as a class of fuels their ignition delay characteristics can be well represented by a single sub-global activation energy.

A further evaluation of additional data on a variety of fuel types has varified the generality of this conclusion for both long chain and cyclic type hydrocarbons. A composite representation of these results is shown in Figure 2, from which a set of recommended values for the pre-exponential factors, a, and the activation energy, $E_{Q.G.}$, were determined as follows:

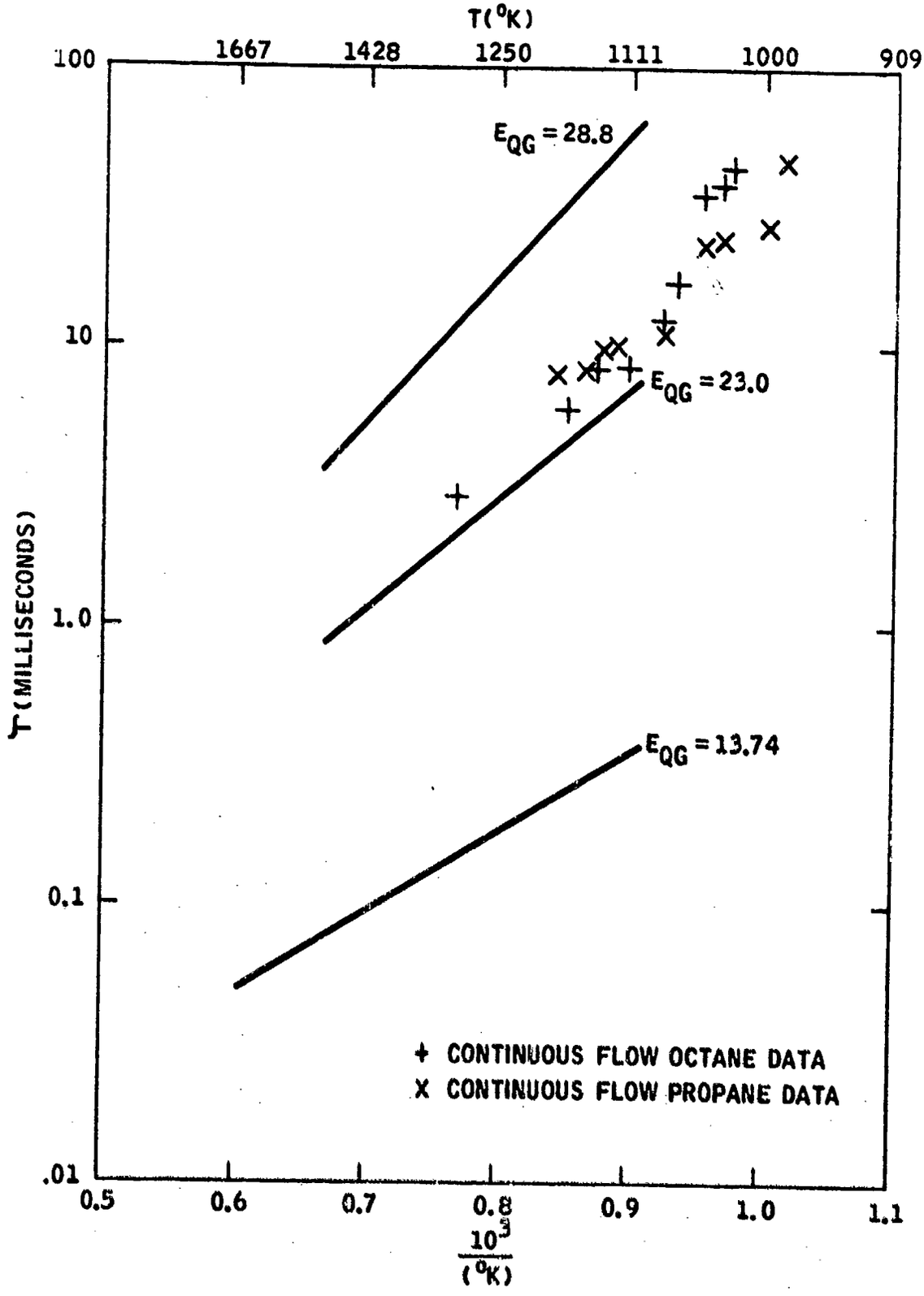

FIGURE 1 EFFECTS OF VARYING THE QUASI-GLOBAL ACTIVATION ENERGY (E_{QG}) UPON IGNITION DELAY

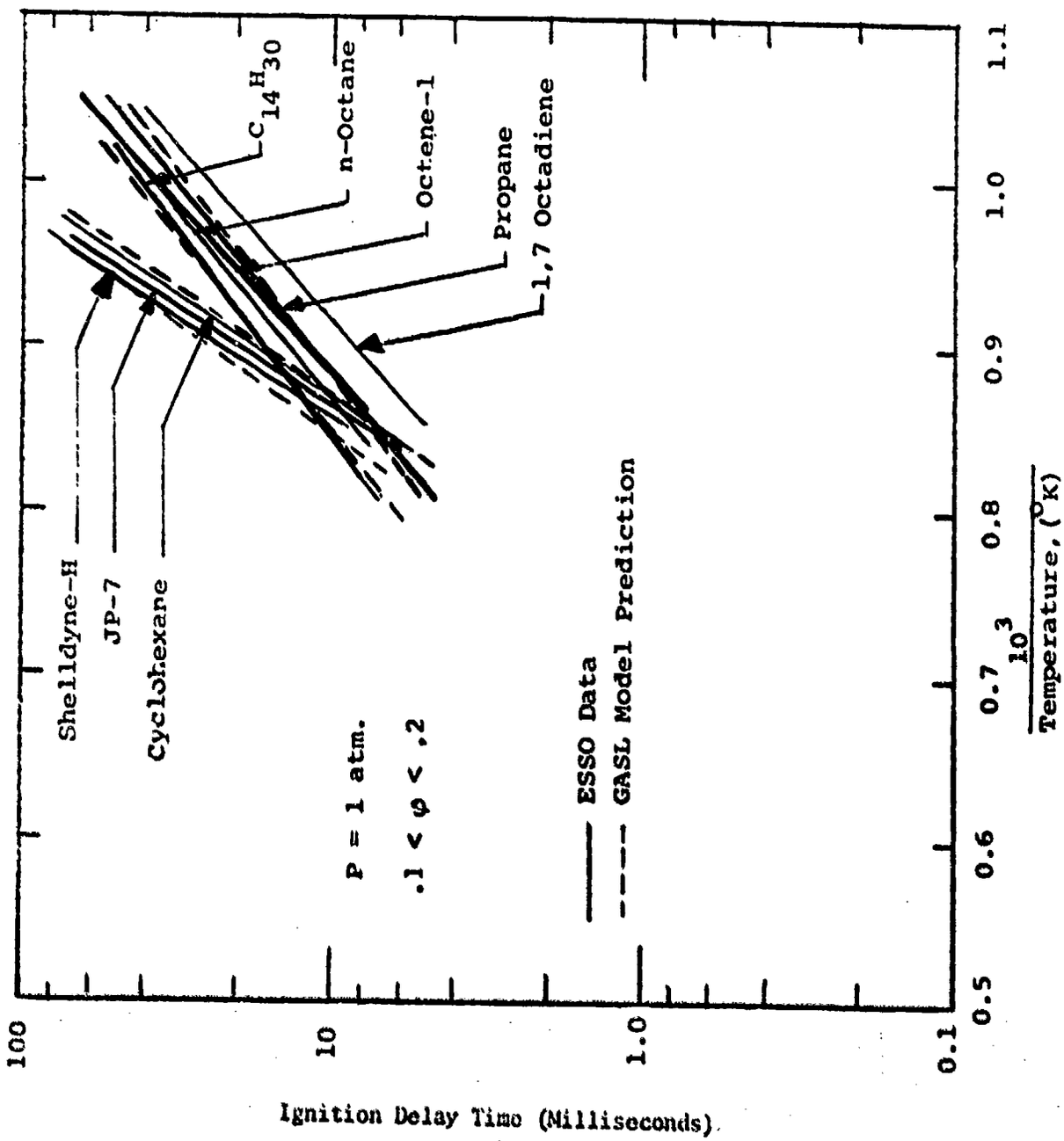

Figure 2 Esso Pure Fuel/Air System Experimental Ignition Delay Time Data - Comparison With GASL Theory.

	Alkanes & Alkenes	Cyclic
a	1	347.
$E_{QG}(\frac{K\ Cal}{mole})$	24.4	39.3

2. SIMULATION OF ADDITIVES

The previous results have served to demonstrate the ability of a relatively simple kinetics scheme to represent the ignition characteristics of neat hydrocarbon fuels. The addition of additives to these neat fuels, however, introduces complex thermal and kinetic mechanisms which, as cited earlier, are not fully understood. Never-the-less, the success of representing the neat fuel behavior suggested that a relatively simple effective means of simulation could be devised to represent any given fuel system (neat fuel plus additive). For this purpose the added free radical approach cited above in Section II was employed. Specifically, the highly reactive OH radical was used in varying percentages of the fuel in an attempt to simulate the effect of the actual additive in reducing the ignition delay time. Initially, theoretical calculations were performed to establish the trends in the relative reduction in ignition delay time as a function of the operating conditions. The results of this study are shown in Figures 3, 4 and 5. Figure 3 shows the effect of initial temperature upon the reduction in ignition delay time. The effect is most pronounced at the lower concentrations and the percent reduction in ignition delay time increases as the temperature is reduced. These trends are identical with those observed with the actual additives, Reference 1. Figure 4 shows the effect of pressure at two temperatures which illustrates that, at least for pressure levels at or above one atmosphere, the pressure has a relatively small effect compared with temperature. Note however as pointed out in Reference 1 that at lower pressures the effect of both parameters can be equally important. Although, the experimental data was limited to essentially the 1 atmosphere level the predicted results appear reasonable in terms of enhancement of the rate of recombination of free radicals with presure. Finally to assess the difference in performance as a consequence of the selection of the free radical simulator a comparison was made using atomic oxygen in place of the hydroxyl radical. These results are shown in Figure 5 for a n-octane/air system. The difference in performance is quite small even at the larger concentration levels. This comparison implies that the choice of effective additive is not a crucial consideration in establishing the utility of the basic simulation technique.

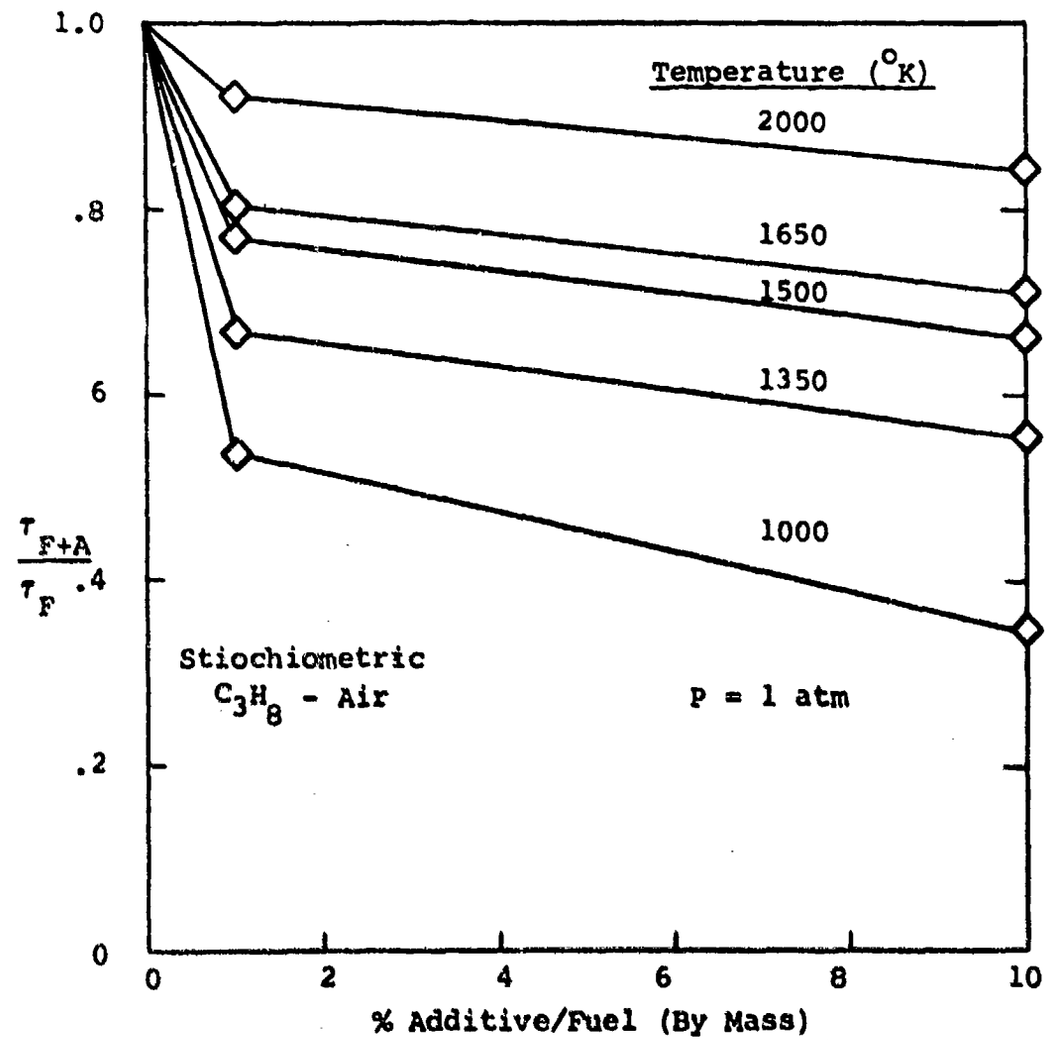

FIGURE 3 Affect of Temperature Upon Additive Performance

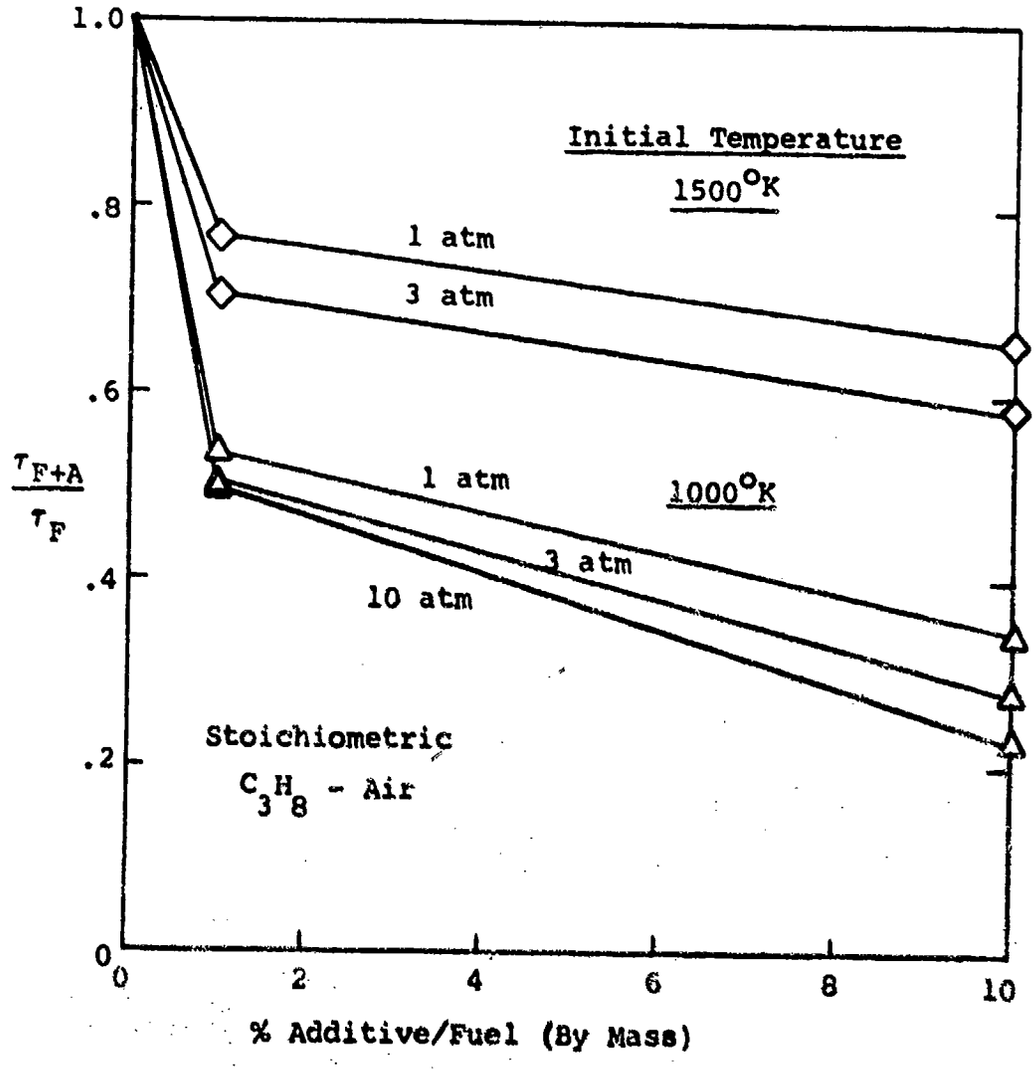

FIGURE 4 Affect of Pressure Upon Additive Performance

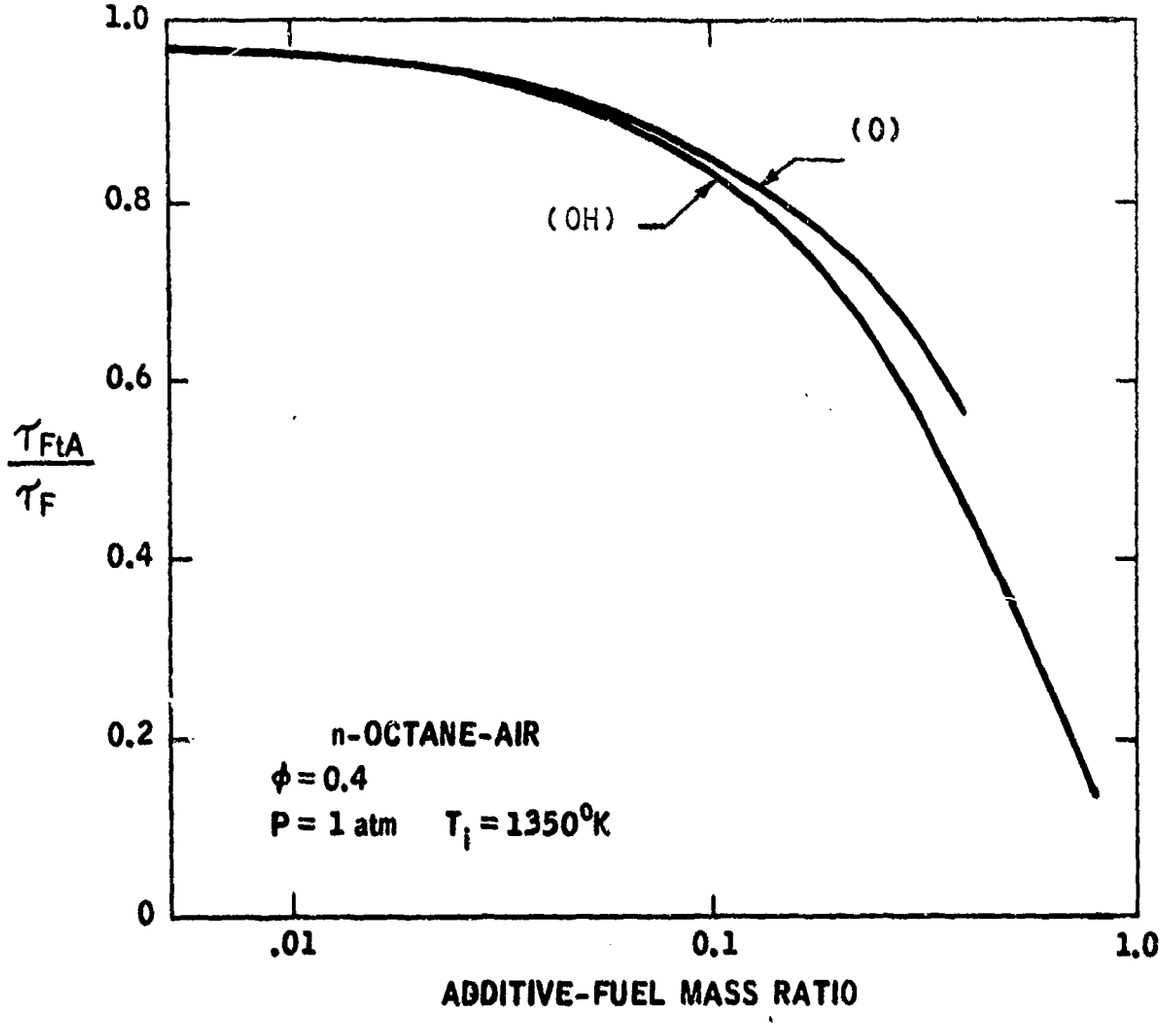

FIGURE 5. INFLUENCE OF ADDITIVE SPECIE AND QUASI-GLOBAL ACTIVATION ENERGY UPON IGNITION DELAY PERIOD

Now, Figures 6, 7 and 8 show some direct comparisons of theory with experimental data involving various additives. In general the experimental data covers a relatively small span in temperature making it somewhat difficult to accurately compare the predicted behavior with the observations. Never-theless, upon comparing the data with the predictions for the various fuels including Shelldyne-H it appears that a value of the effective additive/fuel ratio can be found that reasonably well simulates the behavior for each actual fuel-additive combination. A further refinement is also indicated by these comparisons. Specifically, it appears that the agreement can be made as close as desired by re-evaluating the pre-exponential constant, a, and the sub-global activation energy. This control permits both translation and rotation of the predicted ignition delay curve such that the straight line, τ_{ID} vs. 1/T, data can be predicted more precisely for any given fuel/additive system. Thus, it appears that the complex reaction mechanisms involved in both the neat hydrocarbon and hydrocarbon/additive systems can be simulated given a minimum of τ_{ID} data for each fuel system.

3. TWO DIMENSIONAL EFFECTS

The various comparisons described above were based upon a simplified version of the coupled mixing and kinetics analysis presented in Section II. In particular, the reactants were assumed fully mixed at the entrance section of the Esso Dynamic Flow Facility. Furthermore, wall effects were neglected and the reacting flow was assumed to be one dimensional and adiabatic at constant pressure.

The question that arises pertains to the generality of the assumption of uniform flow in the prediction of ignition delay times. The non-uniform velocity profiles across the duct results in increased residence times near the wall compared with the bulk of the flow. To assess potential effects

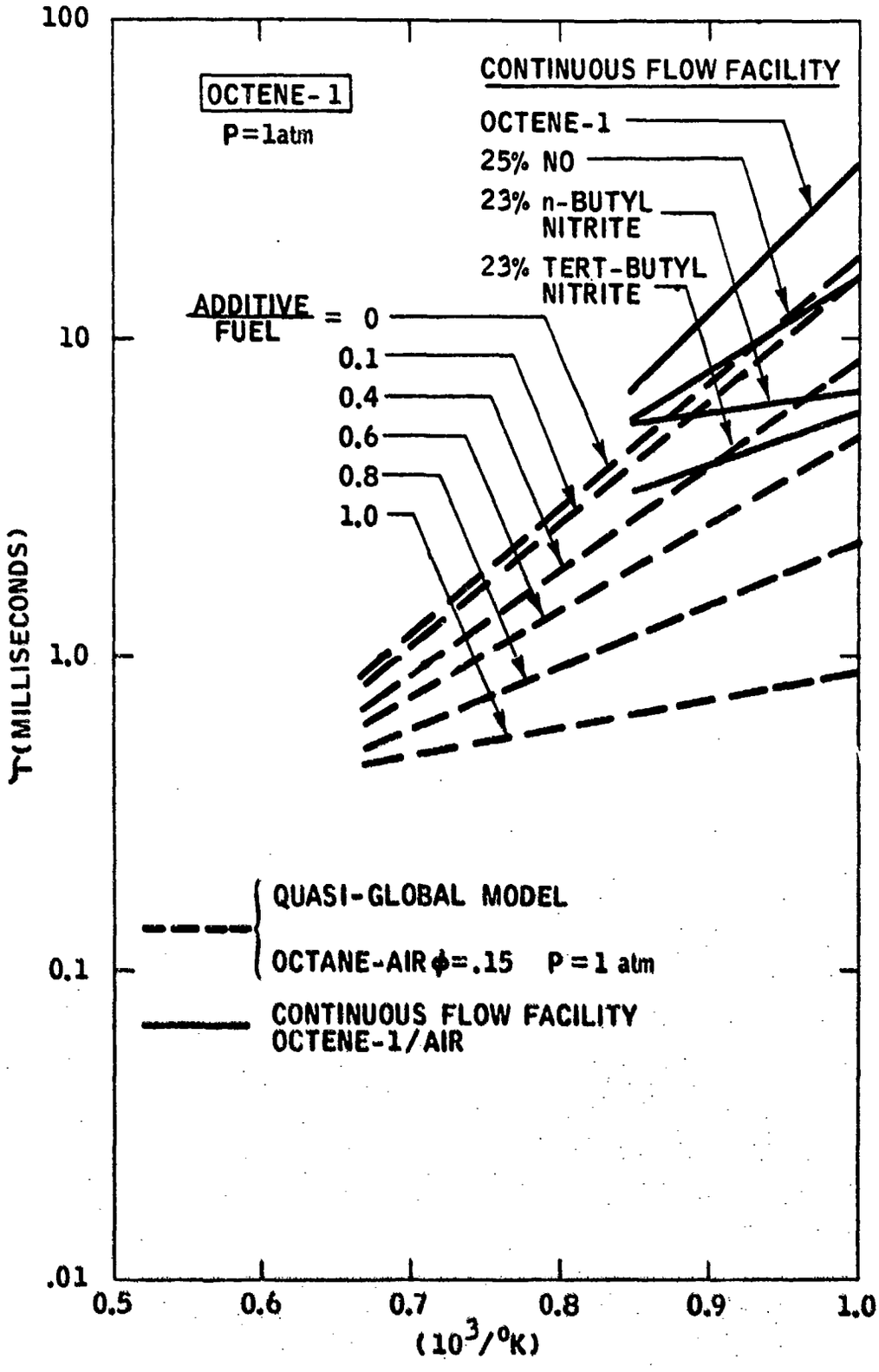

FIGURE 6 . COMPARISON OF THE EFFECT OF ADDITIVES IN THE CONTINUOUS FLOW FACILITY AND THE GASL ANALYTIC MODEL

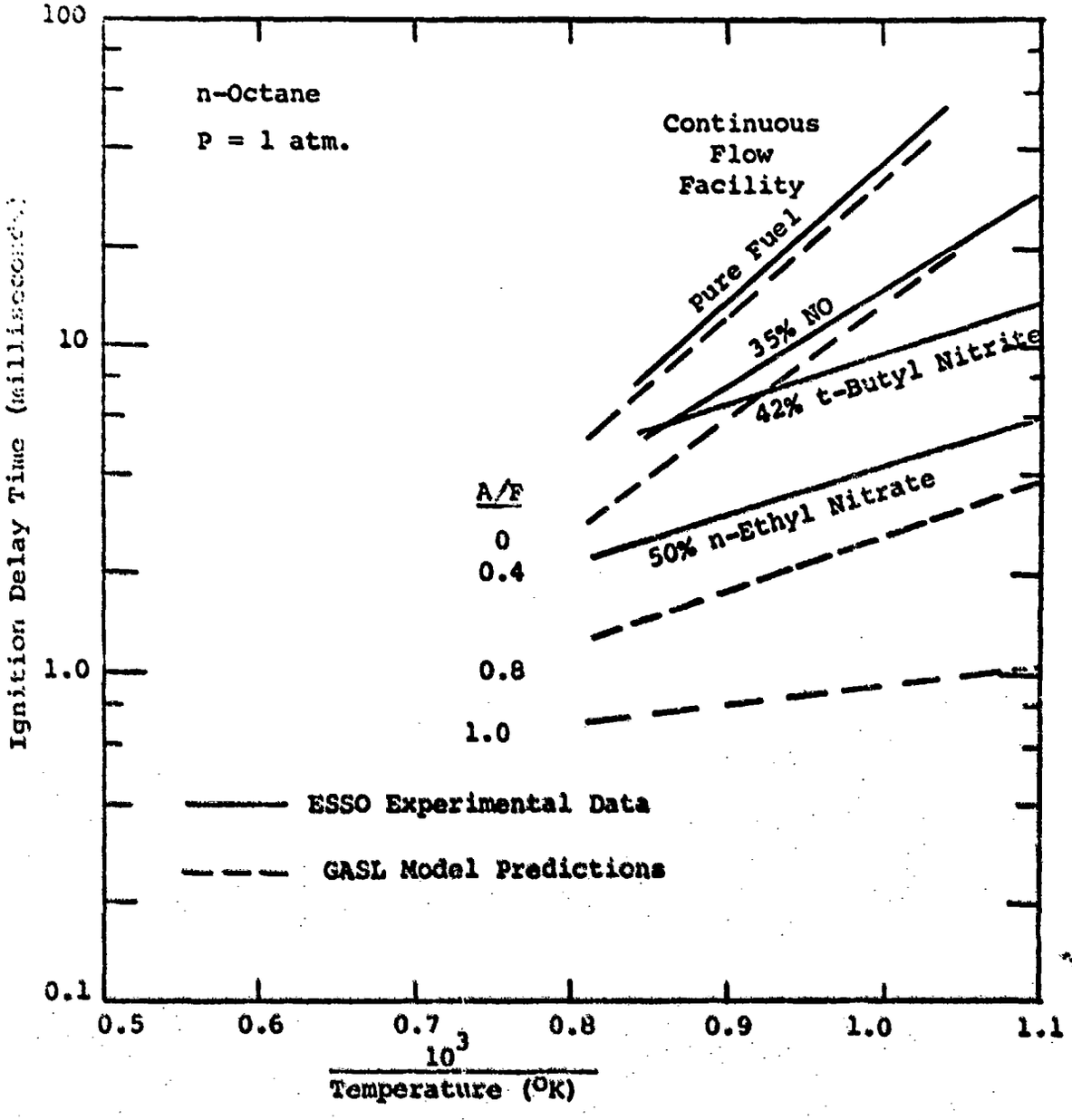

Figure 7 Comparison of Predictions of the GASL Quasi-Global Combustion Model with Esso Experimental Ignition Delay Times for A n-Octane-Additive-Air System.

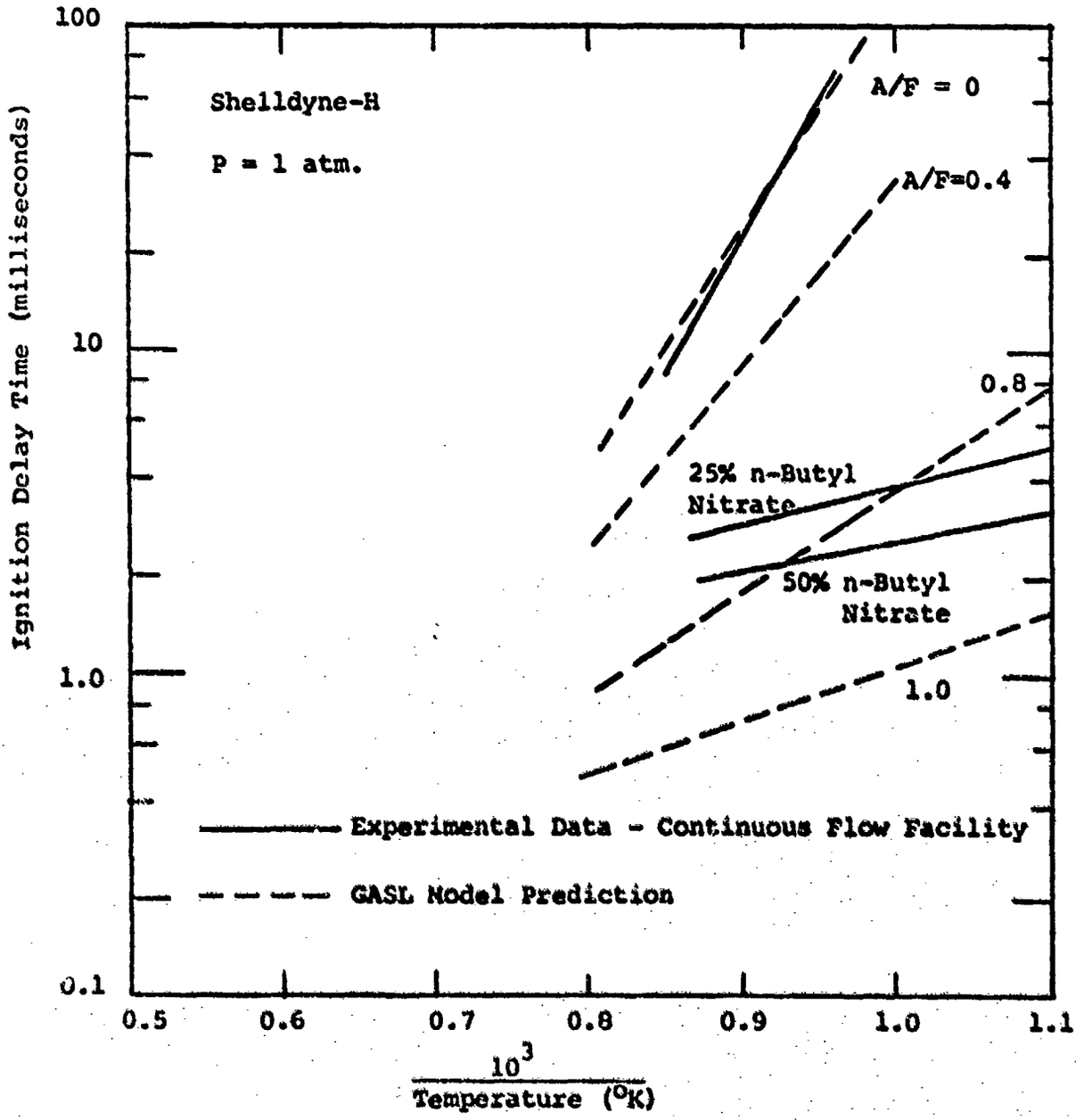

Figure 8 Comparison of a Quasi-Global Model for Cyclic Hydro-Carbon Fuels with Esso Experimental Ignition-Delay Times for the Shelldyne-H-Additive-Air System.

of this residence variation with the attendant result of early ignition occuring at the wall a study was made using the full mixing and combustion analysis described in Section II. In carrying out this analysis turbulent mixing and the adiabatic wall condition were assumed to prevail. The eddy viscosity in the near (potential core) region was taken to be

$$\mu = .0004\ \rho_e\ x\left(u_{\mathcal{L}} - u_e\right)$$

while in the fully developed region the eddy viscosity representation was

$$\mu = .018\ r_{\frac{1}{2}}\ (\rho u)_{\mathcal{L}}$$

where $(\ )_e$ denotes the local values in the outer stream, $(\ )_{\mathcal{L}}$ denoted centerline values and the quantity $r_{\frac{1}{2}}$ represents the radial distance corresponding to the point where the mass flux ρu takes on its average value. Typical results are shown in Figures 9 through 11 for an n-octane case at the operating conditions shown on the figures. Figure 9 shows the velocity profiles which are characteristic of fully developed turbulent pipe flow. Figures 10 and 11 are of particular interest showing the development of the species field during the induction period. It is noted that for x/D's $\leq$ 24 there is a build up of OH near the wall, Figure 10. However, the transport of the free radicals due to turbulent mixing is sufficient to accelerate the reaction process in the interior part of the flow. Thus, the combination of pure mixing and the associated increase in the reaction rate rapidly uniformizes the species profiles. This is also noted in Figure 11 in connection with the growth and development of the major species, CO_2 and H_2O. Finally, Figure 12 shows the development of the axial temperature distributions along the wall and centerline compared with the inviscid, one-dimensional theory. Although there is some difference it is not sufficient to be detected experimentally.

These results explain the consistency and generally excellent agreement that was obtained for the ignition delay comparisons presented earlier in this section. Namely, the behavior is predicted strictly on kinetic grounds rather than upon coupled fluid mechanical/chemical kinetics effects.

In summary the analysis has been shown to predict the neat fuel ignition delay characteristics. In addition, the results on additives indicate that fuel systems (neat fuel plus additive) can also be represented utilizing the relatively simple quasi-global mechanism. Finally, an evaluation of two-dimensional effects has shown that the Esso Dynamic Flow Facility does provide an effective premixed, one dimensional adiabatic flow.

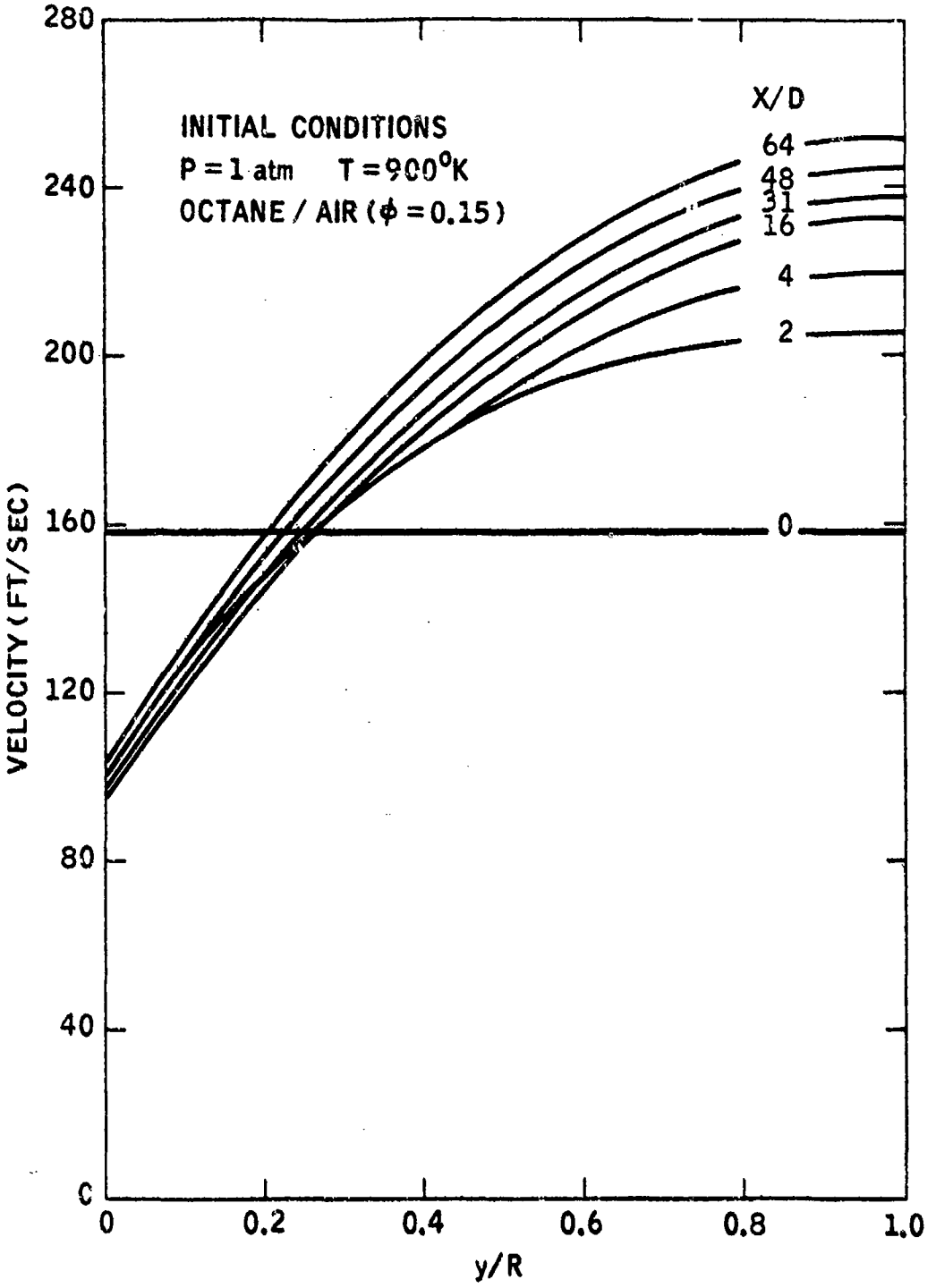

FIGURE 9 VELOCITY PROFILES AS PREDICTED BY THE GASL FINITE DIFFERENCE MIXING AND COMBUSTION MODEL

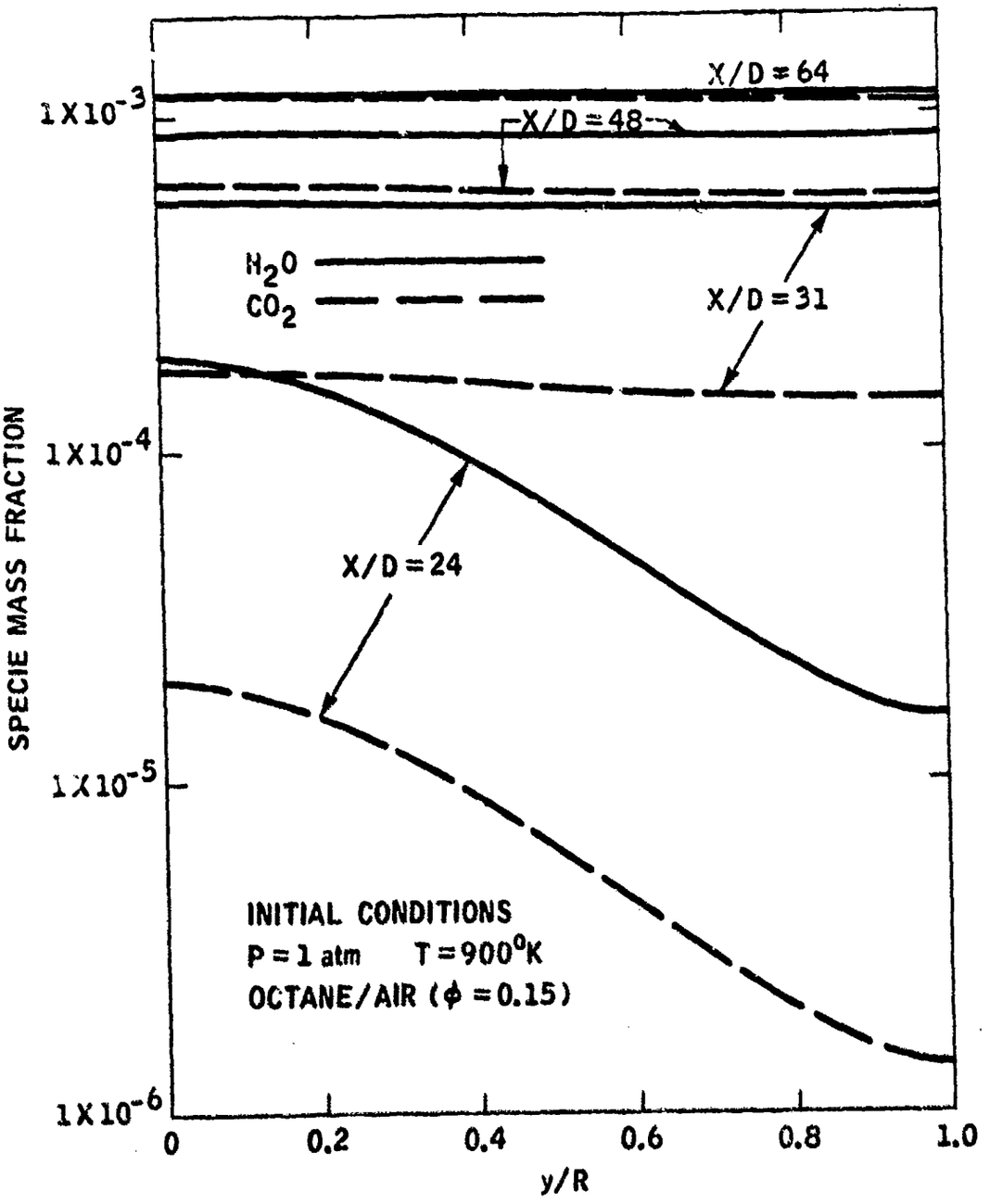

FIGURE 10 RADIAL DISTRIBUTION OF CO_2 AND H_2O AS PREDICTED BY THE GASL QUASI-GLOBAL CHEMISTRY MODEL

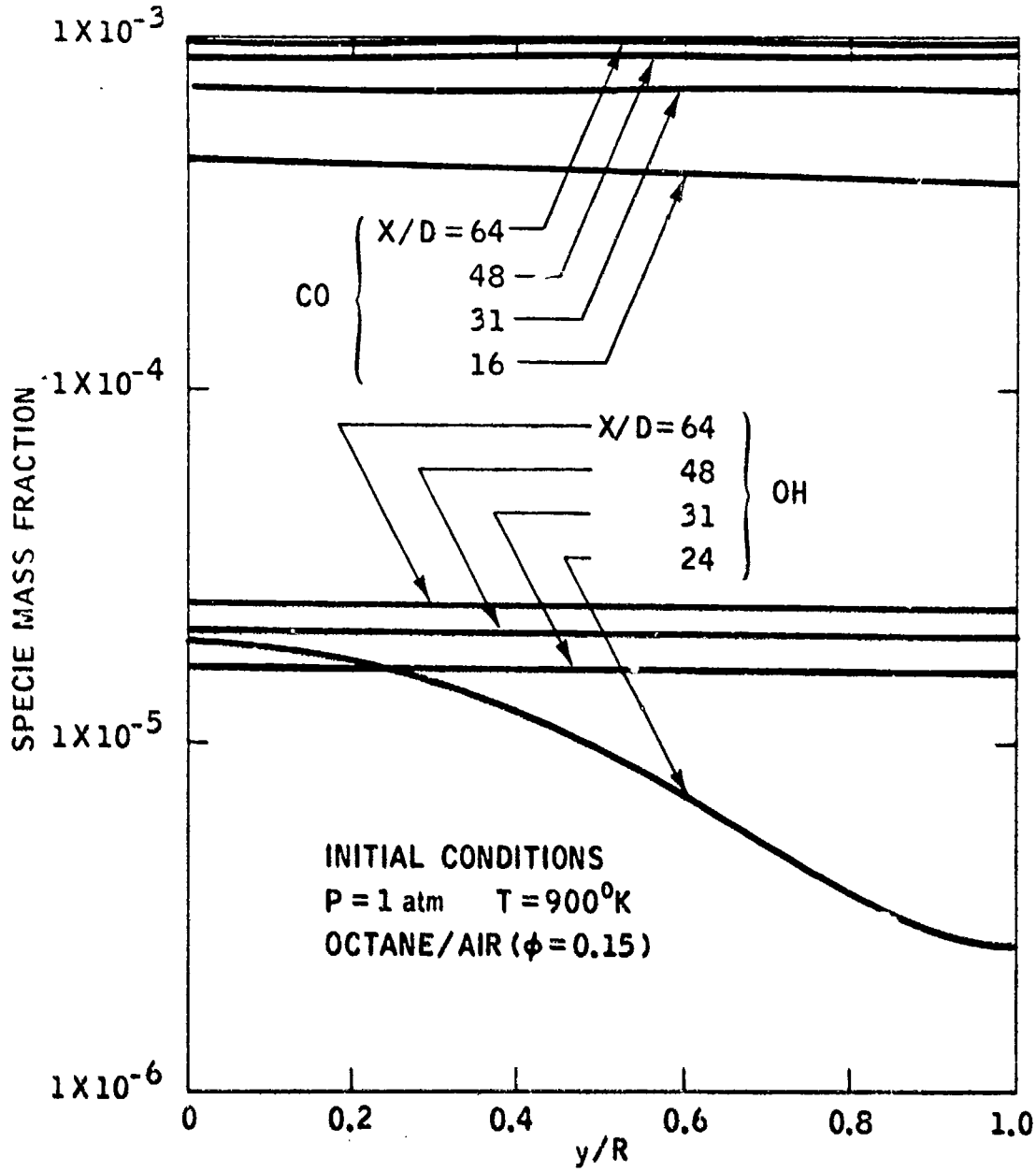

FIGURE 11 RADIAL DISTRIBUTION OF CO AND OH AS CALCULATED BY THE GASL QUASI-GLOBAL CHEMISTRY MODEL

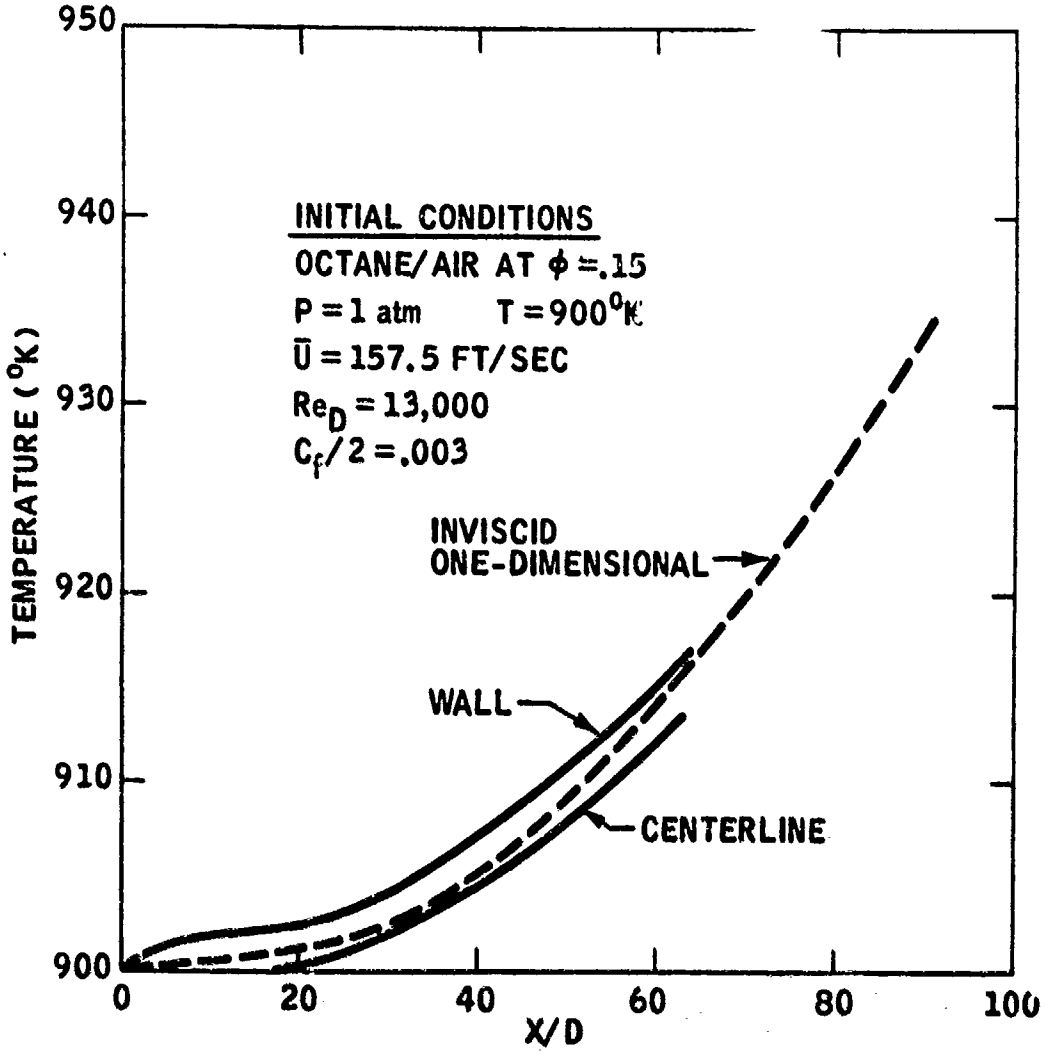

FIGURE 12 CENTERLINE AND WALL AXIAL TEMPERATURES AS PREDICTED BY THE GASL ANALYTIC MODEL

IV

EXPERIMENTAL ASPECTS

1. INTRODUCTORY REMARKS

In this section the supersonic combustion tests conducted by General Applied Science Laboratories is described. The primary objective of this phase (Phase III) of the program was to establish the relative performance of the candidate fuels under conditions approximating those occurring in a supersonic ramjet burner.

The candidate fuels, selected on the basis of the ranking and evaluation carried out in Phases I and II of this program, were Shelldyne-H and H-MCPD, with n-Propyl nitrate chosen as the candidate additive. To provide a basis for comparison, propane and hexane were also tested under identical conditions.

The original test configuration involved coaxial injection of vaporized fuel into an axisymmetric Mach 1.5 air stream with subsequent piloted ignition, mixing and combustion under free-jet type conditions (see Figure 13 (a) and 14). Only part of the test program utilized this test configuration. The program was completed using a test configuration which involved lateral injection of liquid fuel into a two-dimensional Mach 2 air stream with piloted ignition, mixing and combustion in a constant area duct. (See Figure 13(b)).

The change in test configuration was motivated by difficulties encountered in vaporizing the high density hydrocarbon fuels. In particular, it was found that pyrolysis and/or oxidation reactions caused considerable deposition of carbonaceous materials on the walls of the flow through fuel vaporizer (c.f. Figure 14). These deposits were sufficient to clog the system and render it inoperable despite the use of a high pressure water scrub.

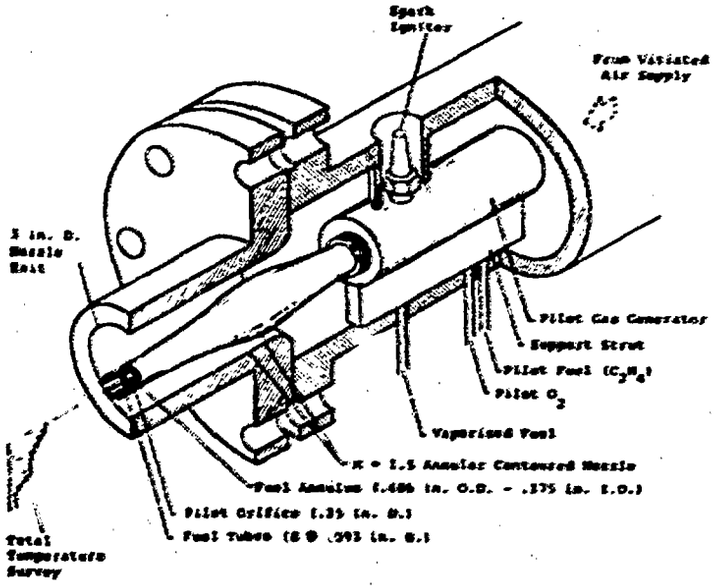

(a) Axial Rig

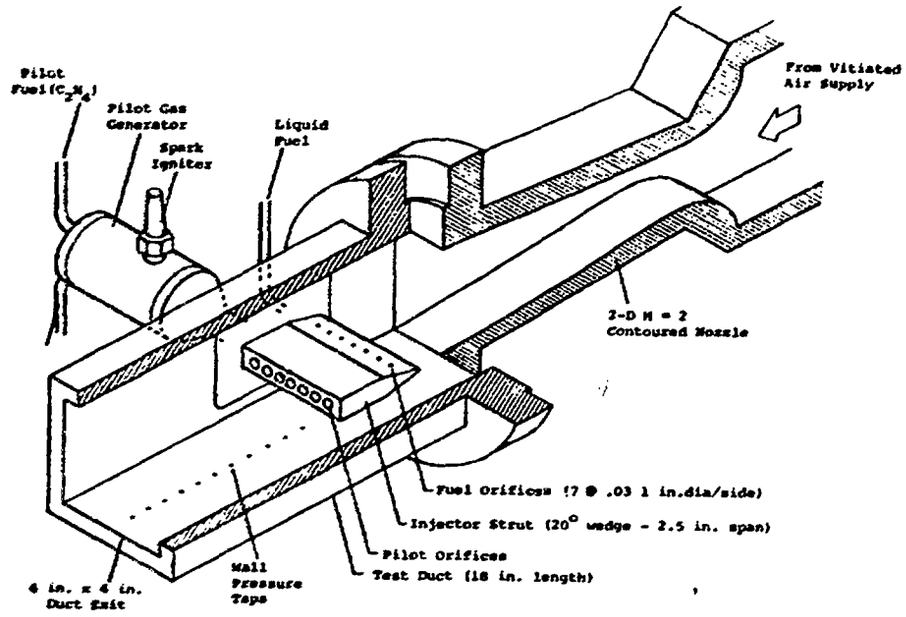

(b) 2-D Rig

Figure 13 SCHEMATICS OF EXPERIMENTAL APPARATUS

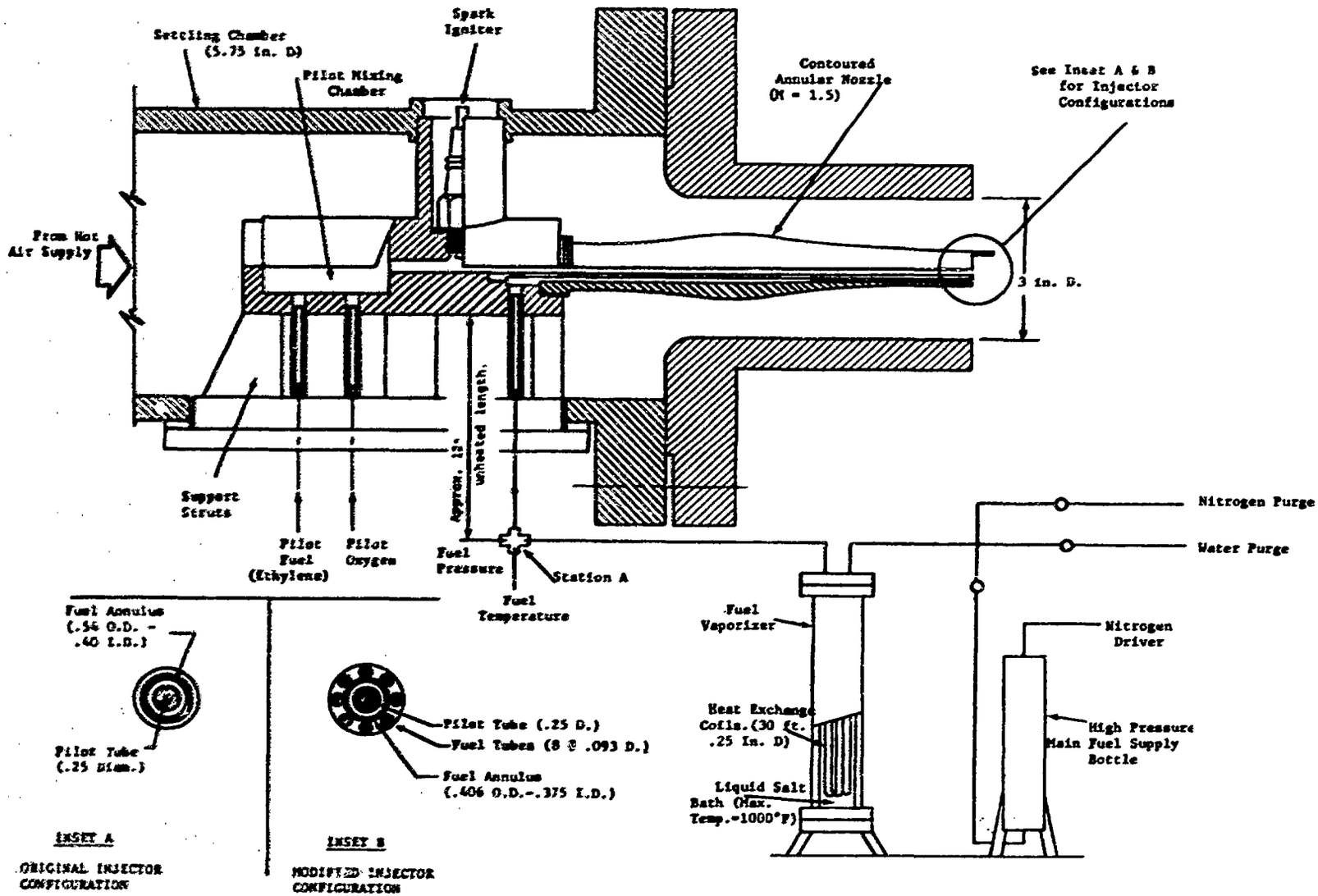

Figure 14 DETAILS OF AXIAL TEST CONFIGURATION

With Air Force approval the test program was completed with direct liquid injection. In this case a coaxial mode of injection cannot provide the flame holding characteristics needed to achieve combustion in short axial distances. Break-up of the fuel jet into a cloud of discrete droplets is required to provide the proper oxidizing environment for the bulk of the raw fuel. This is best accomplished by lateral injection of the liquid fuel into the supersonic main stream since the high shear and dynamic loads associated with the resulting interactions provide a very efficient mechanism for jet breakup. These interactions also give rise to localized high temperature regions which further enhance the evaporation and ignition of the fuel droplets. Accordingly a lateral injection configuration was adopted for the liquid fuel case utilizing an existing test rig. In the ensuing dicussion these two distinct test configurations will be referred to as "Axial" and "2-D" for the sake of brevity.

Another important difference between the two types of tests is the manner in which the combustion characteristics of the fuels were derived and compared with each other. For the axial tests total temperature surveys were obtained at various axial stations downstream of the duct exit. These results were utilized as a basis of comparison. For the 2-D tests the effect of combustion on the duct pressure distribution was used as the diagnostic.

In the next section the range of environmental conditions for these tests is presented. Then the details of the experimental equipment, instrumentation and test procedure are described. Finally, the results obtained are presented and discussed with particular emphasis on the relative performance and ranking of the various neat and neat/additive fuel systems both with respect to each other as well as with the base fuels. Within each of these individual sections, the axial results are presented first followed by the corresponding onos for the 2-D case.

2. ENVIRONMENTAL CONDITIONS

In addition to the geometric configurations which will be described in the next section, the environmental conditions for both the axial and 2-D tests are completely characterized by specification of the following parameters:

- The air stream total temperature (T_{t_∞}), Mach number (M_∞) and static pressure (p_∞), where $(\ )_\infty$ denotes conditions occurring at the respective nozzle exits.
- Main fuel type (including percent additive), mass flow rate ($\dot{m}_f$), total temperature (T_{t_f}) and exit Mach number (M_f) or exit velocity (V_f).
- Pilot gas equivalence ratio (φ_p), mass flow rate ($\dot{m}_p$), and exit Mach number (M_p). Note that since the pilot reactants for all tests are oxygen-ethylene φ_p is related to the O/F ratio by $\varphi_p = 3.429/(O/F)$.

Derivable from these data are certain other parameters of interest including total air mass flow ($\dot{m}_T$), global equivalence ratio (φ_T), pilot adiabatic flame temperature (T_{t_p}) and pilot to fuel mass flow ratio ($\beta=\dot{m}_p/\dot{m}_f$).

The overall range of these parameters for both the axial and 2-D tests are given in Table IV . The specific conditions for the individual tests as well as the manner in which these were determined experimentally are discussed in subsequent sections.

3. EXPERIMENTAL APPARATUS

a. Axial Rig

As may be seen in Figures 13 (a) and 14 the major components of this set-up include

- High temperature air source
- Wind tunnel nozzle
- Pilot gas generator

TABLE IV

OVERALL RANGE OF ENVIRONMENTAL CONDITIONS

PARAMETER	RANGE	
	AXIAL	2-D
M_∞	1.5	2.0
T_{t_∞} (^oR)	530-2730	490-2530
p_∞ (atm)	.96-1.07	.69-.99
Fuel Type	. neat Propane . neat Hexane . neat Shelldyne-H . Shelldyne-H + 15% n-propyl nitrate	. neat Hexane . neat Shelldyne-H . neat H-MCPD . Shelldyne-H + 15% n-propyl nitrate . H-MCPD + 15% n-propyl nitrate
$\dot{m}_f$ (pps)	.032-.048	.071-.180
T_{t_f} (^oR)	910-1230	530
M_f	1.0	-
V_f (fps)	-	30-70
ω_p	.17-.32	.166-.189
$\dot{m}_p$ (pps)	.0043-.0135	.0051-.0164
M_p	1.0	1.0
$\dot{m}_T$ (pps)	2.61-6.77	10.5-23.4
ω_T	.065-.232	.045-.176
T_{t_p} (^oR)	3830-4890	3800-4040
β	.119-.415	.041-.232

Notes:

1. For the 2-D tests M_p = 1.0 corresponds to conditions at the pilot orifice where d* = .086 inches.
2. For the 2-D tests the values of p_∞ appearing here and in Tables VI and VII correspond to readings obtained at pressure tap No. 4 whose location is given in Table V
3. The values of V_f have been estimated from the measured mass flow rates by using a discharge coefficient for the fuel orifices of C_D = 0.60.

o Fuel supply and vaporizer system

Each of these components is described in detail below.

(1) High Temperature Air Source

The high temperature air was supplied by vitiation heating of dry air in a hydrogen combustion heater. Sufficient make-up oxygen is added to produce a working fluid with a composition of 23% oxygen by mass plus nitrogen and water vapor in varying proportions depending on the desired total temperature as shown in Figure 15. The effect of this vitiation on the nozzle exit conditions is discussed below. This facility can provide mass flows up to 20 pps with maximum total temperature and pressure levels on the order of 3300°R and 500 psia, respectively. The dry air is obtained from a 1000 ft^3 - 2000 psi air storage facility. High pressure hydrogen and oxygen is obtained by manifolding a number of standard high pressure cylinders.

(2) Wind Tunnel Nozzle

The wind tunnel nozzle which expands the working fluid to supersonic velocity is formed by a contoured center body aligned concentrically within a nominally 3 inch diameter constant area duct. This center body is supported by a structure located upstream of the tunnel throat within which the pilot gas generator is also housed. As may be seen in Figure 14, passages are provided within the center body to supply fuel and pilot gas to the injector exit located at the extreme downstream end. The injector-pilot configuration itself will be described later in Section IV-6. The minimum area of the wind tunnel nozzle corresponds to an annulus of 3 inches O.D. by 1.35 inches I.D. The corresponding values at the exit (located 4.5 inches downstream of the throat) are 3 inches O.D. by .604 inches I.D. This yields an overall geometric expansion ratio of 1.2 which, for a specific heat ratio, γ, of 1.4

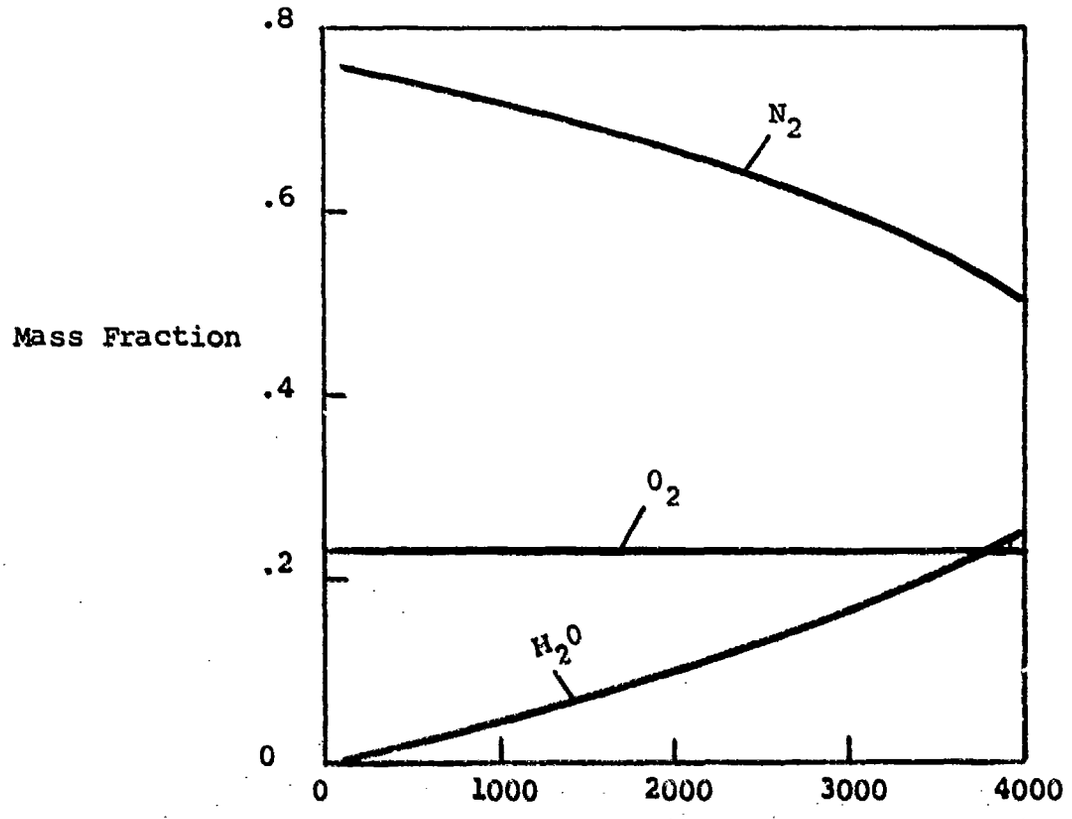

Figure 15 COMPOSITION OF VITIATED AIR AS A FUNCTION OF COMBUSTION TEMPERATURE FOR HYDROGEN COMBUSTION
(Initial Temperature of Reactants = 100°F)

would correspond to a Mach number of approximately 1.53[1]. With vitiation, of course, γ varies according to the degree of vitiation. This would, in turn, lead to some variation in the exit Mach number, static-to-stagnation pressure ratio etc. as shown in Figure 16 which is based on an extensive study performed at GASL to investigate these effects (24) As may be noted therein the effect is relatively minor and will not be considered in the further discussion.

(3) Pilot Gas Generator

The pilot gas generator which is housed in the center body support consists of a small mixing chamber (1.25 inches diameter by 2.5 inches long) into which the reactants (oxygen-ethylene) are introduced through stainless steel tubing in the desired proportions. The combustible mixture then expands into the 0.25 inch diameter tube and is ignited by an aircraft-type spark plug. Once ignition has been initiated the spark plug can be deactivated and combustion sustained so long as the reactant flows are maintained. The performance of the gas generator in terms of flow rates, mixing chamber pressure, equivelence ratio and adiabatic flame temperature is shown in Figures 17 and 18 for the range of conditions of interest here.

(4) Fuel Supply and Vaporizer System

Fuel was supplied to the injector by means of the system shown schematically in Figure 14. The fuel was stored in a high pressure supply bottle with a volumetric capacity of approximately 0.28 ft.^{3}. A regulated high pressure nitrogen source was used to drive the fuel from this bottle and through the vaporizer coils which were immersed in a liquid salt bath maintained at the desired temperature. The heat exchange medium utilized in this vaporizer was a commercially available mixture of inorganic salts specifically designed for this application. It is referred to as HITEC heat transfer salt and is manufactured by DuPont of Wilmington, Deleware. Heating of the salt bath is by means of six 1000 watt electrical

---

1. In these considerations displacement thickness effects have been neglected since for the condition under which these tests were conducted the displacement thickness at the exit is estimated to be on the order of .015 inches.

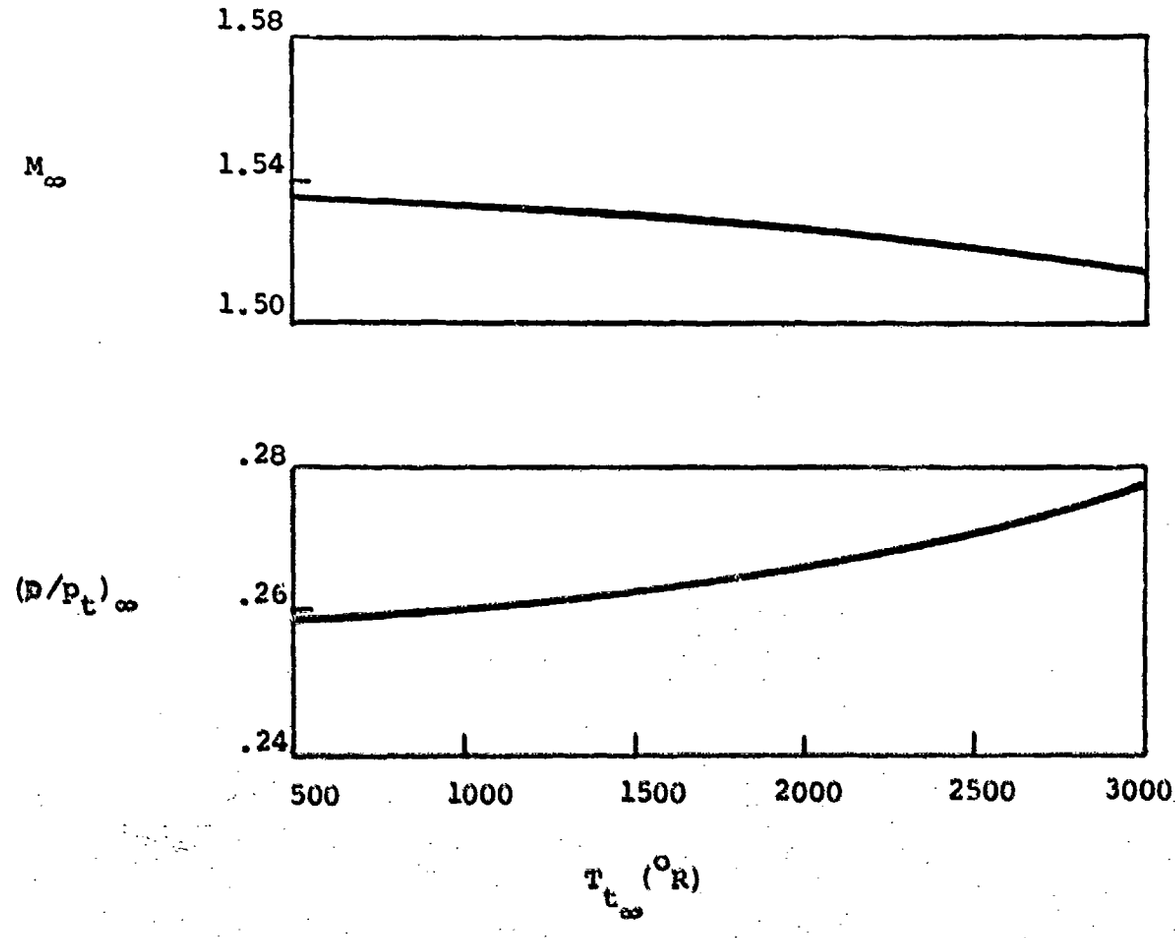

Figure 16 EFFECT OF VITIATION ON PERFORMANCE OF THE AXIAL NOZZLE ($A/A_* = 1.2$)

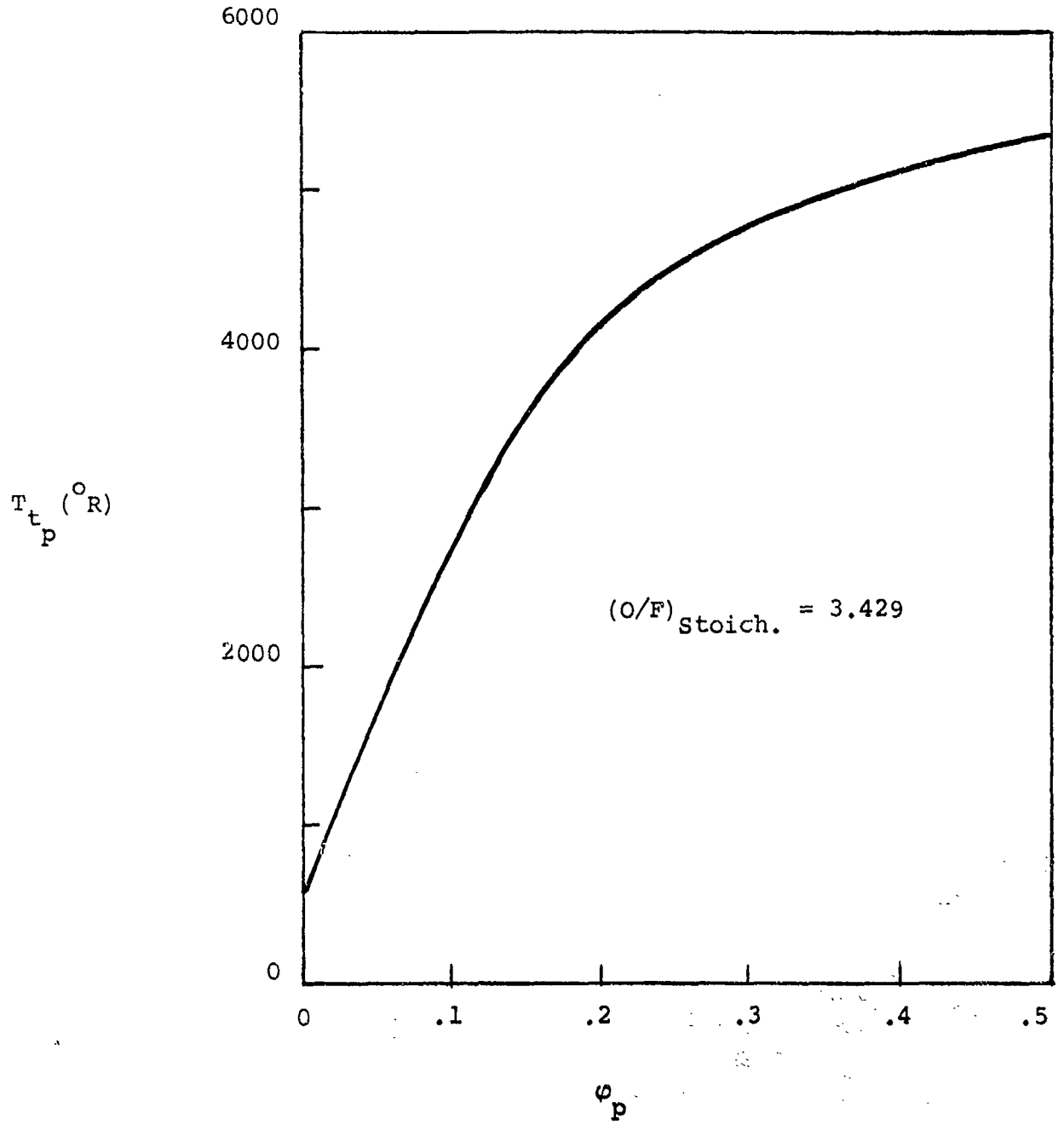

Figure 17 ADIABATIC FLAME TEMPERATURE OF GASEOUS ETHYLENE - OXYGEN PILOT

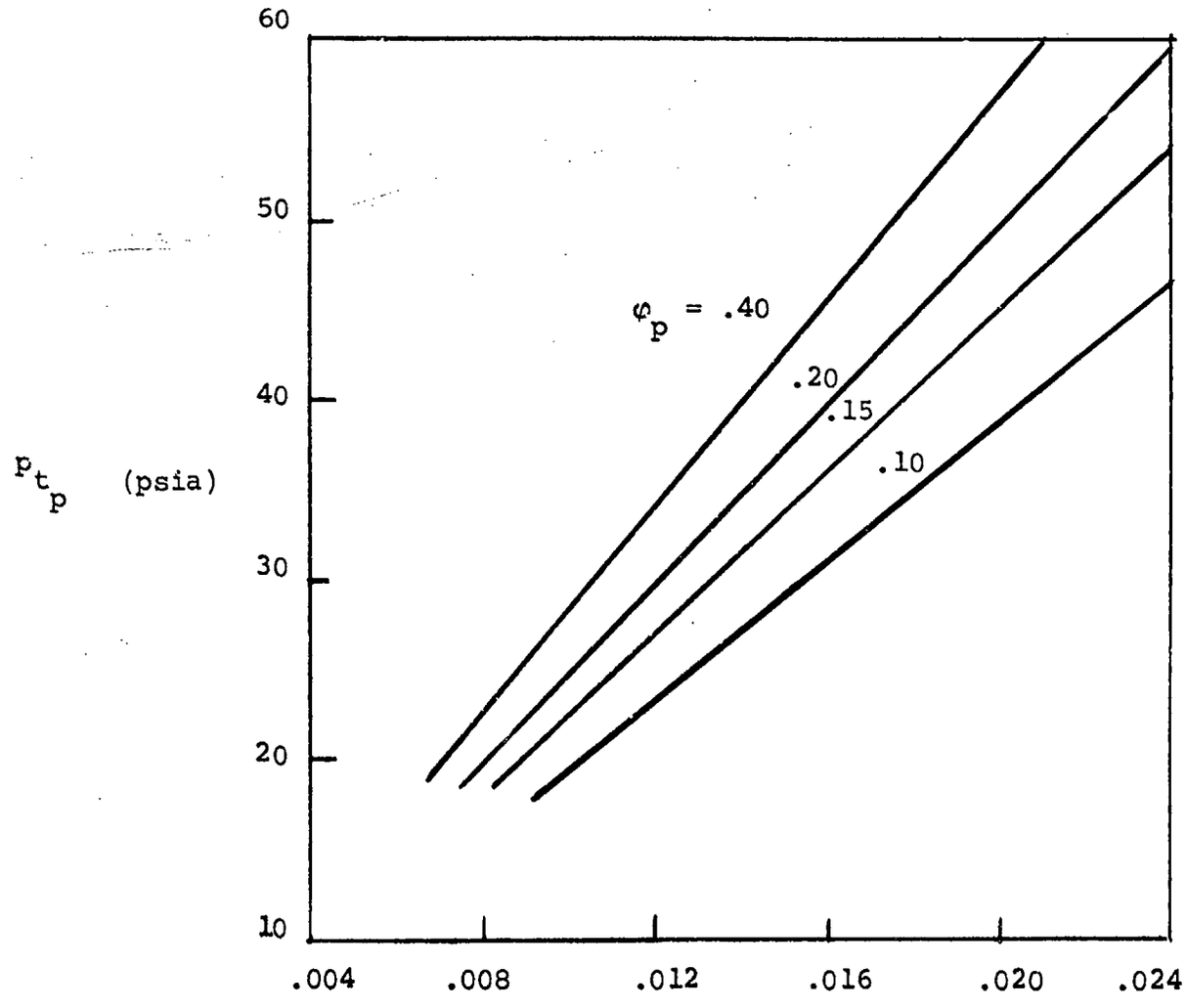

Figure 18 PERFORMANCE OF PILOT GAS GENERATOR FOR AXIAL TEST SERIES

resistance heating elements. The vessel in which the salt is contained is a flanged, 48 inch vertical section of 3"xx-316 stainless steel pipe which is vented to atmosphere. The volumetric capacity of this vessel is approximately 0.12 ft.^{3}. A total of 30 ft. of 0.25 inch I.D. by .035 inch wall stainless steel tubing make-up the heat exchange coils.

b. 2-D Rig

As shown in Figure 13 (b) the major components of this facility include

- o High temperature air source
- o Wind tunnel nozzle
- o Test duct
- o Pilot gas generator
- o Injector strut

The features and characteristics of these components are as follows:

(1) High Temperature Air Source

The supply of high temperature air for the 2-D test series was also obtained by vitiation heating but utilized a different GASL facility, Combustor No. 1, a schematic of which is shown in Figure 19. This facility is capable of somewhat higher performance insofar as total temperature (up to 3600°R) and total pressure (up to 600 psi) are concerned. In all other respects the operating procedures are essentially identical to those previously described including the data shown in Figure 15 .

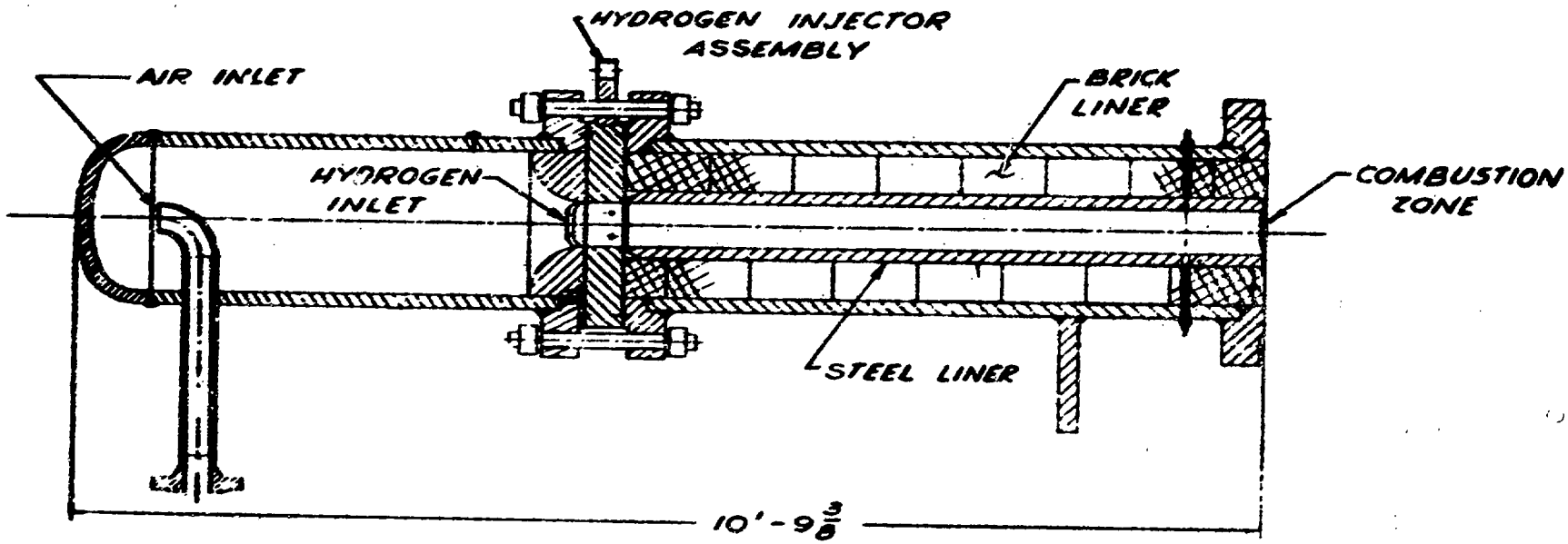

FIGURE 19. COMBUSTOR No. 1 SCHEMATIC

(2) Wind Tunnel Nozzle

For the 2-D tests expansion of the working fluid was accomplished by means of a two-dimensional set of contoured nozzle blocks providing a nominal exit Mach number of two. The pertinent dimensions of this nozzle are

Throat: 2.1 inches by 4.05 inches
Exit: 4.05 inches by 4.05 inches
Length: 20 inches from throat to exit.

The geometric expansion ratio is therefore 1.92 corresponding to a Mach number of 2.15 for $\gamma=1.4$. The effect of vitiation on the nozzle characteristics for this case are given in Figure 20. The wind tunnel nozzle was provided with a series of flush static pressure taps located in accordance with the schedule given in Table V.

(3) Test Duct

The test duct consisted of an 18 inch long nominally constant area extension of the wind tunnel nozzle. This extension was designed to accomodate the injector-strut-gas generator assembly on one of the side walls. On the opposite wall, viewing ports were provided consisting of two air-cooled 3 inch by 4 inch pyrex windows[2]. A typical photograph of the test duct showing the windows and the relative position of the injector strut within is shown in Figure 38. The test duct was also provided with a series of flush .040 inch diameter static pressure taps. Their location as well as the location of the injector strut is indicated in Table V.

(4) Pilot Gas Generator

As indicated in Figure 13(b), the gas generator used in the 2-D experiments is mounted external to

2. The window frames reduce the clear viewing area to 2.5 inches by 3.5 inches.

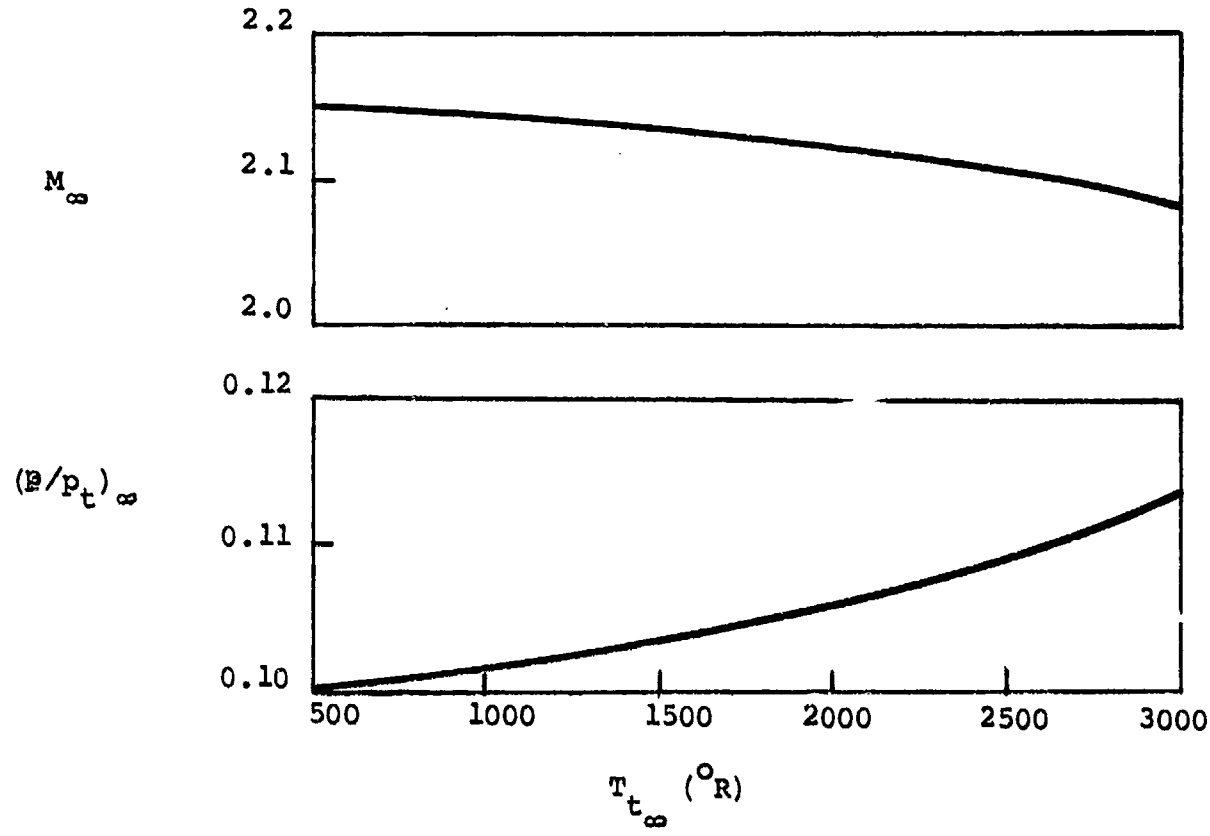

Figure 20 EFFECT OF VITIATION ON PERFORMANCE OF THE 2-D NOZZLE ($A/A_* = 1.92$)

TABLE V Schedule of coordinates and pressure tap locations for the 2-D wind tunnel facility.

Identification Pressure Tap Number	Distance From Nozzle Throat In Inches	Orientation
110	10.1	B
111	11.1	B
112	12.1	B
113	13.1	B
1	14.25	B
2	15.25	B
3	16.25	B
4	17.25	B
5	18.37	B
10	22.75	F
11	22.75	D
12	22.13	E
13	23.63	E
14	24.63	E
15	25.63	E
16	26.63	E
17	27.63	E
18	28.63	E
19	29.63	E
20	30.63	E
21	31.63	E
22	32.63	E
23	33.63	E
24	34.63	E
25	35.75	E
26	22.13	A
27	23.13	C
28	24.13	A
29	25.13	C
30	26.5	A
31	27.4	C
32	28.13	A
33	29.13	C
34	30.13	A
35	31.13	C
36	32.13	A
37	33.13	C
38	34.13	A
39	35.13	C
40	36.13	A
Nozzle Exit	20.0	
Strut Leading Edge	26.2	
Leading Edge of First Window	26.37	
Leading Edge of Second Window	31.13	
Test Duct Exit	38.0	

KEY TO PRESSURE TAP ORIENTATION

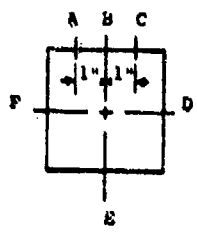

View Of Test Duct Looking Upstream

the test duct. A schematic of this device showing pertinent dimensions is shown in Figure 21. In this case the reactants (oxygen-ethylene) are pre-mixed upstream of a "mushroom" type flame holder around which they expand into the low speed combustion chamber proper. Ignition of the combustible mixture is again accomplished by means of an aircraft-type spark plug which is deactivated once ignition has been achieved. The hot products of combustion then issue out through a single 0.25 inch diameter orifice and flow into the injector-strut-pilot gas manifold to which the gas generator is connected by means of a threaded fitting. The performance of this device is shown in Figures 17, 6 and 22.

(5) Injector Strut

The injector strut consists of a two-dimensional 20° total angle wedge followed by a constant thickness afterbody which spans the test duct. The maximum thickness of the strut is 0.5 inches and the overall chord width is 2.5 inches. The strut is installed at zero angle of attack and is located symmetrically with respect to the horizontal plane of symmetry of the duct with the leading edge 26.2 inches downstream of the nozzle throat. The leading edge is blunted with a nose radius of .062 inches.

The strut is provided with two internal manifolds which feed the fuel and pilot gas orifices. The pilot orifices are located in the rearward facing base of the strut, are equally spaced across the span and consist of 7-10° conical orifices with exit diameter of 0.25 inches and throat diameter of .086 inches. For the operating conditions utilized in this test program, this geometry leads to over-expanded operation of the orifices sufficient to cause a stationary shock system to occur within the conical portion leading to subsonic, and therefore, matched pressure operation at the exit.

The fuel orifices are located in the upper and lower surfaces of the wedge and consist of a total of 14 equally spaced .031 inch diameter holes drilled through to the manifold normal to the wedge surfaces. The fuel orifices are located at a point approximately 0.80inches downstream of the strut leading edge.

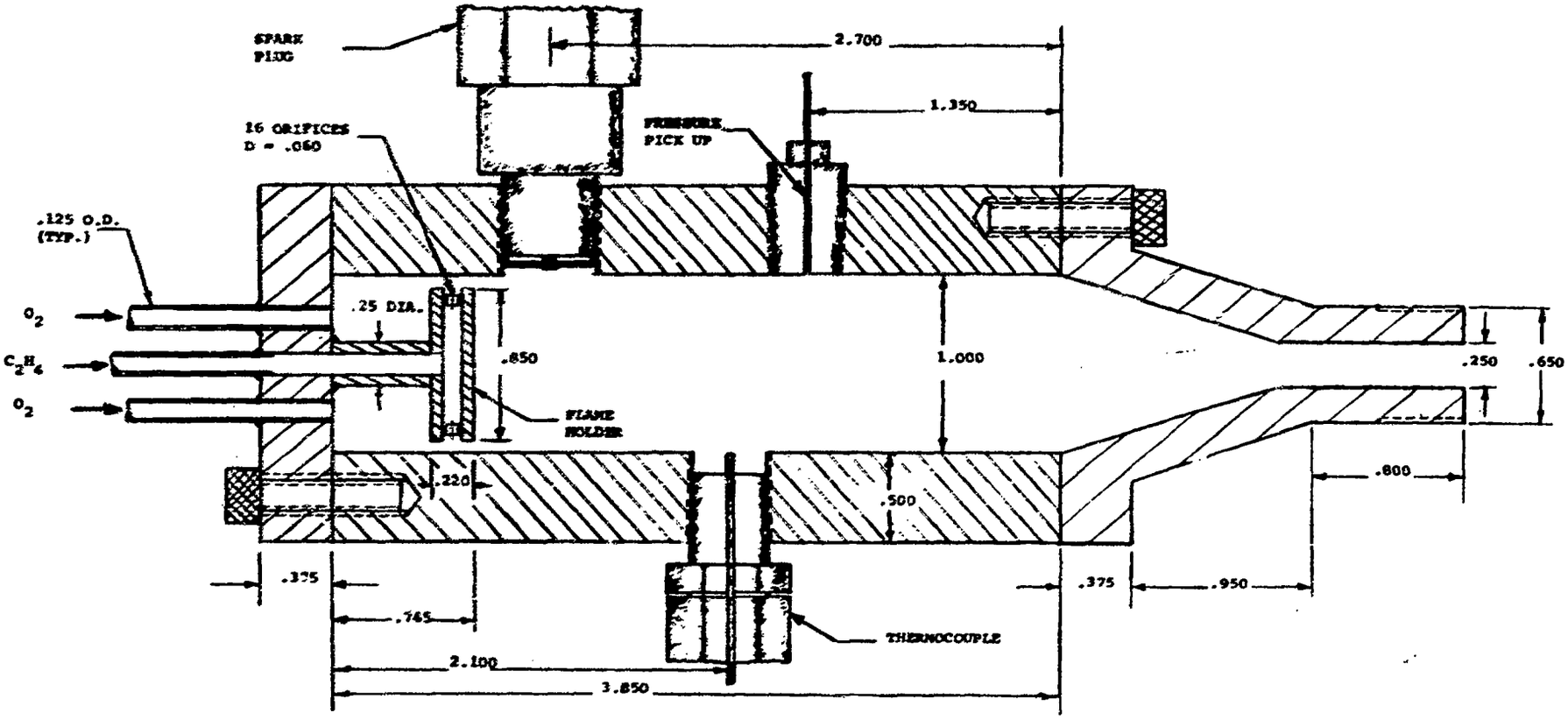

Figure 21 DETAILS OF PILOT GAS GENERATOR FOR 2-D TEST SERIES

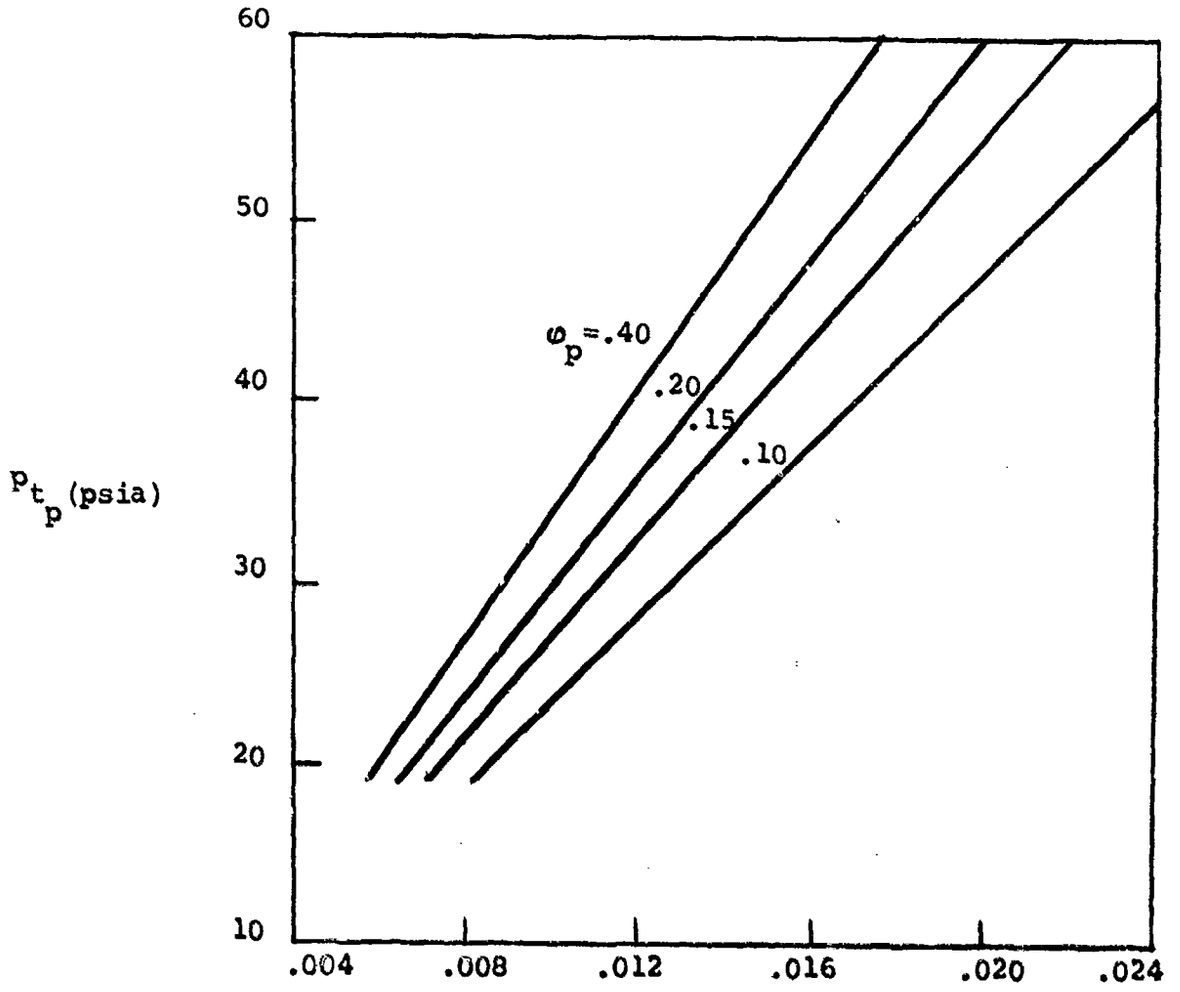

Figure 22 PERFORMANCE OF PILOT GAS GENERATOR FOR THE 2-D TEST SERIES

The fuel plenum is supplied by means of a 0.25 inch O.D. by 0.180 inch I.D. stainless steel tube welded to one end of the strut. The fuel supply system in this case is essentially identical to that used for the axial tests except that the vaporizer is removed from the system.

The pilot gas is introduced into the manifold directly from the pilot gas generator to which it is attached by means of threaded fittings.

4. MEASUREMENTS AND INSTRUMENTATION

a. Axial Tests

Data retrieval during a typical axial test included the following items:

- Stagnation and static pressures associated with standard gas venturi meters monitoring mass flow of tunnel air, tunnel oxygen, tunnel hydrogen, pilot ethylene, pilot oxygen.

- Stagnation and static pressure associated with a cavitating venturi meter used to monitor the fuel flow rate. This device, which is manufactured by the Fox Valve Development Co., Inc. of Mountain Lakes, New Jersey, is designed to reduce pressures within the venturi below supercritical values causing cavitation and effectively providing a chocked orifice (i.e., downstream pressure feedback is suppressed). Steady state flow rates are assured thereby regardless of any downstream disturbances. The actual mass flow rate is determined from the measured pressures from calibration curves such as that shown in Figure 23 . Note that the abscissa represents the difference between the measured pressure and the vapor pressure of the particular liquid fuel.

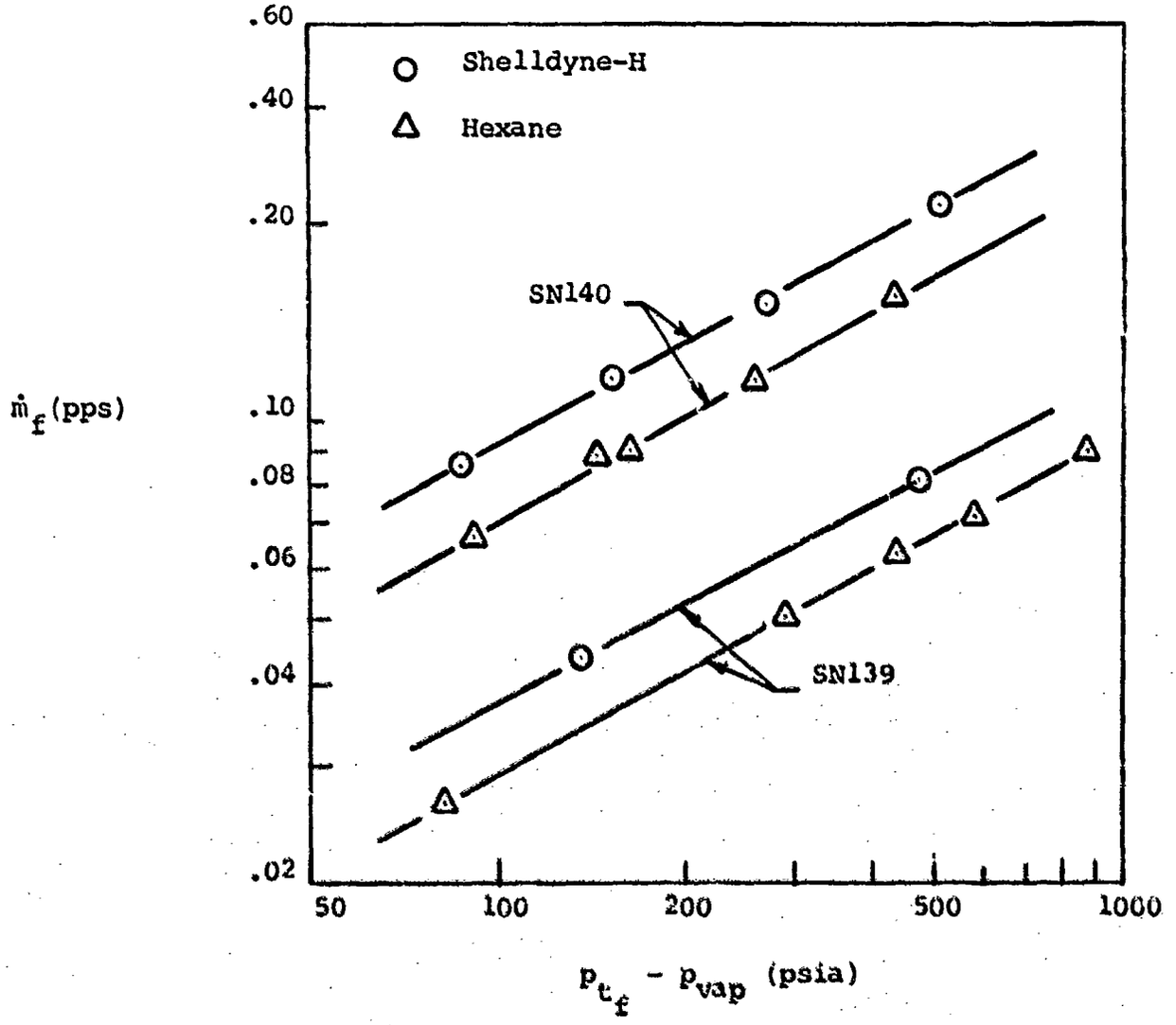

Figure 23 CALIBRATION CURVES FOR CAVITATING VENTURIES

- Stagnation pressure in the wind tunnel settling chamber ($p_{t\infty}$), the pilot gas generator mixing chamber (p_{tp}) and in the main fuel line (p_{tf})[3].
- Static pressure at the nozzle exit.
- Stagnation temperature in the wind tunnel settling chamber ($T_{t\infty}$) and in the main fuel line (T_{tf})[3].
- Radial distribution of total temperature and pitot pressure across the jet at a fixed downstream station.
- Motion and still color photographs of the mixing zone.

The flow phenomena were also monitored visually by means of a closed circuit TV system.

The pressures were sensed by Statham pressure transducers of appropriate range and their analog signals were recorded on Minneapolis-Honeywell Model 1508 Visicorders via Model 658 Sanborn amplifiers. The temperature sensors were either chromel-alumel or Pt-pt/10% RH thermocouples and recorded in the same manner as the pressures.

The camera equipment utilized included a Crown Graph -lex camera with Polaroid back for the stills and a Bolex H-16 Rex 16 mm motion picture camera. The films utilized were Polaroid Type 48 and Kodak Ektachrome No. 7242 respectively. To obtain the pitot and total temperature surveys the rake shown in Figure 24 was used. This rake was mounted on a DC motor driven traverse mechanism part of which can be seen, for example, in the photograph shown as Figure 27(a). During any given run the rake was slowly traversed (~0.5 ips) through the vertical plane of symmetry of the jet with the analog signals from the pitot and total temperature probes recorded continuously. The position of

---

3. The point where p_{tf} and T_{tf} were measured is denoted as Station A in Figure 14.

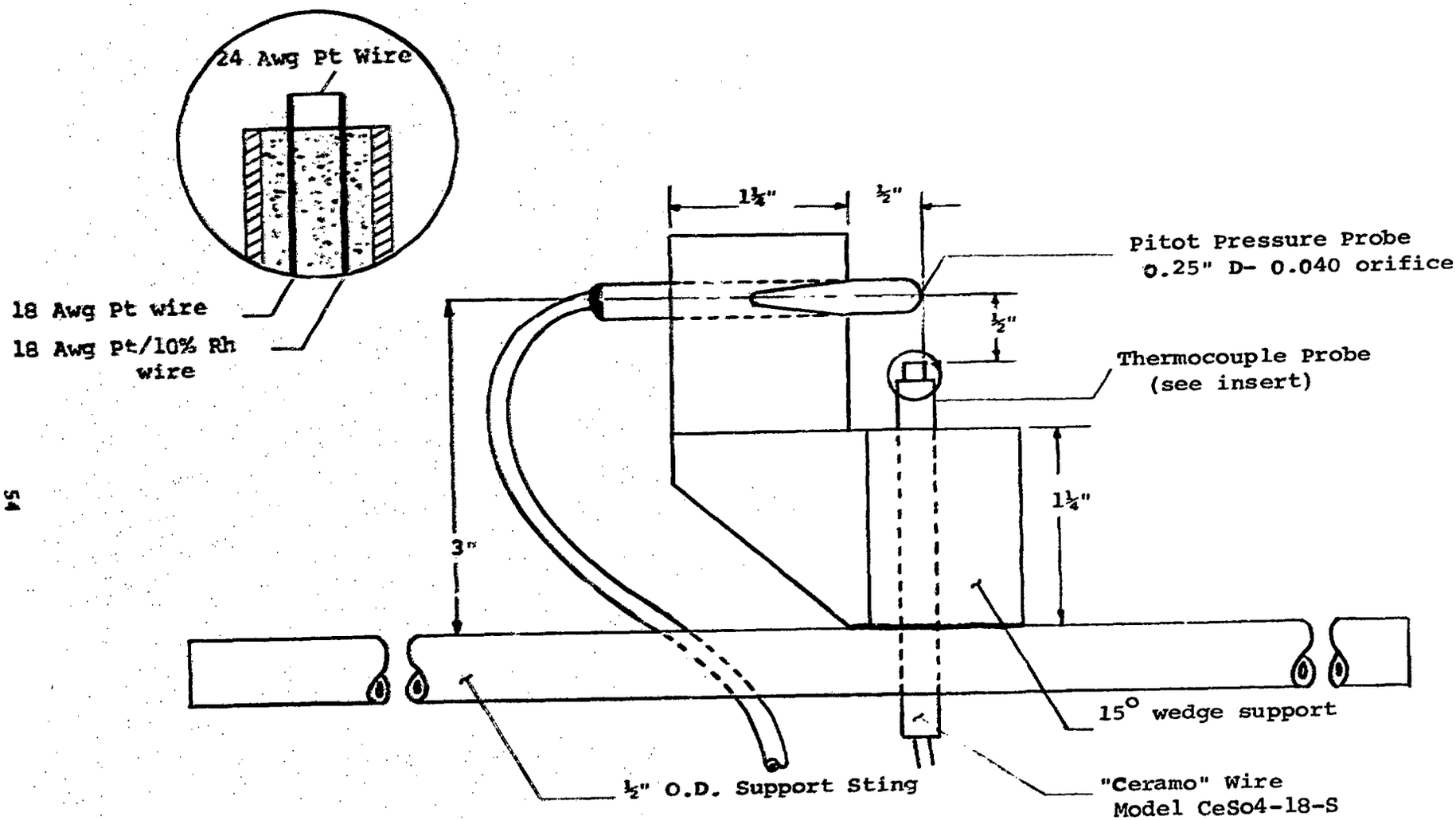

Figure 24 SCHEMATIC OF RAKE USED IN AXIAL TESTS

the rake was determined at each instant by simultaneously recording the output of a slide wire potentiometer mechanically attached to the supporting mechanism. The rake can be seen in various positions relative to the jet axis in several of the photographs discussed in Section IV-6.

The pitot pressure leg of the rake consisted of a 0.25 inch hemisphere cylinder with a .040 inch orifice located in the nose. The total temperature leg utilized a 0.25 inch O.D. sheathed thermocouple wire (trade name CERAMO as manufactured by Thermo-Electric Co., of Saddlebrook, New Jersey) with a Pt-Pt/10% RH calibration. The bare thermocouple junction itself was formed by welding a 24 gauge platinum wire across the two 18 gauge leads of the CERAMO thermocouple. The junction was oriented so that the thin wire was aligned with the primary flow direction. This configuration provides for improved response, needed because of the motion of the probe, and combines it with a relatively high strength arrangement, also required because of the high temperature environment to which the probe is exposed.

b. 2-D Tests

Data retrieval during a typical 2-D test included the following items.

- Stagnation and static pressures associated with standard gas venturi meters monitoring the mass flow of tunnel air, oxygen and hydrogen, and pilot ethylene and oxygen.

- Stagnation and static pressure associated with the cavitating venturi used to monitor the fuel flow rate. This device was located immediately downstream of the high pressure fuel supply bottle. The pressure of the nitrogen driver gas at the head end of this bottle was also monitored.

- Stagnation pressure in the wind tunnel settling chamber and the pilot gas generator combustion chamber.
- Static pressures in the nozzle and the test duct.
- Stagnation temperature in the wind tunnel settling chamber.
- Motion and still color photography of the mixing zone.

In this case, of course, the fuel stagnation temperature was simply the ambient temperature as recorded within the high pressure supply bottle. The fuel total pressure which is reported is the pressure recorded on the high pressure side of the cavitating venturi.

Recording of these data was identical with that for the axial tests except that the static pressure data in the nozzle and test duct were sensed by a single 0-50 psia transducer by means of a scanning type pressure sampling valve (SCANIVALVE - CO., San Diego, California).

The type of film utilized was also the same as that used for the axial tests and the tests were also monitored visually via the TV set up.

5. TEST PROCEDURE

a. Axial Tests

The test procedure involved the following sequence of events:

- o Establish steady state tunnel operation.
- o Initiate pilot gas generator operation.
- o Initiate main fuel flow and verify steady state combustion visually.
- o Actuate probe traverse mechanism.
- o Shutdown and purge all systems.

The data acquisition system and the motion picture camera were actuated prior to all of these events and continued throughout the entire sequence. The still photographs were generally obtained shortly after the probe traversing had been initiated.

With the exception of tunnel air the flow of all fluids was established by means of quick acting, remotely actuated solenoid valves. The flow rates were controlled by presetting of regulators in accordance with pre-established calibration curves. The air flow was controlled manually by means of a Fisher Air Valve (Fisher Governor Co., Marshalltown, Iowa), the desired flow rate being established by monitoring the high pressure side of the air venturi. Steady state tunnel operation was also verified by monitoring T_{t_∞} on a strip chart recorder.

Actuation of the traverse mechanism and the Crown Graphlex camera shutter was also accomplished by remotely operating switches.

Shutdown and purging of all systems occurred as soon as the probe traverse had been completed. This was accomplished by a single switch which is wired so as to override all flow valve solenoids and automatically activates the nitrogen purge supply valves.

The overall time required to complete this entire sequence was on the order of 30 seconds with about 10 seconds required to achieve steady state tunnel operation and an additional 5 seconds required to complete the probe traversing.

b. 2-D Tests

The test procedure for the 2-D tests was identical to that for the axial series except that no probe traverse was involved. Here steady state combustion was allowed to continue for a sufficient period of time to allow a minimum of three complete cycles of analog signal output from the scanivalve to be recorded. In this way any transient behavior in the pressure field existing within the test duct would be either eliminated or observed. In this connection it should be noted that the scanning frequency utilized during these tests was 20 cycles per minute so that with 3 scans the presurres were monitored for a period of approximately 10 seconds.

6. AXIAL RESULTS

a. Preliminary Remarks

The test run log of axial tests is presented in Table VI . As will be noted this series begins with Run No. 36, corresponding to the first test in which ignition and combustion of the main fuel was successfully achieved. Before discussing the results obtained starting with Run 36, it is appropriate here to review briefly the difficulties encountered prior to this point.

During this initial plase, the experimental apparatus differed from that which ultimately proved successful in two important respects. First of all, the reactants utilized in

TABLE VI

SUMMARY OF AXIAL TEST RESULTS

Run No.	T_{t_m} (°R)	P_m (psia)	Fuel Type	$\dot{m}_f$ (pps)	T_{t_f} (°R)	P_{t_f} (psia)	$\dot{m}_f$ (pps)	σ_p	T_{t_p} (°R)	β	$\dot{m}_T$	σ_T	Location Of Survey Station	Maximum Temperature Recorded	Character Of Observed Flame
36	2710	14.6	Hexane	.038	1110	56	.0123	.32	4890	.323	2.61	.222	-	-	Steady
37	2630	14.6	Hexane	.039	1050	80	.0119	.31	4840	.305	2.56	.232	-	-	Steady
38	2100	14.8	Hexane	.038	1230	81	.0119	.31	4840	.313	2.97	.194	12.5	3285	Steady
39	540	14.3	Hexane	.040	1140	88	.0120	.30	4810	.300	6.43	.095	12.5	1835	Steady
41	2320	14.6	Propane	.032	1130	132	.0129	.31	4840	.403	2.95	.169	12.5	3500	Steady
42	540	14.8	Propane	.033	1140	131	.0127	.31	4840	.384	6.45	.080	12.5	1510	Steady
43	520	14.8	Propane	.045	950	161	.0126	.30	4810	.280	6.56	.117	8.25	685	Intermittent
44	2190	14.5	Propane	.032	940	125	.0133	.29	4750	.415	2.92	.171	8.25	3300	Intermittent
45	2260	14.1	Propane	.034	910	126	.0116	.17	3830	.361	2.87	.185	8.25	1855	Intermittent
46	2200	15.0	Propane	.034	920	124	.0120	.25	4550	.353	3.05	.174	8.25	3105	Steady
47	530	14.8	Propane	.033	930	120	.0120	.25	4550	.363	6.52	.079	8.25	1550	Intermittent
48	2210	15.0	Propane	.041	1070	162	.0120	.17	3830	.292	2.96	.216	8.25	2940	Steady
49	530	14.7	Propane	.033	1100	125	.0119	.17	3830	.360	6.58	.078	8.25	1320	Steady
51	2160	15.2	Neat Shelldyne-H	.048	960	55	.0135	.29	4750	.282	3.17	.206	8.25	2760	Steady
54	2190	14.9	Neat Shelldyne-H	.036	1102	37	.0128	.24	4490	.364	3.05	.161	8.25	2925	Steady
55	530	14.5	Neat Shelldyne-H	.036	1090	37	.0114	.26	4600	.316	6.71	.074	8.25	665	Intermittent
56	530	14.9	Neat Shelldyne-H	.036	1080	36	.0121	.32	4890	.336	6.63	.074	8.25	580	Intermittent
57	2170	15.8	Neat Shelldyne-H	.035	1085	35	.0120	.17	3830	.342	3.03	.158	8.25	2910	Steady
58	2210	15.2	Neat Shelldyne-H	.035	1080	30	.0125	.31	4840	.357	3.00	.159	8.25	2935	Steady
59	540	14.6	Shelldyne-H + 25% n-propyl Nitrate	.036	1090	59	.0133	.22	4340	.369	6.77	.065	8.25	1230	Steady
60	540	14.8	"	.036	1180	59	.0052	.24	4490	.144	6.66	.066	8.25	-	Steady
61	540	14.9	"	.036	1210	64	.0043	.24	4490	.119	6.75	.065	8.25	610	Steady

Notes:

1. The numbers given under "Location of Survey Station" represent axial distance from the duct exit, in inches, to the survey station.

2. Runs 40 and 50 thru 52 were aborted for the following reasons:
   - Run 40 - pilot oxygen flow not initiated
   - Run 50 - fuel supply (propane) exhausted during run
   - Run 51 and 52 - fuel (neat Shelldyne-H) did not vaporize due to low vaporizer temperature setting.

the pilot gas generator were oxygen-hydrogen rather than oxygen-ethylene and secondly, the injector configuration differed from that utilized from Run 36 onward as indicated by the insets appearing in Figure 14 .

With regard to pilot gas generator performance, steady operation could not be achieved with the use of oxygen-hydrogen despite considerable effort to rectify this situation. The sequence of events associated with the gas generator operation is; initiate oxygen flow; activate spark; initiate hydrogen flow. Typically, the behavior which was observed at this point was a small rise in temperature within the burner indicating ignition followed almost immediately by quenching of the embryonic flame which had been established. Since this device had been used successfully many times in the past with these reactants (cf 25,26) the possibility of small leaks somewhere in the fuel lines being responsible seemed the likeliest explanation for the observed behavior. Efforts to detect the presence of such leaks were unsuccessful. We note here that the hydrogen flow rates which are involved are quite small (~.0001 pps) so that even a relatively minor leak could have a profound effect on the burner performance. Ultimately, the use of hydrogen as the fuel was abandoned and ethylene selected as a substitute. No difficulty with the gas generator operation was encountered thereafter.

With this new mode of operation for the gas generator and the original injector configuration approximately thirty tests were made using both propane and hexane as the main fuel and with air total temperatures as high as 3600°R. No combustion was achieved except when a blunt body was introduced downstream of the injector to act as a flame holder. A photograph of this situation is shown in Figure 25(a). Note that there is no evidence of combustion upstream of the blunt probe despite the fact that the injector itself is glowing cherry red due to the combined effects of the hot fuel ($T_{t_f} \sim 1300^{\circ}R$) and the elevated air temperature ($T_{t_a} \sim 3000^{\circ}R$). The corresponding conditions for the pilot gas were $\omega_p = 0.36$ ($T_{t_p} \simeq 5000\ ^{\circ}R$) and $\dot{m}_p = .035$ pps.

(a) Run No. 28
Flow is from right to left.

$T_{t_\infty} = 3000^\circ R$

$T_{t_f} = 1300^\circ R$

$\varphi_p = .36$

$\dot{m}_p = .035$ pps

$\beta = .70$

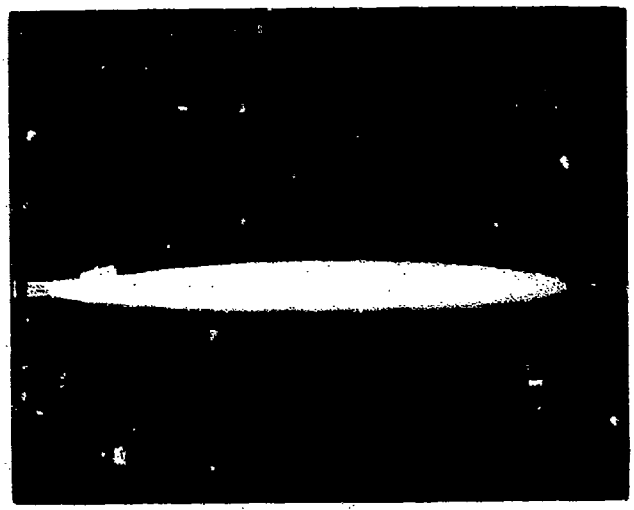

(b) Run No. 36
Flow is from left to right.

$T_{t_\infty} = 2730^\circ R$

$T_{t_f} = 1110^\circ R$

$\varphi_p = .32$

$\dot{m}_p = .0123$ pps

$\beta = .323$

Figure 25 COMPARISON OF FLAME CHARACTERISTICS FOR THE ORIGINAL AND MODIFIED INJECTOR CONFIGURATIONS

At this point in the program it was determined that modifications to the injector-pilot configuration would be required to facilitate ignition and combustion in the free jet. The rationale for the change was as follows: provide a higher temperature ignition source; improve the mixing between the main fuel and the main stream air. As indicated in inset B of Figure 14 this was accomplished by dividing the total flow of main fuel into two parts one of which (approximately 25%) was allowed to come into contact with the ignition source in a manner essentially identical to the original configuration. The remaining 75% of the main fuel was introduced into the main stream through a series of eight tubes arranged peripherally around the injector support at a point somewhat downstream of the exit of the pilot jet. (The fuel tubes are ~.94 inches long).

With this arrangement no difficulty whatsoever was encountered in initiating combustion. Figure 25 (b) shows the flame pattern obtained on the first test made using this configuration.

A comparison of Figures 25 (a) and 25 (b) indicates in a striking way the efficacy of this modification particularly if one also notes that, in terms of the respective environmental parameters (i.e.: T_{t_∞}, T_{t_f}, etc.), the conditions of Run No. 36 are definitely inferior insofar as combustion enhancement potential is concerned, relative to Run No. 28.

The improved performance obtained with this modification can be attributed to the development of a higher temperature ignition source by virtue of the smaller amount of main fuel reacting with the free oxygen in the gas generator effluent plus the enhanced mixing of the remaining fuel with the tunnel air, thereby providing improved fuel-air ratio distribution.

b. Vaporizer Performance

In Figure 26 the performance of the vaporizer is characterized in terms of the stagnation conditions occurring at Station A as defined in Figure 14. The values of p_{t_f} vs. T_{t_f} for the various fuels are compared with their respective vapor pressure curves[4]. As may be noted, in virtually all cases the data lies on the vapor side of the curves. Since the fuels are subjected to additional heating between this point and the injector station, as well as a reduction in pressure, it would appear that all the fuels can be considered to be nominally vaporized at the point of injection.

c. Relative Fuel Performance Based On Photographic Data

In Figures 27 and 28 the relative performance of the various fuel systems are indicated qualitatively by comparison of the flame patterns obtained photographically. These figures represent black and white reproductions of the original color photographs.

The comparison in Figure 27 corresponds to ambient temperature main air flow and further demonstrates the efficacy of the piloting technique. Recall that the static temperature of the supersonic air at the injector station is on the order of only 370°R, with a corresponding velocity of 1400 fps.

These photographs also indicate, rather clearly, the favorable effect of the additive insofar as combustion enhancement is concerned. It is apparent, for example, that the flame

---

4. The vapor pressure curve to which the neat Shelldyne-H and Shelldyne-H + 25% n-propyl nitrate results are compared actually corresponds to data for Shelldyne as provided by the Shell Development Company. Data for Shelldyne-H with or without additive is not available.

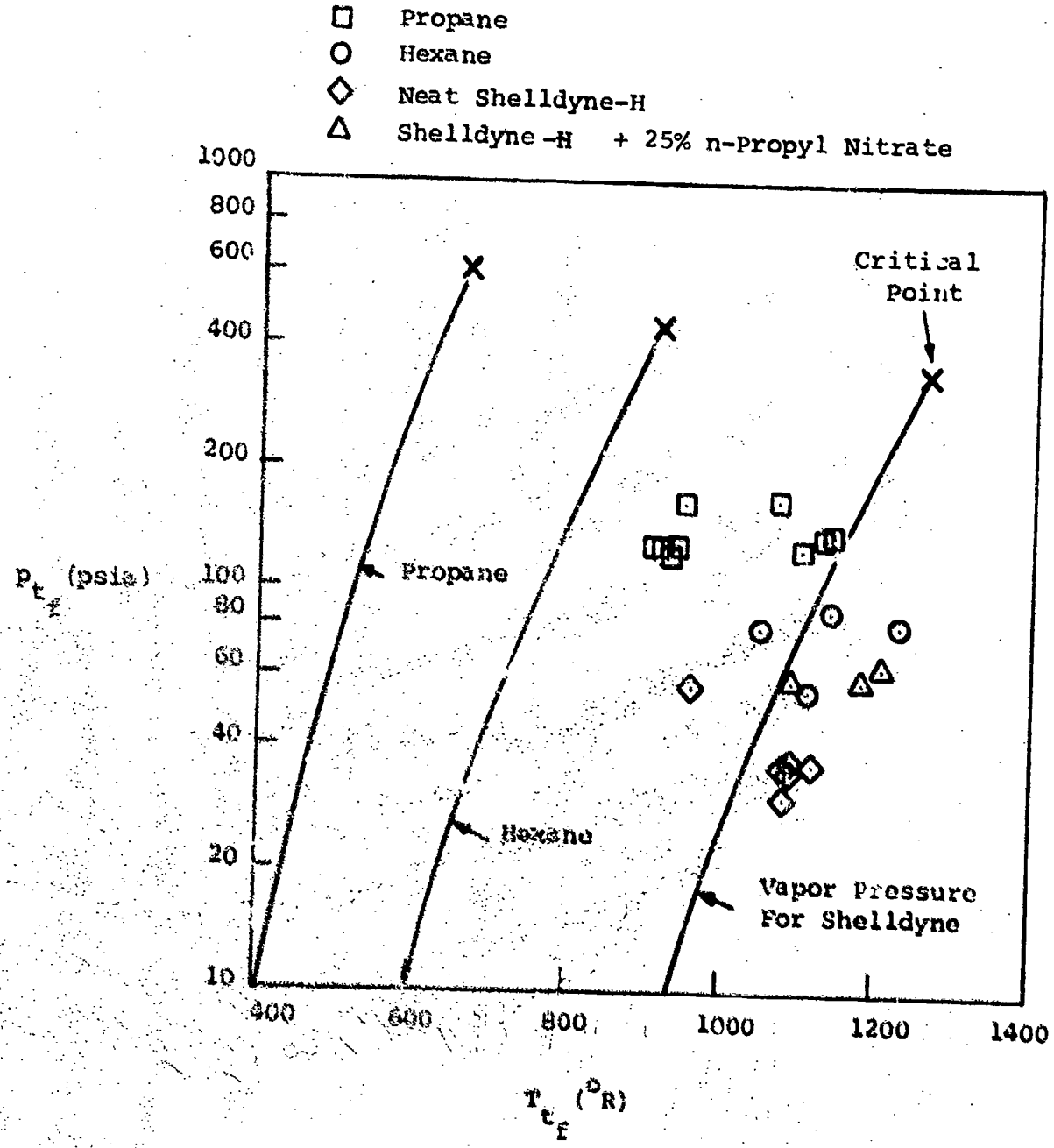

Figure 26 PERFORMANCE OF FUEL VAPORIZER

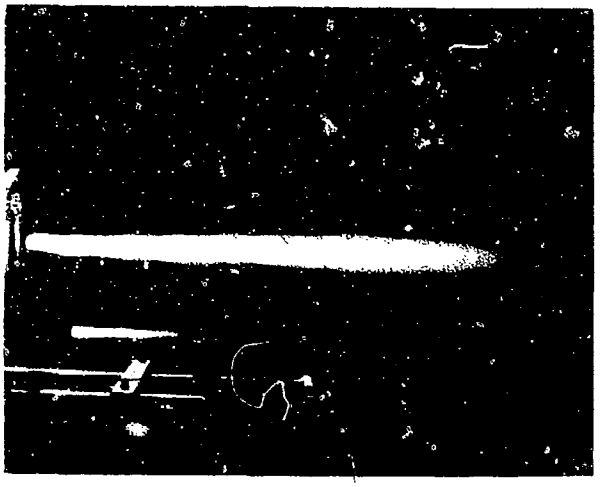

(a) Run No. 49
Fuel:propane

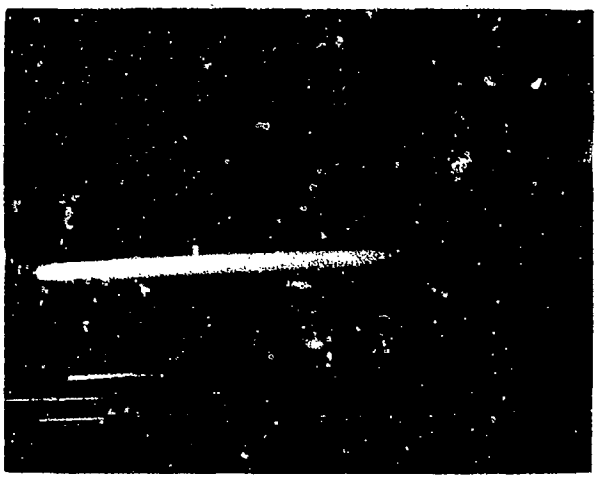

(b) Run No. 56
Fuel:neat Shelldyne-H

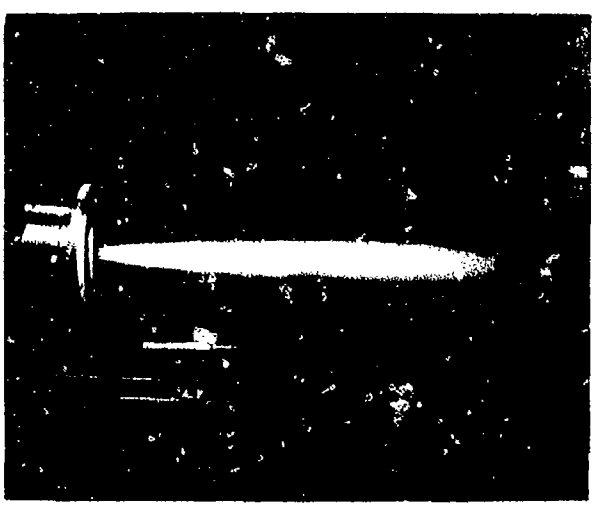

(c) Run No. 59
Fuel:Shelldyne-H
+25% n-propyl nitrate

Figure 27 RELATIVE PERFORMANCE OF SEVERAL FUEL SYSTEMS AT AMBIENT TEMPERATURE

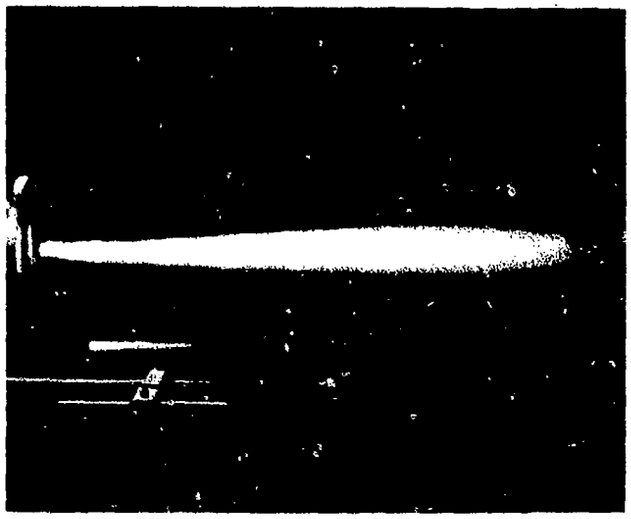

(a) Run No. 48
Fuel:propane

(b) Run No. 58
Fuel:neat Shelldyne-H

Figure 28 RELATIVE PERFORMANCE OF PROPANE AND NEAT-SHELLDYNE-H AT ELEVATED TEMPERATURE

obtained in Run No. 59 is more intense than that observed in Run No. 56. This is even more significant if one recognizes that the pilot φ in the latter case is substantially higher (i.e.: 0.32 vs. 0.22).

Of course this is only a qualitative result, but will be shown to also be quantitatively correct by virtue of the total temperature measurements which will be discussed in the next section.

Continuing with this qualitative comparison we note that the flame obtained in Run No. 59 with Shelldyne-H + 25% n-propyl nitrate is fuller but somewhat shorter then that observed in Run No. 49 corresponding to propane combustion. In this case it would be difficult to estimate which of these represents more intense energy release.

A similar comparison for neat Shelldyne-H vs. propane at elevated temperature is shown in Figure 28 . The relative performance represented by these flames is roughly equivalent to that observed between Runs 49 and 59. That is, the performance of neat Shelldyne-H relative to propane at elevated temperatures appears to be roughly comparable to that of Shelldyne-H + 25% n-propyl nitrate relative to propane at ambient temperatures. In any case, it is apparent that the relative performance of neat Shelldyne-H has improved dramatically with increasing T_{t_∞} as can be seen by comparing Figures 28 (a) and 28 (b), on the one hand, to Figures 27 (a) and 27 (b).

Again these qualitative estimates will be verified by the total temperature measurements which were obtained.

In addition to permitting comparison of relative performance between various fuel systems, these photographs can also be utilized to demonstrate the effect of variation in the environmental conditions. In Figure 29, for example, the effect of varying the pilot flow rate is demonstrated. It is apparent that at the lower value of β rapid quenching of the flame occurs due to mixing of the hot gases with the cold ambient air.

(a) Run No. 59

β = .369

(b) Run No. 61

β = .119

Figure 29 EFFECT OF PILOT FLOW RATE ON COMBUSTION OF SHELLDYNE-H + 25% N-PROPYL NITRATE AT AMBIENT TEMPERATURE

In Figure 30 the effect of fuel total temperature on combustion performance is shown for propane. Note that this effect could not be established for the high density fuels since the vaporizer had to operate at maximum temperature to assure vaporization of these fuels.

As may be noted the effect for propane is quite pronounced and is also borne out by the corresponding total temperature measurements.

Finally, the combined effect of pilot equivalence ratio and fuel total temperature is shown in Figure 31 . In this case the flame zones are virtually identical despite substantial differences in φ_p and T_{t_p} . The practical implications of this result is clear; i.e.: trade-offs between heating of the fuel and pilot gas generator operating conditions are possible.

d. Relative Fuel Performance Based on Total Temperature Measurements.

Some typical examples of the total temperature profiles are shown in Figures 32 thru 34 . For convenience in characterizing the relative performance of the various fuels from these data the maximum indicated temperature from each of the traverses has been listed in Table VI . From these results the summary graphs shown in Figures 35 and 36 were prepared. With these plots the various effects and conclusions alluded to in the previous section can now be conveniently examined in a quantitative way.

Consider for example, the effect of fuel temperatures on the performance of propane. The data shown in Figure 35 not only confirms the conclusion reached on the basis of the photographs shown in Figure 30 but indicate that this trend prevails over the entire range of air stream total temperature investigated; i.e.: compare the $T_{t\ max}$ values obtained for Runs 42 and 43. In both cases (Run 45 vs. Run 48 and Run 42 vs. Run 43) a drop in fuel temperature of less than $200^{\circ}R$ results in a reduction in $T_{t\ max}$ of more than 1000° R [5].

---

5. It should also be noted here that the value of $T_{t\ max}$ for Run No. 42 was obtained at the 12.5" survey station which implies even higher performance relative to Run No. 43.

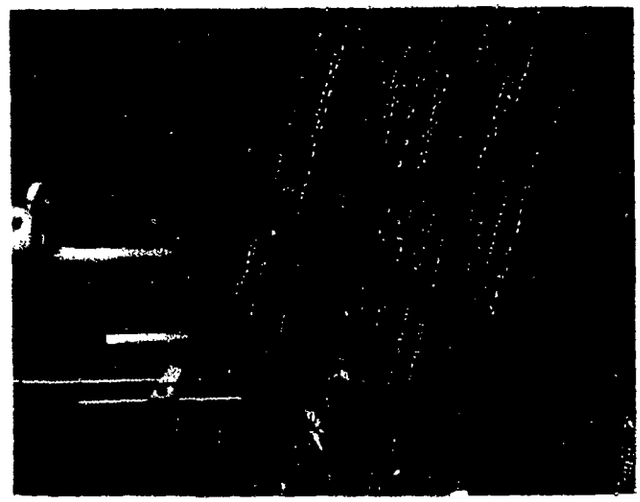

(a) Run No. 45

$T_{t_f} = 910^{\circ}R$

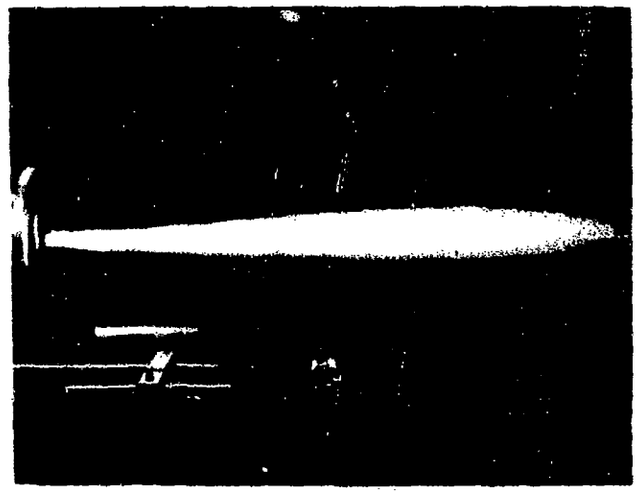

(b) Run No. 48

$T_{t_f} = 1070^{\circ}R$

Figure 30 EFFECT OF FUEL TEMPERATURE ON COMBUSTION OF PROPANE AT ELEVATED TEMPERATURE

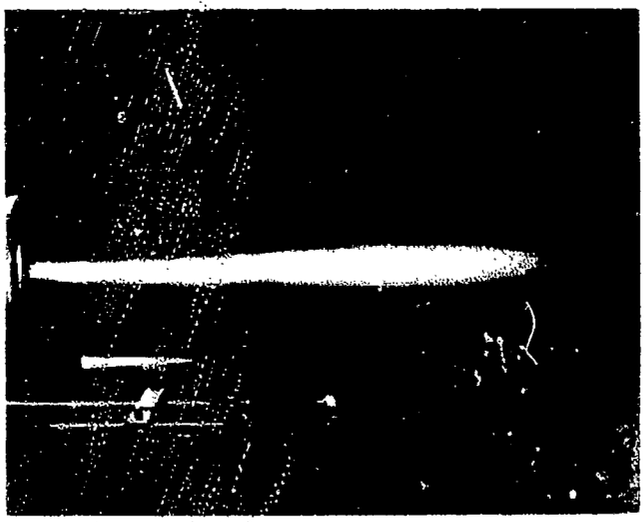

(a) Run No. 47

φ_p = .25

T_{t_f} = 930^{0}R

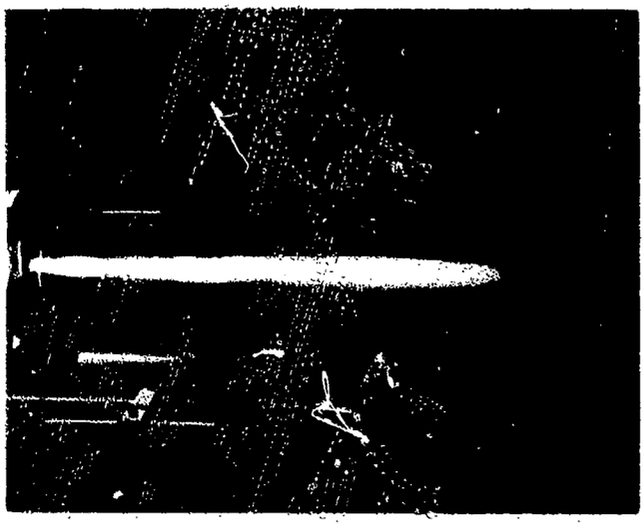

(b) Run No. 49

φ_p = 0.17

T_{t_f} = 1100^{0}R

Figure 31 COMBINED EFFECT OF PILOT EQUIVALENCE RATIO AND FUEL TEMPERATURE ON COMBUSTION OF PROPANE AT AMBIENT TEMPERATURE

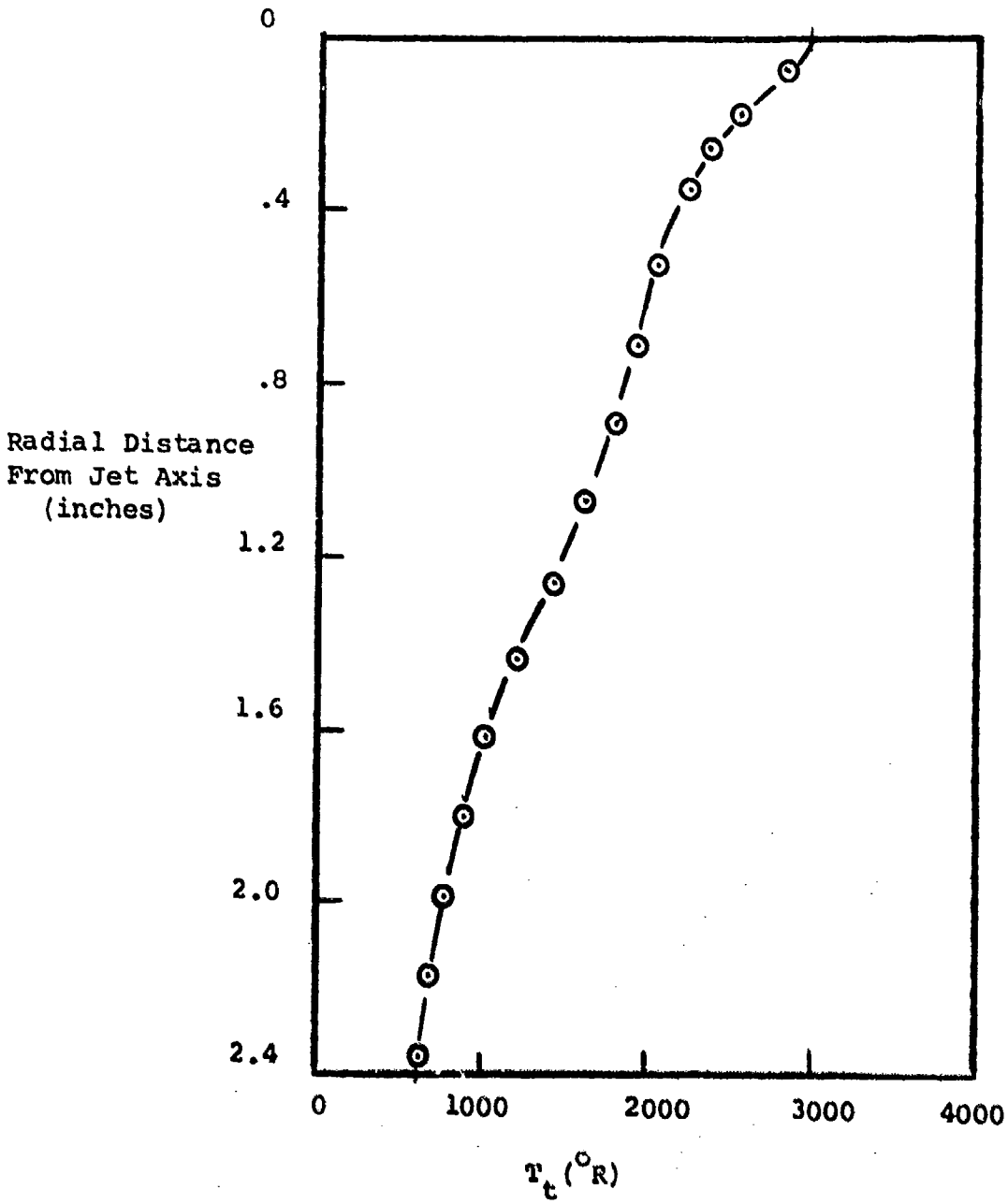

Figure 32 TOTAL TEMPERATURE PROFILE OBTAINED DURING RUN NO. 54

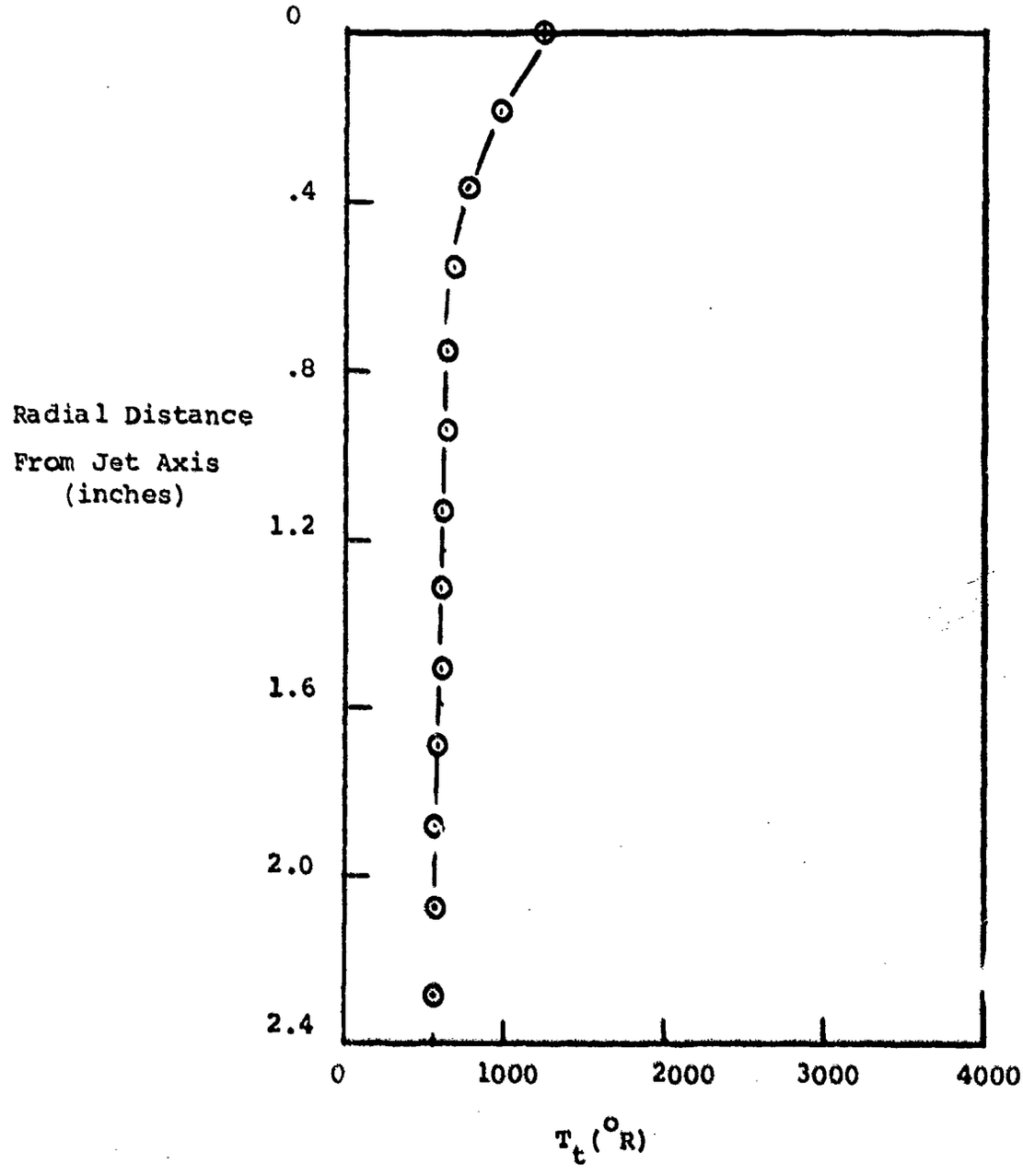

Figure 33 TOTAL TEMPERATURE PROFILE OBTAINED DURING RUN NO. 59

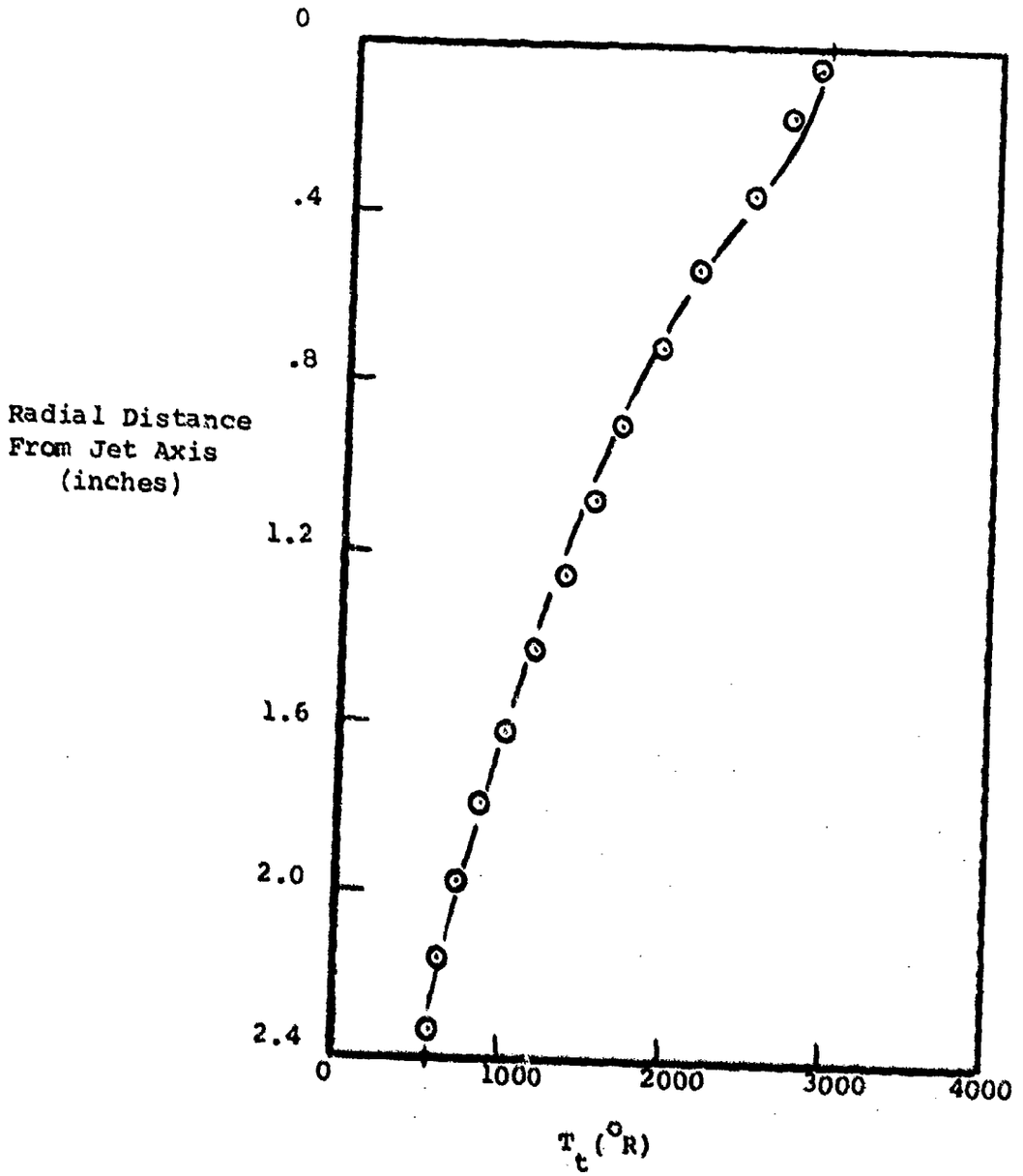

Figure 34 TOTAL TEMPERATURE PROFILE OBTAINED DURING RUN NO. 57

The data shown in Figure 35 also allows us to decide which of the configurations shown in Figure 31 represents the higher heat release case. Since the recorded value of T_{t_f} for Run No. 47 is significantly higher it would appear that the more energetic pilot (φ_p = .25 vs. φ_p = 1.7) has more than compensated for the lower fuel temperature. A similar situation prevails between Runs 44, 46 and 48 where the effect of pilot equivalence ratio can be seen to cause a monotonic decrease in $T_{t\ max}$ independent of fuel temperature variation.

Of more pertinence to the present discussion is the performance of Shelldyne-H and Shelldyne-H/additive relative to the base fuel. This is depicted in Figure 36 . We note first of all that, insofar as the neat Shelldyne-H is concerned, the performance appears to have been optimized with regard to pilot equivalence ratio; i.e.: very little variation in T_{t_f} occurs in the range $.17 \leq \varphi_p \leq .32$. We note also that the qualitative behavior represented by the photographs shown in Figure 28 is completely verified quantitatively; i.e.: both the intensity of the luminous flames and the corresponding temperature measurements obtained in Runs 48 and 58 are virtually indistinguishable implying that the neat Shelldyne-H and propane exhibit essentially equal performance at elevated temperature.

Insofar as the ranking discussed in connection with the photographs shown in Figure 27 again it is apparent the data of Figure 36 confirm the previous conclusions; i.e.: at ambient temperature the performance of the Shelldyne-H/additive system is roughly equivalent to propane (Run No. 60 vs. Run No. 49) and is significantly superior to that of the neat Shelldyne-H (Run No. 60 vs. Run No. 56).

e. Summary

The results of the axial tests presented in this section and the implications thereof may be summarized as follows:

- At ambient temperature levels the performance of neat Shelldyne-H is clearly inferior to both propane and the Shelldyne-H/additive system. On

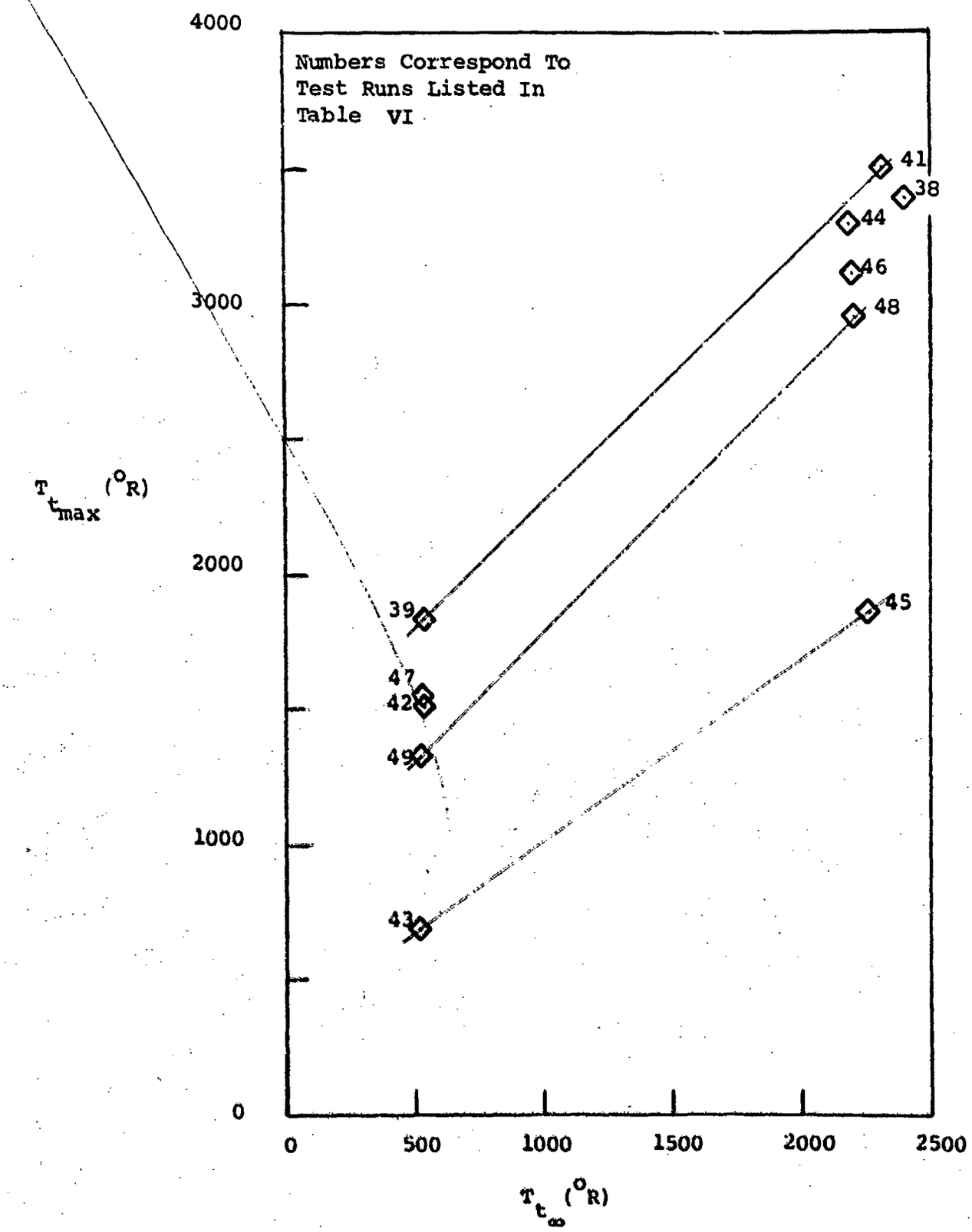

Figure 35 EFFECT OF ENVIRONMENTAL CONDITIONS ON BASE FUEL RELATIVE COMBUSTION PERFORMANCE

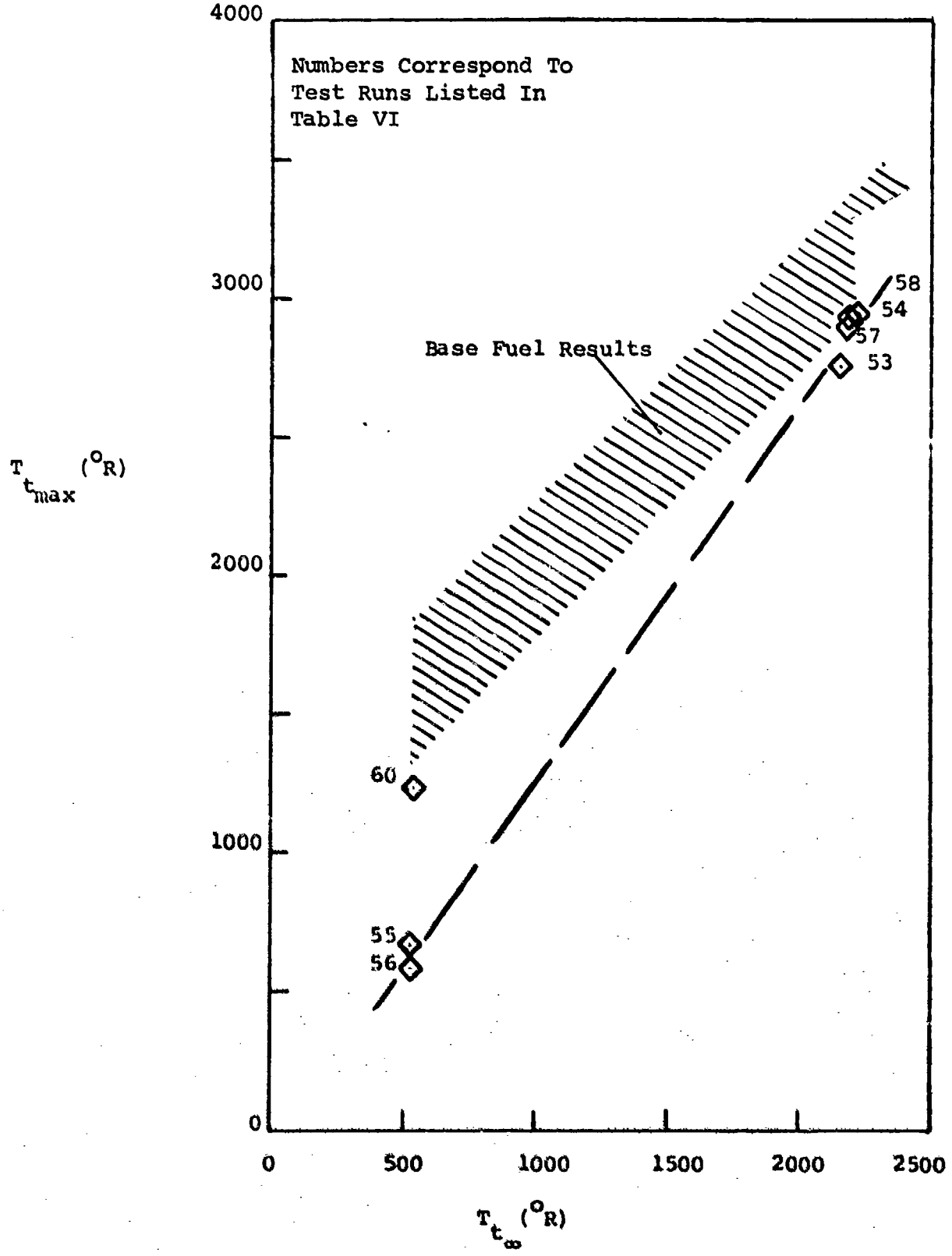

Figure 36 COMPARISON OF COMBUSTION PERFORMANCE OF NEAT SHELLDYNE-H AND SHELLDYNE-H/ADDITIVE WITH BASE FUEL RESULTS

the other hand, the performance of the latter approaches that observed with propane.

- o At higher temperature levels the performance of neat Shelldyne-H improves dramatically relative to that of propane; i.e.: note the "crossover" implied by the dashed line drawn through the available data in Figure 36 . If this trend were to also prevail for the Shelldyne-H/additive system it is apparent that at scram burner conditions (i.e. $T_{t\ max} \sim 2000^{\circ}R$) its performance would be superior to that of propane.

7. 2-D RESULTS

a. Preliminary Remarks

In addition to air stream total temperature and fuel type, the primary variable in this series of tests was the pilot to fuel mass flow ratio β. This procedure was adopted primarily for the purpose of establishing minimum piloting requirements (ignition limits) for the various candidate fuels.

In principal, such a procedure results in a set of data from which a curve similar to that shown in Figure 37 can be prepared. Evidentially, it would be of considerable interest to establish this type of curve for each of the fuels, since comparison of these curves would provide a convenient means of ranking their ignition and combustion performance.

Obviously, it is inherent in this procedure that, in most cases, very low combustion efficiencies will be involved. In terms of the duct pressures which were measured here, this would be manifested by very slight changes in the pressure levels compared to those existing prior to

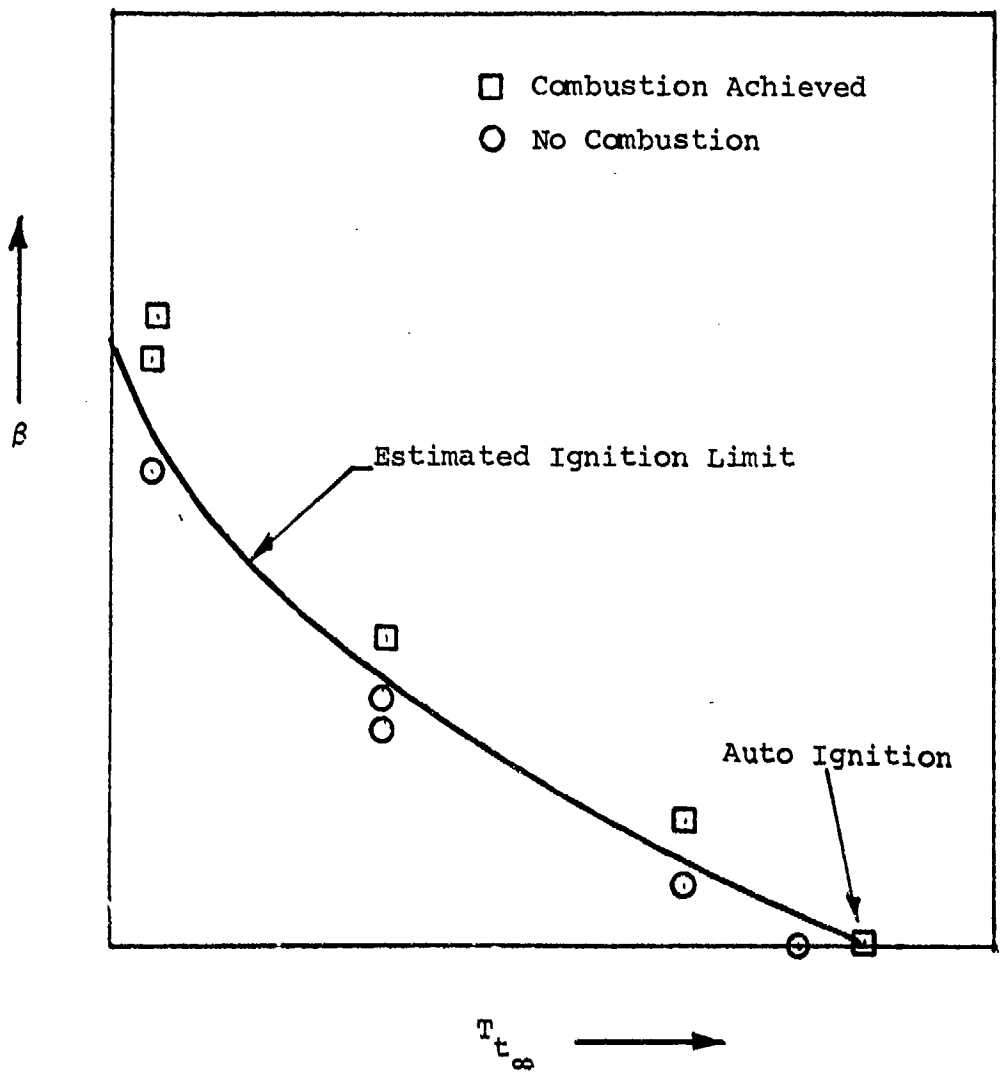

Figure 37 IDEALIZED GRAPH SHOWING DETERMINATION OF IGNITION LIMITS FOR A TYPICAL FUEL

injection and ignition of the main fuel. In particular, the absence of any significant changes can be utilized as a quantitative criterion for establishing the desired ignition limits. This was the procedure utilized in the present investigation as will be discussed in detail below.

Before proceeding with this discussion one further point should be made here. In order to provide a sufficiently wide range for β, it is found necessary to vary both the fuel flow rate, $\dot{m}_f$ as well as the pilot flow rate, $\dot{m}_p$. That is, $\dot{m}_p$ cannot be reduced to arbitrarily small values since accurate metering of the reactant flow rates ultimately is impossible, nor can they be increased beyond a certain point due to supply pressure limitations. Note, for example, that ethylene is supplied commercially at a pressure of only 1200 psia. A similar situation prevails for the fuel flow $\dot{m}_f$.

Since both of these are varied, slight changes in the aerodynamic configuration will occur as β is varied due to corresponding changes in the injection velocity V_f. As an example, consider the data given for Runs 74 and 75 in Table VII, which represents the log of test runs conducted for the 2-D test series. As may be noted, β was roughly doubled between these runs by increasing $\dot{m}_p$ from .0092 to .0163 pps while simultaneously reducing $\dot{m}_f$ from .127 to .112 pps. As a result, the ratio of V_f between the two runs is ~ 1.13 which implies that the penetration of the respective liquid fuel jets will be different. Thus, it must be recognized that Runs 74 and 75 differ, not only in their respective values of β, but that the penetration in the latter is on the order of 30% lower, according to the correlation of Reference 27. Whether or not such a variation can have a significant effect on the ignition limit for an otherwise identical flow configuration is not known at this time, nor could it be established within the scope of the present study whose primary objective was fuel ranking rather than optimization of injection configurations. Any future work in this area should include, in part, an examination of this particular effect.

TABLE VII

SUMMARY OF 2-D TEST RESULTS

Run No.	T_{t_∞} (°R)	P_∞ (psia)	Fuel Type	$\dot{m}_f$ (pps)	P_{t_f} (psia)	V_f (fps)	$\dot{m}_p$ (pps)	ω_p	T_{t_p} (°R)	θ	$\dot{m}_T$ (pps)	ω_T	π
62	510	10.9	Hexane	.071	555	31.7	.0163	.172	3850	.232	23.4	.045	1.36
63	510	10.4	Hexane	.090	875	50.6	.0163	.173	3860	.182	22.6	.059	1.67
64	510	10.6	Hexane	.092	928	51.8	.0126	.181	3960	.137	21.9	.063	1.33
65	510	10.3	Hexane	.093	945	52.4	.0092	.187	4020	.099	22.2	.062	1.02
66	510	10.5	Shelldyne-H+15% n-propyl	.091	593	28.3	.0092	.183	3970	.101	22.8	.051	1.08
67	510	10.2	Nitrate	.175	357	54.4	.0093	.185	4000	.053	22.7	.099	1.08
73	1440	12.0	"	.125	185	38.8	.0051	.179	3940	.041	14.8	.108	1.06
74	1530	13.2	"	.127	190	39.6	.0092	.189	4040	.073	14.1	.115	1.03
75	1520	12.9	"	.112	150	34.8	.0163	.171	3840	.146	14.4	.097	1.92
76	1600	12.7	H-MCPD + 15% n-propyl	.098	127	37.5	.0163	.172	3850	.166	11.7	.099	1.48
77	1400	12.2	Nitrate	.101	135	38.7	.0107	.170	3830	.106	14.0	.092	1.02
78	490	10.3	"	.089	110	34.0	.0088	.180	3950	.099	22.7	.051	1.03
79	490	10.4	"	.180	420	68.9	.0088	.178	3920	.049	22.4	.103	1.05
80	1500	12.3	Hexane	.096	187	56.0	.0163	.172	3850	.170	14.0	.101	1.70
81	1509	12.7	Hexane	.094	177	53.0	.0105	.174	3890	.112	14.2	.098	1.01
82	1510	13.0	Hexane	.123	297	69.3	.0093	.183	3970	.076	14.2	.128	-
83	2530	12.6	Hexane	.096	187	54.0	0	-	-	0	9.3	.156	-
84	1930	12.9	Hexane	.124	300	69.8	.0093	.183	3970	.075	10.5	.176	1.93
85	2345	14.0	Shelldyne-H + 15%n-propyl	.100	120	31.1	0	-	-	0	10.9	.117	-
86	2100	13.9	Nitrate	.126	190	39.2	.0091	.188	4030	.072	11.1	.144	1.45
87	2360	14.1	"	.120	167	37.3	.0052	.166	3800	.044	10.9	.139	1.04
88	2320	14.6	H-MCPD + 15% n-propyl Nitrate	.114	180	43.7	.0052	.166	3800	.046	10.8	.136	1.05
89	1520	12.6	Neat Shelldyne-H	.112	152	34.8	.0164	.171	3840	.146	14.0	.107	1.63
90	1560	12.2	Neat Shelldyne-H	.111	147	34.5	.0161	.173	3860	.145	13.3	.111	1.63

Notes:

1. Runs 68 thru 72 were tare runs.
2. Cavitating venturi No. S/N 139 was used during Runs 62 thru 66. No S/N 140 was utilized thereafter (c.f. Figure 23).

b. Photographic Results

In contrast to the axial test series, no correlation between the observed flame patterns and the quantitative measurements was found. This will become evident in the course of the ensuing discussion.

In Figures 38 thru 40 some of the photographs of these flames are presented. Again, it should be noted that these are not originals but black and white reproductions thereof.

In Figure 38 the performance of neat Shelldyne, H-MCPD + 15% n-propyl nitrate and the base fuel (neat hexane) at essentially identical environmental conditions are compared. An interesting feature of all these photographs is the appearance of a diamond-shaped luminous pattern downstream of the test duct. These probably correspond to shock-induced localized combustion due to compression waves reflected from the free shear layer of the jet. The existence of such a shock-expansion wave system is entirely consistent with the underexpanded state of the test duct when substantial heat release occurs therein.

On a luminosity basis, one would be tempted to conclude that the most intense heat release is associated with Run No. 90 (neat Shelldyne-H), the least with Run No. 77 (H-MCPD/additive) with the hexane performance (Run No. 80) intermediate between them. However, this tentative ranking is found to be inconsistent with the ranking established quantitatively by means of the test duct pressure measurements.

A similar result is depicted in Figure 39. Here again, the Shelldyne/additive system (Run 86) would appear to be significantly more reactive then the base fuel (Run 84) at nominally identical environmental conditions. Nevertheless, the pressure data which will be presented in the next section indicates that the contrary is true.

The most stricking example of the unreliability of the photographic results is shown in Figure 40. In this case

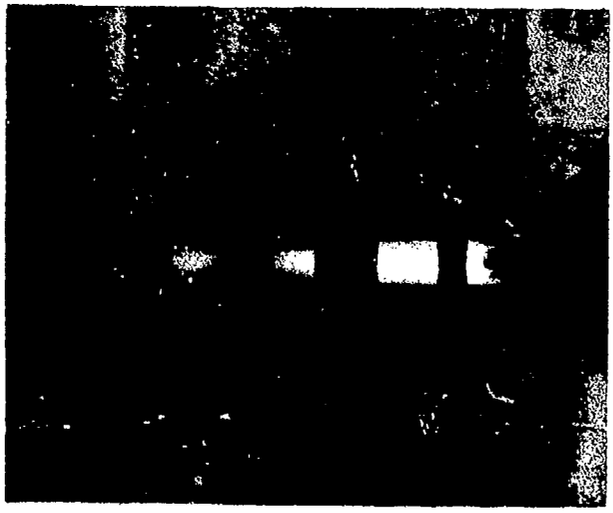

(a) Run No. 77

Fuel: H-MCPD +
15% n-propyl nitrate

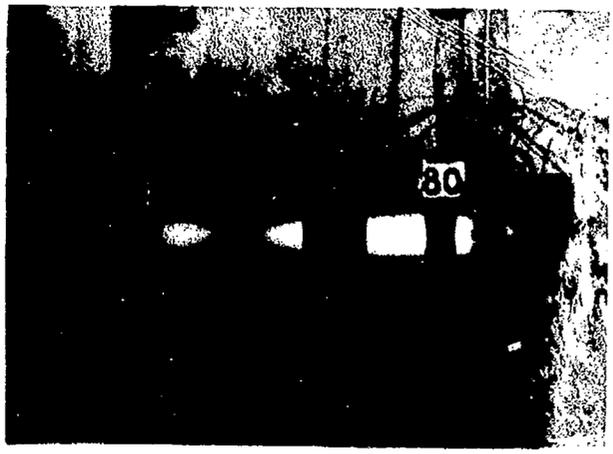

(b) Run No. 80

Fuel: Hexane

(c) Run No. 90

.el: Neat Shelldyne

Figure 38 COMPARISON OF FLAME PATTERNS OBSERVED WITH VARIOUS FUEL SYSTEMS AT INTERMEDIATE TEMPERATURE LEVEL

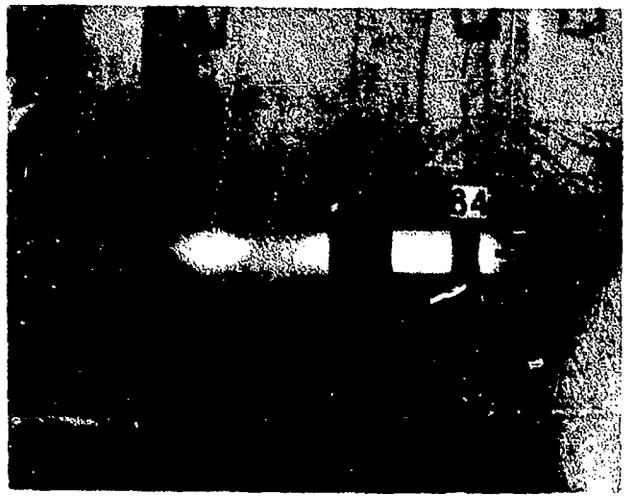

(a) Run No. 84

Fuel: Hexane

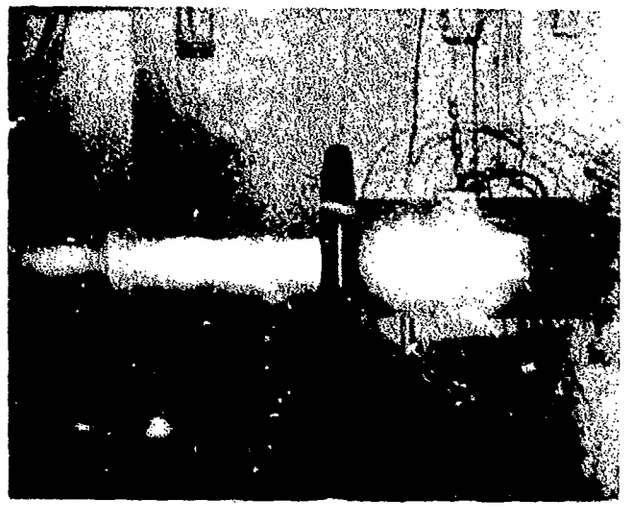

(b) Run No. 86

Fuel: Shelldyne-H
+ 15% n-propyl nitrate

Figure 39 COMPARISON OF FLAME PATTERNS OBSERVED WITH HEXANE AND SHELLDYNE-H/ADDITIVE AT HIGH TEMPERATURE LEVEL

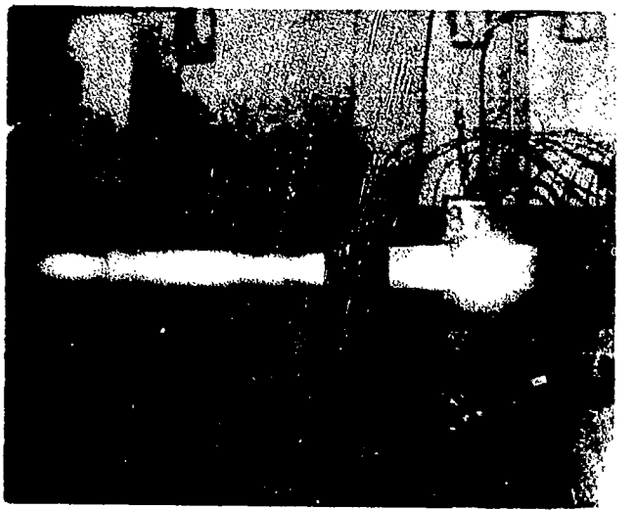

(a) Run No. 87

Fuel: Shelldyne-H
+ 15% n-propyl nitrate

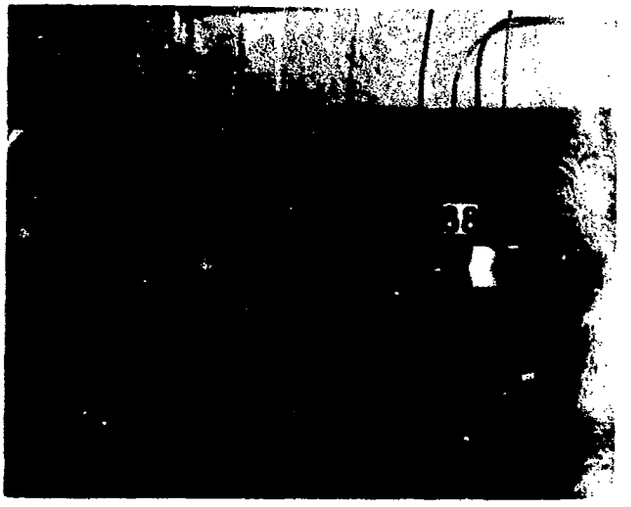

(b) Run No. 88

Fuel: H-MCPD
+ 15% n-propyl nitrate

Figure 40 COMPARISON OF FLAME PATTERNS OBSERVED WITH SHELLDYNE-H/ADDITIVE AND H-MCPD/ ADDITIVE AT HIGH TEMPERATURE LEVEL

the comparison is between the Shelldyne/additive (Run 87) and the H-MCPD/additive (Run 88)* systems. Despite the fact that there appears to be a tremendous difference in the two configurations, examination of the corresponding pressure data showed that, in both cases, virtually no pressure rise occurred.

It is interesting to speculate as to the reason for this anomalous behavior. One possibility is to ascribe the intense luminosity of the Shelldyne-H results to the presence of high concentrations of carbon particles (soot) in these flows. The radiative properties of such particulate matter at relatively low temperatures are well known. Evidently, this result is ultimately connected with an inherent property of this particular fuel, i.e., its high carbon-hydrogen ratio. However, the same fuel was used for both the vaporized and liquid injection tests. Thus, the question arises, why was the anomaly observed only in the liquid injection case and not when the fuel was injected in a vaporized state. If the luminosity is attributed to the presence of higher concentrations of soot the question can be asked in a somewhat different way; i.e., why is the concentration level of soot higher in the liquid injection case?

Several mechanisms can be postulated which could give rise to such a result. First of all since the liquid droplets are initially exposed to the relatively low temperature environment of the main stream air prior to their contacting the ignition source, substantial pyrolisis of the fuel may occur prior to the initiation of oxidation. Further, since this oxidation occurs in a region surrounding the individual particles, much of the oxidation will occur at a very fuel rich condition further enhancing the possibility of soot formation. Finally, vaporization of the fuel prior to initiation of combustion tends to suppress soot formation by virtue of the cracking which occurs prior to actual injection of the fuel. The carbon deposition sufficient to cause clogging of the vaporizer system which has been referred to earlier is clear evidence of this effect and indicates that the fuel issuing from the injector is not Shelldyne-H proper but a mixture of low molecular weight hydrocarbons.

---

* It should be noted that the differences in background appearance between Run 88 and all of the others was caused by the fact that the test cell gate was inadvertently left open during the former run.

With regard to the above remarks it is interesting to note that in all axial tests the flame zones for all fuels exhibited the characteristic blue-bluish white color of a hydrocarbon flame whereas in virtually all Shelldyne-H 2-D runs no such hue was observed. In general, these flames were of a yellowish white coloration without any bluish trace.

c. Relative Performance Based On Duct Pressure Measurements

Typical examples of the duct pressure distributions obtained with and without injection and combustion of the main fuel are shown in Figures 41 to 47 . In each case the static pressures have been normalized with respect to the tunnel stagnation pressure p_{t_∞} and plotted with respect to axial distance measured from the nozzle throat.

The solid line in these figures represents the "tare" pressure observed without combustion. The large pressure rise occurring just downstream of the nozzle exit reflects, of course, the presence of the strut injector. The subsequent wave pattern is also apparent in the tare distribution.

The dashed line in these figures represents the steady state pressure distribution which developed once the combustion had been initiated. It may be noted that three distinct types of behavior are represented in these figures. For convenience these will be referred to here as "least reactive", intermediate and "highly" reactive.

Figure 43 is an example of one of the least reactive cases. As may be noted, whatever heat release occurred resulted in only a slight perturbation in the tare pressure distribution. This situation could be associated with the ignition limit for this particular case.

Figures 42, 44, 46 and 47 are examples of the intermediate situation. Here, the heat release due to combustion is sufficient to generate compression waves downstream of the strut which in some cases are stronger than the shock emanating from the leading edge of the strut. Note also that

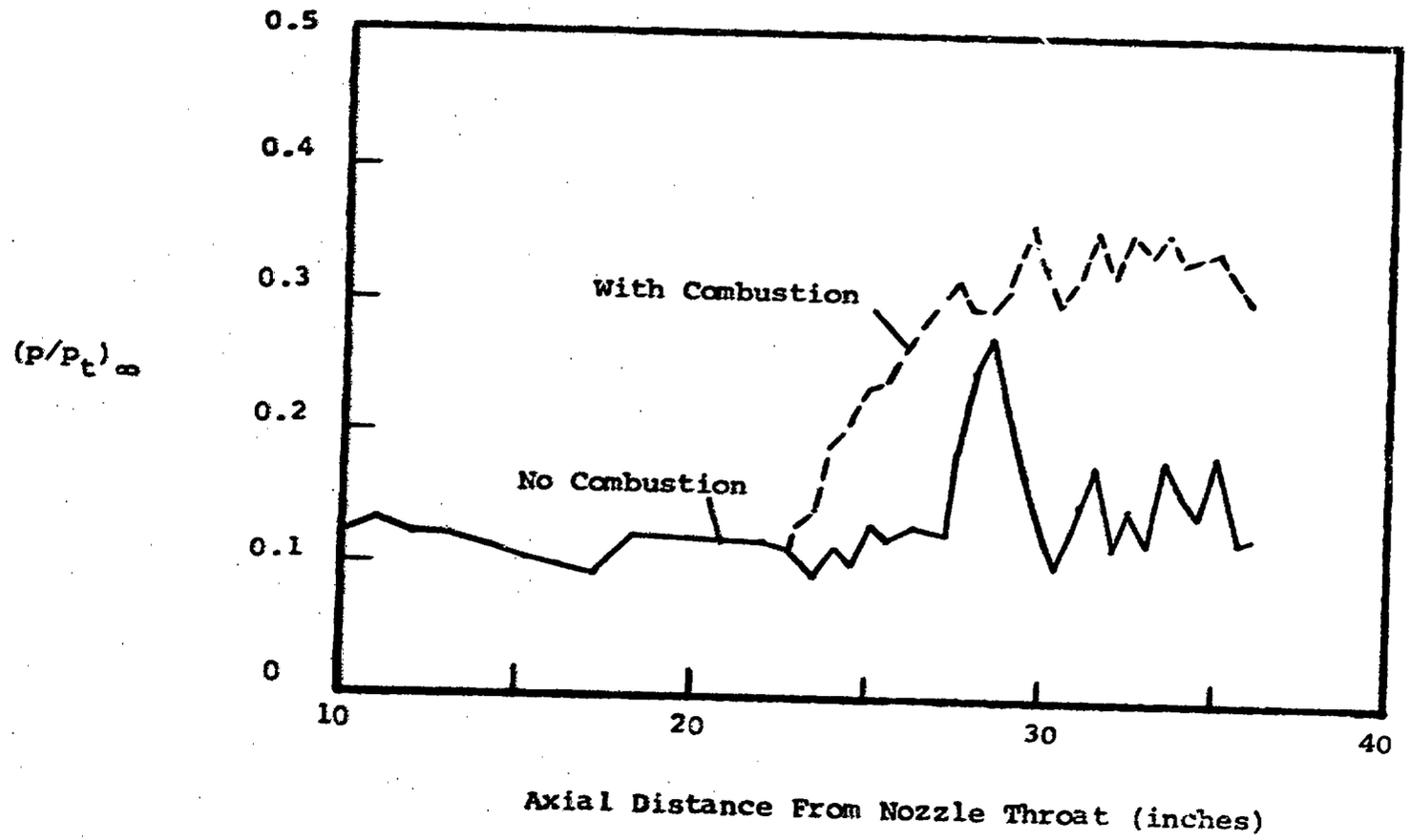

Figure 41 PRESSURE DISTRIBUTION IN THE TEST DUCT FOR RUN NO. 75

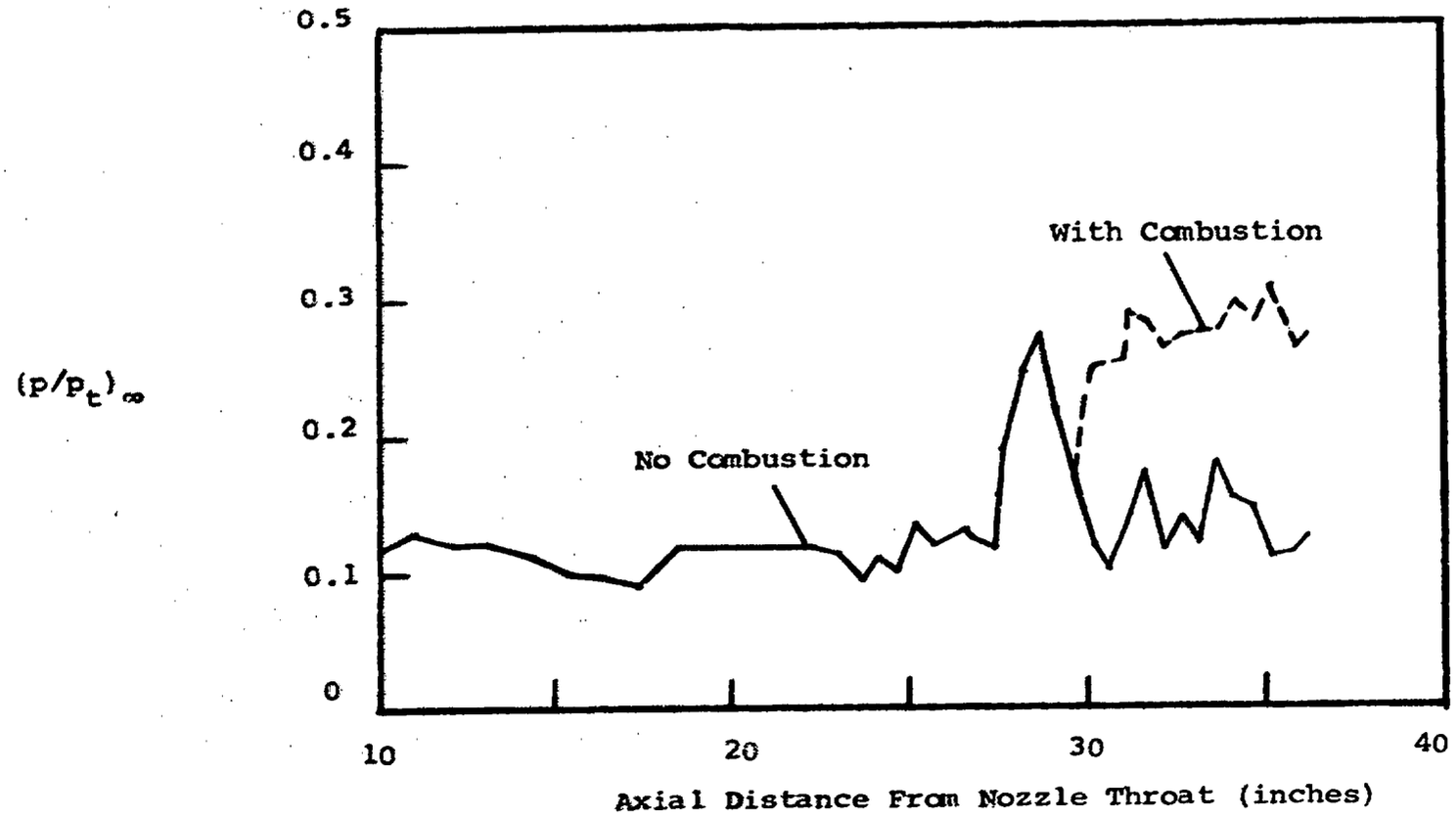

Figure 42 PRESSURE DISTRIBUTION IN THE TEST DUCT FOR RUN NO. 76

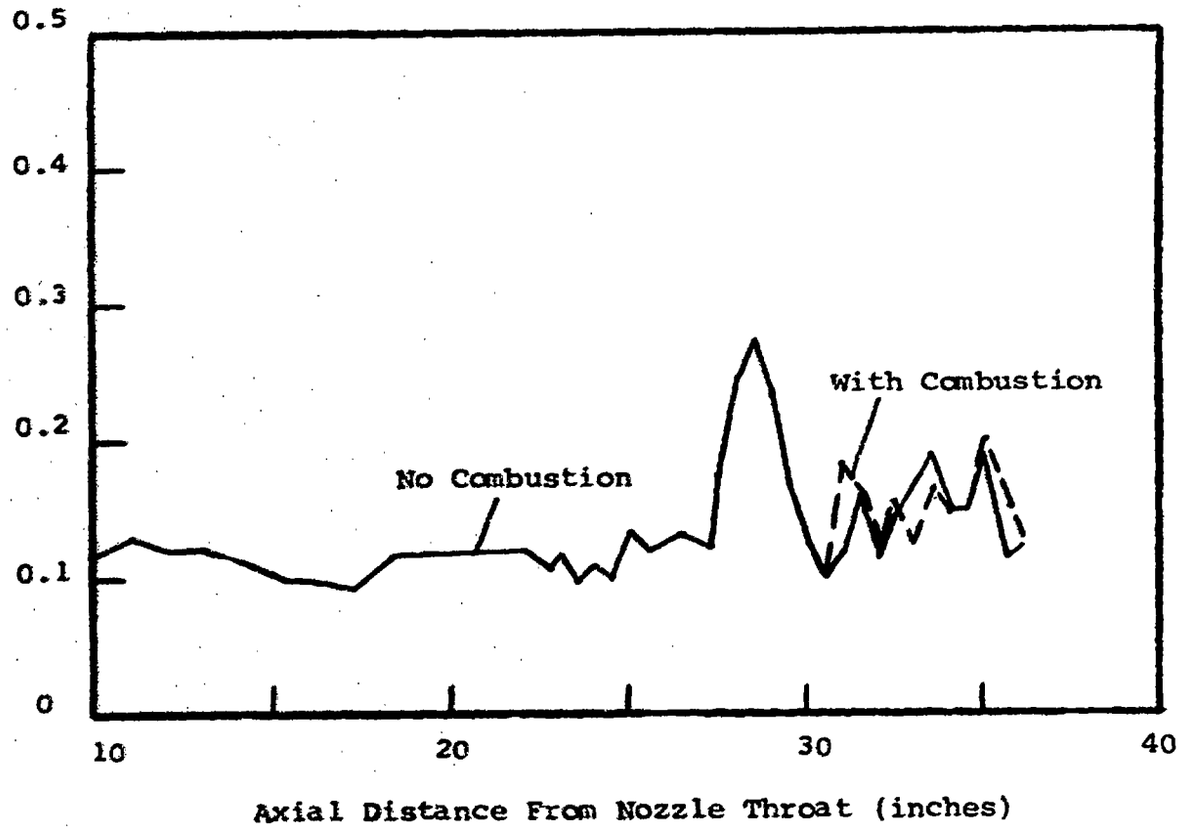

Figure 43 PRESSURE DISTRIBUTION IN THE TEST DUCT FOR RUN NO. 77

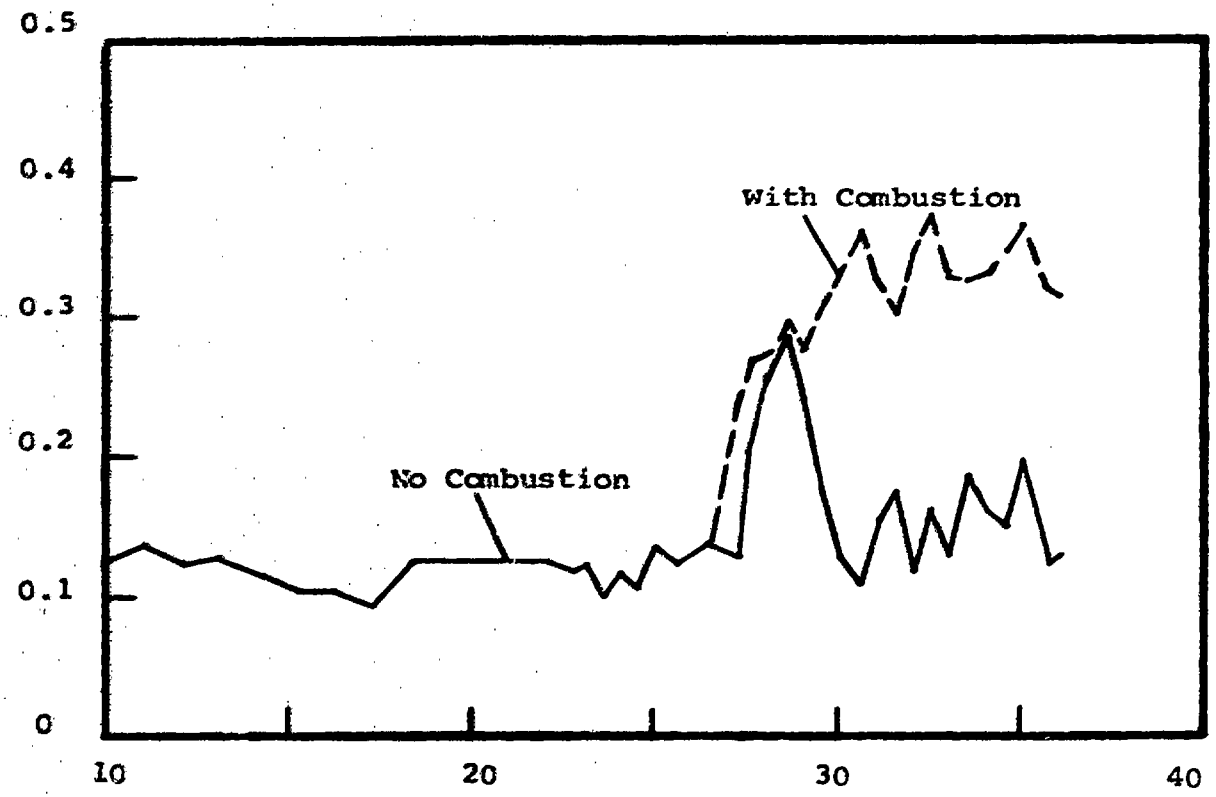

Figure 44 PRESSURE DISTRIBUTION IN THE TEST DUCT FOR RUN NO. 80

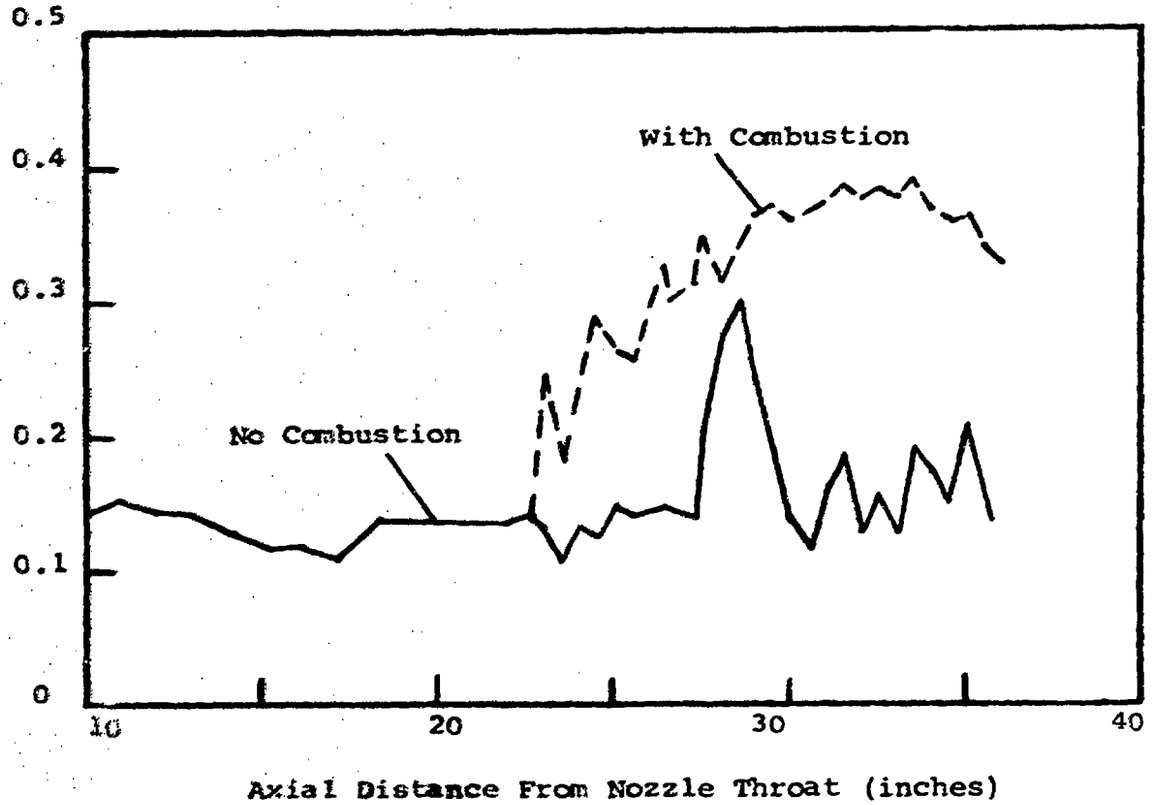

Figure 45 PRESSURE DISTRIBUTION IN THE TEST DUCT FOR RUN NO. 84

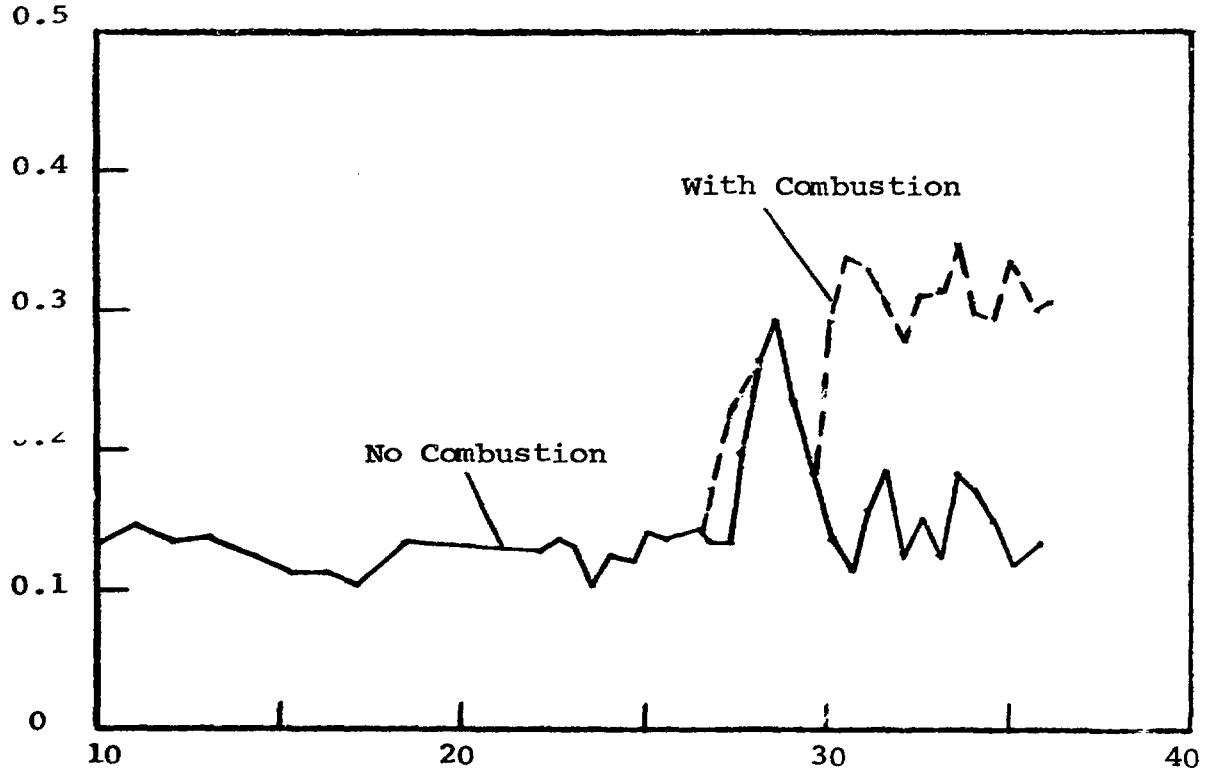

Figure 46 PRESSURE DISTRIBUTION IN THE TEST DUCT FOR RUN NO. 86

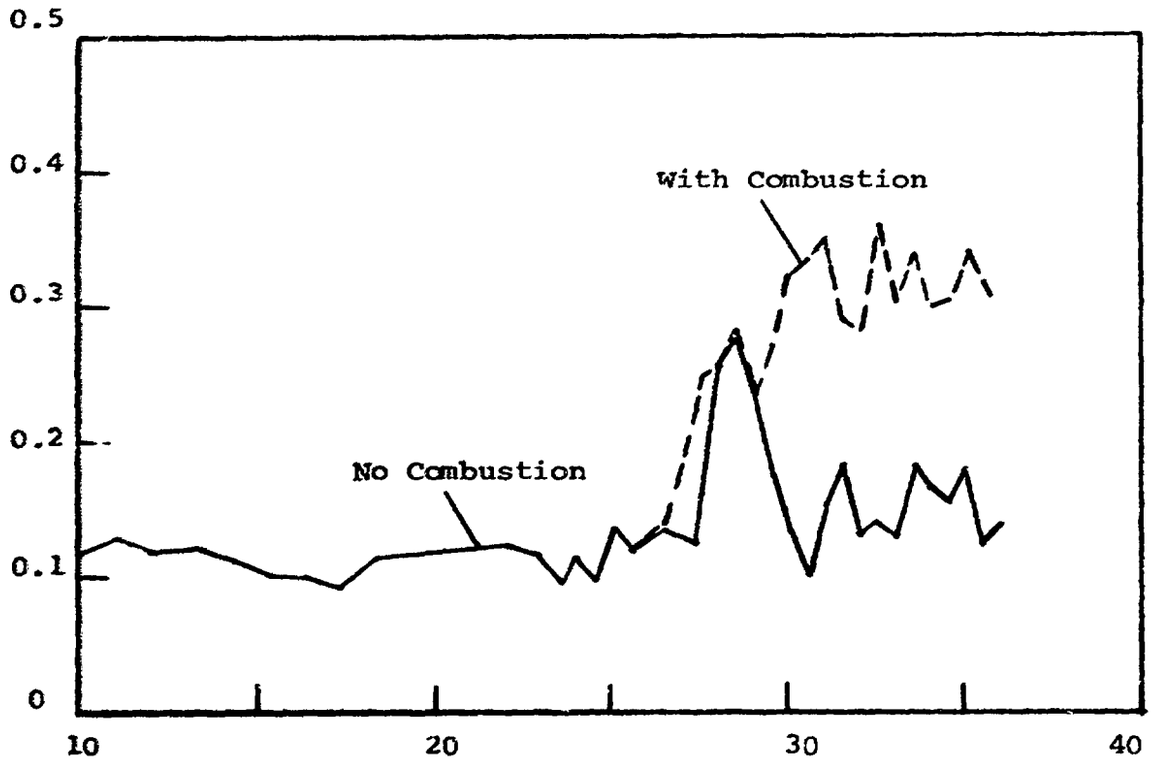

P/P_{t_∞}

94

Figure 47 PRESSURE DISTRIBUTION IN THE TEST DUCT FOR RUN NO. 90

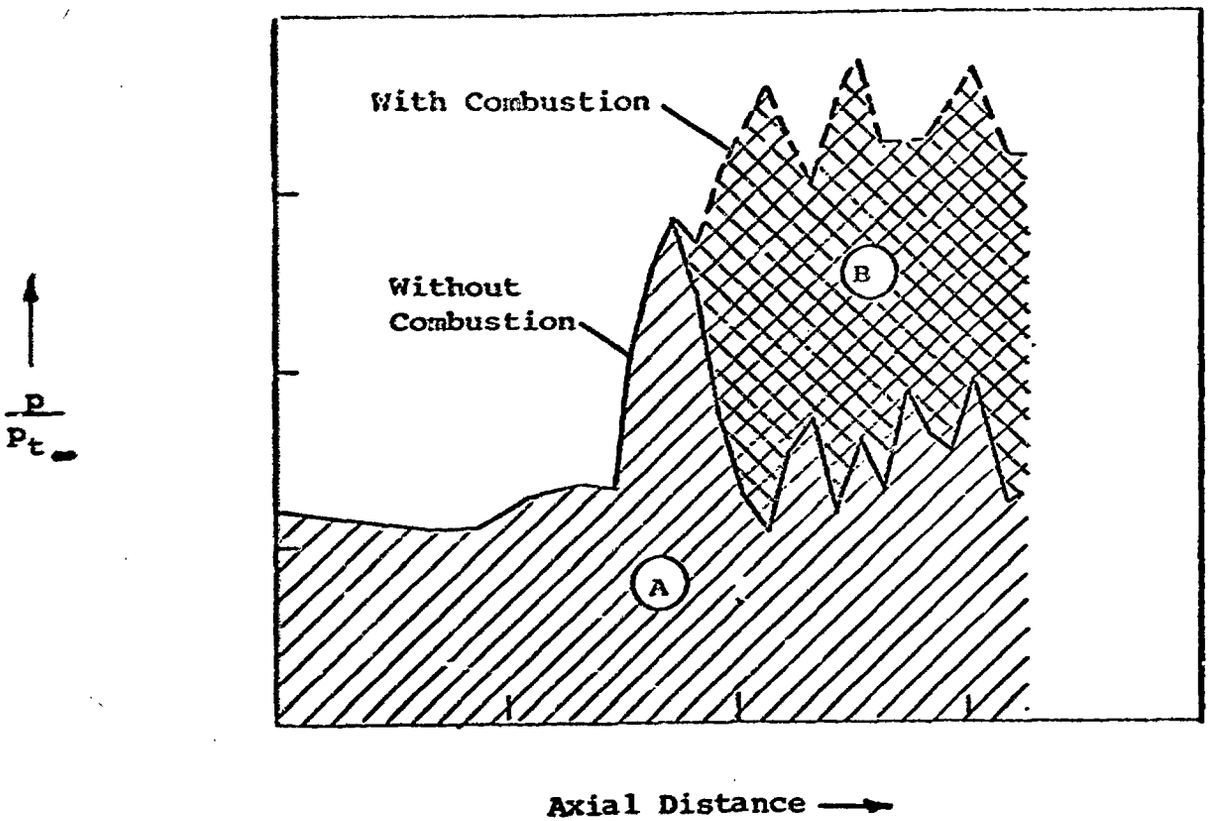

The "duct pressure integral" π is defined as $\pi = A + B/A$ where A and B are the shaded areas shown above.

Figure 48 DEFINITION OF DUCT PRESSURE INTEGRAL

some disturbance is propagated upstream of the aforesaid shock impingement point indicating the possibility of shock boundary layer interaction.

The highly reactive examples shown in Figures 41 and 45 confirm this possibility. Here it is apparent that the heat release has given rise to compression waves sufficient to cause substantial boundary layer separation.

To facilitate comparison of relative performance, this pressure data has been utilized to compute a "duct pressure integral" π defined in accordance with the sketch shown in Figure 48. The resulting values have been listed in Table VII for each of the tests conducted in this series.

We can now verify quantitatively the comments made in the previous section regarding the unreliability of the photographs which were obtained.

Consider, for example, the comparison which had been shown in Figure 38. Based on these photographs it would have been anticipated that π for Run No. 90 would be substantially higher than that for Run No. 80. The pressure measurements themselves indicate that this is not true and that π is slightly higher in the latter case.

The anomaly is even more apparent for Runs 84 and 86, (cf Figures 39, 45 and 46). Note that Run 84 corresponds to one of the "highly reactive" cases leading to boundary layer separation.

Finally, we note that in the case involving Runs 87 and 88 (cf Figure 40) the two values of π are virtually indistinguishable and that both represent examples of "least reactive" cases.

d. Summary

The relative performance and ranking of the various fuel systems examined during the 2-D tests is summarized by means of the bar diagram shown in Figure 49. Points of interest

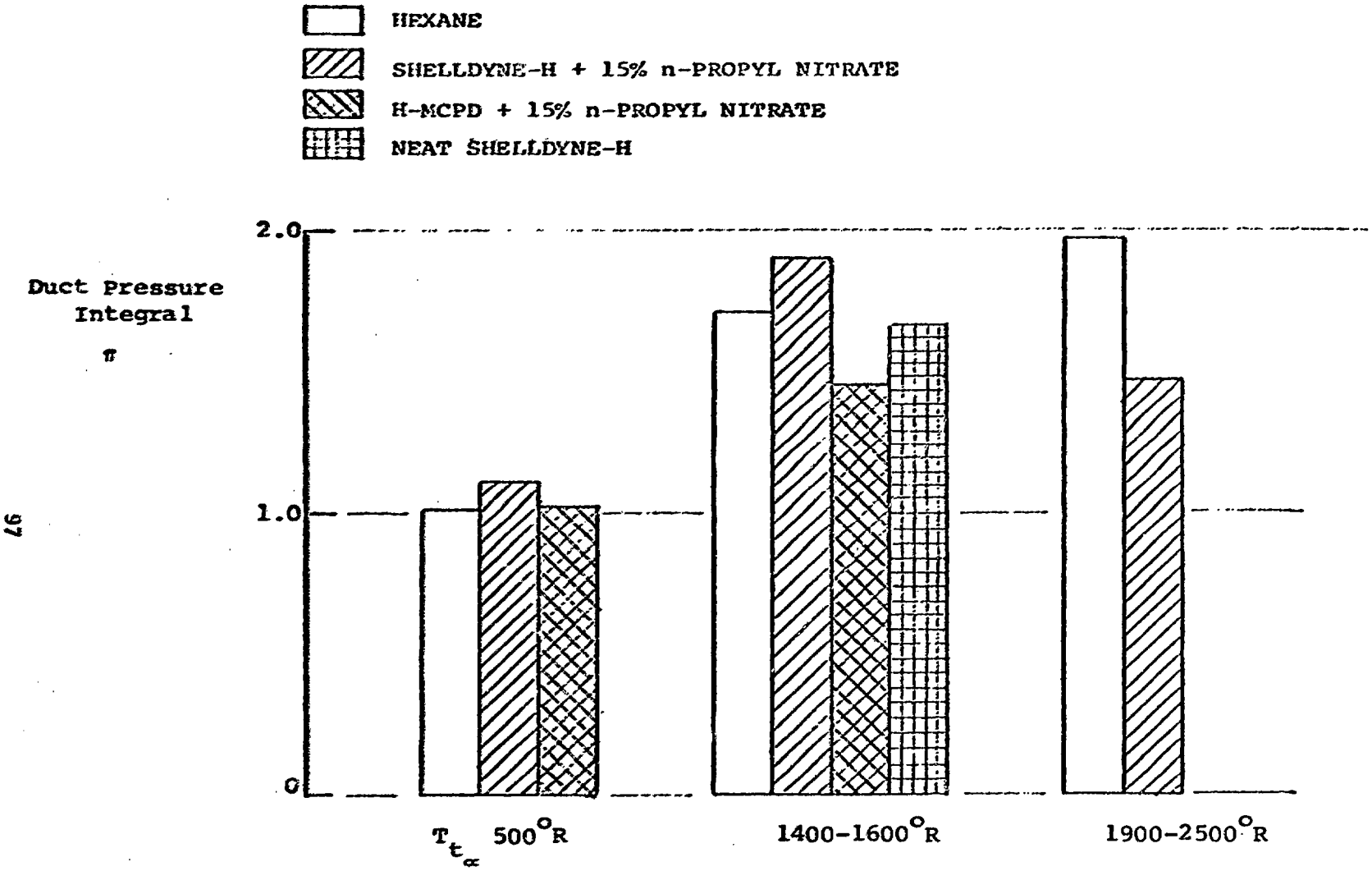

Figure 49 EFFECT OF AIR TUNNEL TEMPERATURE ON RELATIVE PERFORMANCE AND RANKING OF VARIOUS FUEL SYSTEMS AS DETERMINED IN THE 2-D TEST SERIES

are as follows. At low temperature (~ 500 ^{o}R) both the Shelldyne-H/additive and H-MCPD/additive demonstrated some superiority in performance relative to the base fuel (Hexane). At the intermediate temperature level (1400-1600 ^{o}R) the Shelldyne-H/additive system maintains this superiority; however, the H-MCPD/additive system falls somewhat below both. Note also the improved performance of Shelldyne-H with additive relative to the neat Shelldyne-H. At the highest temperature level (1900-2500 ^{o}R) the superiority of Shelldyne-H with additive relative to the base fuel vanishes. It is not clear at this time what the reason for this crossover in performance is due to, particularly if it is recalled that a diametrically opposite trend was observed in the axial tests.* One possible mechanism for that effect can be postulated in terms of a trade-off between the vaporization and combustion kinetics of the two fuels. This is best accomplished by referring to the data shown in Figures 3 and 26. Figure 26, of course, merely shows the monotonic increase of vapor pressure with temperature for both fuel systems. In contrast to this parallel behavior, Figure 3 shows that for a fixed value of percent additive the next reduction in ignition delay time <u>decreases</u> rapidly with increasing temperature. In view of these opposing trends it is likely that an optimum situation can prevail at some intermediate temperature level, leading to the observed behaviour. Additional study would be required, however, to fully verify this contention and to establish definitivly how any possible optimization could be achieved in a practical burner configuration.

---

* It is important to emphasize here that this "crossover" is a relative rather than an absolute one. That is, the performance of Shelldyne-H + 15% n-propyl nitrate at a fixed value of $\mathcal{R}$ (~ .07) continues to improve with increasing temperature as may be seen by comparing the respective values of $\mathcal{R}$ obtained in Runs 66, 67, 74 and 86.

V

REFERENCES

1. "Research On Methods Of Improving The Combustion Characteristics of Liquid Hydrocarbon Fuels", Volume I "Low Speed Experiments" AFAPL No. 72-24 1972, Esso Research and Engineering Company, Linden, New Jersey.

2. Libby, P. A., Pergament, H. S., and Bloom, M. H., "A Theoretical Investigation of Hydrogen-Air Reactions. Part I - Behavior with Elaborate Chemistry," GASL TR 250, Aug. 1961.

3. Westenberg, A. A., "Hydrogen-Air Chemical Kinetic Calculations in Supersonic Flow," JHU-APL CM-1028, Dec. 1962.

4. Westenberg, A. A., and Favin, S., Ninth International Symposium on Combustion, Academic Press, New York, 1963.

5. Montchiloff, I. N., Tabach, E. D., and Buswell, R. F., Ninth International Symposium on Combustion, Academic Press, New York, 1963.

6. Sarli, V. J., Blackman, A. W., and Migdal, D., "Non-equilibrium Chemistry and Nozzle Losses in Hypersonic Ramjets," Presented at the AIAA-ASME Hypersonic Ramjets Conference, White Oak, Md., April 1963.

7. Chinitz, W., "A Theoretical Analysis of Non-Equilibrium Methane-Air Combustion," AIAA Preprint No. 64-542, May 1964 (to be published in Pyrodynamics).

8. Burwell, W. G., Sarli, V. J., and Zupnik, T. F., "Analytically Determined Nonequilibrium Mixture Properties in High Expansion Ratio Nozzles," Presented at 3rd Conference on Performance of High Temperature Systems, Dec. 7-9, 1964.

9. Mayer, S. W., Cook, E. A., and Schieler, L., "Non-equilibrium Recombination in Nozzles," Aerospace Corp. Report No. TDR-269 (4210-10)-6, Sept. 18, 1964.

10. Baurer, T., "Discussion of Non-Hydrogen Fuels for Extension of Scramjet Technology," GASL TR 533, May 8, 1965.

11. Hawthorn, R. D., and Nixon, A. C., "Shock Tube Ignition Delay Studies of Endothermic Fuels," AOAA Preprint No. 65-594, June 1965.

12. Fristrom, R. M., Prescott, R., Neumann, R. K., and Avery, W. H., Fourth Symposium (International) on Combustion, Williams and Wilkins, Baltimore, 1953.

13. Fristrom, R. M., Avery, W. H., Prescott, R., and Mattuck, A., J. Chem. Phys., 22, 106 (1954).

14. Prescott, R., Hudson, R. L., Foner, S. N., and Avery, W. H., J. Chem. Phys., 22, 145 (1954).

15. Fristrom, R. M., J. Chem. Phys., 24, 888 (1956).

16. Fristrom, R. M., Sixth Symposium (International) on Combustion, Reinhold, New York, 1957.

17. Fristrom, R. M., Prescott, R., and Grunfelder, C., Combustion and Flame 1, 102 (1957).

18. Fristrom, R. M. and Westenberg, A. A., Combustion and Flame, 1, 217 (1957).

19. Fristrom, R. M., Westenberg, A. A., and Avery, W. H., "The Study of the Mechanism of Propane-Air Reaction Based on the Analysis of Flame Front Profiles," JHU-APL Paper, 1957.

20. Semenov, N. N., Some Problems of Chemical Kinetics and Reactivity, Pergamon Press, New York, 1958.

21. Magnus, D. E. and Schechter, H. S., "Analysis and Application of the Pade Approximation for Integration of the Chemical Kinetics Equations," GASL TR 642, March 1967.

22. Edelman, R., and Fortune, O., "Mixing and Combustion in the Exhaust Plumes of Rocket Engines Burning RP1 and LOX," GASL TR 631, November 1966.

23. Edelman, R., and Fortune, O., "Some Recent Developments on the Analysis of Exhaust Plume Afterburning," Presented at the Rocket Plume Specialists' Meeting, Aerospace Corp., San Bernardino, Calif., July 11-12, 1968.

24. Edelman, R. B., et. al. - Analytical Investigation of the Effects of Vitiated Air Contamination on Combustion and Hypersonic Airbreathing Engine Ground Tests, GASL TR 676, February 1969; also AEDC-TR-69-148, Oct. 1969.

25. Tamagno, J. Fruchtman, I., and Slutsky, S.: "Supersonic Combustion in Premixed Hydrocarbon-Air Flow", GASL TR-602 (Also AFOSR 66-0872), May 1966.

26. Chinitz, W., and Spadaccini, L. J.: "Research on Vaporizing and Endothermic Fuels For Advanced Engine Application," GASL TR-635 (Also APL-TDR-64-100), Feb. 1967.

27. Catton, I., Hill, D. E., and McRae, R. P., Study of Liquid Jet Penetration In A Hypersonic Stream, A/AA Journal Vol. 6, No. 11, Nov. 1968, pp. 2084-2089.

Unclassified

Security Classification

DOCUMENT CONTROL DATA - R & D

(Security classification of title, body of abstract and indexing annotation must be entered when the overall report is classified)

1. ORIGINATING ACTIVITY *(Corporate author)*

Esso Research and Engineering Co., Linden, N.J. and General Applied Science Laboratories, Westbury, N.Y.

2a. REPORT SECURITY CLASSIFICATION: Unclassified

2b. GROUP:

3. REPORT TITLE

RESEARCH ON METHODS OF IMPROVING THE COMBUSTION CHARACTERISTICS OF LIQUID HYDROCARBON FUELS

4. DESCRIPTIVE NOTES *(Type of report and inclusive dates)*

Final Report (Volumes I and II) January 1, 1969 - December 31, 1971

5. AUTHOR(S) *(First name, middle initial, last name)*

Vincent J. Siminski
Franklin J. Wright
Raymond Edelman
C. Economos
Owen Fortune

6. REPORT DATE	7a. TOTAL NO. OF PAGES	7b. NO. OF REFS
February 1972	216	86

8a. CONTRACT OR GRANT NO.	9a. ORIGINATOR'S REPORT NUMBER(S)
F33615-69-C-1289	
b. PROJECT NO. 3048	AFAPL-TR-72-24 Vol. I and Vol. II
c. Task 304805	9b. OTHER REPORT NO(S) *(Any other numbers that may be assigned this report)*
d.	

10. DISTRIBUTION STATEMENT

Distribution limited to U.S. Government Agencies only; test and evaluation of commercial products. Other requests for this document must be referred to the Fuels Branch (AFAPL/SFF) Fuels and Lubrication Division, Air Force Aero Propulsion Laboratory, Wright-Patterson AFB, Ohio 45433

11. SUPPLEMENTARY NOTES

12. SPONSORING MILITARY ACTIVITY

Air Force Aero Propulsion Lab.
Fuels Branch (AFAPL/SFF)
Fuels and Lubrication Div.
(Project Engineer; Capt. S. G. Hill)

13. ABSTRACT

The purpose of this program was to determine, analytically and experimentally the extent to which the autoignition delay times of liquid hydrocarbons could be reduced by modification of the molecular structure or through the utilization of homogeneous additives and heterogeneous catalysts. To this end the autoignition delays of a number of different hydrocarbons were determined in three different experimental apparatus; a well-stirred reactor, a constant flow subsonic duct and a supersonic detached jet or ducted flow system. At one atmosphere pressure the velocity and temperature of the test devices were varied from subsonic to supersonic and from 300° to 1600°K respectively. No quantitative relationship could be established between the ignition lags measured in the constant flow system and the average residence times determined in the stirred reactor at the blow-out point. However, it is clear that the stirred reactor data more closely describe the total hydrocarbon combustion time than any "pseudo ignition lag" associated with the hydrocarbon. Of the more than 25 different homogeneous additives tested, the strongest ignition promoters, by far, were found to be the alkyl nitrates and nitrites or nitric oxide and nitrogen dioxide. The presence of a platinum surface on the walls of the combustion chamber reduced the autoignition temperature of various hydrocarbons by 350°K. Fuel blends consisting of 15 volume percent n-propyl nitrate in either H-MCPD or Shelldyne-H were ignited and combusted in a piloted supersonic flow (Mach 1.5) over a temperature range of 300 to 1300°K. An ignition model based upon quasi-global kinetics and involving 10 basic chemical reactions has been shown to be able to predict within a factor of 5, the ignition delay of neat hydrocarbons or blends of hydrocarbons with homogeneous additives. The development of the model and the experimental results of the supersonic ignition tests are discussed.

DD FORM 1473 REPLACES DD FORM 1473, 1 JAN 68, WHICH IS OBSOLETE FOR ARMY USE.

Unclassified

Security Classification

14. KEY WORDS	LINK A		LINK B		LINK C	
	ROLE	WT	ROLE	WT	ROLE	WT
Hydrocarbon Ignition Delay Time						
Auto-Ignition						
Combustion of Hydrocarbon Fuels						
Supersonic Combustion						
Subsonic Combustion						
Homogeneous Ignition Promoters						
Heterogeneous Ignition						
Chemical Promoters						
Platinum Catalyst						